

**IMAGING FUNCTIONAL AND
STRUCTURAL NETWORKS
IN THE HUMAN EPILEPTIC BRAIN**

Serge Vulliémoz, MSc, MD

DEPARTMENT OF CLINICAL AND EXPERIMENTAL EPILEPSY
INSTITUTE OF NEUROLOGY
UNIVERSITY COLLEGE LONDON (UCL)
UNITED KINGDOM

THESIS SUBMITTED TO UNIVERSITY COLLEGE LONDON
FOR THE DEGREE OF DOCTOR OF PHILOSOPHY, 2012

DECLARATION OF OWN WORK

I, Serge Vulliemoz confirm that the work presented here is my own. Where information has been derived from other sources, I confirm that this has been indicated in the thesis.

The scientific studies presented in this thesis reflect the contributions of a team of researchers including other colleagues from the DCEE, IoN UCL. However, this thesis presents only studies where I conducted most steps of data analysis and the complete interpretation of the results following discussions at supervision meetings. All the figures and illustrations are my own.

Information derived from other sources has been indicated and referenced in this thesis.

I have outlined my own individual contribution to each of the studies published here and the contributions of my main co-workers and collaborators.

Signature

ABSTRACT

Epileptic activity in the brain arises from dysfunctional neuronal networks involving cortical and subcortical grey matter as well as their connections via white matter fibres. Physiological brain networks can be affected by the structural abnormalities causing the epileptic activity, or by the epileptic activity itself. A better knowledge of physiological and pathological brain networks in patients with epilepsy is critical for a better understanding the patterns of seizure generation, propagation and termination as well as the alteration of physiological brain networks by a chronic neurological disorder. Moreover, the identification of pathological and physiological networks in an individual subject is critical for the planning of epilepsy surgery aiming at resection or at least interruption of the epileptic network while sparing physiological networks which have potentially been remodelled by the disease.

This work describes the combination of neuroimaging methods to study the functional epileptic networks in the brain, structural connectivity changes of the motor networks in patients with localisation-related or generalised epilepsy and finally structural connectivity of the epileptic network. The combination between EEG source imaging and simultaneous EEG-fMRI recordings allowed to distinguish between regions of onset and propagation of interictal epileptic activity and to better map the epileptic network using the continuous activity of the epileptic source. These results are complemented by the first recordings of simultaneous intracranial EEG and fMRI in human. This whole-brain imaging technique revealed regional as well as distant haemodynamic changes related to very focal epileptic activity. The combination of fMRI and DTI tractography showed subtle changes in the structural connectivity of patients with Juvenile Myoclonic Epilepsy, a form of idiopathic generalised epilepsy. Finally, a combination of intracranial EEG and tractography was used to explore the structural connectivity of epileptic networks. Clinical relevance, methodological issues and future perspectives are discussed.

TABLE OF CONTENTS

DECLARATION OF OWN WORK.....	2
ABSTRACT.....	3
TABLE OF CONTENTS.....	4
LIST OF FIGURES.....	11
LIST OF TABLES.....	12
LIST OF ABBREVIATIONS.....	13
ACKNOWLEDGMENTS.....	15
FUNDING SOURCES.....	17
FOREWORD.....	18
OUTLINE AND PERSONAL CONTRIBUTION.....	20
PUBLICATIONS ASSOCIATED WITH THIS THESIS.....	23

SECTION 1: LITERATURE REVIEW

CHAPTER 1: EPILEPSY.....	30
1.1 Epilepsy: a frequent and severe neurological disease.....	30
1.1.1 Definitions.....	30
1.1.2 Epidemiology, morbidity and mortality.....	30
1.2 The Epilepsies.....	31
1.2.1 Epileptic Seizures and epileptic syndromes.....	31
1.3 Pharmaco-resistance and epilepsy surgery.....	36
1.3.1 Pharmaco-resistance.....	36
1.3.2 Non-invasive presurgical evaluation.....	37
1.3.3 Intracranial EEG Recordings.....	41
1.3.4 Post-operative outcome.....	43
1.4 Conclusion and clinical issues addressed by this work.....	45
CHAPTER 2: FUNCTIONAL IMAGING OF EPILEPSY: EEG (MEG) SOURCE IMAGING AND EEG-fMRI.....	47
2.1 Introduction.....	47
2.2 Neurophysiological background.....	50
2.2.1 Origin of the EEG signal.....	50
2.2.2 Origin of the fMRI signal.....	51
2.3 EEG Source Imaging.....	55
2.3.1 Methodological principles and limitations.....	55

2.3.2	Clinical ESI studies in focal epilepsy.....	60
2.4	MEG and Magnetic Source Imaging of epileptic networks	63
2.4.1	Data acquisition and processing	63
2.4.2	Detection of epileptic activity	63
2.4.3	Effect of conductivity.....	64
2.4.4	Clinical MSI studies in focal epilepsy	65
2.5	Resting state EEG-fMRI for mapping epileptic networks.....	65
2.5.1	Methodological principles and limitations	65
2.5.2	Clinical EEG-fMRI studies in focal epilepsy	71
2.6	Combination of ESI and EEG-fMRI.....	75
2.6.1	Intrinsic discrepancies between EEG and fMRI measurements	75
2.6.2	Symmetrical and asymmetrical combination of ESI and EEG-fMRI	76
2.7	Further methodological perspectives	83
2.7.1	EEG-fMRI and ESI studies in the frequency domain.....	83
2.7.2	Cortical potential imaging	83
2.7.3	Can fMRI inform about network dynamics ?	84
2.8	Perspectives on the combination of ESI and EEG-fMRI.....	85
2.9	Conclusion.....	86

CHAPTER 3: DIFFUSION MAGNETIC RESONANCE IMAGING AND
TRACTOGRAPHY IN EPILEPSY

		87
3.1	Introduction.....	87
3.2	Diffusion imaging: physical and radiological principles.....	88
3.2.1	Diffusion: physical background	88
3.2.2	Measurement of diffusion with MRI.....	89
3.3	Tractography	90
3.3.1	Principles.....	90
3.3.2	Methodological limitations and validation studies.....	91
3.4	Diffusion MRI applied to Epilepsy imaging	93
3.4.1	Structural brain modification associated with epileptic activity : evidence from animal studies	93
3.4.2	Status epilepticus in humans	94
3.5	Diffusion imaging as a lateralising or localising tool : Post-ictal and interictal clinical studies	95
3.5.1	Post-ictal diffusion imaging	95
3.5.2	Interictal Diffusion imaging.....	96
3.6	Tractography studies in focal epilepsy	100

3.6.1	Temporal lobe Epilepsy: Alteration of the limbic network and reorganisation of cognitive networks.....	101
3.6.2	Memory	102
3.6.3	Language	102
3.6.4	Visual pathways.....	103
3.6.5	Motor system.....	104
3.6.6	Malformations of cortical development.....	105
3.6.7	Tracking the propagation pathways of the epileptic activity.....	106
3.7	Perspectives.....	110
3.7.1	Structural connectivity of functional neuronal networks.....	110
3.7.2	Ongoing developments in MR tractography.....	110
3.8	Conclusion.....	112

SECTION 2: EXPERIMENTAL STUDIES

CHAPTER 4:	COMMON METHODS	114
4.1	EEG-fMRI.....	114
4.1.1	EEG acquisition.....	114
4.1.2	MRI acquisition.....	115
4.1.3	EEG artefact correction and IED identification.....	115
4.1.4	EEG Source Imaging (ESI).....	116
4.1.5	fMRI processing and statistical analysis	117
4.2	Diffusion imaging and tractography.....	119
4.2.1	Acquisition and preprocessing.....	119
4.2.2	Tractography and quantitative tract analysis.....	119
CHAPTER 5:	SPATIO-TEMPORAL MAPPING OF EPILEPTIC NETWORKS USING SIMULTANEOUS EEG-fMRI AND EEG SOURCE IMAGING	121
5.1	Summary.....	121
5.2	Introduction.....	122
5.3	Methods.....	123
5.3.1	Patients and electro-clinical data	123
5.3.2	EEG-fMRI acquisition	125
5.3.3	Analysis.....	126
5.3.4	Assessment of concordance.....	126
5.4	Results	127
5.4.1	Concordance at IED onset (ESIo).....	129

5.4.2	Concordance in IED propagation areas (ESIp)	130
5.4.3	Comparison with intracranial EEG results.....	130
5.4.4	Illustrative cases	131
5.5	Discussion	136
5.5.1	Concordance and sources of uncertainties	138
5.5.2	ESI and EEG-fMRI of IED in the medial cortex	139
5.5.3	ESI and EEG-fMRI in temporal lobe IED	140
5.5.4	ESI as a marker of propagation	142
5.5.5	Revisiting the importance of the cluster containing the most significant BOLD increase	143
5.5.6	ESI and negative BOLD responses	144
5.6	Conclusion.....	146
CHAPTER 6: CONTINUOUS EEG SOURCE IMAGING ENHANCES ANALYSIS OF EEG-fMRI IN FOCAL EPILEPSY.....		147
6.1	Summary	147
6.2	Introduction.....	148
6.3	Methods.....	149
6.3.1	Patients and electro-clinical data	149
6.3.2	EEG-fMRI acquisition	149
6.3.3	EEG analysis and Electrical Source Imaging (ESI)	151
6.3.4	Source activity based on continuous ESI (cESI)	151
6.3.5	fMRI analysis.....	153
6.3.6	Assessment of Concordance	154
6.3.7	Exploration of factors influencing the degree of concordance	155
6.4	Results	156
6.4.1	Concordance and clinical relevance	156
6.4.2	Illustrative case reports.....	157
6.4.3	Factors that influence the degree of concordance	166
6.5	Discussion	168
6.5.1	Methodological considerations.....	169
6.5.2	Neurophysiological and clinical relevance.....	172
6.6	Conclusion.....	174

CHAPTER 7: SIMULTANEOUS INTRACRANIAL EEG AND fMRI OF INTERICTAL EPILEPTIC DISCHARGES IN HUMANS	175
7.1 Summary	175
7.2 Introduction.....	176
7.3 Methods.....	177
7.3.1 Patients	177
7.3.2 Case reports.....	177
7.3.3 Data acquisition.....	179
7.3.4 icEEG analysis	179
7.3.5 fMRI.....	180
7.4 Results	181
7.4.1 Patient 1	187
7.4.2 Patient 2	189
7.5 Discussion	191
7.5.1 Methodological considerations.....	191
7.5.2 Neurophysiological relevance.....	194
7.5.3 Clinical relevance	195
7.6 Conclusion.....	197
 CHAPTER 8: CONNECTIVITY OF THE SUPPLEMENTARY MOTOR AREA IN JUVENILE MYOCLONIC EPILEPSY AND FRONTAL EPILEPSY	 198
8.1 Summary	198
8.2 Introduction.....	199
8.3 Methods.....	200
8.3.1 Patients and controls	200
8.3.2 Motor fMRI.....	201
8.3.3 Diffusion Tensor imaging acquisition and preprocessing	202
8.4 Results	204
8.4.1 SMA tractography.....	204
8.4.2 Juvenile Myoclonic Epilepsy	204
8.4.3 Frontal Lobe Epilepsy	205
8.4.4 Comparison between FLE and JME	205
8.5 Discussion	210
8.5.1 Juvenile Myoclonic Epilepsy	210
8.5.2 Frontal Lobe Epilepsy.....	213
8.5.3 Methodological considerations.....	214
8.6 Conclusion.....	215

CHAPTER 9: STRUCTURAL CONNECTIVITY OF EPILEPTIC NETWORKS	216
9.1 Summary	216
9.2 Introduction.....	217
9.2.1 Epileptic networks.....	217
9.2.2 Mapping the structural connectivity of epileptic networks.....	220
9.2.3 Combined icEEG and DTI study of the structural connectivity of the seizure onset zone	222
9.3 Case Report	223
9.4 Methods.....	225
9.4.1 Localisation of the seizure onset zone as tractography seed	225
9.4.2 Tractography: one-seed vs two-seed.....	225
9.4.3 Tractography in healthy controls.....	226
9.4.4 Qualitative tractography and commonality maps	226
9.4.5 Quantitative tract analysis.....	227
9.4.6 Voxel-based analysis of FA maps.....	227
9.5 Results	227
9.5.1 Qualitative tractography and commonality maps	227
9.5.2 Quantitative tract analysis.....	229
9.5.3 Voxel-based analysis of FA maps.....	229
9.6 Discussion	233
9.6.1 Neuroanatomical significance	233
9.6.2 Methodological considerations:.....	234
9.6.3 Perspectives.....	236
9.7 Conclusion.....	237

SECTION 3: DISCUSSION

CHAPTER 10: OVERALL DISCUSSION	239
10.1 Summary of the principal findings and methodological considerations.....	239
10.1.1 Combining ESI and EEG-fMRI.....	239
10.1.2 Interictal epileptic networks in focal epilepsy.....	239
10.1.3 Intracranial EEG-fMRI	240
10.1.4 Structural connectivity of physiological and epileptic networks.....	241
10.2 General discussion and future research directions	242
10.2.1 Methodological discussion and perspectives	242
10.2.2 Neurobiological discussion and perspectives	250

10.3 Clinical implications and perspectives.....	255
10.3.1 Mapping epileptic networks for epilepsy surgery.....	255
10.3.2 Mapping epileptic networks for neuromodulation	257
CHAPTER 11: GENERAL CONCLUSION	259
LIST OF REFERENCES.....	260

LIST OF FIGURES

Chapter 5 :

Figure 5.1 : ESI concordant with very small positive BOLD changes

Figure 5.2 : ESI concordant with negative BOLD changes

Figure 5.3 : Discordant ESI and BOLD changes

Chapter 6 :

Figure 6.1 : Summary of the analysis strategy

Figure 6.2 : IED model vs parametric model : temporal lobe focus

Figure 6.3 : IED model vs parametric model : occipital focus

Figure 6.4 : IED model vs parametric model : frontal focus

Figure 6.5 : Discordant case

Chapter 7 :

Figure 7.1 : Intracranial EEG outside and inside the MR scanner : patient 1

Figure 7.2 : Intracranial EEG outside and inside the MR scanner : patient 2

Figure 7.3 : Intracranial electrode position and BOLD changes : patient 1

Figure 7.4 : Intracranial electrode position and BOLD changes : patient 2

Chapter 8 :

Figure 8.1 : Commonality maps of SMA connectivity for Juvenile Myoclonic Epilepsy

Figure 8.2 : Fractional anisotropy of SMA connectivity for patients and controls

Chapter 9 :

Figure 9.1 : Connectivity of epileptic networks on intracranial EEG

Figure 9.2: Intracranial seizure onset in focal cortical dysplasia

Figure 9.3 : Commonality map of seizure onset zone connectivity

Figure 9.4: Seizure propagation: tract of interest

Figure 9.5: Quantitative tract analysis

Figure 9.6: voxel-based analysis of FA maps: patient > control group

LIST OF TABLES

Chapter 2:

Table 2.1: Revised classification of focal seizures

Chapter 5:

Table 5.1: Clinical, electrophysiological and radiological data

Table 5.2: EEG Source imaging and EEG-fMRI results

Chapter 6:

Table 6.1: Clinical, electrophysiological and radiological data

Table 6.2: Results of ESI, conventional and parametric EEG-fMRI analysis

Table 6.3: Factors influencing the degree of concordance

Chapter 7:

Table 7.1: Description of intracranial interictal epileptiform discharges

Chapter 8:

Table 8.1: Clinical characteristics for patients and controls

Table 8.2: Quantitative SMA tractography analysis

LIST OF ABBREVIATIONS

ADC	Apparent Diffusion Coefficient
AED	Anti-Epileptic Drug(s)
ANOVA	Analysis of Variance
BOLD	Blood Oxygen Level Dependant
ECD	Equivalent Current Dipole
ECG	Electrocardiogram
EEG	Electroencephalography, Electroencephalogram
EEG-fMRI	Simultaneous EEG and fMRI
EPI	Echo Planar Imaging
ESI, cESI	Electric Source Imaging, continuous Electric Source Imaging
FCD	Focal Cortical Dysplasia
CT	Computer Tomography
DCM	Dynamic Causal Modelling
DSI	Diffusion Spectrum Imaging
DT/DTI	Diffusion Tensor / Diffusion Tensor Imaging
DWI	Diffusion Weighted Imaging
FA	Fractional Anisotropy
(FDG)-PET	(Fluoro-Deoxy-Glucose) Positron Emission Tomography
FLAIR	Fluid Attenuation Inversion Recovery
fMRI	functional Magnetic Resonance Imaging
FLE, TLE	Frontal Lobe Epilepsy, Temporal Lobe Epilepsy
FWE	Family Wise Error
GLM	General Linear Model
HRF	Haemodynamic Response Function
HS	Hippocampal Sclerosis

icEEG	Intracranial electroencephalography
icEEG-fMRI	Simultaneous intracranial EEG and fMRI
IED	Interictal Epileptic Discharges
IGE	Idiopathic Generalised Epilepsy
ILAE	International League Against Epilepsy
JME	Juvenile Myoclonic Epilepsy
MD	Mean Diffusivity
MEG	Magnetoencephalography, Magnetoencephalogram
MR/MRI	Magnetic Resonance / Magnetic Resonance Imaging
NHNN	National Hospital for Neurology and Neurosurgery, London, UK
NSE	National Society for Epilepsy, UK, renamed Epilepsy Society in 2009
nTV	Normalised Tract Volume
PET	Positron Emission Tomography
ROI	Region of Interest
SAR	Specific Absorption Rate
SMAC	Spherical Model with Anatomical Constraints
SEEG	Stereo-Electroencephalography
SISCOM	Substraction of Ictal SPECT coregistered to MRI
SMA	Supplementary Motor Area
SOZ	Seizure Onset Zone
SPECT	Single Photon Emission Computed Tomography
S_{soz}, S_p	Tractography seed underlying the seizure onset/propagation zone
SPM	Statistical Parametric Mapping
SPM{t}/F	t- / F- contrast on Statistical Parametric Maps
TE/TR	Echo Time / Time of Repetition of MRI acquisition sequences
VOI	Volume of Interest

ACKNOWLEDGMENTS

I am deeply grateful to Professors John S. Duncan, my principal supervisor and Louis Lemieux, my subsidiary supervisor for their warm welcoming in their research groups, inspiring guidance and constant support throughout the course of this thesis. I would also like to thank Professor Mathias Koepp for his co-supervision in the tractography study described in Chapter 8 and for a memorable landlordship. I am also very grateful to Professor Christoph M. Michel in Geneva, Switzerland, for his support and guidance during this PhD and beyond for all matters related to EEG source imaging.

Rachel Thornton, David Carmichael and Roman Rodionov were my main companions and guides in the field of EEG-fMRI research and Mark Symms, Mahinda Yogarajah and Christian Vollmar brought crucial scientific and methodological input in the tractography studies. I am also thankful to all other researchers of the Epilepsy Research Group met during my time at the National Society for Epilepsy (NSE): Silvia Bonelli, Maria Centeno, Mar Matarin, Karin Rosenkrantz, Anna San Juan, Anna Vaudano, Umair Chaudhary, Vasily Kokkinos, Jason Stretton and Gavin Winston. With all, I had enthusiastic scientific exchanges and friendly chats. Some other researchers, Afraim Salek-Haddadi, Khalid Hamandi, Helmut Laufs and Rob Powell had recently left the lab but had left a legacy that allowed my studies to take place. The radiographers at NSE offered their experience for high quality data acquisition and friendly collaboration: Philippa Bartlett, Jane Burdett, Elaine Williams as well as Sajitta Cannadathu for EEG acquisition. Peter Gilford patiently listened to and solved my IT issues.

Methodological guidance for study design and statistics was kindly given by Prof. Karl Friston, Will Penny and Jean Daunizeau from the Wellcome Trust Centre for Neuroimaging.

At the National Hospital for Neurology and Neurosurgery, Beate Diehl, Catherine Scott and Stjepana Kovac together with the clinical team of the Telemetry ward were

very helpful in discussing electro-clinical findings of patients included in this work. Together with Mr Andrew McEvoy, the epilepsy neurosurgeon, they greatly facilitated the logistics of simultaneous intracranial EEG and fMRI recordings. John Thornton, head MR physicist and the MR radiographers Lisa Strycharczuk, Catherine Green, Alison Duncan, Prashanth Kesara, Bruce Metheringham also played a key role in that study. Fergus Rugg-Gunn, kindly provided the MEG results included in Chapter 7.

I am also very indebted to my clinical mentors in the University Hospital of Geneva, Switzerland: Professor Margitta Seeck, and Professor Pierre Jallon who introduced me to the clinical and scientific aspects of the fascinating universe of epileptology and encephalography. I am also very grateful to Professor Theodor Landis, former chairman of the Neurology Department, who welcomed and mentored me during my neurological training and career development. Denis Brunet and Laurent Spinelli, were very precious supports with practical aspects of EEG source analysis.

Many other people contributed to my research work with interesting discussions, useful suggestions, precious advice or experimental assistance and all should be anonymously acknowledged here.

I would also like to thank both examiners of this thesis work, Dr Rod Scott and Dr Andrew Bagshaw, for their critical reading and interesting comments, which improved the quality of this thesis.

My parents always encouraged me on the path of scientific and medical education and their loving support helped me to make the best choices during my training.

Finally, this work would not have been possible without the constant love, joy, support and motivation given to me by Lindsey, Jules and Margot. They made this British experience a unique adventure.

FUNDING SOURCES

During this PhD thesis, I was supported by the “Fonds de Perfectionnement” of the University Hospital of Geneva, Switzerland, by a fellowship for advanced researcher from the Swiss National Research Foundation and by a grant from the same institution (33CM30-124089, SPUM Epilepsy). I also acknowledge the financial support of the UK Medical Research Council (MRC grant G0301067) which funded the scalp EEG-fMRI research group and the Wellcome Trust grants 079474, 083148 which funded the tractography project. This work was undertaken at UCLH/UCL who received a proportion of funding from the Department of Health’s NIHR Biomedical Research Centres funding scheme. I am grateful to the Big Lottery Fund, Wolfson Trust and National Society for Epilepsy for supporting the 3T MRI scanner at the Epilepsy Society (formerly National Society for Epilepsy).

FOREWORD

This thesis investigates functional and structural properties of pathologic and physiologic networks in the brain of persons with epilepsy. The scientific studies performed to pursue this goal and presented in this work are based on the combination of several neuro-imaging methods to take advantage of their specific strengths. These individual methods each result from years of methodological development and an in-depth description of the underlying physical and methodological principles is beyond the scope of this thesis. References for further reading are given along the work.

Likewise, none of this work could have been possible without the precious work of several persons more or less closely involved with my specific projects, from the identification of the patients, to the optimisation of MR acquisition sequences and data storage. All the work presented here was realised in the context of collaborations internal and external to the UCL Institute of Neurology. The main scientific collaborations are acknowledged below and other collaborators are mentioned in the acknowledgement section.

The first three studies represent advances in EEG-fMRI to map the neuroelectric and haemodynamic changes related to epileptic activity in a multimodal approach with a combination of EEG source imaging and EEG-fMRI on the one hand and the first simultaneous recording of simultaneous intracranial EEG and fMRI on the other hand. In the fourth study, I investigated the association between epilepsy and alteration of specific structural connections of the motor network. This was done by combining fMRI to localise the supplementary motor area with MR tractography to map its connections with other brain regions. The term “epileptic networks” will be used in this work to describe all brain regions in which the activity is estimated to be modified in relation to epileptic activity. For the mapping of these epileptic networks, the

combination of functional and structural methods would be very beneficial to study the structural connections underlying the functional pathological networks. The fifth study is a step in this direction and represents an exploratory study of using various functional mapping techniques (ESI, EEG-fMRI, intracranial EEG) to localise the epileptic focus in combination with MR tractography to map its structural connectivity.

OUTLINE AND PERSONAL CONTRIBUTION

This thesis is structured as follows:

SECTION 1: LITERATURE REVIEW

- **Chapter 1** introduces clinical background on epilepsy.
- **Chapter 2** describes the functional neuroimaging methods that are important for the understanding of the following work, namely EEG source imaging (ESI) and simultaneous EEG-fMRI recordings. The physical principles and methodological considerations are discussed together with a review of neurophysiological and clinical applications in patients with epilepsy. Portions of this chapter feature in a review article published in the context of this research work.
- **Chapter 3** introduces structural brain imaging using diffusion imaging and tractography based on diffusion tensor imaging. The physical principles, methodology and clinical studies in epilepsy are reviewed.

SECTION 2: EXPERIMENTAL STUDIES

- **Chapter 4** describes common methods used in more than one of the experimental studies of this thesis and chapters 4 to 8 describe the experimental studies
- In **Chapter 5**, I combined Electrical Source Imaging and simultaneous EEG-fMRI recordings to benefit from the exquisite temporal resolution of ESI and the better spatial resolution and whole-brain coverage of fMRI. In this first application of ESI on the EEG recorded during fMRI acquisition, I was able to distinguish between haemodynamic changes related to the onset vs the propagation of interictal epileptic discharges, thereby adding temporal information to EEG-fMRI results.
- In **Chapter 6**, I combined further ESI and EEG-fMRI to improve the information extracted from the EEG for fMRI analysis. By estimating the source of the epileptic

activity with ESI and then mapping haemodynamic changes related to this source activity, I showed that this technique improved the localisation of the epileptic focus and the mapping of the epileptic networks.

Personal contribution: For those 2 studies, based on a largely overlapping group of patients, I was responsible for part of the data acquisition in collaboration with R. Thornton. I was primarily involved in study design, data analysis and interpretation, in the context of a collaboration with Professor C.M. Michel of the Functional Brain Mapping Laboratory of the Faculty of Medicine of the University of Geneva, Switzerland. The principal investigator was Prof. Louis Lemieux.

- In **Chapter 7**, I present the first results of the mapping of epileptic networks in focal epilepsy using recordings of simultaneous intracranial EEG and fMRI in human.

Personal contribution: I was primarily responsible for the clinical recruitment and supervision of the patients, analysis of the quality of intracranial EEG obtained during fMRI acquisition, EEG coding and data analysis to map epileptic network. I collaborated closely with David W. Carmichael who had been responsible for previous safety and feasibility studies and had designed the project together with the principal investigator Prof. Louis Lemieux.

- In **Chapter 8**, I showed the alteration of the motor network structural connectivity in patients with different forms of epilepsy with motor manifestations: Juvenile Myoclonic Epilepsy and Frontal Lobe Epilepsy.

Personal contribution: I was primarily responsible for study design and data analysis. The recruitment of patients and data acquisition was done by Christian Vollmar in the context of a larger project on functional imaging in frontal lobe

epilepsy and juvenile myoclonic epilepsy led by Prof. Mathias J. Koepp. The principal supervisor of my specific project was Prof. John S. Duncan.

- In **Chapter 9**, I explored the structural connectivity of the epileptic network starting from the seizure onset zone. A combination of intracranial EEG and DTI tractography was used. The currently available methodology and its limitations are discussed.

Personal contribution: I was primarily responsible for study design and data analysis. Dr Beate Diehl, National Hospital for Neurology and Neurosurgery participated in study design and patient selection by helping define patterns of intracranial EEG activity that were suitable for analysis and providing clinical interpretation of intracranial EEG.

SECTION 3: DISCUSSION

- **Chapter 10** summarises the principal experimental findings, presents a overall discussion of the neurophysiological and clinical relevance of these results. Future research directions and ways to address current methodological limitations are presented.
- **Chapter 11** is the general conclusion.

PUBLICATIONS ASSOCIATED WITH THIS THESIS

Parts of the introduction (chapter 2) and experimental studies (chapters 5-9) presented in this thesis have been published as a first author in peer-reviewed journals:

Chapter 2:

Vulliemoz S, Michel CM, Daunizeau J, Lemieux L, Duncan JS ; *The combination of EEG source imaging and EEG-correlated functional MRI to map epileptic networks*; *Epilepsia* 2010 Apr 51(4): 491-505.

Chapter 5:

Vulliemoz S, Thornton R, Rodionov R, Carmichael DW, Guye M, Lhatoo S, McEvoy AW, Spinelli L, Michel CM, Duncan JS, Lemieux L ; *The spatio-temporal mapping of epileptic networks : Combination of EEG-fMRI and EEG source imaging*; *Neuroimage* ; 2009, Jul 1;46(3):834-43.

Chapter 6:

Vulliemoz S, Rodionov R, Carmichael DW, Thornton R, Guye M, Lhatoo S, Michel CM, Duncan JS, Lemieux L ; *Continuous EEG Source Imaging enhances analysis of EEG-fMRI in focal epilepsy*; *Neuroimage* ; 2010, Feb 15 ; 49(4):3219-29.

Chapter 7:

Vulliemoz S, Carmichael DW, Rosenkranz K, Diehl B, Rodionov R, Walker M, McEvoy AW, Lemieux L; *Simultaneous intracranial EEG and fMRI of interictal epileptic discharges in humans*; *Neuroimage*, 2011 Jan 1;54(1):182-90.

Chapter 8:

Vulliemoz S, Vollmar C, Yogarajah M, Carmichael DW, Stretton J, Symms MR, Koepp M, Duncan JS; *Connectivity of the supplementary motor area in juvenile myoclonic epilepsy and frontal lobe epilepsy*; *Epilepsia*. 2011 Mar; 52(3):507-14.

In addition to the studies mentioned above in chapters 5-9, I was involved as co-investigator in the following studies and publications performed at the DCEE:

Thornton R, Laufs H, Rodionov R, Cannadathu S, **Vulliemoz S**, Salek-Haddadi A, McEvoy A, Harkness W, Smith S, Lhatoo S, Elwes RDC, Walker M, Lemieux L, Duncan JS; *EEG-correlated fMRI and post-operative outcome in focal epilepsy*; Journal of Neurology, Neurosurgery and Psychiatry, 2010 Aug; 81(8):922-7.

Personal contribution: I participated in data acquisition, EEG and fMRI analysis for some of the patients and redaction of the manuscript.

Thornton R, Rodionov R, Laufs H, **Vulliemoz S**, Vaudano A, DW Carmichael, Cannadathu S, Guye M, McEvoy A, Bartolomei F, Chauvel P, Diehl B, Walker M, Duncan JS, Lemieux L; *Imaging Haemodynamic Changes related to Focal Seizures: Comparison of EEG-based general linear model, independent component analysis of fMRI and intracranial EEG*; Neuroimage, 2010, Oct 15; 53(1): 196-205.

Personal contribution: I participated in data acquisition, EEG and fMRI analysis for some of the patients, as well as interpretation of the results and redaction of the manuscript.

Thornton R, **Vulliemoz S**, Rodionov R, Carmichael DW, Diehl B, Elwes RDC, Laufs H, McEvoy AW, Walker MC, Bartolomei F, Guye M, Chauvel P, Lhatoo S, Duncan JS, Lemieux L; *Epileptic Networks in Focal Cortical Dysplasia revealed using EEG fMRI*; Annals of Neurology, in press.

Personal contribution: I participated in data acquisition, EEG and fMRI analysis for some of the patients as well as interpretation of the results and redaction of the manuscript.

Carmichael DW, **Vulliemoz S**, Rodionov R, Thornton J, McEvoy AW, Lemieux L; *Simultaneous intracranial EEG-fMRI: safety and data quality*; in revision.

Personal contribution: I was involved in clinical recruitment and supervision of these first 2 patients undergoing simultaneous intracranial EEG and fMRI recordings, in intracranial EEG acquisition and analysis and I participated in the interpretation of the results and redaction of the manuscript.

Carmichael DW, **Vulliemoz S**, Rosenkranz K, Thornton J, Rodionov R, McEvoy AW, Lemieux L; *Measuring oscillatory human brain activity across scales and states using the first simultaneous intracranial EEG and fMRI recordings*, in preparation.

Personal contribution: In this same dataset as described above, I participated in recruitment, data acquisition and analysis as well as interpretation of the results and redaction of the manuscript

CONFERENCE POSTERS AND TALKS RELATED TO THIS THESIS

Carmichael DW, **Vulliemoz S**, Thornton J, Rodionov R, McEvoy AW, Lemieux L; *Feasibility of simultaneous intracranial EEG-fMRI in humans: data quality*; International Society for Magnetic Resonance in Medicine, Montreal, June 2011

Carmichael DW, **Vulliemoz S**, Thornton J, Walker M, Rosenkranz K, Rodionov R, McEvoy AW, Lemieux L; *Simultaneous intracranial EEG-fMRI in humans suggests that high gamma frequencies are the closest neurophysiological correlate of BOLD fMRI*; International Society for Magnetic Resonance in Medicine, Montreal, June 2011

Carmichael DW, **Vulliemoz S**, Rodionov R, Rosenkranz K, Diehl B, Walker M, McEvoy AW, Lemieux L; *Simultaneous intracranial EEG and fMRI of interictal epileptiform discharges in patients with epilepsy*; Annual meeting of the American Epilepsy Society, San Antonio, Dec 2010

Carmichael DW, **Vulliemoz S**, Rosenkranz K, Diehl B, Walker M, , Rodionov R, McEvoy AW, Lemieux L; *Simultaneous intracranial EEG-fMRI in patients with epilepsy*; 9th European Congress on Epileptology, Rhodes, June 2010

Vulliemoz S; *Identifying the connectivity of the epileptogenic zone, discussion group*, 9th European Congress on Epileptology, Rhodes, June 2010

Vulliemoz S, Carmichael DW, Rosenkranz K, Diehl B, Rodionov R, Walker M, McEvoy AW, Lemieux L; *Simultaneous intracranial EEG and fMRI of interictal epileptic discharges in humans*; Annual meeting of the Organisation for Human Brain Mapping, Barcelona, June 2010

Thornton R, **Vulliemoz S**, Laufs H, Rodionov R, Chaudhary U, Carmichael DW, Diehl B, McEvoy AW, Elwes R, Lhatoo S, Bartolomei F, Walker MC, Guye M, Duncan JS, Lemieux L; *EEG fMRI in the pre-surgical evaluation of patients with focal cortical dysplasia and epilepsy*; Annual meeting of the Organisation for Human Brain Mapping, Barcelona, June 2010

Carmichael DW, **Vulliemoz S**, Rosenkranz K, Rodionov R, McEvoy AW, Lemieux L; *Feasibility of simultaneous intracranial EEG-fMRI in humans : first results*; Annual meeting of the Organisation for Human Brain Mapping, Barcelona, June 2010

Vulliemoz S, Rodionov R, Carmichael D, Thornton R, Guye M, Spinelli L, Michel C, Duncan J, Lemieux L; *Continuous EEG Source imaging enhances EEG-fMRI analysis*, Annual Meeting of the Swiss Society for Neurosciences, Lausanne, Switzerland, March 2010

Vulliemoz S, Rodionov R, Carmichael D, Thornton R, Guye M, Spinelli L, Michel C, Duncan J, Lemieux L; *Continuous EEG Source imaging enhances EEG-fMRI analysis*, Alpine Brain Imaging Meeting, Champéry, Switzerland Jan. 2010

Vulliemoz S, Vollmar C, Yogarajah M, Stretton J, Thompson P, Koepp M, Symms MR, Duncan J; *Connectivity of the supplementary motor cortex in frontal lobe epilepsy: an fMRI based tractography study*; Annual meeting of the American Epilepsy Society, Boston, Dec 2009

Thornton R, Rodionov R, Laufs H, **Vulliemoz S**, Carmichael DW, Diehl B, Guye M, Bartolomei F, Lhatoo S, Walker MC, McEvoy AW, Smith SM, Chauvel P, Duncan JS, Lemieux L; *Exploring Haemodynamic Changes in Focal Seizures* ; Annual meeting of the American Epilepsy Society, Boston, Dec 2009

Vulliemoz S, Rodionov R, Carmichael D, Thornton R, Guye M, Spinelli L, Michel C, Duncan J, Lemieux L; BOLD correlates of *Continuous EEG Source imaging in patients with focal epilepsy*; International Epilepsy Congress, Budapest, June 2009

Vulliemoz S, Vollmar C, Yogarajah M, Stretton J, Thompson P, Koepp M, Symms MR, Duncan J; *Connectivity of the supplementary motor cortex in frontal lobe epilepsy: an fMRI based tractography study*; Annual meeting of the Organisation for Human Brain Mapping, San Francisco, June 2009

Vulliemoz S, Thornton R, Rodionov R, Carmichael D, Guye M, Spinelli L, Michel C, Lemieux L ; *The epileptic networks in space and time: simultaneous electric source imaging and EEG-fMRI*; Annual meeting of the American Epilepsy Society, Seattle, Dec. 2008

Thornton R, Rodionov R, Laufs H, **Vulliemoz S**, Cannadathu S, Carmichael DW, Guye M, Bartolomei F, Lhatoo S, Walker MC, Smith SM, McEvoy AW, Chauvel P, Duncan JS, Lemieux L; *EEG-fMRI in Seizures: Imaging the Epileptic Network* ; Annual meeting of the American Epilepsy Society, Seattle, Dec. 2008

Vulliemoz S, Thornton R, Rodionov R, Guye M, Spinelli L, Michel C, Lemieux L ; *Hemodynamic response related to initiation vs propagation of interictal spikes can be*

discriminated using EEG source imaging and EEG-fMRI data; 8th European Congress on Epileptology, Berlin, Sept. 2008

Vulliemoz S, Thornton R, Rodionov R, Carmichael D, Guye M, Spinelli L, Michel C, Lemieux L ; *The epileptic networks in space and time: simultaneous electric source imaging and EEG-fMRI*; UK chapter of the International League against Epilepsy, Dundee, UK, July 2008

SECTION 1

LITTERATURE REVIEW

1 EPILEPSY

1.1 Epilepsy: a frequent and severe neurological disease

1.1.1 Definitions

According to the recent definition provided by the International League Against Epilepsy (ILAE), an **epileptic seizure** is “a transient occurrence of signs and/or symptoms due to abnormal excessive or synchronous neuronal activity in the brain” (Fisher, van Emde Boas et al. 2005). This can take a variety of forms, depending on the origin and the propagation of this pathological activity.

Epilepsy is a neurological disorder caused by the recurrence of unprovoked seizures. According to the definition by the ILAE, “Epilepsy is a disorder of the brain characterized by an enduring predisposition to generate epileptic seizures and by the neurobiologic, cognitive, psychological and social consequences of this condition” (Fisher, van Emde Boas et al. 2005). An epileptic condition is therefore defined by the occurrence of at least two unprovoked seizures or the occurrence of an inaugural seizure in an individual presenting evidence of a functional or structural brain abnormality that predisposes him to recurring seizures.

1.1.2 Epidemiology, morbidity and mortality

Epilepsy is the most common debilitating neurological condition. Its incidence is estimated to be 40-70/100,000 persons per year in developed societies (not considering febrile seizures in young children and single seizures). The incidence has a J-shaped curve as a function of age, with a high incidence in infants and in the elderly population: epilepsy associated to abnormal brain development, metabolic disorders or perinatal insults starts early in life while acquired brain lesion such as stroke, tumor and trauma increase the risk of epilepsy in the elderly. Studies in

developing countries, have found higher incidence and factors explaining such differences are not clearly identified. The prevalence of epilepsy in a developed society is 5-10 per 1000 persons (again, excluding febrile convulsions, single seizures and inactive cases) (Hauser, Annegers et al. 1993; MacDonald, Cockerell et al. 2000). Data from developing countries have shown higher or lower prevalence values depending on the region studied, with higher rates in rural areas (Sander and Shorvon 1996).

Epilepsy is associated with neurological, cognitive, psychiatric and socio-professional co-morbidities. Moreover, the mortality of epileptic patients is 2-3 times higher than the general population, especially in the first 15 years following diagnosis. Common causes of death in persons suffering from epilepsy include bronchopneumonia (especially in the elderly population), tumors, seizure-related death (such as status epilepticus and Sudden Unexplained Death in Epileptic Patients, SUDEP) and accidents. A higher risk of suicide is present among persons suffering from epilepsy (Bell and Sander 2009) and the existence of affective disorders (depression, anxiety) appears as a clear risk factor (see (Kanner 2009) for a review).

1.2 The Epilepsies

1.2.1 Epileptic Seizures and epileptic syndromes

Epileptic seizures can be characterised by a wide range of clinical manifestations with sensory, motor, neuro-vegetative, cognitive or psychic symptoms and signs. An epileptic syndrome is a characteristic clinical entity defined by epidemiological factors, seizure type, electro-encephalographic patterns, treatment response and prognosis. A standardised classification and terminology to describe the different forms of epileptic seizures and epileptic conditions (epilepsies) is very important to allow

precise communication between members of medical professions and consistent clinical research.

Until very recently, the prevailing classification scheme was the international classification of epileptic seizures, revised in 1981 (ILAE 1981) and the classification of epilepsy syndromes and epilepsies, revised in 1989 (ILAE 1989) (<http://www.ilae-epilepsy.org/ctf/>). In 2010, a new classification strategy has been proposed to take into account the recent important technological developments, notably in imaging and genetics, which are now playing a critical role in our understanding of epileptic seizures and epilepsies and their classification (Berg, Berkovic et al. 2010). Since this new scheme has only been published in 2010, the literature and this thesis are based on the preexisting terminology which is still widely used.

1.2.1.1 1981 Classification of epileptic seizures

In the 1981 classification of seizures, the epileptic **seizures are** classified according to observation of characteristic patterns of symptoms and signs during the seizure (ictal semiology) together with the associated electrographic features measured by electroencephalographic recordings (EEG). The seizures are first classified as generalised or focal onset type, and the second level of classification is based on semiology, i.e. clinical manifestations : generalised seizures can be either myoclonic, clonic, tonic, tonic-clonic, atonic or absence seizures. Focal onset seizures are separated into simple partial (awareness is preserved) and complex partial seizures (awareness is altered or lost) and further labelled as motor, somato-sensory, special sensory (visual, auditory, olfactory, gustatory), autonomic or psychic seizures.

1.2.1.2 1989 Classification of epileptic syndromes

The revised classification of epileptic syndromes and epilepsies (1989) is based on the distinction between focal and generalised types as well as on five hierarchical axes describing the available knowledge of the condition (Engel 2006) :

- 1) Ictal semiology
- 2) Seizure type
- 3) Syndrome
- 4) Etiology (if available)
- 5) Impairment

This classification is not static but has been periodically modified by the ILAE with changes in terminology and recognition of new syndromes. The etiological classification distinguishes “idiopathic” (no identified cause, presumably polygenic factors), “symptomatic” (known structural, metabolic or genetic cause) and “cryptogenic” (from the Greek roots “*kryptos*”, hidden, and “*genein*”, to produce: a focal origin is suspected but the cause is unknown).

Focal epilepsies are further classified according to the affected hemisphere and lobe (left/right, frontal, temporal, parietal, occipital, insular) and this can be further detailed with sublobar classification associated with specific clinical and EEG features (i.e. medial and lateral temporal lobe epilepsy, orbito-frontal, fronto-polar). This is especially the case for epilepsies affecting the temporal and frontal lobes which represent the vast majority of focal epilepsies.

The following terminology is used in the description of focal epileptic activity, mainly **from** the perspective of surgical management (Rosenow and Luders 2001) :

- **Symptomatogenic zone**: The cortical area that produces the ictal symptoms of the individual patient when it is activated by the epileptic discharge. It is defined by history and video-EEG semiology.

- **Irritative zone:** the cortical area that generates interictal epileptiform activity. It is estimated by scalp EEG, magnetoencephalography, or intracranial EEG.
- **Ictal onset zone:** the zone capable to generate spontaneous seizures. It is a subset of the irritative zone. It can be estimated with the same tools as the irritative zone except that MEG rarely captures seizures due to recording sessions generally limited to less than one hour.
- **Epileptogenic zone:** area of brain tissue that is necessary to generate the seizures and which needs to be surgically removed to obtain seizure freedom. It is estimated by a combination of all the above zones estimated during presurgical evaluation.
- **Epileptogenic lesion:** structural brain abnormalities with the potential of generating interictal and ictal epileptic activity. It is identified by neuroimaging or by post-operative histological examination.
- **Eloquent cortex:** cortical region that is identified as crucial for neurological or cognitive functions (i.e. motor, sensory, visual, language cortex).

1.2.1.3 Changes in the new 2010 classification scheme

For clarification, the old and new classifications of the seizures and of the epileptic syndromes and epilepsies are detailed in Table 2.1.

The changes in the classification of epileptic seizures mainly concern terminology and classification of generalised seizures (Berg, Berkovic et al. 2010). Generalised epileptic seizures are defined as “originating at some point within, and rapidly engaging, bilaterally distributed networks”. Focal seizures are defined as “originating within networks limited to one hemisphere. They may be discretely localized or more widely distributed”. For focal seizures, the new terminology has abandoned the terms “simple partial” “complex partial” and “secondary generalised” because these were frequently misused and misunderstood. The description of impairment of

consciousness and other ictal manifestations should be done according to the clinical symptoms and signs occurring during the seizure. For that purpose, the use of the glossary of ictal semiology (Blume, Luders et al. 2001) is encouraged.

2010 classification of focal seizures		Previous description
Without impairment of consciousness	With observable motor or autonomic components	Simple partial seizure
	Involving subjective sensory or psychic phenomena only	Aura
With impairment of consciousness	“Dyscognitive”	Complex partial seizure
Evolving to bilateral convulsive seizure	Involving tonic, clonic or tonic and clonic components	Secondary generalised

Table 2.1: Revised classification of focal seizures

Adapted from (Berg, Berkovic et al. 2010)

The main change between the 1989 and the 2010 classification of the epilepsies is that epilepsies are no longer classified as “idiopathic” (with no cause), “symptomatic” (related to a structural or metabolic cause) and “cryptogenic” (with a presumed but unidentified cause). These terms are replaced by “genetic”, when a genetic cause has been identified, “structural-metabolic”, when imaging or laboratory tests reveal a cause and “unknown” in the other situations.

In this thesis, most studies refer to focal seizures in patients with “structural” (when a lesion has been identified by MRI) or “unknown” cause (when the lesion has not been identified). One study recruited patients with Juvenile Myoclonic Epilepsy (JME), previously coined “idiopathic” epilepsy and now classified as genetic. These patients have generalised tonic-clonic seizures or generalised myoclonic jerks, which designation is unaffected by the nomenclature change. This work does not include the study of patients with other specific epileptic syndromes.

1.3 Pharmaco-resistance and epilepsy surgery

1.3.1 Pharmaco-resistance

Around 30% of patients suffering from epilepsy will endure recurring seizures despite multiple anti-epileptic drug (AED) treatments. The introduction of the first anti-epileptic drug will lead to seizure freedom in 47% with the first drug, 30% with the second drug, 10% with the third and 5% with the fourth (Kwan and Brodie 2000). Pharmacoresistance is defined as the persistence of seizures despite a well conducted anti-epileptic drug treatment with at least two drugs during at least 2 years.

In some carefully selected patients, epilepsy surgery, consisting in removing the cortical zone necessary for the initiation of epileptic seizures (the epileptogenic zone), can lead to seizure freedom or significant improvement of the seizure control. The determination of which brain structures should be targeted by surgery is tailored to the individual patients. Epilepsy surgery can consist in resection of a radiologically visible lesion (lesionectomy), removal of epileptogenic cortex (cortectomy), partial or total resection of a lobe (lobectomy), multiple lobectomies. Disconnective surgery, interrupting major white matter tracts such as the corpus callosum (callosotomy) as well as disconnection of a whole hemisphere (functional hemispherectomy) can also be performed in specific cases.

It is estimated that around 3% of patients who develop epilepsy should be evaluated for the possibility of epilepsy surgery with half of them estimated to proceed to surgery (Lhatoo, Solomon et al. 2003). Studies suggest that, every year, 1000 individuals for every 50 million people in the developed world would require such evaluation.

1.3.2 Non-invasive presurgical evaluation

1.3.2.1 Long term scalp video-EEG

Long-term scalp video-EEG recordings (telemetry) with ictal recordings of clinical and electrical manifestations of seizures are the core of presurgical evaluation. Consistent electro-clinical patterns across several seizures are needed to ensure that the epilepsy is unifocal. The localising value of EEG changes is greater when the onset of ictal EEG changes precede the clinical manifestations because the latter reflects the involvement of the symptomatogenic zone that could occur by propagation from a “silent” brain region (seizure onset zone). However, scalp video-EEG per se is not sufficient to delineate which brain structures need to be surgically removed and additional structural/functional imaging is needed to find concordant areas of tissue damage or dysfunction.

1.3.2.2 Structural imaging

MRI is currently the gold standard for structural imaging and it has radically transformed the field of epilepsy surgery thanks to its sensitivity in revealing brain lesions in patients with pharmaco-resistant epilepsy. The most common causes include hippocampal sclerosis, malformation of cerebral development such as focal cortical dysplasia or heterotopia, low grade tumors, cavernoma, traumatic or ischemic lesions, parasitic lesions such as cysticercosis (Duncan 2010). The use of modern MRI scanners (3 Tesla) and sequences and interpretation by expert neuroradiologists

can turn previously non-lesional MRI studies into positive detection of a lesion. The neuroimaging commission of the ILAE has established technical recommendations for clinical MRI in epilepsy to optimize the yield of the procedure in detecting other focal epileptogenic abnormalities (ILAE 2005). Patients with previously unremarkable scans should therefore be rescanned with the required protocol when significant improvement of the technique become available and their scans reviewed by neuroradiologists experienced in epilepsy imaging. CT scans (Computed Tomography) are not useful in epilepsy imaging outside of an emergency situation except to detect calcified lesions notably in neurocysticercosis and this technique should be replaced by MRI if available.

Quantitative volume measurements (volumetry) of the hippocampus can be helpful in indicating unilateral or bilateral hippocampal damage. This can be done either visually by trained personnel or with automated segmentation techniques (Chupin, Hammers et al. 2007). Advanced imaging strategies to identify subtle structural abnormalities include voxel-based, and other computational models of grey/white matter segmentation and description, mostly aiming at detecting subtle focal cortical dysplasia (Bernasconi, Bernasconi et al. 2011). These can help localise previously undetected lesions and therefore dramatically influence surgical management. Diffusion imaging is another technique to detect subtle structural changes and related studies are reviewed in Chapter 3. All these techniques with improved sensitivity are affected by higher rate of false positive findings and their results need to be corroborated by other imaging findings.

1.3.2.3 Isotopic imaging

Isotopic imaging techniques such as PET (Positron Emission Imaging) and SPECT (Single Photon Emission Computerised Tomography) are based on the intravenous injection of radio-labelled tracers and can be used as functional imaging tools to help localise the epileptic focus.

¹⁸F-Fluoro-Deoxy-Glucose (FDG-)PET can show a focal interictal hypometabolism (lower glucose consumption) at the site of focal epileptic activity. This hypometabolism usually extends beyond visible MRI lesions and some overlap with the resection area is associated with a good outcome. This technique can be particularly relevant in patients with no detectable MRI lesion. A focal hypometabolism can point to an undetected focal cortical dysplasia which can sometimes be retrospectively recognised on the MRI. In MRI negative temporal lobe epilepsy, the presence of a unilateral anterior temporal hypometabolism is highly predictive of a good post-operative outcome (Carne, O'Brien et al. 2004). The use of specific PET ligands, such as the benzodiazepine antagonist ¹¹C-flumazenil (Ryvlin, Bouvard et al. 1998) or ¹¹C-alpha-methyl-tryptophane (AMP) (Wakamoto, Chugani et al. 2008) is currently hampered by their very restricted availability and is limited to a few centres where they are mainly used for research purposes.

SPECT allows a qualitative measure of focal cerebral blood flow via the amount of tracer uptake in the brain. A hypoperfusion of the epileptic focus is expected in the interictal period with a relative focal hyperperfusion when the tracer is injected during the seizure. The precision of the localisation is higher when the tracer is injected earlier in the seizure. The maximal hyperperfusion focus tends to indicate sites of seizure spread rather than onset so that ictal SPECT rather reveals regional epileptic activity and affected hemisphere (Van Paesschen, Dupont et al. 2007). Digital subtraction between the ictal and interictal images coregistered to the structural MRI (SISCOM: Substraction Ictal SPECT COregistred to MRI) allows a better identification of the epileptic focus than side-by-side visual analysis of interictal and ictal images (Van Paesschen 2004).

PET and SPECT are mostly useful for lending support to hypotheses about localisation of the epileptic focus in lesional cases with ambiguous electroclinical

findings and in non-lesional cases. In most cases, the information from PET and SPECT is used to refine the placement of intracranial electrodes (see below).

1.3.2.4 Neuropsychological and psychiatric assessment

Neuropsychological evaluation should always be performed to assess the functional ability of the patient and to detect specific domains of cognitive impairment related to epilepsy. These deficits can suggest a lateralised or bilateral dysfunction (for instance impairment of language or verbal memory suggests involvement of the hemisphere that is dominant for language). The assessment can also point towards the involvement of frontal vs temporal structures and add concordance or discordance to the electro-clinical and imaging findings (Baxendale and Thompson 2010). More specifically, the assessment of memory function is important when estimating the risk of post-operative memory decline in temporal lobe resections. Classical risk factors pointing towards a greater risk of post-operative symptomatic decline include an intact preoperative verbal memory, surgery in the language-dominant hemisphere, older age at seizure onset or at surgery and the absence of hippocampal sclerosis on MRI (Chelune 1995; Hermann, Seidenberg et al. 1995; Alpherts, Vermeulen et al. 2006; Baxendale, Thompson et al. 2006). In addition, all candidates to epilepsy surgery should also benefit from psychiatric assessment to reveal past or current psychiatric conditions, especially affective disorders, obsessive-compulsive disorders and psychoses, that make them at risk for post-operative worsening of their psychiatric symptoms and require careful consideration of the risk/benefit of epilepsy surgery and close post-operative follow-up (Foong and Flugel 2007).

1.3.2.5 Additional functional imaging tools

Magnetic Resonance Spectroscopy indicates metabolic changes that suggest neuronal damage co-localised with the epileptic focus. Such changes can also occur at distance from the focus and can be reversible following resective surgery so that

their use in predicting surgical outcome is still uncertain (Simister, McLean et al. 2009). Localisation of the epileptic focus and its associated network using Electric Source Imaging (ESI), Magnetic Source Imaging (MSI) and simultaneous EEG-fMRI is addressed specifically in Chapter 3.

Aside from localisation of the epileptic focus, there are tremendous developments in the mapping of the eloquent cortex, that are progressively translating from the research labs into the clinical decision making (see (Koepp and Woermann 2005; Duncan 2009; Duncan 2010) for reviews and references for further reading). However, the current state of non-invasive mapping techniques is such that direct cortical mapping with intracranial electrodes is required if eloquent regions appear to be close to the planned resection site.

Functional MRI is increasingly used to localise the motor cortex as well as the expressive and receptive language areas. fMRI mapping of language areas has similar lateralisation precision as invasive tests such as the Wada test (injection of the anaesthetic agent amobarbital into one carotid artery to test the language performance of the rest of the brain (Binder 2010)). The function of the bilateral hippocampal formations in the memory network can be measured with fMRI using memory paradigms and there is increasing evidence that the results are predictive of surgical outcome in patients with TLE (Bonelli, Powell et al. 2010).

1.3.3 Intracranial EEG Recordings

In some patients, the non-invasive tests do not allow an unequivocal decision to be made on whether surgery is possible and which structures should be removed, and invasive EEG recording with subdural or depth stereotactic electrodes is needed (Seeck and Spinelli 2004).

The oldest and still widely used approach uses depth electrodes implanted into the brain via a stereotactic procedure (StereoEEG, SEEG) (Munari, Hoffmann et al. 1994). This approach is based on brain atlases to localise the coordinates of a targeted brain structure. Subdural electrodes involve a variable combination of grids (NxM contacts) and strips (usually 1-2xN contacts). SEEG allows a very good recording of deep brain structures, notably the medial temporal lobe. It allows sampling of discrete structures on both hemispheres. However, the technique is less suited for mapping the eloquent cortex.

Subdural electrode techniques are widely used in neo-cortical focal epilepsies as they allow covering of large patches of cortex to pinpoint the irritative zone and seizure onset zone. They also allow electro-corticography via brief electrical stimulations to map the areas of eloquent brain functions that need to be spared by resection. The inferior and medial temporal lobes can be recorded with infra-temporal strip electrodes or a combination of depth electrodes and subdural electrodes.

Surgically, insertion of electrodes needs to be preceded by precise targeting and is therefore more time-consuming than subdural electrode implantation. Large grids used for mapping the lateral neo-cortex require a craniotomy for their insertion, while strips can be inserted via small “burr-holes”.

Despite these relative pros and cons of both techniques, the choice for using depth vs subdural electrodes remains largely centre-specific, relying on the experience of local epileptologists and neurosurgeons. Intracranial recordings used in this thesis were performed mostly at the NHNN where a combination of subdural and depth electrodes is generally used: subdural for the lateral and medial neocortex, depth for medial temporal structures and lesions extending into the white matter (focal cortical dysplasia, tubers). A few patients were investigated in La Timone hospital in Marseille, France using exclusively depth electrodes as developed in this precise

centre by Talairach and Bancaud in the 1960's. One patient was investigated in North Bristol Hospital, UK with depth electrodes.

With both SEEG and subdural electrodes, each electrode contact samples the average local field potential within a volume of brain tissue of around 1 cm³ (Lachaux, Rudrauf et al. 2003). The number of electrodes and contacts is limited both by surgical considerations and number of available channels of EEG recording systems (typically 64-128 channels). This illustrates the fact that intracranial EEG only samples a limited portion of brain tissue. Therefore, prior hypothesis about possible localisations of the epileptic focus are required to select the regions to be covered by intracranial EEG and yield meaningful results for surgical decision making.

Following electrode implantation, imaging with CT or MRI and state-of-the art coregistration of the electrode position on the structural MRI and fusion with the other imaging techniques greatly enhances the interpretation of intracranial EEG findings regarding the epileptic network and the involved eloquent cortex.

1.3.4 Post-operative outcome

1.3.4.1 Seizure control

In temporal lobe epilepsy, the most frequent pharmaco-resistant epileptic syndrome in adults, the resection of a unilateral hippocampal sclerosis can lead to seizure freedom in up to 85% of patients at one year follow-up (Spencer and Huh 2008). However, long-term studies show that seizures can recur even after a long seizure free interval and the seizure-freedom decreases over time to reach around 40% at 10 years post-operatively (McIntosh, Kalnins et al. 2004). A randomised study showed that seizure freedom was more likely and mortality was reduced after 2 years in patients undergoing epilepsy surgery compared to those continuing medical therapy only with anti-epileptic drugs (Wiebe, Blume et al. 2001). In patients with focal

malformations of cortical development, the second most frequent cause of refractory epilepsy in adults, up to 60% of patients can be seizure-free after surgery (Fauser, Schulze-Bonhage et al. 2004), with the complete resection of the abnormal cortex being an important prognostic factor (Kim, Lee et al. 2009). The absence of a detectable lesion (MRI-negative patients) is not incompatible with surgical strategies and a seizure-free outcome but requires additional imaging tests and intracranial EEG recordings in most cases (McGonigal, Bartolomei et al. 2007). Odds for a seizure-free outcome tend to be lower than in lesional cases but can be as high as 50-60% (Wetjen, Marsh et al. 2008; Bell, Rao et al. 2009). These findings illustrate the importance of brain imaging for detecting focal brain abnormalities in the management of patients suffering from epilepsy. The chances of seizure freedom are greater for shorter disease duration and younger age at surgery (Yoon, Kwon et al. 2003).

1.3.4.2 Risk of post-operative deficits

The general risk of complication for epilepsy surgery compares to other neurosurgical therapies with around 2% of severe morbidity or mortality related to haemorrhage or infection (Lüders 2008). The risk and type of permanent neurological deficit is of course dependant of the resection site: memory decline (hippocampus) and visual field defect (optic radiation) in temporal lobe surgery, motor deficits in pericentral frontal regions, sensory deficits in parietal resections. A variable combination of non-invasive and invasive tools is used during the presurgical assessment in each epilepsy surgery centre to help localise the epileptogenic zone in relation to the eloquent cortex. The risk of post-operative deficit can be estimated preoperatively based on electro-clinical findings, neuropsychological assessment and functional MRI. Invasive tests include the amobarbital test, whose reliability is debated (Baxendale 2009) and electrocorticography during intracranial EEG (Niedermeyer and Lopes da Silva 2005). The neurosurgical procedures are increasingly monitored

online with electrophysiological monitoring (intraoperative corticography, motor and sensory evoked potentials) allowing online tailoring of the resection if neurophysiological signals are altered.

1.4 Conclusion and clinical issues addressed by this work

This clinical review chapter stressed the fact that a large proportion of patients suffering from epilepsy are refractory to anti-epileptic drugs. Epilepsy surgery can be a life changing intervention, provided the epileptic generators and the eloquent cortex have been properly localised. Most epilepsy surgery centres use a variable combination of advanced imaging techniques (FDG-PET, SPECT, EEG source imaging, Magnetoencephalography, EEG-fMRI, voxel-based morphometry, spectroscopy) to localise the epileptic activity and the eloquent cortex and to help planning resective surgery or the placement of intracranial electrodes. All these techniques are used with centre-specific methodology. Therefore, much work remains to be done for improving and validating the diagnostic and prognostic value of these promising new mapping techniques, with the expectation that combination of different techniques (“multimodal” imaging) will be precious for the confirmation of clinically relevant findings and the understanding of the underlying pathology.

In this work, I have used various combinations of functional and structural imaging tools (EEG-fMRI and EEG source imaging, intracranial EEG and fMRI, fMRI and tractography, intracranial EEG and tractography) to improve the description of functional and structural epileptic networks and have tried to assess the clinical relevance with the best available evidence.

These new imaging techniques have also shed a new light on the mechanisms underlying several epileptic syndromes, to the point that they have participated to a reappraisal of the international classification. Moreover, they increasingly help to understand the alteration in physiological neuronal networks in patients with epilepsy.

In this context, this work also investigates the alteration of motor networks in focal and generalised (“idiopathic”) forms of epilepsy and contributes to cast further doubt on the “idiopathic” label attached to Juvenile Myoclonic Epilepsy.

2 FUNCTIONAL IMAGING OF EPILEPSY: EEG (MEG) SOURCE IMAGING AND EEG-fMRI

2.1 Introduction

Functional neuro-imaging of epileptic networks involved in the initiation and propagation of epileptic activity could help better understanding the physiopathological mechanisms underlying the disease, to monitor treatment efficacy and to better define target for epilepsy surgery. In the following, much emphasis is placed on the current status and the future perspectives of functional neuro-imaging derived from Electroencephalography (EEG) which are the core methodologies used in this work: EEG source imaging (ESI) and EEG-correlated functional Magnetic Resonance Imaging. Magnetoencephalography (MEG) and MEG Source Imaging (MSI) can also be used in the functional mapping of brain networks and these techniques share similarities with EEG and ESI techniques. Methodological aspects and clinical applications of MEG for localising focal epileptic activity will be briefly described.

After the first report of EEG recording of the human brain performed by Hans Berger in 1929, application to the study of the brain of epileptic patients quickly followed, notably through the inventiveness of William Grey Walter who applied a larger number of smaller electrodes to localise physiologic and pathologic patterns of electric activity (Niedermeyer and Lopes da Silva 2005). Clinically, analysis of conventional EEG monopolar or bipolar EEG traces is still the mainstay of EEG interpretation to localise abnormal electrical activity, notably epileptiform discharges. The development of digital EEG recording in the 1980s allowed the study of scalp voltage maps to better understand the location and orientation of the underlying electric sources that generate them. More recently, complex computer models have allowed the development of EEG Source Imaging (ESI) to estimate the distribution of

three-dimensional intra-cerebral electrical activity giving rise to the recorded scalp activity (He, Zhang et al. 2002; Michel, Murray et al. 2004). ESI has transformed conventional EEG analysis into a modern three-dimensional imaging tool for the localisation of epileptic sources (Michel, Murray et al. 2004; Plummer, Harvey et al. 2008) and evoked potentials (Michel, Thut et al. 2001) with a time resolution of milliseconds, that allows the investigation of dynamic changes in neuronal networks.

EEG-correlated functional Magnetic Resonance Imaging (EEG-fMRI) has emerged as another non-invasive brain imaging technique based on EEG recording (Hamandi, Salek-Haddadi et al. 2004; Gotman, Kobayashi et al. 2006; Laufs and Duncan 2007). The EEG is recorded inside an MRI scanner in order to map the brain regions where haemodynamic changes are coupled to specific EEG features. This imaging tool was first developed to map focal brain haemodynamic changes time-locked to interictal epileptic spikes, in an attempt to provide a new method for localising epileptic activity that would be useful for pre-surgical evaluation of pharmaco-resistant patients. After an initial “proof-of-concept” report showing that EEG could be recorded during the hostile magnetic environment of fMRI recordings (Ives, Warach et al. 1993), patient safety and data quality was investigated in detail (Lemieux, Allen et al. 1997) and clinical series exploring the localisation of focal epileptic activity followed (Seeck, Lazeyras et al. 1998; Krakow, Woermann et al. 1999; Lazeyras, Blanke et al. 2000). Since then, the evolving data acquisition technology, notably correction of EEG artefacts allowing continuous fMRI recordings, progress in analytical strategies and results from a growing body of methodological and clinical studies have transformed EEG-fMRI into a powerful tool to investigate the haemodynamic changes associated with spontaneous brain activity. The technique has been used to explore epileptic networks, including sub-cortical involvement in the basal ganglia and thalamus, but also to study endogenous brain rhythms of wakefulness and sleep, and evoked brain activity. These studies have brought new insights into the coupling between neuronal

activity, cerebral metabolism and focal brain perfusion changes in the epileptic and non-epileptic brain (for reviews, see (Gotman, Kobayashi et al. 2006; Ritter and Villringer 2006; Laufs, Daunizeau et al. 2008).

A major expectation of any new non-invasive imaging tool in epileptology, is its potential to improve the management of patients who are candidates for surgical treatment of their epilepsy. Formal validation of techniques for localising epileptic sources requires comparison with a gold standard localising measurement, ideally in large homogeneous patient groups, which is very difficult to obtain in clinical practice. Imaging studies of brains with structural lesions do not offer absolute validation since the lesion can be relatively large and the irritative zone can extend beyond the lesion. Validation with data from intracranial recording electrodes is intrinsically constrained to small groups of patients with heterogeneous epileptic syndromes and limited intracranial spatial sampling. Validation can also be based on post-operative seizure-freedom in small groups of patients with the imaged epileptogenic focus included (or not) in the area resected. This has the disadvantage that the areas resected are often much larger than the epileptic zone making it difficult to assess the test's specificity and long-term follow-up is required. Although widely performed, validation based on post-operative imaging is confronted with the problem of coregistration of the post-operative structural brain image and pre-operative imaging (structural and functional) to precisely align brain images. For imaging studies requiring spatial precision at millimetre scale (such as pre-/post-comparison of brain measures (Yogarajah, Focke et al. 2010)) careful non-linear coregistration is mandatory to account for local brain deformation (retraction, "sagging" into the resection zone).

This chapter starts with a brief overview of the neurophysiological background underlying the EEG and fMRI signals. It will then describe the principles, limitations and main clinical studies of ESI and EEG-fMRI. Finally, the potential of combining ESI and EEG-fMRI will be presented as this combination might result in a better imaging

tool giving insight into the spatial and temporal organisation of epileptic networks and their interaction with background cerebral activity. The primary focus is on applications of ESI and EEG-fMRI in patients with epilepsy, but some modelling and methodological developments in cognitive neurosciences using fusion of EEG Source Imaging or MEG Source Imaging with fMRI will be referred to, especially those that may be relevant to the investigation of epileptic networks and their interactions with background or evoked brain activity.

2.2 Neurophysiological background

2.2.1 Origin of the EEG signal

Scalp EEG electrodes record fluctuations in electrical potential maps that are generated by cortical pyramidal neurons oriented perpendicularly to the cortical surface, (Niedermeyer and Lopes da Silva 2005). The Scalp EEG corresponds to the summed post-synaptic potentials in response to synaptic activity: Excitatory and Inhibitory Post-Synaptic Potentials. In the case of excitatory activity, this post-synaptic activity in the dendritic tree creates a relatively negatively charged extracellular space while the extracellular distal part of the cell is relatively positively charged, resulting in a current flow so that the neuron can be approximated as a microscopic electric dipole perpendicular to the cortical surface. Hence, the EEG signal is mostly generated in gyral crowns parallel to the surface, whereas the sulcal activity is usually of unfavourable orientation and both walls of a sulcus tend to have electrical fields that cancel each other. The synchronised occurrence of this phenomenon over a large population of neurons with parallel orientation and widespread dendritic trees results in a voltage field measurable with scalp electrodes. Post-synaptic potentials are modulated mostly in a frequency range below 50Hz while higher frequencies are filtered both by the capacitive cell membranes and by volume conduction, especially

across the skull which has low electrical conductivity and attenuates dural potentials (Nunez and Silberstein 2000). However, for the frequency band of interest in this work (i.e. 1-30Hz), the attenuation of the signal is probably not frequency-dependent. The solid angle theory applied to EEG generators explains why short lasting axonal action potentials of about 1 ms duration do not result in a combined macroscopic electric signal, despite frequent firing and high amplitude (Gloor 1985). It also explains the relationship between frequency and amplitude whereby delta waves can summate over a long time window and lead to a high amplitude potential. Simultaneous intracranial and scalp recordings have shown that synchronous cortical activity over at least 6-10 cm² of gyral surface was necessary for pathological events to be clearly detectable with scalp electrodes (Tao, Baldwin et al. 2007). The infolding and multi-laminar structure of the cortex can make the relationship between generators and electrodes complex (Megevand, Quairiaux et al. 2008). In some other instances, neuronal activity can give rise to a “closed” electric field (e.g. stellate cells) which is invisible to scalp electrodes. Whole-head sampling and voltage maps typically provide more information about the localisation and orientation of intracerebral sources than do a restricted number of electrodes (Michel, Murray et al. 2004; Ritter and Villringer 2006).

2.2.2 Origin of the fMRI signal

The fMRI signal relies on the intrinsically delayed coupling between the neuronal activity in the brain, oxygen consumption and focal perfusion changes. In summary, the BOLD changes measured by fMRI are considered to reflect focal haemodynamic changes that are themselves related to changes in neuronal activity as detailed below.

In fMRI studies, differences in magnetic susceptibility between oxy- and deoxyhaemoglobin can be detected using appropriately chosen MRI acquisition

sequence parameters, giving rise to the Blood Level Oxygen Dependant (BOLD) contrast mechanism.

A basic assumption underlying the interpretation of fMRI studies is that an increase of regional “neuronal activity” results in an increase in metabolic demand (of neurons and astrocytes), with increased energy and oxygen consumption. The local decrease in oxygen-saturated haemoglobin and increase of desaturated haemoglobin carbon-dioxide and nitric-oxide is followed by regional dilatation of arterioles, allowing a perfusional overshoot and global decrease in desaturated haemoglobin. These haemodynamic changes occur over several seconds after the triggering changes in neuronal activity and can be described by a “balloon” model (Buxton, Wong et al. 1998). Thus, even though the total oxygen consumption increases, the fraction of oxygen extraction decreases and the percentage of deoxygenated haemoglobin in local venous blood decreases. In this model, BOLD signal increases correspond to increases in neuronal activity compared to a chosen baseline of cerebral activity.

The term “neuronal activity” used here must be understood as the global synaptic product of a local neuronal population (associated to the action of metabolically demanding ionic pumps for maintaining/restoring homeostasis), in response to inhibitory and excitatory inputs and interneural feed-forward and feedback activity. In other words “neuronal activity” must not be interpreted as an equivalent to the resulting output of the network in terms of spiking frequency but as the result of total inhibition and excitation in the network, as well as the balance between them (neuromodulation) (See (Logothetis 2008) for a detailed review on the neurophysiological basis of the fMRI signal and (Buzsaki, Kaila et al. 2007) for a review on inhibitory activity). A notable consequence is that networks with “silent output” do not necessarily coincide with zero metabolic changes and constant BOLD signal. Moreover, the EEG signal reflects synchronous activity of a regional neuronal population rather than the number of cells firing. Therefore, reduced regional

inhibitory (but metabolically demanding) activity allowing strong synchronised activity of a subpopulation would generate a stronger EEG signal with a reduced metabolic demand that could translate into negative BOLD changes related to epileptic activity (Nunez and Silberstein 2000).

Experimental work in monkeys showed that BOLD increases correlated better with increases in local field potential (representing perisynaptic activity around an extracellular intracranial electrode over a range of a few millimetres) than with multi-unit activity and constitutes, therefore, a model of synaptic activity. In contrast, the firing of action potentials by neurons is probably too short to trigger a measurable metabolic-vascular response (Logothetis, Pauls et al. 2001). However, the local field potential is only an imperfect measure of synaptic activity as its fluctuations are not specific to selective changes in network activity. Moreover, it is also influenced by post-synaptic activity and has a natural bias to preferentially reflect synaptic activity of pyramidal cells because of their spatial alignment (Logothetis 2008).

Animal and human studies have shown that the neuronal activity and the haemodynamic changes giving rise to BOLD signal changes occur over very different time scales. In accordance with the “balloon” model (Buxton, Wong et al. 1998), the Haemodynamic Response Function (HRF) triggered by a neuronal event lasting a few milliseconds and measured with fMRI is slower and long lasting: after an initial decrease, it slowly rises to peak between 5-6 seconds after the event onset, and decreases with an undershoot before going back to baseline in about 20 seconds (Glover 1999). This HRF shows inter-individual but also intra-individual variations depending on the brain regions studied. The initial dip seems to represent a more focal contribution of the capillary bed, reflecting a brief insufficiency of the vascular supply before a relative focal hyper-perfusion that is a response to increased metabolism (Yacoub and Hu 1999). On a cellular level, the initial “dip” is thought to be the result of the oxidative response of neurons while the later response results from a

combination of neuronal and astrocytic metabolism (Aubert, Pellerin et al. 2007). This slow-reacting vascular supply is regional (millimetre scale) (Tolias, Sultan et al. 2005) and not limited to individual or small groups of neurons in specific networks in a volume containing millions of neurons (Logothetis 2008). Functional MRI studies typically use voxel sizes of around 50 mm^3 and are well suited to the anatomical scale of the haemodynamic changes.

With the above mentioned considerations about the origin of the BOLD signal, the interpretation of sustained negative BOLD responses observed in cognitive as well as in epilepsy studies is difficult and probably context dependent. The concomitant measurement of cerebral blood flow is important to decide if there is a simultaneous decrease in metabolism or if the negative BOLD response is the result of an impaired coupling between arterial oxygenation and metabolism (Stefanovic, Warnking et al. 2005; Carmichael, Hamandi et al. 2008; Hamandi, Laufs et al. 2008). Negative BOLD changes have been related to visual perceptual suppression in humans (Shmuel, Yacoub et al. 2002) with concomitant electrophysiological studies in monkeys showing a decrease in local field potential in monkeys (Shmuel, Augath et al. 2006; Maier, Wilke et al. 2008). A decrease in metabolism may be associated with a selective increase in neuronal activity, observable with scalp EEG, such as synchronised firing of a small neuronal population that was inhibited by other energy-demanding neurons, as in the case of the alpha rhythm (Laufs, Holt et al. 2006). The widespread cortical negative BOLD response observed in relation to generalised spike and wave discharge might also reflect increased cortical synchrony with reduced total cerebral blood flow (Aghakhani, Bagshaw et al. 2004; Hamandi, Salek-Haddadi et al. 2006). As a correlate of focal interictal epileptic discharges on scalp EEG, negative BOLD changes have been found both near to and distant from the presumed epileptic focus and it is not clear whether they reflect surround inhibition, altered neurovascular coupling, distant downstream/upstream metabolic decrease vs

propagated epileptic activity or, less probably, a vascular theft mechanism (Kobayashi, Bagshaw et al. 2006; Salek-Haddadi, Diehl et al. 2006).

2.3 EEG Source Imaging

2.3.1 Methodological principles and limitations

The EEG (and MEG) source imaging process has three main ingredients: the choice of a model of the source or sources, a way of calculating the fields generated by any possible configuration of the source model at the location of the electrodes or magnetometers (**the forward problem**), and a source parameter estimation procedure (data fitting, **the inverse problem**).

2.3.1.1 The “forward problem”: spherical and realistic head models

The relationship between a specific distribution of postulated electric sources in the brain and the resulting scalp voltage map is determined by modelling the so-called “forward model” (for details on EEG source imaging see the reviews of (Michel, Murray et al. 2004; Leijten and Huiskamp 2008; Plummer, Harvey et al. 2008). The most important step in that respect is the construction of a mathematical model of the head’s electromagnetic and geometrical properties to calculate the volume conduction across different biological tissue and calculate the lead field that will offer a unique solution of scalp potential for any distribution of cerebral sources. The simplest of such models are spherical head models, which can include one layer or multiple overlapping shells (brain, cerebro-spinal fluid, bone, skin) and have the advantage of linearity and ease of calculation. However, they are not well suited for the study of the activity of basal brain regions (orbito-frontal, inferior and medial temporal) commonly involved in epileptic activity. Further, these models generally do not account for inter-individual variations in brain anatomy, which is crucial for epilepsy imaging, in which brains with large lesions are frequently encountered. By

contrast, realistic and subject-specific head models, implemented as Boundary Element Models (BEM) or Finite Element Models (FEM) account more precisely for the details of head anatomy but are more computationally demanding. Finite Element Models can incorporate information derived from Diffusion Tensor MRI to account for effects of conduction anisotropy of the white matter to provide a detailed model of the head's conductivity (Tuch, Wedeen et al. 2001; Gullmar, Hauelsen et al. 2011). Finally, a hybrid head model based on individual brain anatomy constrained in a spherical head model offers the advantage of linear computation combined with individual brain and head features (Spinelli, Andino et al. 2000). Nevertheless, the lack of precise knowledge over the ratio of tissue conductivity between brain and bone tissue adds significant uncertainty to all head models (Plummer, Harvey et al. 2008). In their pioneering work based on in vitro measurements, Rush and Driscoll proposed a ratio between brain/skin to skull conductivity of 80:1 (Rush and Driscoll 1969). More recent work suggests that this value might be inaccurate with a ratio closer to 1:20. This would mean that the scalp EEG can actually be recorded with much higher spatial resolution and justifies the use of high density EEG systems. In newborn, the skull is 7-8 times thinner so that the ratio in pediatric population is lower than in adults and spatial resolution therefore higher. This uncertainty regarding the skull conductivity value is related to the difficulty to accurately measure it in physiological conditions. Fast changing electrical properties make post-mortem measurements not representative of in vivo values. Per-operative measurements using electrodes applied either part of the skull during neurosurgery can be relied upon only if bone temperature and humidity were maintained at their physiological level. New methods for estimating conductivity based on magnetic imaging in individual subjects are in development (Wendel, Vaisanen et al. 2009).

2.3.1.2 Solving the “inverse problem”: equivalent current dipoles and distributed sources

For a given distribution of the scalp electric field (scalp EEG), there is not a unique distribution of current density (sources) within the head. More generally, if electric sources are unrestricted within the volume enclosed by the sphere on which the electric field is measured, there exist indeed an infinite number of possible source configurations, giving rise to the ambiguity of the inverse electromagnetic problem as described in the XIXth century by von Helmholtz ((Helmholtz 1853) in (Michel, Murray et al. 2004)). In consequence, solving this inverse problem requires assumptions about the source distribution, allowing reduction of the extent of the solution space (number and spatial configuration of solution elements). Since the EEG generators are localised in the grey matter, we can restrict the distribution of sources to the grey matter rather than to the whole brain, narrowing the ambiguity of the inverse problem. Dipolar models seek to explain the scalp electric field with one or a few Equivalent Current Dipoles (ECD). Some approaches use spatio-temporal dipole modelling to take into account the onset and propagation of interictal discharges (Scherg, Bast et al. 1999). The localisation of this ECD should however not be assumed to be the localisation of the IED generator as it only represents the centre of mass of a theoretical point source giving rise to an equivalent scalp voltage map. Careful interpretation of its orientation is required to identify the corresponding patch of activated cortex. Other models based on dipolar sources do not fit an ECD to the EEG data but rather scan all possible dipole locations to find the source location providing the best fit of the data (e.g. MUSIC, Beamformer, see (Sekihara and Nagarajan 2004) for review). When combined with spherical head models, dipole locations of known medial temporal lobe sources are classically displaced up to 30 mm rostrally and localised to the frontal lobe which represents a major discordance (Cuffin 1996; Roth, Ko et al. 1997). The estimation of the correct number of sources is

the most critical step in these models, which are not optimal to describe activation of widespread neuronal networks, as in the case of propagation of IED. Model comparison using Bayesian statistics has recently been proposed to solve this particular problem (Kiebel, Daunizeau et al. 2008).

In contrast to ECD models, distributed source models reconstruct electric activity at each point of the solution space in the brain. They avoid the difficult choice of the number of active sources and are better suited than ECD to describe the involvement of extended patches of neocortex. With distributed inverse source models, current source density and local field potentials can be estimated throughout the brain, facilitating comparison with intracranial recordings (Michel, Grave de Peralta et al. 1999). However, these solutions are highly underdetermined (thousands of possible solution points for 30-250 electrodes) and a priori hypotheses derived from electrophysiological assumptions have to be applied to the inverse solution algorithm. Heuristic constraints have first been proposed, such as minimum norm or maximal smoothness of the solution (e.g., LORETA) (Michel, Murray et al. 2004). Moreover, "regularisation" strategies ("depth weighting") have to be applied to compensate for a mathematical bias that favours solutions localised on the brain convexity since they are nearer to scalp electrodes. More recent techniques rely on increasingly realistic spatial (Daunizeau, Mattout et al. 2006, Friston, Harrison et al. 2008) and temporal constraints (Kiebel, David et al. 2006, Fastenrah, Friston et al. 2008). Variational Bayesian methods can be used to statistically select the optimal class of regularising constraint (i.e. prior hypothesis) (Friston, Harrison et al. 2008). Dipolar and distributed linear solutions have been compared, most often using simulated EEG data (Grova, Daunizeau et al. 2006). The result of the comparison depends of course on the nature of the dataset and neuronal generators, with distributed inverse solution being more suitable for extended sources and to estimate the extent of such sources. Dipolar models seem to give more precise localisation but poor estimation of extent.

Concordant findings using different methods of inverse solution provide more reliability.

An increased number of electrodes (at least 64 channels), and spatial coverage including inferior temporal electrodes, increases the precision of ESI (Kobayashi, Yoshinaga et al. 2003; Lantz, Spinelli et al. 2003; Meckes-Ferber, Roten et al. 2004; Sperli, Spinelli et al. 2006). Application of ESI to the IED rising phase leads to a better estimation of the irritative zone of IED while ESI at the IED peak rather reflects propagation (Lantz, Spinelli et al. 2003). The advantages and drawbacks of different ESI strategies as well as the limitations of their clinical validations have recently been discussed in detail (Michel, Murray et al. 2004; Plummer, Harvey et al. 2008).

Some studies have applied non-parametric or parametric statistical mapping to determine source extent thresholds, similarly to the methods applied in functional MR, volumetric MR and quantitative nuclear medicine (PET, SPECT) imaging (Sperli, Spinelli et al. 2006; Zumsteg, Friedman et al. 2006). Validation was obtained by finding an overlap greater than 50% between the calculated source and resection areas in 27/30 seizure-free patients (Sperli, Spinelli et al. 2006) or by comparison with foramen electrode recordings (Zumsteg, Friedman et al. 2006). These statistical analyses provide a spatial threshold to the source extension, reduce the risk of spurious sources and increase sensitivity to weaker source activity (that might otherwise be hidden by dominant activity) (Michel, Lantz et al. 2004; Michel, Murray et al. 2004) thereby strengthening the position of ESI as a modern brain mapping technique.

2.3.2 Clinical ESI studies in focal epilepsy

2.3.2.1 Interictal ESI as a pre-surgical tool in epilepsy and validation with intracranial EEG and surgical series

Clinical studies that compare ESI results with invasive EEG recordings have been carried out with simultaneous scalp ESI and *foramen ovale* recording in patients with temporal lobe epilepsy. ESI was able to differentiate between medial and lateral temporal spikes (Dinesh Nayak, Valentin et al. 2004) as well as to identify patterns of propagation within the temporal lobe. Concordance between intracranial EEG and dipolar sources has been found in over 90% of technically feasible cases in two studies of temporal and frontal lobe epilepsy using ECD and dipole scanning algorithms (Gavaret, Badier et al. 2004; Gavaret, Badier et al. 2006). In another large study of patients with both temporal and extra-temporal epilepsies recorded with dense-array EEG (128 electrodes), a distributed linear ESI model showed concordant findings at a lobar level in 94% of 32 patients including 100% of patients with temporal lobe epilepsy (Michel, Lantz et al. 2004). In the perspective of epilepsy surgery, lobar concordance as a validation criterion cannot be considered sufficient, particularly in the frontal lobe. However, when the same study estimated the concordance between ESI and the resection area in post-operative seizure-free patients, there was good concordance in 79% of 24 adults. The drawback of these studies is that they were not blinded, none was prospective, e.g. in order to guide or refine intracranial electrode placement and the additional localisation information compared to other imaging modalities was not analysed. There is also an ongoing debate about the ability of EEG and ESI to visualise medial temporal IED or only their basal or lateral propagation (Lantz, Ryding et al. 1997; Pacia and Ebersole 1997; Merlet and Gotman 2001; Gavaret, Badier et al. 2004; Zumsteg, Friedman et al. 2006). Strong arguments supporting the ability of EEG recording to "see" the medial temporal structures have recently been provided by the localisation of evoked

responses to the human medial temporal lobe (James, Britz et al. 2008) with confirmation by intracranial EEG recordings from the hippocampus (Nahum, Gabriel et al. 2011). Finally a recent study confirmed that ESI can be accurate in patients with large brain lesions: multichannel EEG recordings and a realistic head model yielded ESI results that were localised within the resection area in all 12 post-operatively seizure-free patients (Brodbeck, Lascano et al. 2009).

Despite these robust validation studies, ESI is not used widely in epilepsy surgery centres. One reason might be that until now, no standard “good-practice” has been widely established as to which class of head models and inverse algorithms should be used, whatever the detailed application. This means that the choice remains mainly a matter of informed user choice and software availability.

To compare directly the performances of different source localisation models, two datasets with real scalp interictal discharges were analysed by different research groups, who applied either dipolar or distributed solutions while being blinded to the results of intracranial EEG localisation (temporal polar and medial parietal) (Ebersole 1999): multiple spatio-temporal dipolar analyses and dipole scanning showed correct localisation of these well localised generators although dipole scanning solution showed some contamination of the orbito-frontal region for the temporal source. The distributed solution performed well for the parietal source but could not reach sub-lobar precision for the temporal polar source, although additional inferior temporal electrodes could have helped if available.

In children, ESI performed on standard telemetry recordings (29 electrodes) showed 50% overlap with the resection zone and ESI for 90% of 30 children after application of a statistical threshold and the localisation of ESI in this group was better than with PET or SPECT (Sperli, Spinelli et al. 2006). Moreover, the use of dense-array EEG increased the concordance to 100% in the same group of children.

2.3.2.2 Ictal ESI studies

A key advantage of ESI over other techniques for ictal imaging is the wide availability of ictal EEG data. ESI has also been applied to ictal EEG, although there are methodological difficulties due mainly to the non-stationary EEG pattern, motion artefacts and the difficulty recording multiple identical events. Nevertheless some studies showed good localizing value when using approaches in the time-domain (Lantz, Michel et al. 2001; Holmes, Tucker et al. 2010) or localising the dominant frequency at ictal onset (Blanke, Lantz et al. 2000). A large study on patients with temporal lobe epilepsy using spatio-temporal dipoles for ESI showed a very good predictive value of the dipole orientation with respect to the location of the seizure onset zone (Assaf and Ebersole 1997). Boon et al. applied a similar technique that yielded results in 31/93 patients with ictal recordings and concluded that ESI was mostly useful to reject patients from intracranial recording or surgery (Boon, D'Have et al. 2002). Another study on temporal lobe epilepsy with simultaneous scalp and depth electrodes using ECD, found that results of ESI of the first ictal changes seen on scalp EEG were all in the lateral neocortex with the concomitant intracranial recording showing propagated activity in both temporal lobes with a maximum in the temporal medial contacts (Merlet and Gotman 2001). Finally an interesting very recent study classified seizures according to ictal EEG patterns and compared various source localisation techniques (Koessler, Benar et al. 2010). The authors suggested that ECD techniques were more concordant with intracranial depth electrodes findings than distributed source techniques but the very sparse spatial sampling of depth electrodes could constitute a bias towards more focal sources such as those provided by dipole solution. Further work is warranted as ictal events are unstable by nature compared to IED and hence more difficult to model.

2.4 MEG and Magnetic Source Imaging of epileptic networks

MEG is based on the detection of magnetic currents which are a component of the electro-magnetic signal emitted by neuronal activity. MEG is therefore a complementary technique to EEG with a lot of similarities in the methodology and some major differences. These are briefly described and compared below.

2.4.1 Data acquisition and processing

MEG availability is intrinsically limited by its cost related to the need for superconductive materials. MEG sensors are not in contact with the patient's scalp and there is therefore no need for contact gel. Modern EEG electrode caps and nets have reduced the time of preparation and the need for contact gel making preparation time similar for both techniques. EEG can be recorded over much longer periods than MEG, a definite advantage for recording seizures and IED during sleep. The heavy equipment of MEG prevents simultaneous recording with other imaging modalities except with EEG, whereas EEG can be recorded simultaneously to PET, SPECT or fMRI. The general principles of MEG source imaging are similar to those applied to EEG datasets (see section 2.3).

2.4.2 Detection of epileptic activity

Epileptic activity can be detected by EEG, MEG or both. As the magnetic field is oriented perpendicularly to the electric field, MEG detects sources oriented tangentially to the scalp (in the walls of a sulcus or in the interhemispheric fissure) but is insensitive to sources with radial orientation (top of gyrus or bottom of sulcus). MEG seems to have a higher sensitivity for superficial neocortical areas whereas EEG is better at detecting deeper sources (Goldenholz, Ahlfors et al. 2009).

Therefore, MEG principally detects activity in the sulcus that is not opposed by the opposite sulcal wall and most recorded IED are generated in gyral crowns that are perpendicular to the scalp or in major fissures (base of the brain, superior temporal plane, medial sagittal cortex) (Agirre-Arrizubieta, Huiskamp et al. 2009). Simultaneous recording of EEG would therefore add value to MEG recordings (Ebersole and Ebersole 2010). MEG source imaging has been rigorously validated (Barnes, Furlong et al. 2006; Brookes, Zumer et al. 2011) and showed lobar colocalisation with the resection area in 54-80% of patients with epilepsy who are post-operatively seizure free (Stefan, Hummel et al. 2003).

2.4.3 Effect of conductivity

Unlike electric fields which are strongly influenced by differences in conductivity between the brain, skull and soft tissues, the magnetic fields are unaffected. This gives an advantage to MEG over EEG as MEG recordings and algorithms of magnetic source imaging (MSI) can use simple models of volume conductors and do not need to account for conductivity changes. While head models with individual anatomy can give reliable localisation with ESI, even in patients with large lesions (Brodbeck, Lascano et al. 2009), conductivity issues are a limiting factor in patients who are evaluated after previous neurosurgery: the bone defects severely distort EEG voltage maps and ESI results but have no influence on MSI. Bone model defects and their effect on local skull conductivity can be modelled by realistic head models (Benar and Gotman 2002) but are computationally demanding and not widely used.

2.4.4 Clinical MSI studies in focal epilepsy

Comparative studies evaluating the precision of source localisation with EEG and MEG are confounded by the fact that study centres are more expert in one technique than the other and most of these studies use much fewer EEG electrodes than MEG sensors. MSI can give valuable localising information, thereby increasing the number of patients who are selected for intracranial recording and refining intracranial electrode placement (Knowlton, Elgavish et al. 2008; Sutherling, Mamelak et al. 2008; Stefan, Rampp et al. 2010). Validation studies comparing MSI results to FDG-PET, SPECT and intracranial EEG recordings have also suggested that MSI can have predictive value on post-operative outcome (Knowlton, Elgavish et al. 2008). Apart from localisation of visually identified IED, analysis of high (Guggisberg, Kirsch et al. 2008) or low frequency in the MEG signal (Kaltenhauser, Scheler et al. 2007) could also help localising focal epileptic activity.

2.5 Resting state EEG-fMRI for mapping epileptic networks

2.5.1 Methodological principles and limitations

Technical details regarding EEG-fMRI data acquisition and safety issues have been reviewed recently (Hamandi, Salek-Haddadi et al. 2004; Gotman, Kobayashi et al. 2006; Laufs, Daunizeau et al. 2008).

2.5.1.1 Interactions between EEG system and MR system: subject's safety and data quality

Special care has to be given to the EEG set-up to allow safe and good-quality recording of simultaneous EEG and MR signal and minimising undesired or potentially dangerous interaction between the two systems that could harm the patient or affect data quality (Lemieux, Allen et al. 1997).

In the scanner environment, electrodes and conductive leads are prone to induced current caused by head movement, scanner vibration or variations in the magnetic field such as radiofrequency pulses. The occurrence of such currents in resistive materials causes heating of electrodes and could lead to scalp burns. These currents can be reduced to a safe level by a dedicated design of the EEG set-up (non-ferrous electrodes, short leads, avoiding loops, additional resistors). It is also important to minimise displacement of EEG components by stabilising head position with a vacuum cushion and EEG set-up with sand/salt bags to reduce electrode heating as well as perturbation of the EEG signal.

The EEG recording in the MR environment is contaminated by two major sources of artefacts caused by induced electrical currents via variation of the magnetic field or motion of the electrodes: the MR gradient-artefact and the pulse-artefact (Hamandi, Salek-Haddadi et al. 2004; Gotman, Kobayashi et al. 2006). The periodic switch of the scanner's gradients during MRI acquisition (time-varying magnetic magnetic gradients) causes induced currents altering the EEG, the interpretation of which is impossible without correction. Pulse-artefacts are time-locked to cardiac activity that can mimic epileptiform activity. Recent simulation studies suggested that they are mostly caused by small-amplitude head pitch caused by the arterial pulse rather than by magnetic field changes caused by the flow of arterial blood towards the head (Yan, Mullinger et al. 2010).

On the other hand, metal electrode wires, resistors and conductive gel produce inhomogeneities of the magnetic field, leading to susceptibility artefact, image distortion and signal drop-out (Krakow, Allen et al. 2000). Even objects with only weak magnetic properties cause small distortion of the magnetic field when placed inside it. The shift of the nuclear magnetic radiofrequency induced by the field inhomogeneities cause image distortion when the frequency offset becomes of the order of magnitude of the voxel-size. Moreover, large frequency variations across a

slice (as commonly observed at the interface between water containing intracranial structure and air cavities) cause regions of signal drop-out. Metallic electrodes cause both image distortion and small areas of signal drop-out in underlying tissue that can be limited to the skull by choosing optimal components for the EEG system (electrodes, resistors) and minimal amount of conductive gel (Krakow, Allen et al. 2000). Next to these alterations of the static magnetic field, metallic electrodes also act like a screen to the radiofrequency pulses and the related magnetic field used to rotate the nuclear magnetisations to create the image. This can lead to intensity variations of the image and increased resistance of the RF coil, both of which represent sources of noise (Debener, Mullinger et al. 2008).

2.5.1.2 Data Acquisition

Initial EEG-fMRI studies used a reduced number of electrodes, usually 10 or even only a few electrodes over a region of interest of the scalp with the goal of simply detecting the occurrence of spikes for the analysis of the fMRI signal (Warach, Ives et al. 1996; Seeck, Lazeyras et al. 1998; Krakow, Woermann et al. 1999; Patel, Blum et al. 1999; Lazeyras, Blanke et al. 2000; Al-Asmi, Benar et al. 2003). Currently, commercially available MRI compatible devices are based **on** the international 10-20 montage and include up to 64 recording electrodes that allow better spatial and morphological classification of EEG events. MRI-compatible amplifiers are placed and immobilised inside the scanner bore and connected to the recording computer outside the scanner room through optic fibres. This non-conductive connection avoids disruption of the shielding of the scanner room and the consequent perturbation of the magnetic field and image quality. It also avoids the need for additional electronic devices in the scanner room that would need to be specifically designed. Synchronisation between the scanner and the EEG recording system is very important to allow correct detection and correction of MR gradient-related artefacts (Mandelkow, Halder et al. 2006). It is based on a commercially available

synchronisation component or on a separate recording of a slice timing signal (Allen, Polizzi et al. 1998). Sampling frequency greater than 1000Hz and adequate dynamic range of the amplifiers (to avoid saturation from gradient artefact) are prerequisites for a good-quality off-line artefact correction. Low-quality on-line artefact correction is usually available to monitor patient collaboration (eyes closure) and safety (occurrence of seizures).

The electrocardiogram also needs to be recorded for subsequent correction of pulse-related artefacts caused predominantly by pulse-related head motion (Yan, Mullinger et al. 2010). Electromyographic activity is sometimes useful and has been used to investigate the BOLD correlate of cortical myoclonus (Richardson, Grosse et al. 2006) or detect seizure activity (Salek-Haddadi, Diehl et al. 2006).

The acquisition of MR images by a “transmit-receive” head coil rather than a body coil reduces heating and safety issues but several centres use a configuration of body transmit and head receive coil and such system is perfectly compatible with standard scalp EEG-fMRI acquisition. Multiple sessions of recording for a total of up to 2 hours of scanning (more than 1000 volume scans) can be necessary to capture a sufficient number of EEG events and scans for statistical analysis. Different methods of fMRI acquisition have been developed to avoid or overcome MR gradient-related artefact on the EEG recording. Early EEG-fMRI studies of patients with epilepsy used EEG-triggered fMRI, where online identification of IED would trigger the image acquisition (Warach, Ives et al. 1996; Seeck, Lazeyras et al. 1998; Krakow, Woermann et al. 1999; Patel, Blum et al. 1999; Lazeyras, Blanke et al. 2000; Al-Asmi, Benar et al. 2003). Other studies used interleaved EEG-fMRI to study evoked potentials or brain state fluctuations (Goldman, Stern et al. 2000; Bonmassar, Schwartz et al. 2001). Finally, most recent studies use continuous fMRI acquisition and off-line artefact correction.

2.5.1.3 Data processing

Correction of gradient artefact can be successfully performed by subtracting a sliding average of the artefact followed by adaptive filtering of the EEG (Allen, Josephs et al. 2000). Several strategies have been proposed for the subsequent correction of the pulse-artefact related to cardiac activity (Grouiller, Vercueil et al. 2007). Each correction strategy has a different effect on the EEG frequency spectrum so that the correction used should be chosen to spare the frequency band of interest for analysis. The most commonly applied is average template subtraction time-locked to the ECG similarly to the gradient-artefact correction (Allen, Polizzi et al. 1998).

In most applications of EEG-fMRI in epilepsy, artefact-corrected EEG recordings are reviewed by experts to identify IED that are marked as events of interest and entered into a General Linear Model (GLM) after convolution with a model of the HRF. Centre-specific choices of confounds including motion regressors, and cardiac confounds are added to model other sources of variance of the BOLD signal. The statistical estimation of this model and the use of t- or F-contrasts will identify the voxels in which the BOLD signal time course is significantly correlated with the occurrence of the IED, i.e. the brain regions where cerebral perfusion and metabolism show changes time-locked with IEDs. Correction can be applied to account for multiple voxel comparison and reduce the chance of false positive results (Friston, Frith et al. 1991; Genovese, Lazar et al. 2002).

2.5.1.4 Methodological limitations

Image distortion and signal drop-out is particularly important at the vicinity of air-tissue interfaces (basal temporal lobe and the orbito-frontal regions) as well as in the presence of metal foreign body (clips, electrodes) or haemosiderin deposits (cavernomas, trauma, surgical sites). The amount of signal loss in these regions influences the probability of obtaining a response in patients with temporal lobe epilepsy (Bagshaw, Aghakhani et al. 2004). Motion, especially when studying ictal

recordings, and incomplete correction of pulse-related artefact can hamper rigorous analysis. The use of stronger magnetic fields decreases the participation of potentially confounding draining veins to the signal but increases pulse artefacts and susceptibility artefacts (Mullinger, Brookes et al. 2008).

As EEG patterns differ between individuals, a model describing all IED as individual identical events is not always appropriate. Taking into account the duration of prolonged epileptic discharges increases sensitivity to detect BOLD changes (Bagshaw, Hawco et al. 2005; Salek-Haddadi, Diehl et al. 2006). In rhythmic discharges, the spectral power of a specific frequency band has been used successfully to identify brain regions associated with its fluctuations (Salek-Haddadi, Lemieux et al. 2003; Laufs, Hamandi et al. 2006). Independent Component Analysis (ICA) has been applied to the EEG to select an “epileptic regressor” for fMRI analysis and this led to an improved localisation compared to conventional IED marking although no formal validation with intracranial EEG or post-operative follow-up was reported (Jann, Wiest et al. 2008). ICA has also been used to perform “data-driven” analysis of the fMRI signal and revealed interictal haemodynamic signatures that were concordant with IED-based event-related EEG-fMRI analysis (Rodionov, De Martino et al. 2007). An interesting perspective of this analysis strategy would be to apply it to cases in whom no IED was recorded during EEG-fMRI and the usual fMRI contrast could not be obtained. The finding of interictal haemodynamic changes concordant with the irritative or seizure onset zone, despite the absence of IED on the scalp EEG, would increase the sensitivity of EEG-fMRI studies.

Intracranial electrodes can record abundant epileptic activity which is not detected with scalp electrodes: a factor of 60 for amplitude attenuation of epileptic discharges across the skull (Nunez and Silberstein 2000), a scalp:cortex spike ratio up to 1:2000 (Alarcon, Guy et al. 1994) and a threshold of 6-10 cm² of excited gyral surface for detecting changes on the scalp (Tao, Ray et al. 2005). Precise modelling of the

BOLD baseline is needed, therefore, in order to be able to reveal significant contrast time-locked to epileptic discharges measured on the scalp. Integration of physiologic background rhythms (Tyvaert, Levan et al. 2008) as well as the use of ICA of the BOLD signal (Mantini, Perrucci et al. 2007; Rodionov, De Martino et al. 2007) could improve the sensitivity of EEG-fMRI studies. Notably, simultaneous scalp and intracranial EEG could help to explain why some patients with very frequent IED do not show any significant correlated BOLD changes. Ongoing studies are currently evaluating the interaction between intracranial electrodes and MR imaging (Carmichael, Thornton et al. 2008; Carmichael, Thornton et al. 2010) with promising data from study of fMRI in patients with deep brain stimulation electrodes (Carmichael, Pinto et al. 2007). Models of BOLD fluctuations based on intracranial EEG recordings would certainly help to directly address the questions raised above.

2.5.2 Clinical EEG-fMRI studies in focal epilepsy

2.5.2.1 Interictal studies

Most EEG-fMRI studies in epilepsy are exploratory whole-brain studies aiming at demonstrating BOLD changes throughout the brain linked to any pathological discharges on scalp EEG. Since studies of combining ESI and EEG-fMRI have almost exclusively focused on focal epilepsy, we will not review here the EEG-fMRI studies on generalised epileptic activity. As for ESI clinical studies, EEG-fMRI studies on focal epilepsy mostly consist of heterogeneous patient groups. The yield of BOLD responses is predominantly affected by EEG criteria (IED frequency) of included patients. In two large EEG-fMRI studies (63 and 38 patients) with temporal, extra-temporal, lesional or cryptogenic epilepsies, lobar concordance between electro-clinical data and the most significant cluster of BOLD response was found in about 75% of the cases who showed BOLD activation (Al-Asmi, Benar et al. 2003; Salek-

Haddadi, Diehl et al. 2006). Complex patterns of multiple positive and negative responses can be observed locally and distant to the presumed irritative zone. In temporal lobe epilepsy, responses to unilateral spikes involved the temporal lobe in 73% (mostly the neocortex or both medial and lateral cortex), often with bilateral temporal involvement and additional extra-temporal positive and negative responses (Kobayashi, Bagshaw et al. 2006). The maximum activation was located in the temporal lobe or frontal operculum in 50% of activations whereas the maximum deactivation was only rarely in the ipsilateral temporal lobe.

Malformations of cortical development (MCD) are highly epileptogenic and often associated with frequent IED on the EEG. Pathological changes and epileptic zones often extend beyond MRI-demonstrable lesions. EEG-fMRI on patients with MCD (polymicrogyria, nodular or band heterotopia, focal cortical dysplasia) found relatively consistent patterns of positive responses correlated with structural abnormalities and distant negative responses (Salek-Haddadi, Lemieux et al. 2002; Kobayashi, Bagshaw et al. 2005; Kobayashi, Bagshaw et al. 2006; Salek-Haddadi, Diehl et al. 2006).

In 13 children with focal epilepsy aged 1-17 year-old, the responses could be related to the lesion or the presumed epileptogenic area (based on EEG scalp maps) in 84% (Jacobs, Kobayashi et al. 2007). Deactivations were more frequent than activations, suggesting a possible effect of sleep, sedation or age.

2.5.2.2 Validation of EEG-fMRI in epilepsy: intracranial EEG and surgical series

Comparison of EEG-fMRI results with other localising tools has recently shown promising results regarding the clinical relevance of EEG-fMRI findings. EEG-fMRI results were concordant with interictal hypometabolism on FDG-PET and ictal hyperperfusion on SPECT in 7 adults with various epileptic syndromes (Lazeyras, Blanke et al. 2000). When available, intracranial recordings (combination of data

reflecting IED and ictal onset zone from depth or subdural electrodes and interictal intra-operative corticography) confirmed the findings in 5/6 patients. Concordance with PET (2 patients) and SPECT (2 patients) was also reported in a pediatric study (De Tiege, Laufs et al. 2007). Looking at all the BOLD clusters and intracranial IED localisations in 5 patients, Benar et al. found good agreement between clusters of BOLD response and intracranial spiking contacts but the authors did not analyse the correlation between the most significant BOLD cluster and the most active interictal contact or the ictal onset zone, which would have clearly increased the clinical relevance of this study (Benar, Grova et al. 2006). In another study on an overlapping group of patients, congruence between interictal SEEG and interictal BOLD changes was found in 3 of 8 patients in whom SEEG was available (Grova, Daunizeau et al. 2008). More interestingly, propagation of IED documented by intracranial electrodes has been shown to occur from the vicinity of one BOLD cluster to another (Grova, Daunizeau et al. 2008). Finally, BOLD response to focal slow EEG activity instead of IED was shown to be concordant with the ictal onset zone on intracranial EEG in one patient with frontal lobe epilepsy (Laufs, Hamandi et al. 2006) suggesting that modelling other events than IED could have a localising value in pre-surgical focal epilepsy.

The localisation of the most significant BOLD changes within the volume resected has been related to a better outcome in some case-series (Lazeyras, Blanke et al. 2000; Thornton, Laufs et al. 2010). Comparison between studies is limited due to the application of study specific inclusion criteria (patients selected for the presence of detectable interictal activity vs all consecutive presurgical patients vs all patients with subsequent intracranial EEG or surgery). Evaluating the potential role of EEG-fMRI findings in clinical decision making, Zijlmans et al. obtained BOLD responses in 8/29 patients prompting the decision to reconsider surgery or intracranial recording in 4/8 patients that had previously been rejected because the epileptic focus was poorly

localised with other diagnostic modalities (Zijlmans, Huiskamp et al. 2007). Surgery was done in 1/4 so far leading to improvement but not seizure freedom and larger studies are needed to clarify the potential role of EEG-fMRI in clinical decision making. BOLD maps are often complex, involving multifocal cortical and subcortical regions considered to be involved in the epileptic network. Most studies investigate only the concordance of one cluster i.e. the global statistical maximum or any cluster in a given region of interest. A detailed report of maps of BOLD signal changes would be preferable to assess the validity and specificity of EEG-fMRI and allow comparison between studies. For this purpose, a graded assessment of concordance is useful, e.g. “Concordant” = all clusters are within the same lobe as the epileptic focus, “Concordant plus” = statistical maximum in the concordant lobe and additional remote clusters, “Discordant” (Salek-Haddadi, Diehl et al. 2006)).

2.5.2.3 Ictal EEG-fMRI studies in focal epilepsy

Ictal (EEG-)fMRI recordings are a relatively rare finding and are difficult to model because of frequently associated confounding motion and the event’s neurophysiological complexity. Nonetheless, these are extremely interesting studies due to their potentially greater yield in terms of networks involved. In some studies, BOLD changes have been detected prior to visible scalp EEG changes or clinical onset (Salek-Haddadi, Merschhemke et al. 2002; Federico, Archer et al. 2005). Results showed different involvement of cerebral networks compared to interictal imaging and give new insights into the mechanism underlying seizure generation. Intracranial recording in 2 patients showed ictal onset zones corresponded to the maximal ictal BOLD response with maximal statistical score (Tyvaert, Hawco et al. 2008). Thus, ictal EEG-fMRI findings are complementary to interictal studies and may help better discriminate between irritative and seizure onset zones in presurgical patients.

2.6 Combination of ESI and EEG-fMRI

2.6.1 Intrinsic discrepancies between EEG and fMRI

measurements

The combined analysis of electro-physiological and haemodynamic measurements can theoretically benefit from the temporal resolution of EEG and the spatial resolution of MRI and can increase our understanding of the underlying neurovascular processes. However, a prerequisite for such analysis is the recognition of the intrinsic limitation that both measurements do not reflect the same underlying biophysical phenomena, as discussed above (2.2.2). fMRI responses reflecting high metabolic activity can occur and be invisible on the EEG because of brain architecture such as deep-seated sources, source orientation tangential to the scalp, opposing source orientation in sulci or concentric neuronal architecture (Connors and Gutnick 1990). A non-synchronised increase in neuronal activity would cause a metabolic increase with haemodynamic consequences but no change in the EEG trace. On the other hand, an EEG signal can occur without an fMRI signal if a small proportion of a neuronal population behaves in a highly synchronised pattern.

Furthermore, the BOLD signal is created by oxygenation changes in both the micro-vascular tissue bed and the downstream venous pooling system, leading to potential confounding responses in draining veins. In anaesthetised monkeys, sensory cortex mapping with fMRI and microelectrode arrays showed an overlap of 55% (Disbrow, Slutsky et al. 2000), while in patients with epilepsy, intracranial EEG studies showed that IED sources and IED-correlated fMRI responses share spatial proximity but not complete concordance (Benar, Grova et al. 2006; Grova, Daunizeau et al. 2008) and the changes in neuronal activity related to distant BOLD responses are largely unknown. The coupling between neuronal activation, perfusion and oxygenation seems to be preserved in the irritative zone (Stefanovic, Warnking et al. 2005),

including during IED (Carmichael, Hamandi et al. 2008; Hamandi, Laufs et al. 2008), but this coupling was altered in electrographic seizures (Bahar, Suh et al. 2006). Structural brain lesions, notably of cerebro-vascular origin, can affect neuro-vascular coupling (Rossini, Altamura et al. 2004). This should be considered when modelling the BOLD response in regions potentially affected by abnormal haemodynamic properties such as vascular lesions, vascular malformations or tumours. Finally, there is recent puzzling evidence of regional cerebral blood flow changes prior to the onset of a stimulus and unrelated to intra-cranially recorded extra-cellular neuronal activity (Sirotin and Das 2009). Such changes have also been found prior to IED measured by scalp electrodes (Hawco, Bagshaw et al. 2007; Moeller, Siebner et al. 2008) questioning the assumed causal link between neuronal and vascular changes.

In the following sections, the possibilities and existing literature of integrating inverse models of electro-magnetic and vascular measurement will be discussed. Such models have variously been developed to combine fMRI data with either EEG or MEG results. Although this review does not focus on MEG, relevant methodological developments regarding combination of MEG and fMRI will be mentioned. An advantage of EEG over MEG in multi-modal fusion is the possibility of obtaining simultaneous recordings of EEG and fMRI, which is not possible with MEG.

2.6.2 Symmetrical and asymmetrical combination of ESI and EEG-fMRI

There are various methodological options to combine ESI or EEG and fMRI data, depending on the hierarchy that is applied to the analysis. First, in the conventional EEG-fMRI analysis scheme described above (2.5.1.3), events of interest extracted from the EEG can be used as regressors for fMRI analysis and fusion of the two modalities is achieved through correlation in time in an “**EEG-informed EEG-fMRI**

modelling". In the spatial domain, the localising ability of the two modalities offers the possibility of other forms of data fusion. As the general starting hypothesis is that EEG and BOLD signals should be correlated over time in some parts of the brain, a degree of concordance between the two forms of localisation in relation to a specific phenomenon is to be expected. Therefore, a sensible first step in EEG-fMRI fusion in the spatial domain is to compare independently derived localisations via "**ESI and EEG-fMRI comparative studies**" in which the EEG signal is used in parallel for both the analysis of the BOLD signal and the ESI. Assuming a good degree of spatial concordance one may exploit the superior temporal resolution of EEG to try to reveal dynamic patterns in those regions. Second, at a higher degree of integration, the results of one of the analyses can be used to constrain the other modality, resulting in an **asymmetrical** combination: Clusters of BOLD responses can be used to constrain ESI solutions obtained with underdetermined distributed source models: "**fMRI constrained EEG solutions**". Conversely, ESI results can be used as predictors of the BOLD signal changes: "**ESI-informed EEG-fMRI analysis**". Finally, based on the assumption that EEG and fMRI signals are generated by the same cortical region with a specific neurono-glial population, biophysical generative models can be developed to "**invert**" both EEG and BOLD signals: datasets of simultaneously acquired, signals are entered into a comprehensive model of brain activity and neurovascular coupling realising a non-hierarchical "**symmetrical fusion model of EEG and fMRI**". The interested reader is referred to (Daunizeau, David et al. 2009) for a recent review of these techniques.

2.6.2.1 ESI and EEG-fMRI comparative studies

The vast majority of studies comparing ESI and EEG-fMRI localisation are based on recordings obtained from different sessions: EEG-fMRI is often performed with a relatively small number of scalp EEG electrodes and ESI is performed on data obtained with better electrode coverage outside the scanner environment. The first

confirmation of EEG-fMRI findings in epilepsy with electric source localisation (distributed inverse solution LORETA) and intracranial recording was reported by Seeck et al. using a distributed inverse solution (Seeck, Lazeyras et al. 1998), while other studies used ECD.

Lemieux et al. 2001 compared the localisation of IED-related BOLD responses and EEG source localisation (Lemieux, Krakow et al. 2001). They used spike-triggered fMRI on 6 patients (5 with lesions) and compared the results with ESI based on 64-channel EEG acquired separately outside the scanner. Two different models of ECD sources, namely free moving dipole or spatio-temporal source modelling, were used with a realistic head model (Boundary Element Model). The concordance between both modalities was generally good. In all cases at least one dipole was located in the same lobe for each BOLD cluster, with an average peak-to-peak distance of 2.2 cm for positive and 3.5 cm for negative responses. Concordance of EEG-fMRI results with lesion localisation was also good but no intracranial recording was available for validation.

In a similar study, Bagshaw et al. performed spatio-temporal dipole modelling and EEG-fMRI in 17 patients (Bagshaw, Kobayashi et al. 2006). Distance between the ECD and the closest activated voxel was 32-34 mm but was much greater when the most active voxels were considered (58.5 to 60.8 mm). The authors pointed rightly to the mislocalisation caused by the dipolar model that fits sources out of the grey matter and deep into the brain. In another study from the same group, Benar et al. studied the concordance between EEG-fMRI BOLD clusters, EEG source localisation and intracranial EEG in 5 patients, some of them included in the study by Bagshaw et al. (Benar, Grova et al. 2006). In both studies, EEG for ESI was recorded in a separate session, after adding 21 electrodes to the 19 electrodes used inside the MR scanner. EEG source localisation was based on multiple dipolar sources using a realistic head model (Boundary Element Model). Stereotactic depth electrodes or

subdural grid electrodes were used during intracranial recording. The main finding was that whenever there was an intracranial electrode in the vicinity (20-40 mm) of BOLD clusters or ESI, this electrode contained recorded epileptic activity. This was true for positive and negative BOLD responses. There was better concordance between BOLD clusters and intracranial EEG than between ESI and intracranial EEG, stressing the limitation of ECD-based ESI models and the sampling limitations of intracranial EEG. However, sources identified using ESI were revealed that had no BOLD correlate in the temporal lobe and the reverse was also found, with isolated BOLD clusters in the supplementary motor cortex. In both studies, no information was given regarding the most active BOLD cluster, the main ESI source and the main intracranial focus. Although no clear-cut match is expected, even in direct cortical EEG recording (Disbrow, Slutsky et al. 2000) because of the fundamental difference of both signals discussed above, these distances are clearly larger than those from studies comparing the localisations of BOLD response and ECD source models of evoked responses to external stimuli (Strobel, Debener et al. 2008).

With the above considerations in mind, distributed source models might be better suited for widespread IED that are the most likely to be associated with significant BOLD responses. A more refined study on the same patient group as Bagshaw et al. used geodesic distance to measure concordance between BOLD cluster, a distributed source localisation based on maximum entropy of the mean and a Bayesian framework to assess fMRI concordance and relevance. It showed a good concordance between ESI and BOLD for 24% of BOLD cluster in 6/7 patients and the localisation was confirmed by intracranial EEG recording in 3 patients (Grova, Daunizeau et al. 2008).

In a series of 11 children with benign rolandic epilepsy, Boor et al. compared EEG-fMRI BOLD patterns (using a parametric estimate of the spike frequency, and interleaved MR acquisition with no artefact correction) with the results of multiple

source analysis (spatio-temporal dipole modelling), again with two separate acquisition sessions (Boor, Jacobs et al. 2007). In 4/11 patients, BOLD clusters were concordant with the locations of the initial dipoles and in 3 of these patients, there were additional areas of activation extending into the central fissure and the insula, corresponding to dipolar sources of propagated activity. The authors concluded that ESI helped to define a pattern of propagation in the EEG-fMRI results.

An important methodological issue in all these studies is the choice of statistical thresholding techniques used for the different techniques. Indeed, the majority of ESI studies do not include a statistical estimation of the extent of the source. Some statistical methods have been proposed (see section 2.3.1.2 and (Sperli, Spinelli et al. 2006; Zumsteg, Friedman et al. 2006)), a point which becomes particularly crucial when assessing concordance (overlap) between modalities for validation.

2.6.2.2 “fMRI-constrained ESI”

The ill-defined nature of the EEG inverse problem undermining ESI can be addressed by making a priori assumptions on the nature of the generator. The ESI solution space can be constrained by anatomical information, e.g. limiting the space of solutions to the cortical grey matter. Constraining ESI solutions based on knowledge derived from fMRI results has been considered. This technique has been mostly applied to the field of cognitive neuroscience with promising results (Ahlfors, Simpson et al. 1999; Babiloni, Babiloni et al. 2002; Liu and He 2006). Similar developments have taken place in the field of the MEG inverse solution (Ahlfors, Simpson et al. 1999; Dale, Liu et al. 2000). However, in general, the application of fMRI constraints to ESI should be considered with extreme caution, given the fundamental differences between regional metabolic/vascular and electrical changes, as described above. Starting with an EEG-based inverse solution and applying fMRI-based constraints to the solution in order to increase agreement with fMRI data carries the risk of spatial bias with false positive and false negative solutions (Brookings, Ortigue et al. 2009).

Moreover, the “static” fMRI constraint will be applied to successive EEG time frames with very different scalp maps and source activity (Gonzalez-Andino, Blanke et al. 2001). Preliminary studies with dipolar constrained ESI have shown good correlation with focal fMRI results. However, fMRI-constrained ESI in the case of spatially distributed networks remain a difficult challenge. Nevertheless, some recent studies suggest that distributed ESI is more suited than dipolar ESI for such scenarios, involving large areas of cortex (Liu and He 2006; Grova, Daunizeau et al. 2008). Currently, when studying epileptic activity, an fMRI-informed constraint on ESI is not recommended, unless it includes flexible weighting and proper model comparison tools to assess the relevance of the BOLD clusters as ESI priors, for instance within a Bayesian framework for an *a posteriori* assessment of the relevance of the fMRI constraints (Daunizeau, Grova et al. 2007).

A recent EEG-fMRI study compared the localisation of the generators of the spike and wave components of Generalised Spike Wave activity identified on EEG (Daunizeau, Vaudano et al. 2010). BOLD clusters related to Generalised Spike Wave activity were used as priors in a bayesian model comparison of EEG source models and found bilateral fronto-temporo-parietal regions associated with spikes while the frontal components were lacking for slow-waves.

2.6.2.3 “ESI informed fMRI analysis”

Using the reverse analytical asymmetry, ESI results can be used for fMRI analysis in the General Linear Model. Liston et al. combined EEG source imaging and fMRI with the objective of improving sensitivity and reducing EEG observer bias in one patient (Liston, De Munck et al. 2006). They used an automated spike classification and subsequently projected the EEG in the source space on an ECD. Analysing the time course of the ECD and applying an amplitude threshold led to the detection of an additional 61% of IED to those previously visually detected IED, thus increasing the explained variance of the MR signal. Such modelling represents the equivalent in

source space to ICA techniques described above (section 2.5.1.4) and used for selecting a continuous marker of interictal epileptic activity at the level of the electrodes (sensor space).

2.6.2.4 Neural mass models and “Symmetrical fusion model of EEG and fMRI”

EEG and fMRI data could be entered into a combined inverse model of the BOLD signal and the scalp EEG with the prospect that characterisation of multiple variables will allow better estimation of the mechanisms generating macroscopic electrical signal and haemodynamic changes (Trujillo-Barreto, Martinez-Montes et al. 2001; Daunizeau, Grova et al. 2007; Brookings, Ortigue et al. 2009). While local changes in synaptic activity can be detected by scalp electrodes these changes also trigger metabolic and haemodynamic cascade that cause local changes in vasodilatation and significant changes in BOLD signal that are detected by fMRI. Thus the inversion of these two forward models could lead to a symmetrical fusion of EEG (or MEG) and fMRI data that might better localise active neural sources. This requires a detailed model of the relationship between neuronal activity and haemodynamic response, which is generally based on neural mass models and a variant of the “balloon model” (Buxton, Wong et al. 1998; Babajani and Soltanian-Zadeh 2006). Recent work in this field relies mainly on simulated data to generate event-related potentials in response to a input into the neural mass model (stimulus) (Deneux and Faugeras 2006; Sotero and Trujillo-Barreto 2007; Valdes-Sosa, Sanchez-Bornot et al. 2009). Up to now, there has not been a validation of such a symmetrical technique in the context of EEG-fMRI data from patients with focal or generalised epilepsy.

2.7 Further methodological perspectives

2.7.1 EEG-fMRI and ESI studies in the frequency domain

The BOLD signal correlates of physiological scalp EEG rhythms have revealed distinct patterns of “resting state activity” both in healthy subjects (Mantini, Perrucci et al. 2007) and interictally, in patients with epilepsy (Tyvaert, Levan et al. 2008). Theoretical work suggests that an increase of neuronal activity is associated with a shift of the frequency spectrum towards the high frequencies and regional BOLD signal increases (Kilner, Mattout et al. 2005). Frequency-based approaches have been applied to ESI of ictal EEG (Lantz, Michel et al. 1999; Blanke, Lantz et al. 2000). In EEG-fMRI, the spectral power of focal slowing was associated with localised BOLD changes with a close spatial relationship with the ictal onset zone in a single case report (Laufs, Hamandi et al. 2006). Generalised 3Hz slow waves showed regions with associated positive (thalamic) and negative (diffuse cortical) BOLD changes (Salek-Haddadi, Lemieux et al. 2003; Siniatchkin, van Baalen et al. 2007) and spectral power has been used to model the associated BOLD signal. There is no report of combined ESI and EEG-fMRI approach in the frequency domain but this technique would be interesting to map focal haemodynamic changes regions linked to features of the frequency spectrum of interictal epileptic activity.

2.7.2 Cortical potential imaging

Scalp EEG data can be also used to reconstruct cortical potentials using realistic head models and it has been suggested that the use of fMRI-weighting of the cortical potential computation could help to increase the spatial resolution (Liu, Kecman et al. 2006). This technique has been used to map evoked potentials with validation through intra-operative electro-corticography (He, Zhang et al. 2002). Its future

application to interictal discharges could provide very valuable information in the context of cortical mapping in epilepsy surgery candidates.

2.7.3 Can fMRI inform about network dynamics ?

The typical interval between fMRI volumes (repetition time, TR) is in the order of 2-3 seconds which is adequate to sample the profile of the HRF. However, this sampling frequency and the slow response of the HRF limit our ability to study fast changes in EEG activity which occur at the time scale of milliseconds. Perfusional and metabolic changes in regional brain activity can occur before the occurrence of detectable scalp EEG events and suggest that processes on a slower timescale might play a facilitating role in the generation of epileptic activity (Hawco, Bagshaw et al. 2007; Moeller, Siebner et al. 2008). Recently, new analytical tools based on neural mass models, such as Dynamic Causal Modelling (DCM) (Friston, Harrison et al. 2003), have been developed to obtain information on directionality and causality relationships between clusters of activations shown by fMRI studies. DCM models electromagnetic signals as arising from a network of sources, where each source is considered to be a point process; i.e., an ECD linked to the other sources by effective connectivity. Initially developed to model the response of neural populations to an external stimulus, such as in cognitive fMRI, DCM has recently been validated by intracerebral recordings in animal models of absence epilepsy (David, Guillemain et al. 2008) and applied to human epileptic brains to identify neural drivers of fMRI signals in focal epilepsy (Hamandi, Powell et al. 2008) or idiopathic generalised epilepsy (Vaudano, Laufs et al. 2009). Identifying the directionality of the interaction between cerebral structures revealed by fMRI, with a comprehensive underlying neuronal model, would be a major step in understanding the dynamics of epileptic networks. Therefore, fMRI analysis based on these models could infer directionality of processes that occur at much lower temporal scale than the fMRI sampling rate and

inform about network dynamics. These models could help bridge the gap between our understanding of epileptic activity at a cellular level and on a whole-brain scale.

2.8 Perspectives on the combination of ESI and EEG-fMRI

Studies comparing or combining ESI and EEG-fMRI suggest that the combination of these techniques could provide complementary localising information, with potential clinical relevance. Unfortunately, the equivalent dipole technique used in most studies combining ESI and EEG-fMRI is not a real localiser of the cortical generators but rather a representation of their “centre of mass”, which make it conceptually difficult to assess overlap or distances between results of both techniques. More studies are needed using distributed electric sources that represent a better model of epileptic activity affecting extended patches of cortex. There is also a lack of clinical studies properly combining ESI and fMRI, starting from applying ESI and EEG-fMRI to the same dataset to avoid intrasession fluctuations of spontaneous brain activity. In addition, clinical EEG-fMRI studies have only recently started to move from simple spike-based event-related model design to more advanced use of EEG and ESI features to guide fMRI analysis. Last but not least, the feasibility of intracranial EEG-fMRI in patients with epilepsy could have clinical relevance while carrying great scientific interest. All these points are addressed in the current experimental work and their clinical relevance is estimated and discussed.

2.9 Conclusion

In the pre-surgical work-up of patients with epilepsy, ESI has been shown to be a valuable localising tool in most patients, with validation using intracranial EEG or post-operative follow-up. Recent studies also suggest a good concordance between EEG-fMRI findings and similar gold standard localisation tools. However, such surgical series potentially suffer from a recruitment bias towards unifocal epileptic activity and good outcome and many cases remain complex and difficult to analyse or interpret.

There are exciting ongoing biophysical modelling and experimental developments attempting to solve the combined “electro-vascular inverse problem” and to uncover the precise nature of microscopic and macroscopic neuro-vascular coupling but most of these developments are still at the stage of computer simulation or application to simple experimental paradigms using evoked-responses. Their future translation from group studies of cognitive evoked-related potentials to individual patients with spontaneously occurring epileptic discharges is far from simple but is likely to help us to better understand the underlying mechanisms of the generation, propagation and termination of epileptic discharges. The assessment of clinical relevance, especially with respect to planning epilepsy surgery or intracranial electrode placement will require intracranial EEG studies or post-operative follow-up. These techniques may also have wider application, in the investigation of the interaction between epileptic activity and other brain networks involved in resting state, cognitive processes and sleep.

3 DIFFUSION MAGNETIC RESONANCE IMAGING AND TRACTOGRAPHY IN EPILEPSY

3.1 Introduction

Diffusion MR imaging and tractography are new developments of MRI that are increasingly involved in clinical studies of neurological disorders (Ciccarelli, Catani et al. 2008). Diffusion imaging reveals subtle structural abnormalities, not detected by conventional structural MRI and tractography techniques allow the mapping of neural tracts in the white matter. Applied to epilepsy imaging, these techniques may potentially improve the understanding of the reciprocal interaction between abnormal connectivity and epileptic activity. In patients suffering from focal pharmaco-resistant epilepsy who are being evaluated for possible epilepsy surgery, these techniques allow the detection of previously unrecognised structural abnormalities. In other patients, they allow mapping important white matter tracts (motor, language, vision) that are potentially altered by neurological diseases and could be applied for mapping structural connections underlying epileptic networks.

This chapter presents a brief technical survey of the physical and radiological principles of diffusion and its measurement, followed by a review of the application to epilepsy and epilepsy surgery.

3.2 Diffusion imaging: physical and radiological principles

3.2.1 Diffusion: physical background

Random motion of water molecules is caused by thermal energy. This molecular displacement is called **diffusion**. When the molecules can diffuse equally in all directions of a tridimensional space, the medium is described as **isotropic**, like the free diffusion of a drop of ink in a glass of water, which is limited only by the walls of the glass. In a biological structure, the diffusion of water molecules is limited by cellular membranes delimitating the the intra-cellular and the extra-cellular spaces as well as by intracellular structures (cytoskeleton, organelles). In a tissue where the intracellular volume is high compared to extracellular volume, the cell membranes limit long range diffusion compared to a tissue where the extracellular volume predominates. Therefore, the diffusion coefficient will be low in the former tissue and high in the latter. These structural properties can be used to detect regions of high intracellular volume like cell swelling in cytotoxic oedema (e.g. early status epilepticus, acute stroke) or abnormally packed neurons (disorders of brain development). Similarly, regions of increased extracellular volume can be detected and occur in vasogenic edema (late status epilepticus, subacute stroke) and cellular loss (gliosis).

In a highly organised structure like the brain, nerve fibres are tightly packed in white matter bundles. Therefore, the diffusion is favoured in certain directions and restricted in others because of resistance of the cellular membranes to the crossing of water molecules. The myelin sheets and intra-axonal skeleton (microtubules) seem to play a minor role in the diffusion properties (Beaulieu 2002). The diffusion in such structures is called **anisotropic**. A **Diffusion Tensor (DT)** is a mathematical representation to describe the diffusion properties of a tissue with 6 variables: 3 for the position at which the diffusion is measured and 3 for principal orthogonal directions to represent anisotropic properties. The DT can be mathematically

transformed (diagonalisation) to contain non-null elements only in its diagonal. These elements are the eigenvalues, describing the diffusivity in the axis of principal diffusivity and two orthogonal directions (eigenvectors). The **Fractional Anisotropy (FA)** measures the deviation from isotropy in a given point in space. The highest eigenvalue shows the direction of preferred diffusion (axial diffusivity, parallel to fibre bundle axis) while the other eigenvalues represent radial (perpendicular) diffusivity. The **Mean Diffusivity (MD = trace of the Diffusion Tensor = sum of eigenvalues)** represents the mean molecular motion, **independently of the directions of diffusion measures** (For a review of these physical principles, see (Tuch, Reese et al. 2003; Hagmann, Jonasson et al. 2006)).

3.2.2 Measurement of diffusion with MRI

Magnetic Resonance Imaging (MRI) offers a unique tool to measure the diffusion properties through **Diffusion Tensor Imaging (DTI)**, where additional gradients in the magnetic field are designed to enhance effect of diffusion on the MR signal. The magnetic properties of the water molecules which move into a given volume element (voxel) during the acquisition sequence will be different from those of immobile molecules (phase shift), causing a decrease of the signal intensity. By measuring the diffusion properties at each position (voxel) in 3 perpendicular directions, the diffusion tensor can be obtained. Diffusion Weighted Images (DW, DWI) and maps of Apparent Diffusion Coefficient (ADC, an equivalent to MD) which is obtained by subtracting the T2 effect from DWI, are now recorded in routine clinical structural MRI (Pierpaoli, Jezzard et al. 1996; Tuch, Reese et al. 2003; Hagmann, Jonasson et al. 2006).

Analysis of the images can then be performed either by comparing selected regions of interest across the population studied or by voxel-based whole-brain techniques. While they remove the investigator selection bias, the voxel-based techniques allowing statistical parametric mapping suffer from the limitations associated with the

necessary normalisation of the images, regarding anatomical variation in ventricle and gyral anatomy.

3.3 Tractography

3.3.1 Principles

Tractography is a post-processing method used to display the data obtained from the DTI in order to represent white matter tracts in a 3D image or with colour coding. This technique has therefore the potential to use DTI data for in-vivo imaging of white matter pathways. Starting from a given region of interest (seed region), specified by the investigator, the directions of maximal diffusion, assumed to be the direction of axonal bundles in the white matter, can be followed from one voxel to the next (**“streamline” or “deterministic” tractography**). In this way, pathways of maximal water diffusion reflecting white matter neural tracts can be tracked across the brain. The main limitation of the technique is encountered in voxels where there is fibre crossing or “kissing”. There, the diffusion tensor has two “competing” peak-directions and the anisotropy is falsely reduced, which can interrupt the tracking procedure (false negative), alternatively, the tract can be “deviated” to follow another crossing tract (false positive). User-specified thresholds for the maximal angle of a tract at each voxel and for the minimal anisotropy necessary to continue the tract as well as exclusion/inclusion regions can be applied to introduce prior anatomical knowledge and “guide” the tracking procedure. These processing steps can of course introduce an important investigator bias in the data.

Probabilistic tractography is an alternative approach that has been developed to improve the reliability of fibre tracking through voxels with low anisotropy (either due to noise or to multiple crossing/neighbouring fibre tracts with different directions) and to obtain some quantitative measurement regarding the reliability of the tract.

Probabilistic tractography algorithms include some uncertainty in the direction of fibres derived from the 3 eigenvectors of the diffusion tensor. Tracts are then generated according to this uncertainty and the process is repeated iteratively, usually with several thousand iterations. The result is a map of the probability of connection, i.e. the probability of each voxel to be reached by a tract starting from the seed region (Parker and Alexander 2003). The drawback of this iterative analysis is that it is consuming in terms of time (by a multiple of N iterations) and computing power but its significant advantage over streamline tractography is to better cope with crossing/"kissing" fibres, while giving information about the reliability of the connections obtained. The probabilistic tracts can then be compared across subjects using commonality maps (superposition of normalised tracts in each group to obtain probability of connection across the group) or by statistical analysis of the various tract measures (FA, MD, volume of normalised tracts).

3.3.2 Methodological limitations and validation studies

It should be born in mind that tractography shows pathways of least resistance to water diffusion at a millimetric resolution, and is therefore only a crude estimate of bundles of thousands of axons projecting across the white matter. Moreover, it provides no information regarding the directionality of the connections (afferent vs efferent) or the number or density of synaptic connections. However, this technique has the definite advantage over more precise tracer techniques that it can be applied non-invasively *in vivo*. A few studies have investigated the reliability of tractography as an imaging tool of white matter tracts. Intersession and interindividual reproducibility for major tracts in healthy subjects was good for FA and MD (<10%) but less so for the volumes of normalised tracts (Ciccarelli, Parker et al. 2003; Dauguet, Peled et al. 2006; Heiervang, Behrens et al. 2006; Wakana, Caprihan et al. 2007). The stability of the measurement was tract specific, better with two

constraining regions of interest, and did not improve with increased number of diffusion directions (although more direction increased the sensitivity and therefore the tract volumes). Formal comparison with injected tracers in monkeys (Dauguet, Peled et al. 2006; Dyrby, Sogaard et al. 2007), invasive MRI tracer manganese (Dyrby, Sogaard et al. 2007) or with anatomical dissection in humans (Lawes, Barrick et al. 2008) reported an overall good agreement for large white matter tracts. However, such studies are limited by methodological problems, including dye diffusion, tract dissection, image coregistration and are dependent on the algorithm used for tractography and the tuning of tracking parameters such as the FA threshold or the angular threshold that determine the interruption of the tracking algorithm.

In some recent studies, statistics have included parallel but also radial diffusivity measures (as represented by the different eigenvalues of the DT) (Concha, Gross et al. 2006; Widjaja, Blaser et al. 2007; Diehl, Busch et al. 2008) and some authors have proposed that parallel/radial diffusivity of a tract reflects axonal/myelinic integrity (Song, Sun et al. 2002). However, a well documented simulation study challenged this model by showing that individual eigenvalues can not be compared across subjects unless the tensor axes are strictly identical and statistics should therefore be limited to FA and MD (Wheeler-Kingshott and Cercignani 2009).

Tract-Based Spatial Statistics (TBSS) is a whole brain tractography approach consisting in projecting the individual DTI images onto atlases of the major white matter tract and performing statistics on those projected tracts (Hagler, Ahmadi et al. 2009). The advantage is to eliminate the need for smoothing the images before voxel-based analysis and to limit the comparison to major tracts rather than to apply the comparison to every voxel of the brain, with the necessary need to correct for multiple voxel comparisons (Focke, Yogarajah et al. 2008).

Another methodological issue is the distortion affecting the diffusion EPI images which is caused by magnetic field inhomogeneities and induced eddy currents.

Careful image processing is required when co-registering diffusion images with EPI images of fMRI or structural T1-weighted images for defining seed regions or overlaying results. Moreover, clinical studies comparing pre- and post-operative images have to deal with post-operative brain shift and sagging, prompting the need for non-linear co-registration algorithms (Yogarajah, Focke et al. 2010).

3.4 Diffusion MRI applied to Epilepsy imaging

3.4.1 Structural brain modification associated with epileptic activity : evidence from animal studies

Diffusion MRI can image morphologic changes in the brain caused by sustained epileptic activity (status epilepticus). The underlying chain of events is mainly caused by changes in ionic concentration and membrane permeability (Lux, Heinemann et al. 1986; Wang, Majors et al. 1996) and has been described in animal models of epilepsy (bicuculline-induced status epilepticus in rats) (Zhong, Petroff et al. 1993) and spreading depression caused by electroshocks (Prichard, Zhong et al. 1995). In the acute (ictal) phase or shortly after the seizure (post-ictal), cytotoxic edema resulting from seizure-induced increases in membrane permeability, causes cellular swelling in the cortex, and therefore reduction of extra-cellular space of up to 30% (Lux, Heinemann et al. 1986). Consequently the free diffusion of water molecules is focally reduced and this can be visualised by diffusion MRI (reduced ADC). The simultaneous increase in blood perfusion suggests that the cytotoxic edema is directly caused by the electric activity rather than by an accompanying hypoxia (Szabo, Poepel et al. 2005). This phase of cytotoxic edema is followed by another phase of vasogenic edema, during which the vessel permeability rises and the extra-cellular volume increases, leading to increased water diffusion, and, therefore, an increased ADC. These acute changes are followed by a reversal of the diffusion

abnormalities but result in atrophy of hippocampus at the chronic stage (Choy, Cheung et al. 2010). Histological alterations underlying FA changes have been found in models of acquired epilepsy in rats despite unremarkable visual analysis of brain MRI (Sierra, Laitinen et al. 2010).

3.4.2 Status epilepticus in humans

Similar changes in cortical diffusivity have been described in patients suffering from convulsive or non-convulsive status epilepticus of limbic or extra-limbic origin (Wiesmann, Woermann et al. 1997; Lansberg, O'Brien et al. 1999; Scott, Gadian et al. 2002; Szabo, Poepel et al. 2005). Moreover, the subcortical white matter seems to present mainly a vasogenic edema (Lansberg, O'Brien et al. 1999; El-Koussy, Mathis et al. 2002).

The final radiological evolution can be either towards a complete resolution of these changes (as early as day 14 in humans (Szabo, Poepel et al. 2005)) suggesting only a transitory dysfunction or towards permanent abnormalities with an increase of the ADC probably reflecting cellular loss (and hence increased extracellular space and increased diffusivity), tissue atrophy and gliosis (Lansberg, O'Brien et al. 1999; Nedelcu, Klein et al. 1999; Scott, King et al. 2003). The detection of the permanent structural abnormalities has been reported after 1 month in limbic status epilepticus leading to hippocampal sclerosis (Gong, Concha et al. 2008) or 2 months in neocortical status epilepticus leading to regional atrophy (Lansberg, O'Brien et al. 1999). In most patients, the changes in diffusivity were multifocal, pointing to abnormalities affecting various parts of an epileptic network rather than a single epileptogenic region. There is limited evidence that the changes might progress for months after termination of status epilepticus despite seizure freedom (Gong, Concha et al. 2008). Tissue atrophy has also been described in the neocortex in children as soon as two weeks after status-like febrile seizures (> 1h duration) (Takanashi, Oba

et al. 2006). In children with prolonged febrile seizures, there is hippocampal volume increase (acute oedema), followed by volume decrease (atrophy) and subsequent growth (VanLandingham, Heinz et al. 1998).

3.5 Diffusion imaging as a lateralising or localising tool :

Post-ictal and interictal clinical studies

One of the biggest expectations regarding any new imaging tool involved in presurgical work-up of epilepsy is that it could help localising the epileptogenic focus or any underlying structural abnormality that was not revealed by other imaging tests. “Interictal” and “post-ictal” imaging could be useful for localising subtle lesions and epileptogenic foci and help if the standard imaging tests are normal or show multiple abnormalities. “Ictal” imaging remains a rare finding except when selecting patients with status epilepticus.

3.5.1 Post-ictal diffusion imaging

DWI changes after a single seizure have been described but are less consistent and more transient than in studies of status epilepticus. Studies performing serial scans showed resolution of the abnormalities after a few days. Most studies report small heterogeneous patient groups with various delays from seizure to imaging (Diehl, Najm et al. 2001; Hufnagel, Weber et al. 2003; Oh, Lee et al. 2004; Diehl, Symms et al. 2005; Salmenpera, Symms et al. 2006) (see (Briellmann, Wellard et al. 2005) or (Yogarajah and Duncan 2008) for a review of these studies). In most cases where changes were found, local and distant ADC/MD decrease were reported but increases localised to the putative epileptic focus were also observed. The observation of changes in ADC but not FA suggested that simple seizures caused cell swelling without altering the direction of principal diffusion (Diehl, Symms et al.

2005). A study looking at diffusion-weighted focal changes less than an hour after single seizures in 23 patients identified focal changes after 50% of single partial complex and secondary generalized seizures, using a whole-brain voxel-based analysis of DWI rather than regions of interest (Salmenpera, Symms et al. 2006). The involved region corresponded to the putative focus of the seizures only in a minority of the patients suggesting that the method probably revealed networks involved in the seizures rather than the zone of onset. Enhancement of the epileptogenic activity by the GABA-receptor antagonist flumazenil was used on 12 patients in another study (Konermann, Marks et al. 2003). ADC decrease was found in the presumed zone of ictal onset as defined by electro-clinical data and structural MRI and confirmed by post-operative seizure freedom in half of them.

3.5.2 Interictal Diffusion imaging

3.5.2.1 Temporal lobe epilepsy

In patients with temporal lobe epilepsy (TLE) and unilateral hippocampal sclerosis on conventional MRI, increased ADC values reliably lateralised the epileptic focus (Hakyemez, Erdogan et al. 2005; Wehner, Lapresto et al. 2007). When the conventional MRI was not conclusive, the ADC values were not significantly different from the contralateral hippocampus although they were lower in patients than in controls, suggesting probable bilateral structural abnormalities.

Actually, in TLE with unilateral hippocampal sclerosis, diffusion imaging showed structural abnormalities extending far beyond the sclerotic hippocampus and include extratemporal white matter tracts (Gross, Concha et al. 2006). A study using statistical voxel-based mapping confirmed these extensive findings (temporal lobe and extra-temporal limbic system, frontal lobe), more so in left than right TLE (Gong, Concha et al. 2008). The FA of the ipsilateral thalamus was correlated to age at

disease onset in unilateral TLE with hippocampal sclerosis. However, the presence of extensive abnormalities does not seem to indicate a worse surgical outcome (Gross, Concha et al. 2006) and could even be reversible: in about half of the patients who underwent temporal lobe surgery and became seizure free, post-operative imaging showed a resolution of the diffusion abnormalities in the contralateral hippocampus (Thivard, Tanguy et al. 2007). These findings suggest that remote diffusion abnormalities are caused by cytotoxic or vasogenic edema associated with chronic epileptic activity, with resolution after resection of the epileptogenic zone.

A study in 33 patients with unilateral TLE and hippocampal sclerosis showed widespread decrease of FA and increased MD in the limbic structures but also in neocortical temporal and extra-temporal regions which extended contralaterally to the affected hippocampus (Focke, Yogarajah et al. 2008). A comparison between voxel-based Statistical Parametric Mapping and TBSS showed that TBSS was more sensitive to detect white matter abnormalities, whereas SPM was more sensitive to detected MD changes in the affected hippocampus.

In patients with TLE (mixed group with HS or non-lesional TLE), some studies showed a correlation between findings of DTI and clinical characteristics: interictal psychosis correlated with diffusion abnormalities in both temporal lobes (low FA) and both frontal lobes (low FA, high MD) (Flugel, Cercignani et al. 2006). Epigastric aura was associated with lower diffusivity ipsilateral to the epileptogenic focus and a positive history of febrile seizures was associated with bilateral higher anisotropy in the temporal lobe (Thivard, Lehericy et al. 2005).

3.5.2.2 Focal diffusion abnormalities and epileptic activity

In an interesting study with diffusion MRI in 16 patients investigated with intracerebral electrodes (10 TLE, 6 extra-TLE), abnormalities of mean diffusivity (probably reflecting gliosis or cellular loss) were better correlated with seizure onset zones than FA abnormalities that reflected rather a distant disorder of white matter connections

(Thivard, Adam et al. 2006). Moreover, the correlation was better in extra-temporal epilepsy (83%) than in temporal epilepsy (20%). This suggested that diffusion imaging could help to choose electrode placement in difficult cases of cryptogenic partial epilepsy. Another study using voxel-based diffusion mapping in 14 patients with frontal lobe epilepsies found areas of increased diffusivity within the irritative (75%) or epileptic zones (66%) but also, and more often, in connected areas (86%) (Guye, Ranjeva et al. 2007). The extent of these findings was less widespread in MRI-negative patients and was significantly correlated to the disease's duration. The authors concluded that diffusion imaging had poor specificity to detect the epileptic zone but reflected widespread and potentially evolving neuro-glial abnormalities. Another study used non-invasive DTI and magneto-encephalography in children with focal cortical dysplasia and reported decreased FA and increased MD in the white matter underlying visible focal cortical dysplasia but also near distant MEG sources in 11/15 children (Widjaja, Zarei Mahmoodabadi et al. 2009). This study also showed diffusion changes distant to the lesion in white matter tracts projecting to/from these regions of focal cortical dysplasia but did not report results about tracts projecting to/from regions of MEG sources.

3.5.2.3 Malformations of cerebral development

Diffusion imaging is particularly promising for studying normal and pathological patterns of brain development. Dramatic changes in brain architecture and connectivity occur throughout pre- and post-natal maturation through dendritic remodeling, cell death, synaptic pruning and myelination. Increases in fractional anisotropy precede the appearance of myelin while decrease in ADC reflects the progressive increase of the size of neurons and glial cells (see (Grant 2005; Toga, Thompson et al. 2006) for review). As a correlate, diffusion imaging is therefore very informative in developmental disorders. It can reveal very subtle areas of focal cortical dysplasia through changes in mean diffusivity reflecting abnormally packed cells or

through reduced anisotropy of the underlying white matter bundles, caused either by disturbed connectivity or by ectopic neurons located in the white matter (Eriksson, Rugg-Gunn et al. 2001; Gross, Bastos et al. 2005). The abnormal pattern seen in diffusion imaging is often more extensive than the malformation seen on standard MRI. This suggests that the malformed area and possibly the epileptogenic focus may not be restricted to abnormal regions seen on standard MRI. These findings are concordant with histopathological findings that show more widespread abnormal tissue than the extent seen on MRI. It could also explain the frequent bad outcome of epilepsy surgery in patients with cortical dysplasia. Post-operative histopathological analysis revealed subtle gliosis and a very good outcome confirmed that the epileptogenic zone was concordant with the diffusion abnormalities (Rugg-Gunn, Eriksson et al. 2002). Similarly, decreased FA values were found for the white matter underlying regions of polymicrogyric cortex (Trivedi, Gupta et al. 2006; Bonilha, Halford et al. 2007).

Tuberous sclerosis, an autosomal dominant condition with skin lesions and multiple cerebral malformative lesions (tubers) with a high epileptogenicity is another interesting application for diffusion imaging. The malformations are multifocal but resection of the main epileptogenic tuber can lead to significant improvement. Interestingly, epileptogenic tubers have increased ADC values in the white matter underlying them, when compared to non-epileptogenic tubers, whereas a decrease in FA values or the size of the tuber seem to be less specific markers (Jansen, Braun et al. 2003; Chandra, Salamon et al. 2006; Luat, Makki et al. 2007).

3.5.2.4 Cryptogenic focal epilepsy

In 10 patients with normal appearing conventional MRI, focal increase in mean diffusivity (8/10) or reduction in anisotropy (2/10) suggesting occult structural abnormalities that were concordant with electroclinical localisation in 7/10 patients (Rugg-Gunn, Eriksson et al. 2002). In one patient, surgical resection guided by these

findings lead to a marked improvement in seizure control and histopathological exam confirmed a focal cortical dysplasia.

3.5.2.5 Brain trauma and post-traumatic epilepsy

Increase of the mean diffusivity and decrease of the fractional anisotropy can be measured in widespread brain regions after brain trauma and the affected territories can be much more extensive than those seen on standard MR images. These changes probably reflect cell loss, diffuse axonal injury and secondary Wallerian degeneration in the corresponding regions, allowing to map precisely the post-traumatic damages (Wiesmann, Symms et al. 1999). Moreover, a greater extent of the abnormalities observed with diffusion imaging seems to be correlated with a greater risk of developing post-traumatic epilepsy (Gupta, Saksena et al. 2005).

3.5.2.6 “Pharmacological” imaging

Diffusion imaging could also be used to assess the impact of anti-epileptic drug treatment. For instance, transient lesions of the splenium of the corpus callosum (cytotoxic edema of probable glial origin) have been related to rapid AED withdrawal and linked to fluid imbalance via arginin vasopressin (Prilipko, Delavelle et al. 2005; Nelles, Bien et al. 2006). Moreover, long-term phenytoin affects cerebellar tracts (Lee, Mori et al. 2003). Diffusion imaging could also be used as a prognostic marker of cell damage after treatment for status epilepticus as suggested by animal studies (Engelhorn, Weise et al. 2007).

3.6 Tractography studies in focal epilepsy

Through the mapping of individual white matter tracts, there can be several contributions of tractography to epilepsy imaging. First it allows to extract diffusivity measures that relate to a particular tract (mean FA, mean MD, tract volume) and

could therefore be more relevant than the measurement of the same variable at a particular voxel, irrespective of tracts. Group analysis of these data can help understanding disease mechanisms. Analysis of tractography results in patients with focal epilepsy has been primarily done in patients with TLE and hippocampal sclerosis, a group of patients with homogeneous pathology (see below). Different methodology have been applied and have focused on measuring tracts abnormalities ipsi- and contra-lateral to seizure focus, measuring correlations between abnormal tract data and neuropsychological scores and have used tract measurements to predict post-operative deficit (visual field, language) or, rarely, to plan surgical strategy. Alternatively, anatomy of tracts in individual patients can be of great help in surgical planning.

3.6.1 Temporal lobe Epilepsy: Alteration of the limbic network and reorganisation of cognitive networks

Probabilistic tractography from the parahippocampal gyrus in patients with unilateral TLE and HS showed reduced ipsilateral tract volume and mean FA for left TLE but not for right TLE, with no clear correlation with hippocampal volume (Yogarajah, Powell et al. 2008). In other studies, the posterior corpus callosum (linking both temporal lobes) showed reduced FA in unilateral TLE (Kim, Piao et al. 2008), while bilateral changes in the limbic system (fornix and cingulum) have also been observed in unilateral TLE with HS, but not in non-lesional TLE (Concha, Beaulieu et al. 2009). Similarly, the thalamus seems to be affected predominantly in TLE with HS (Kim, Koo et al. 2010). The bilateral changes in diffusion properties of the limbic system (fornix) described above show an interesting evolution after surgery, ipsilateral abnormalities tend to worsen, suggesting post-operative Wallerian degeneration, while contralateral

changes do not normalise, contradicting the hypothesis that these might be reversible rather than clear-cut structural changes (Concha, Beaulieu et al. 2007).

3.6.2 Memory

In left TLE, FA of the tract seeded from the left parahippocampal gyrus was correlated with verbal learning scores and FA of the contralateral tract with non-verbal learning scores (Yogarajah and Duncan 2008). Therefore, tractography seemed to be a more reliable indicator of the integrity of memory networks than the simple measure of hippocampal volume. The lower FA of the ipsilateral uncinate fasciculus was correlated with lower verbal memory scores in left TLE (Diehl, Busch et al. 2008) and earlier age of disease onset (Lin, Riley et al. 2008). Using a tract atlas in TLE patients, changes in the uncinate, arcuate and inferior occipito-frontal fascicula have been found and correlated with neuropsychological scores for verbal memory and language, although no distinction was made between right and left TLE patients in the statistical analysis (McDonald, Ahmadi et al. 2008). A TBSS study explored post-operative changes in patients with TLE and hippocampal sclerosis (Schoene-Bake, Faber et al. 2009). Abnormal FA was found for temporal and extra-temporal tracts both in the ipsilateral and contralateral hemisphere but unfortunately, no pre-operative imaging was available making it difficult to discriminate between effect of disease or surgery.

3.6.3 Language

In patients with left hemispheric epilepsy, intracranial cortical mapping showed a good concordance between the localisation of the arcuate fasciculus mapped with tractography and the language cortex (Ellmore, Beauchamp et al. 2009), although the posterior language regions seem more dispersed than the anterior regions (Diehl,

Piao et al. 2010). FA of the arcuate fasciculus correlated with language fMRI asymmetry indices in right but not left TLE (McDonald, Hagler et al. 2008).

In order to map individual cortico-subcortical functional networks, recent studies have used language fMRI activation maxima as seed regions for tracking structural connectivity of language networks in TLE (Powell, Parker et al. 2007). Interestingly, language networks were less lateralised in left TLE than in right TLE and in controls, showing diffuse changes in extratemporal brain structures of TLE patients. While the principle of fMRI seeding has the advantage of accounting for a possible plasticity of the eloquent cortex in neurological disorders, its validity could be limited by imperfect coregistration between fMRI and diffusion images (see 2.3). In a further study, the same authors found greater post-operative naming difficulties after left temporal lobe surgery in patients with language tracts that were more strongly lateralised to the language dominant hemisphere (Powell, Parker et al. 2008). Post-operative FA increases after left anterior temporal lobe resection, suggesting compensatory plasticity occurred preferentially in the ventromedial language pathways and correlated with language performance (Yogarajah, Focke et al. 2010). In summary, temporal lobe epilepsy seems to be associated with extensive abnormalities of brain structural connectivity both locally and remotely, that are correlated to cognitive deficits. These findings point to the importance of studying subcortical pathways when evaluating functional networks.

3.6.4 Visual pathways

In temporal lobe epilepsy surgery, one of the most feared complications, besides memory decline, is post-operative visual field defect occurring via a lesion of the anterior loop of the optic radiation (Meyer's loop) when it is included in the resection area. Using tractography for mapping the optic radiation in individual patients, two studies found that patients with a resection volume including part of the radiation had

a post-operative visual deficit whereas others with surgery sparing the radiation had not (Powell, Parker et al. 2005; Nilsson, Starck et al. 2007). Two recent studies on larger patient groups (with 14 and 21 patients respectively) documented more precisely the anatomic variability of Meyer's loop, particularly the distance between its anterior aspect and the tip of the temporal lobe. Using deterministic tractography, the first study found that the extent of the post-operative visual field defect was correlated to the distance between the temporal pole and the anterior tip of Meyer's loop but not to the extent of surgical resection (Taoka, Sakamoto et al. 2005). The second study found that the anterior excursion of Meyer's loop was highly variable and more anterior than in the previous study (Yogarajah, Focke et al. 2009). This difference probably reflects a greater sensitivity provided by probabilistic tractography for imaging this region containing multiple crossing and kissing tracts. This study confirmed the association between visual field defect and the extent of surgical resection but also found that the distance from temporal pole to the tip of Meyer's loop was associated with the extent of visual field defect.

Tractography of the optic radiation, as well as other white matter bundles of nervous fibres could thus be used to tailor neurosurgical interventions (Kikuta, Takagi et al. 2008; Thudium, Campos et al. 2010). In a patient with an epileptogenic cerebral malformation (periventricular nodular heterotopia) adjacent to the optic radiation, tractography helped tailor the surgical resection and the patient had no post-operative deficit (Stefan, Nimsky et al. 2006).

3.6.5 Motor system

Tracking of the motor pathways can be based on seed regions defined by motor activation (Guye, Parker et al. 2003) or defined from anatomical landmarks. Tractography of the medial frontal cortex revealed two different clusters of seed voxels with distinct connectivity profiles with the other brain structures (Johansen-

Berg, Behrens et al. 2004). These regions of distinct connectivity showed good spatial concordance with the Supplementary Motor Area (SMA) and the pre-SMA as identified by specific fMRI activations (fingertapping and serial subtraction respectively).

Caution should prevail when planning surgery based on tractography results. A comparative study using both tractography and subcortical electrostimulation in two patients with glioma showed that tractography failed to show parts of the corticospinal tracts that were functionally relevant but the streamline methodology for tractography that was used is not the most sensitive technique (see section 3.3.1) (Kinoshita, Yamada et al. 2005).

3.6.6 Malformations of cortical development

Periventricular Nodular Heterotopia and Band Heterotopia are malformations of cortical development in which some neurons did not migrate from the subependymal region toward the cortex, but stayed packed around the ventricles (Periventricular Nodular Heterotopia) or in the subcortical regions, sometimes producing an appearance of “double cortex” (Band Heterotopia). In these patients, epileptic activity can arise from the heterotopia themselves or from other brain regions that appear normal on the standard MRI. Histopathological studies show that there are generally other sites of brain development disorder, either in the overlying cortex or at distant sites (Aghakhani, Kinay et al. 2005; Tassi, Colombo et al. 2005). The study of the connectivity of those structures indicates that white matter tracts run through or end within the band heterotopia (Eriksson, Symms et al. 2002) confirming histopathological studies and the fact that there is often no focal neurological deficit in these patients.

3.6.7 Tracking the propagation pathways of the epileptic activity

Some studies have proposed tractography to explore the structural connections underlying the propagation of epileptic activity. An important prerequisite to build reliable seed regions for tractography is a localisation of epileptic activity with a good spatial resolution. So far, only a few studies exist, which used localisation information gained from intracranial EEG (with the advantage of a high spatial resolution), MEG or IED-related BOLD changes to seed the tractography.

3.6.7.1 Combining scalp EEG-fMRI and tractography

Hamandi et al. investigated one patient with temporal lobe epilepsy (hippocampal sclerosis and temporal seizure onset on scalp-EEG) with a combination of EEG-fMRI and DTI (Hamandi, Powell et al. 2008). Widespread IED-related BOLD changes with strongest involvement in the medial temporal lobe and occipital lobe were found. Using a seed region in the medial temporal lobe and using probabilistic tractography, they obtained a tract suggesting direct connectivity between these regions. Having documented functional and structural connectivity between these regions involved in the epileptic network, the authors further investigated the effective (directional) connectivity of this network using Dynamic Causal Modelling (DCM, see chapter 2.7.3) on the regions BOLD changes. They found greater evidence for a flow of information from the medial temporal to the occipital region. Structural connections and pathways of propagation of epileptic activity between the occipital and temporal lobes are well documented and can be mapped with DTI (Catani, Jones et al. 2003). Propagation of epileptic activity generally occurs from the occipital to the temporal lobe but there are clinical cases with evidence of backward propagation (Jacobs, Dubeau et al. 2008), possibly through backward projection of the inferior longitudinal fasciculus (Catani, Jones et al. 2003). In this thorough exploration of the various approaches to study network connectivity at a functional and structural level, a quantitative study of the tract was unfortunately lacking. The study did not distinguish

between major tracts found in the occipito-temporal white matter and detectable by DTI such as the inferior longitudinal fasciculus and the optic radiatio (Jacobs, Dubeau et al. 2008). Moreover, the authors did not study whether the tract was altered compared to the contralateral hemisphere or better, to a group of controls. Generally speaking, the demonstration of a physiological tract could be a false positive connection if the tract happened to “cross through” the seed region and without fibres actually starting/ending at that location (like a motorway crossing someone’s backyard does not necessary mean there is an entrance on it). These studies help to understand pathways of propagation but the lack of quantitative description of the involved tracts means that no conclusion can be drawn with respect to the normality of abnormality of the tracts potentially involved in this network.

3.6.7.2 Combining MEG and tractography

As mentioned above (section 3.6.4), MEG was able to localise the source of epileptic activity in nodular heterotopia in the vicinity of the optic radiation mapped with tractography (Stefan, Nimsky et al. 2006). While this case is a good illustration of the benefit of combining multimodal imaging tools in presurgical evaluation, the connectivity of the heterotopic grey matter was not specifically studied.

Mohamed et al reported a case of gelastic seizures arising from a benign tumour (xantho-astrocytoma) located in the anterior cingulate gyrus (Mohamed, Otsubo et al. 2007). The child was seizure-free after removal of the lesion, suggesting seizure-onset in the immediate proximity to the lesion. The visualisation of preserved cingulate fibres with DTI tractography led the authors to postulate a propagation of epileptic activity from the lesion to the medio-temporal structures to explain the ictal semiology concordant with interictal epileptic discharges shown by MEG over the temporal regions. Unfortunately, this case does not provide more than what could have been postulated from anatomical knowledge of the connections of the limbic circuit in the normal brain. The demonstration of altered diffusion properties along the

cingulate fibers, compared to age-matched children would have given more insight into changes of this physiological bundle secondary to the focal lesion.

Two studies combined MEG and DTI to investigate the connectivity of the epileptogenic zone in groups of children. In the first study on localisation-related epilepsy caused by focal cortical dysplasia, reduced FA was found beyond visible lesions but close to MEG sources when results were compared to the contralateral hemisphere at group level (Widjaja, Zarei Mahmoodabadi et al. 2009). The FA of tracts known to project from the location of the lesions (based on published anatomical and neuroimaging studies) was also compared to tracts seeded from contralateral homologous regions. Quantifying changes in tracts rather than FA maps at voxel level gives a better evidence of altered connectivity over a longer range than simply documenting subtle structural changes at the site of a lesion, which could be unrelated to epileptic activity. Even then, analysing specific connections involved in propagation of the epileptic activity documented by other imaging methods would have strengthened the study. Another study from the same research group focused on children with temporal lobe epilepsy and found frontal MEG sources in addition to the temporal source in 6/23 children (Bhardwaj, Mahmoodabadi et al. 2010). In all 6 cases, tracking from a large region of interest in the frontal and temporal white matter revealed tracts connecting both regions via the external capsule in the affected hemisphere but not in the contralateral hemisphere. The authors suggested that these aberrant fronto-temporal connections could be the cause of the temporo-frontal spread of epileptic activity or the consequence of brain plasticity induced by chronic epileptic activity. Early onset of chronic epileptic activity might have prevented the physiological disappearance of these connections. Alternatively, a congenitally miswired brain could have generated fronto-temporal epileptic networks and more difficult to treat epilepsy. To confirm such abnormal tracts and dissociate between both hypotheses regarding their relation to epileptic activity, larger group studies of

patients with similar epilepsies are needed. These should investigate whether the age of onset is later than the habitual disappearance of such tracts in some patients, which would speak against an effect of the epileptic activity on tract remanence. Alternatively, the finding of such tract in patients without epilepsy (or before they develop it) would be in favour of the latter hypothesis.

3.6.7.3 Combining intracranial EEG and tractography

In a study combining icEEG with streamline tractography, Diehl et al, investigated pathways of seizure propagation in four patients with seizure onset in the posterior (occipito-temporo-parietal) cortex and very focal seizure activity for several seconds before distant propagation (Diehl, Tkach et al. 2010). They found reduced connectivity from the seizure onset zone compared to the homologous contralateral regions, suggesting that reduced structural connectivity could explain the delayed propagation. Regions close to the epileptogenic zone and tract originating from there have been shown to have reduced FA (Rugg-Gunn, Eriksson et al. 2001; Widjaja, Zarei Mahmoodabadi et al. 2009). Therefore this interesting icEEG-DTI study would have been enhanced if the tractography analysis had focused on connectivity changes in parts of the tracts involved in seizure propagation as shown by icEEG and not only on the global connectivity from the patch of cortex involved in seizure onset.

3.7 Perspectives

3.7.1 Structural connectivity of functional neuronal networks

The recent tractography studies mapping the structural connectivity of functional networks such as the language system have deepened our understanding of the effect of epilepsy on these networks. In clinical studies, similar seeding techniques allow to take into account the potentially altered localisation of brain function under the effect of the disease. Further studies targeting networks postulated to be altered by specific epileptic conditions are warranted.

Moreover, similar functional localising tools will increasingly be applied to estimate the structural connectivity of regions involved in the initiation and propagation of epileptic activity. However, their spatial accuracy will need to be critically assessed, as the investigated connections are likely to be less robustly tracked than the larger and anatomically well defined tracts subserving language, motor or visual functions. In that respect, the combination between intracranial EEG and tractography, explored in this work (chapter 9) is less prone to such mislocalisation and could be a valuable tool to test connectivity hypothesis in a limited number of patients.

3.7.2 Ongoing developments in MR tractography

In epilepsy surgery planning, the precision of tractography will increase with the development of algorithms solving the problem of fibre crossing. The knowledge of the white matter tracts could be combined with other imaging modalities into neuro-navigation devices helping the monitoring of surgery with imaging during the operation and predicting the occurrence of post-operative deficits, especially when combined with brain areas activated during fMRI tasks.

Recently, the measurement of diffusion in a greater number of directions has partly overcome the ambiguity of tracking in regions with fibre crossing (Behrens, Berg et al.

2007). State-of-the-art imaging includes Diffusion Spectrum Imaging and Q-ball Imaging that are not yet used routinely because of the duration of the acquisition and scientific expertise required for data processing (Hagmann, Jonasson et al. 2006).

Whole-brain connectivity can be represented using “connectivity matrices” containing the results of tracking between all pairs of regions of interest parcellated from the cortex (Hagmann, Cammoun et al. 2008). Initial studies suggested a brain connectivity core consisting in a backbone of connectivity “hubs” (Hagmann, Cammoun et al. 2008; Gong, He et al. 2009). Segregation of brain regions according to their connectivity is also possible with such approaches (Johansen-Berg, Behrens et al. 2004; Hagmann, Cammoun et al. 2008). Application of these techniques in clinical studies could reveal changes in the large-scale brain connectivity pattern related to chronic epilepsy and help explain cognitive deficits, remote imaging abnormalities or simulate the effect of resective surgery on the network.

3.8 Conclusion

Diffusion MRI and tractography allow imaging based on the displacement properties of the water molecules in the brain and these techniques are increasingly applied in research and clinical decision making. The reduction of scanning time and improvement of the imaging of fibre crossing are precious advances for increasing the clinical implementation. More research is needed to understand precisely the significance of quantitative alterations of tracts and determine whether this “miswiring” facilitates epileptic activity or whether it is chronic epileptic activity that alters the structural connectivity. Notably, longitudinal studies looking at the presence of progressing tract abnormalities, post-operative studies exploring modifications in tracts remote from the resection and investigations into structural propagation pathways of epileptic activity would give important insight into this problem. Application of these techniques for investigating the structural connectivity of epileptic networks is emerging and combination with functional localisation will increase our understanding of these networks with potential implications for epilepsy surgery.

SECTION 2

EXPERIMENTAL STUDIES

4 COMMON METHODS

This chapter describes common experimental methods that were used for more than one of the studies described in chapters 5-9. These methods reflect common practice in the epilepsy imaging group of the UCL Institute of Neurology as performed on the MR scanner of the National Society for Epilepsy (Chalfont St Peter, Bucks).

Methods used specifically for one study are described in the relevant chapters.

All research studies were approved by the Research Ethics Committee of the UCL Institute of Neurology and UCL Hospitals. All patients and controls gave written informed consent.

4.1 EEG-fMRI

4.1.1 EEG acquisition

EEG was recorded using MR-compatible systems EEG cap (Brain Products, Munich, Germany). A 32- or 64-channel EEG cap was used according to the 10-20 or 10-10 electrode position convention (30 resp. 62 recording scalp electrodes, 1 ECG electrode and 1 EOG electrode, used as redundant ECG electrode). Prior to MRI, EEG was recorded for 15 minutes with eyes closed outside the scanner.

Patients were then installed in the scanner with the EEG wires straightened and immobilised by sand bags to reduce induced currents. They were asked to lie still in the scanner with their eyes closed and no specific instruction regarding vigilance was given. EEG was recorded continuously during fMRI with a sampling frequency of 5000Hz that was synchronised to the scanner's 20 kHz gradient clock. A high-pass filter of 0.1 Hz and a low-pass filter of 250 Hz were applied after amplification but prior to data recording. ECG was recorded with a single lead on the same amplifier.

4.1.2 MRI acquisition

Each patient underwent 2 or 3 20-minute blocks of EEG-fMRI acquisition on a 3T Signa Excite HDX scanner (GE Medical Systems, Milwaukee, USA). Each fMRI dataset consisted of 404 T2*-weighted single-shot gradient-echo echo-planar images (EPI; TE/TR 30/3000 msec, flip angle 90, FOV 24x24cm², matrix size 64x64 for in-plane resolution of 3.75x3.75 mm, 43 interleaved slices with 3 mm thickness). A slice trigger was generated by the scanner for the acquisition of each EPI slice and was recorded by the EEG software for subsequent artefact correction.

For the purpose of anatomical localisation and EEG source localisation, we also acquired one volumetric 3D T1-weighted image including nasion and inion (matrix size 256x256x170, voxel size 1.1x1.1x1.1 mm³, resampled offline to 1x1x1 mm³ voxels for comparison with isotropic images created with the head model for ESI) as well as one high resolution EPI image.

4.1.3 EEG artefact correction and IED identification

Gradient artefacts from the scanner and pulse-related artefacts were removed offline from the EEG trace recorded during scanning using average artefact subtraction methods described elsewhere (Allen, Polizzi et al. 1998; Allen, Josephs et al. 2000). The artefact-corrected EEG was resampled to 250 Hz. Filtering of the EEG signals was needed to identify IED. Second order Butterworth Low and High pass filters (Low pass 35Hz, High pass 0.3Hz) with -12 db/octave roll-off were used. They were computed linearly with two passes (one forward and one backward), eliminating the phase shift, and with poles calculated each time to the desired cut-off frequency. Interictal Epileptiform Discharges (IED) were identified and marked consensually by two experienced electro-encephalographers (S Vulliemoz, R Thornton) (Salek-Haddadi, Diehl et al. 2006). Selection and

categorisation of IED was based on a) location and morphology of the individual IED and b) EEG voltage topography. In one patient (patient 5) with very frequent IED (>50/min), we used a spike detection software algorithm based on spatio-temporal correlation (BESA, MEGIS software GmbH, Penzberg, Germany) and subsequently reviewed the detected IED to correct for false positive markers.

4.1.4 EEG Source Imaging (ESI)

The IED used for fMRI modelling were analysed using an ESI methodology implemented in *Cartool* (<http://brainmapping.unige.ch/Cartool.htm>).

For the head model, we used a Spherical head Model with Anatomical Constraints (SMAC) based on a 3-shell spherical realistic head model and the patient's individual MRI (Spinelli, Andino et al. 2000). The source space was limited to the grey matter, segmented using the Statistical Parametric Mapping software SPM5 (www.fil.ion.ucl.ac.uk/spm). Solution points were sampled isotropically in the spheric grey matter with around 3000 to 4000 points (intersubject variations) representing a mesh of about 5x5x5 mm (with some distortion caused by the back transformation into the individual brains. A standard localisation of the electrodes according to the 10-20 system was assumed to obtain electrode coordinates.

Estimation of the location of intracranial generators was carried out using a linear distributed inverse solution (LAURA) (Grave de Peralta Menendez, Gonzalez Andino et al. 2001). This source imaging favours a smooth distribution of source activity and incorporates the biophysical constraints that the strength of a source regresses regularly with distance between solution points (Michel, Murray et al. 2004). The parameters used for the LAURA calculation were fixed to a neighbourhood size of 26 solution points and a regression with the inverse of the cubic distance (for vector

fields). The regularization parameter was fixed to Alpha=1 for all maps (Pasqual Marqui, Sekihara et al. 2009).

After filtering (high-pass: 0.3 Hz, low-pass: 35 Hz), IED were averaged and channels containing artefacts were interpolated. To estimate the IED source, we used the time point corresponding to the half maximum of the first rising phase of the global field power of the averaged IED. This was previously reported to be the best estimation of the source of IED onset (ESIo) (Lantz, Spinelli et al. 2003). ESI of propagation areas of IED (ESIp) were defined as maximum source activity around the first or second maximum of the Global Field Power (GFP) that involved a different cortical region than ESIo. The GFP is defined as the sum of all squared potential differences between electrodes which is equivalent to the standard deviation of the potentials (Lehmann and Skrandies 1980):

$$\text{GFP} = \sqrt{\frac{\sum_{i=1}^N (u_i - \langle u \rangle)^2}{N}}$$

Where u_i is the voltage of the map u at the electrode i , $\langle u \rangle$ is the average voltage of all electrodes of the map u and N is the number of electrodes of the map u .

4.1.5 fMRI processing and statistical analysis

After discarding the first four image volumes, necessary to reach T1 stability, the fMRI time-series were realigned and spatially smoothed with a cubic Gaussian kernel of 8 mm full width at half maximum. fMRI time-series data were then analysed using a GLM implemented in the SPM5 software package (www.fil.ion.ucl.ac.uk/SPM) to determine the presence of regional IED-related changes of the BOLD signal. For each patient, a separate set of regressors in the same GLM was formed for each type of epileptiform discharge identified in the EEG, allowing the identification of specific BOLD effects. For this purpose,

discharges were modelled as zero-duration events (unit impulse, or 'delta', functions) and convolved with the canonical Haemodynamic Response Function (HRF) as well as its temporal and dispersion derivatives, to account for deviations from the canonical time course. This resulted in three regressors for each event type (Friston, Fletcher et al. 1998). Motion-related effects were included in the GLM in the form of 24 regressors representing the Volterra expansion of the 6 realignment parameters (Friston, Williams et al. 1996), plus combinations of Heaviside step functions accounting for large motion effects ('scan nulling' regressors with 0.5 mm threshold) (Lemieux, Salek-Haddadi et al. 2007). An additional set of cardiac confound regressors was included to account for pulse-related signal changes (Liston, Lund et al. 2006). A high-pass filter of 128s was included to eliminate BOLD changes caused by slow scanner drift.

SPM-{F} contrasts were used across the three regressors corresponding to each event type to generate F-maps with a significance threshold of $p < 0.05$ corrected for multiple comparisons (family-wise error). The sign of the BOLD response at a given cluster was assessed by plotting the fitted response. In discordant cases (see below for definition), additional uncorrected F-maps ($p < 0.001$, uncorrected, cluster size > 10 voxels) were visually inspected to check for supra threshold changes in the suspected epileptogenic zone. Maps of significant BOLD responses were overlaid onto high-resolution EPI images and T1-weighted volumetric images after co-registration to the EPI images, allowing for anatomical localisation (Ashburner and Friston 1997).

4.2 Diffusion imaging and tractography

4.2.1 Acquisition and preprocessing

Whole brain diffusion-weighted cardiac gated single-shot echo planar images (TE 73 ms, 60 contiguous 2.4 mm thick axial slices) were acquired in the same session as fMRI. Diffusion sensitizing gradients were applied in each of 52 non-collinear directions (maximum b value 1200mm²/s) along with 6 non-diffusion weighted scans (b0) (Cook, Symms et al. 2007). Acquisition time was approximately 25 minutes, depending on heart rate. Field of view was 96x96 filled to 128x128 leading to reconstructed voxel size of 1.875 x 1.875 x 2.4 mm³.

The images were corrected for eddy currents and two diffusion tensors were fitted to the data as previously described (Powell, Parker et al. 2006). For the fitting of the diffusion tensors, the spherical-harmonic voxel classification algorithm was used to select voxels in which one tensor fitted the data poorly (Alexander, Barker et al. 2002). In these voxels, a mixture of two gaussian probability density functions were fitted to the data to obtain the two principal directions of diffusion and estimate the direction of the crossing fibres. The eigenvalues of the diffusion tensor were used to calculate maps of fractional anisotropy (FA image) and mean diffusivity (MD image). A non-diffusion weighted b0 image (mean of the 6 b0 images) was also created.

4.2.2 Tractography and quantitative tract analysis

After selection of a study specific seed region and masks (see chapters 8 and 9), probabilistic tractography was carried out with the PiCo (Probabilistic Index of Connectivity) algorithm extended to cope with multiple fibres, in the Camino package (www.cs.ucl.ac.uk/research/medic/camino/) (Parker and Alexander 2003). All studies used 5000 Monte Carlo iterations (angular threshold 80°, FA threshold 0.1) and tract interpolation (Powell, Parker et al. 2006; Yogarajah, Focke et al. 2009).

The post-processing of the tracts was done in FSL (FMRIB Software Library : www.fmrib.ox.ac.uk/fsl/) and SPM5. The tracts were then normalised to a standard space by normalising the individual FA image to the FA template in FSL (FMRIB58_FA_1mm.nii) using the default non-linear normalisation tool available in SPM5 and by applying the same normalisation matrix to the individual tracts and seeds. The volume of the normalised tract (nTV) was calculated after normalisation to take account of variable head size (Powell, Parker et al. 2006). Commonality maps were then built by averaging the thresholded and binarised normalised tracts seeded from the same regions (Powell, Parker et al. 2006). For each brain voxel, these maps therefore represent the proportion of subjects in whom the voxel belongs to the tract.

5 SPATIO-TEMPORAL MAPPING OF EPILEPTIC NETWORKS USING SIMULTANEOUS EEG-fMRI AND EEG SOURCE IMAGING

5.1 Summary

Objectives: We investigated whether electrical source imaging (ESI) performed on the interictal epileptiform discharges (IED) acquired during fMRI acquisition could be used to study the dynamics of the networks identified by the BOLD effect, thereby avoiding the limitations of combining results from separate recordings.

Methods: Nine selected patients (13 IED types identified) with focal epilepsy underwent EEG-fMRI. Statistical analysis was performed using SPM5 to create BOLD maps. ESI was performed on the IED recorded during fMRI acquisition using a realistic head model (SMAC) and a distributed linear inverse solution (LAURA).

Results: ESI could not be performed in one case. In 10/12 remaining studies, ESI at IED onset (ESIo) was anatomically close to one BOLD cluster. Interestingly, ESIo was closest to the positive BOLD cluster with maximal statistical significance in only 4/12 cases and closest to negative BOLD responses in 4/12 cases. Very small BOLD clusters could also have clinical relevance in some cases. ESI at later time frame (ESIp) showed propagation to remote sources co-localised with other BOLD clusters in half of cases. In concordant cases, the distance between maxima of ESI and the closest EEG-fMRI cluster was less than 33 mm, in agreement with previous studies.

Discussion: Simultaneous ESI and EEG-fMRI analysis may be able to distinguish areas of BOLD response related to initiation of IED from propagation areas. This combination provides new opportunities for investigating epileptic networks.

5.2 Introduction

A few studies have evaluated the concordance between various ESI methodologies (single or multiple equivalent dipole, distributed solutions, Bayesian approaches) and EEG-fMRI results in focal epilepsy (Seeck, Lazeyras et al. 1998; Lemieux, Krakow et al. 2001; Bagshaw, Kobayashi et al. 2006; Benar, Grova et al. 2006; Boor, Jacobs et al. 2007; Grova, Daunizeau et al. 2008) but the ESI and EEG-fMRI analyses were not performed on simultaneously acquired datasets (see Chapter 2.6.2.). All studies found a good degree of spatial concordance between ESI results and EEG-fMRI but also stressed the intrinsically different underlying neurophysiological mechanisms for each measurement: ESI directly images synchronised synaptic activity whereas fMRI measures a resulting mixed contribution of focal metabolic and perfusion changes.

In the present study we combined ESI and EEG-fMRI in patients with focal epilepsy in order to test the following hypotheses:

- 1) BOLD responses coupled to onset vs. propagation of IED can be discriminated using the high temporal resolution of simultaneous ESI.
- 2) The cluster with the most significant positive BOLD response is not always a good localiser of the region of IED onset (as identified using ESI).
- 3) Negative BOLD changes can be spatially concordant with the estimated source of IED onset. They can therefore have localising value and they are not only a reflection of distant upstream or downstream effects.

5.3 Methods

5.3.1 Patients and electro-clinical data

Patients with refractory focal epilepsy undergoing pre-surgical assessment were selected from our database of EEG-fMRI at 3T between January 2004 and July 2008 according to the following criteria:

1) intra-MRI EEG recording with 32 electrodes or more;

2) presence of spikes, spike-waves or sharp waves on the intra-MRI EEG. Interictal epileptic transients in the form of short runs of low amplitude high frequency poly-spikes were not considered as they have poor signal-to-noise ratio for ESI and are best modelled as blocks for the EEG-fMRI analysis (Bagshaw, Hawco et al. 2005);

3) presence of a significant IED-related BOLD response ($p < 0.05$, Family-wise error correction for multiple voxel comparisons).

Nine patients were thus identified fulfilling the criteria (one EEG-fMRI recording each). In total, 12 types of IED were identified and used for analysis, resulting in 12 spike-type specific analyses. Clinical, electrophysiological and imaging data of the patients are given in Table 5.1. All patients had cryptogenic focal epilepsy except for patient 4 who had focal cortical dysplasia in the left medial occipital cortex.

Case	Gender, age	Seizure semiology	IED localisation on scalp EEG used for fMRI modelling	Number of IED used for fMRI modelling (Number of 20 min fMRI sessions)	MRI
1a	M, 31y.	Bizarre undetailed sensation,	R mid temporal	103 (2) *	N
1b		CPS with	R post temporal	17 (2) *	
1c		dystonic posture L hand	R occipito-temporal	69 (2)	
2	M, 30y.	Aphasic SPS No aura, CPS	L temporal	161 (2)	N
3	F, 48y.	No aura, CPS with oral and manual automatisms	L temporal	197 (2)	N
4a	M, 21y.	CPS, oral automatisms, R clonic jerks, SGS	L temporal	312 (2) *	FCD L medial occipital
4b			R temporal	56 (2)	
5	M, 27y.	Cloni R face/arm --> SGS	R frontal	2239 (2)	N
6a	M, 22y.	No aura, CPS with L head version	Bil frontal	269 (3)	N
6b			Bil frontal polyspikes	101 (3)	
7a	F, 37y.	No aura, CPS	L frontal	23 (2)	N
7b			Bil frontal	49 (2)	
7c			R frontal	11 (2) *	
8a	M, 19y.	Epilepsia partialis continua L leg --> rare SGS	R fronto-central	121 (3)	N
8b			central midline	206 (3)	
8c			R frontal	10 (3) *	
9a	M, 25y.	Epigastric , auditory, gustatory or heautosopic aura, tonic posture R hand	L fronto-temporal	38 (3)	N
9b			L fronto-polar	35 (3) *	
9c			L parietal	23 (3) *	

Table 5.1: Clinical, electrophysiological and radiological data

R/L/Bil : right/left/bilateral; post : posterior; SPS/CPS : Simple/Complex Partial Seizure, SGS : Secondly Generalised Tonic Clonic Seizure, FCD : Focal Cortical Dysplasia. *: no significant IED-related BOLD change revealed and not considered individually further for ESI.

Three patients underwent intracranial EEG investigations: In patient 1, a subdural grid with 6x8 contacts was placed over the right temporal cortex. One additional subdural strip electrode (1x8 contacts) was placed over the temporo-parietal cortex and 2 depth electrodes (6 contacts) targeted the right amygdala and anterior hippocampus. In patient 5, 8 depth electrodes with 15 contacts were placed stereotactically in the right hemisphere: 6 orthogonal electrodes (medial/lateral contacts); i) orbito-frontal antero-medial/orbito-frontal lateral; ii) anterior cingulate gyrus/dorso-lateral prefrontal; iii) insula/fronto-opercular (pars opercularis); iv) insula/fronto-opercular (pars orbicularis); v) supplementary motor area/dorsal premotor cortex; vi) amygdala/middle temporal gyrus; 2 oblique electrodes: i) orbito-frontal postero-medial/fronto-polar; ii) dorsomedian thalamus / dorso-lateral-premotor and 1 electrode was placed in the left hemisphere: orthogonal electrode: anterior cingulate gyrus/dorso-lateral prefrontal. In patient 8, 4 electrodes (15 contacts) were implanted in the right hemisphere: 3 orthogonal electrodes: i) anterior cingulate gyrus/dorsolateral prefrontal; ii) supplementary motor cortex/dorsal premotor cortex; iii) paracentral lobule/precentral lateral); 1 oblique electrode: postcentral / medial superior parietal lobule.

5.3.2 EEG-fMRI acquisition

Data acquisition was performed as described in section 4.1.

Patients P4, P8 and P9 had EEG with 62 recording electrodes and the others with 30 recording electrodes.

5.3.3 Analysis

EEG and fMRI analysis were performed as described in section 4.1.

The IED identified on the corrected EEG (see section 4.1.3) were used for ESI (see section 4.1.4) and for fMRI analysis (SPM{F}-maps, see section 4.1.5).

In four patients a total of 7 IED types were found not to be associated with significant BOLD changes (see below for description of fMRI analysis) and therefore were not considered further (see Table 5.1). In patient 1 three sets of IED were identifiable from the scalp EEG (case 1a: right mid-temporal, case 1b: right posterior temporal; case 1c: right occipito-temporal) and were considered separately for fMRI modelling and ESI in an initial analysis, 1c alone being associated with significant BOLD changes. Since their sites of origin were presumably very close to each other we performed an additional fMRI analysis by merging all three types of event, giving a grand total of 13 analyses.

5.3.4 Assessment of concordance

5.3.4.1 Concordance between BOLD changes and ESI

SPM{F}-maps (with FWE corrected threshold) showing BOLD signal changes and ESI results, were overlaid on T1-weighted anatomical MR images. We then selected the anatomically concordant BOLD clusters (i.e. located in the same lobe as the ESI-derived source) whose maxima were closest to ESlo and ESIp, respectively. When visual anatomical concordance was found, the Euclidian distance between ESlo/ESIp maximum and the maximum of the closest BOLD cluster was measured using MRlcro (www.sph.sc.edu/comd/rorden/mricro.html). ESI and BOLD clusters were considered discordant if in different lobes and separated by a major anatomical fissure or sulcus (sylvian or interhemispheric fissure), so that neighbouring frontal/parietal or parietal/temporal regions for instance were not considered

discordant a priori although located in different lobes. ESI and BOLD cluster with lateral vs. medial temporal localisation were also considered discordant. In addition the localisation of the BOLD cluster containing the global maximal positive response was identified for spatial comparison with ESlo and ESlp.

5.3.4.2 Concordance with intracranial EEG results

When available, results of intracranial EEG were compared with our results. The position of the intracranial electrode contacts was assessed visually on MRI T1-weighted images acquired after electrode implantation. The anatomical position of contacts inside the irritative zone was compared to the ESI and EEG-fMRI results.

5.4 Results

ESI and BOLD results are summarised in Table 5.2.

Table 5.2 : EEG-fMRI and ESI results (next page)

FWE : Family Wise Error correction, unc. : uncorrected ; R/L/Bil : Right/Left/Bilateral, ant/post: anterior/posterior, sup/mid/inf : superior/middle/inferior, mes/lat :medial/lateral. NA : not available.

Case	EEG focus (total IED)	Main BOLD+ cluster (F-test, FWE)	ESI onset	closest BOLD (mm) (F-test, FWE)	ESI Propagation	closest BOLD (mm) (F-test, FWE)	Intra-cranial EEG IED
P1c	R occipito-temporal (69)	Only BOLD neg R occipito-temporal	R occipito-temporal	- 25	Idem	+ 19	R lat mid- and post temporal
P1a	R mid-temp	Joint analysis : R ant cingulate	R lat mid-temp	NA	R mes temporal	+ 10	“
P1b	R post temp		R post-temp	(+ unc) NA	-		
P1c	R occip-temp (total 189)		R occip-temp	-			
P2	L temporal (161)	L inf temporo-occipital	L lat temporal	- 19 + (max) 51	L mes temporal	NA NA	
P3	L temporal (197)	L insula & L opercular frontal	L lat temporal	- 6 + 30	L mes temporal	+ 6	
P4b	R temporal (56)	R temporo-parietal (unc: R insula, R inf lat temporal)	R lat ant temporal	NA NA	R mid frontal	NA NA	
P5	R frontal (2239)	R>L mes sup frontal	L>R medial orbito-frontal	+ contralat (max) 10	R lat inf frontal	+ 17	R medio-orbito-frontal and medial prefrontal
P6a	Bil frontal (269)	R sup frontal	R ant frontal	+ 16	L mes frontal	+ 25	
P6b	Bil frontal polyspikes	R sup frontal	NA		NA		
P7a	L frontal (23)	L mid frontal	L inf frontal	+ 32	L mid frontal	+ 11	
P7b	Bil frontal (49)	L mid frontal	L mid frontal	+ (max) 19	R sup frontal	NA (+ unc) NA	
P8a	R fronto-central (121)	R mid frontal (R sup frontal)	R sup frontal	+ (max) 9	L mid frontal	NA NA	R medial fronto-parietal
P8b	central midline (206)	R frontal midline	L frontal midline	+ contralat (max) 31	R mid frontal	NA (+ unc) NA	“
P9a	L fronto-temporal (38)	Only BOLD neg: L opercular fronto-temporal	L lat temporal	- 33	L mes temporal	NA NA	“

5.4.1 Concordance at IED onset (ESIo)

In 1/13 analyses with a significant BOLD response, the averaging of bilateral frontal polyspikes had low SNR, did not show a stable scalp topography and therefore did not allow reliable source localisation, so that this study was discarded (patient 6b). In 9/12 remaining IED studies, we found good anatomical concordance between ESIo and one cluster of BOLD response, which also matched other electro-clinical localisation. In 2 studies with inter-hemispheric source activity (patient 5, patient 8b), ESI showed bilateral medial frontal localisation with maximum activity in the hemisphere contra-lateral to the BOLD maximum which itself was concordant with the electro-clinical localisation; according to our strict definition of concordance based on the localisation of the maximum of the ESI solution these results must be labelled as discordant. In 2 other studies of temporal IED (studies 1a and 4), discordance corresponded to large separation within a lobe (medial vs. lateral temporal lobe in study 1a; temporal-parietal vs. lateral anterior temporal in study 4b).

In 4/12 studies, the BOLD cluster containing the global statistical maximum (and corresponding to positive BOLD changes) was the closest to ESIo. In 4/12 studies the cluster closest to ESIo corresponded to a negative BOLD change. In 2 of these cases, the closest positive BOLD cluster was in the same lobe as ESIo but more distant than the cluster corresponding to negative BOLD changes. In the two other cases, there were only negative BOLD changes.

The mean peak-to-peak Euclidian distance for the concordant cases was 23 ± 9 mm (range: 6-33 mm). When including the two cases with frontal medial ESIo lateralised to the hemisphere contralateral to electro-clinical localisation, the distance values were 20 ± 10 mm (6-33 mm). In these two cases, the maximum voxel was projected across the midline for distance measurement. Distance was

not measured in the remaining 2 discordant cases (patient 1: medial vs. lateral temporal lobe; patient 4b: temporal pole vs. temporo-parietal junction).

5.4.2 Concordance in IED propagation areas (ESIp)

In 6/12 IED studies, ESIp showed good concordance with one BOLD cluster that was positive in each case. The Euclidian distance for these concordant cases was 15 ± 7 mm (6-25 mm). In the 6 other cases, visual inspection of the uncorrected SPM{F}-maps showed concordant uncorrected positive BOLD clusters in 2 cases but no concordant BOLD in the remaining cases.

5.4.3 Comparison with intracranial EEG results

In patient 1, subdural grid electrodes recorded right lateral mid-temporal and lateral posterior temporal IED confirming our ESlo findings of separate temporal IED (Table 5.1). The largest and most diffuse of these lateral temporal IED showed concomitant involvement of the medial temporal lobe (amygdala and anterior hippocampus) and small independent IED were also recorded in isolation in the medial temporal lobe. The joint analysis of the 3 types of temporal/temporo-occipital IED showed right medial temporal BOLD changes and a BOLD maximum in the ipsilateral cingulate.

In patient 5, depth electrodes showed an irritative zone predominating in the right orbito-frontal and medial prefrontal cortex, concordant with ESlo and the associated BOLD cluster. Much fewer IED were observed in the right supplementary motor area (medial posterior frontal) corresponding to the maximum positive BOLD cluster. The maximum negative BOLD change was localised in the ipsilateral precuneus.

In patient 8, depth electrodes showed IED originating from the medial fronto-parietal cortex (para-central lobule and medial superior parietal lobe), confirming the agreement between ESlo and the BOLD response.

5.4.4 Illustrative cases

Figure 5.1 shows an example of concordance (patient 5, right frontal IED). Here, the combination of ESI and EEG-fMRI allowed identification of the orbito-frontal BOLD cluster closest to the source of the irritative zone estimated by ESI and revealed temporal patterns suggestive of propagation from medial to lateral frontal cortex. This localisation of the irritative zone was subsequently confirmed by intracranial recording. However, the maximum positive BOLD cluster (supplementary motor area) did not correspond to the areas principally involved in IED generation. The most significant voxel showing a BOLD decrease in the retrosplenial region was consistent with previous reports of IED-related BOLD changes in cortical regions involved in the “default mode” network (Kobayashi, Bagshaw et al. 2006; Laufs, Hamandi et al. 2007).

Figure 5.2 illustrates patient 3 (left temporal IED) with a negative BOLD cluster as the closest cluster to IEDo (lateral temporal), and subsequent propagation closest to a positive BOLD cluster (medial temporal). The most significant cluster of positive BOLD response was in the left insular cortex. As in patient 5, the maximal negative BOLD response was in regions typical of the default mode network (not seen on the slice presented in this figure). Both positive and maximal were discordant with ESI.

Figure 5.3 shows discordant results for ESlo and the BOLD response in patient 1 (combined right temporal IED). ESlo of case 1a shows a right lateral temporal activity that propagates to right medial temporal regions. There was no concordant

BOLD response for ESlo in the lateral temporal cortex. However, there was a right medial temporal positive BOLD response concordant with ESIp. Intracranial recording confirmed IED originating from the right mid- to posterior temporal neocortex.

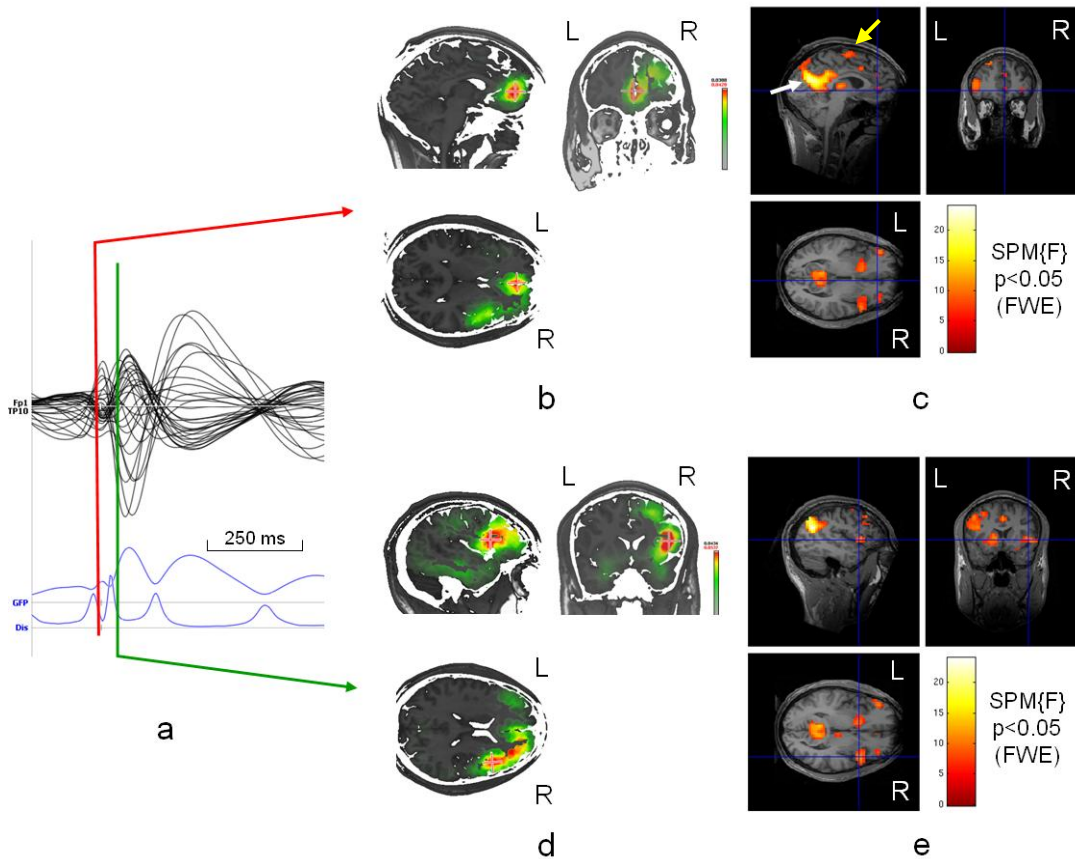


Figure 5.1: ESI concordant with very small positive BOLD changes

Patient 5: a) Averaged intra-MR IED. The first rising phase of the averaged IED and Global Field Power is used for IED onset (ESlo, red line) and a later timeframe for IED propagation (ESlp, +88 ms, just after the second maximum of the averaged IED, green line); b) EEG source imaging at IED onset (ESlo) in orbito-frontal cortex (bilateral but maximum in left hemisphere); c) Right orbito-frontal BOLD cluster concordant to ESlo (positive BOLD response, cross-line at maximum). The positive statistical maximum is localised in the right supplementary motor cortex (yellow arrow). The highly significant BOLD response in the medial parietal cortex corresponds to the maximum negative BOLD response, localised in the “default mode” network (white arrow); d) EEG source imaging just after second maximum of the averaged IED showing a shift of maximal source activity to frontal-opercular region (ESlp); e) Right lateral frontal BOLD cluster closest to ESlp (positive BOLD response, cross-line at maximum). Intracranial EEG was concordant with ESlo (see section 5.4.3).

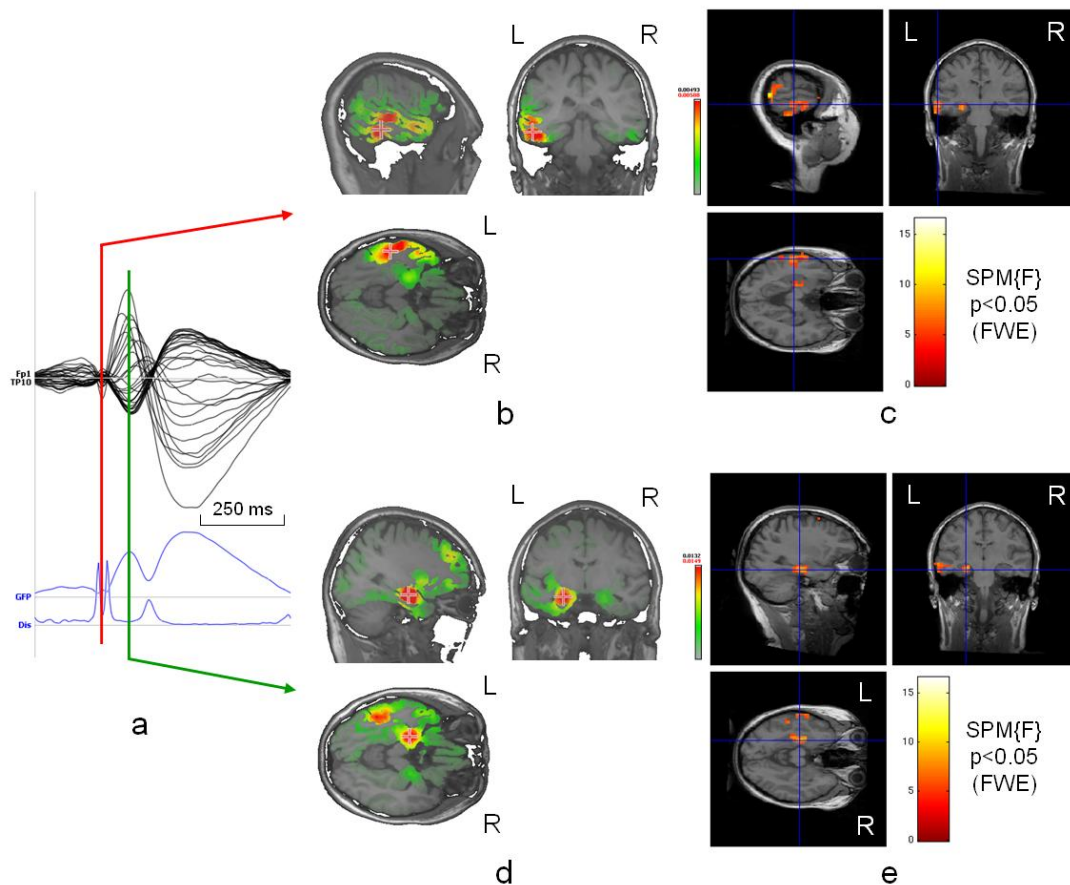


Figure 5.2: ESI concordant with negative BOLD changes

Patient 2: a) Averaged intra-MR IED. The rising phase of the averaged IED and Global Field Power is used for IED onset (ESlo, red line) and a later timeframe for IED propagation (ESlp, +96 ms, second maximum of the averaged IED, green line); b) EEG source imaging at IED onset (ESlo) in left lateral temporal cortex; c) Left lateral temporal BOLD cluster concordant to ESlo (negative BOLD response, cross-line at maximum), the positive statistical maximum is in the left insula (not seen); d) EEG source imaging of the second maximum phase of the averaged IED showing a shift of maximal source activity to left medial temporal lobe (ESlp); e) Left medial temporal BOLD cluster concordant with ESlp (positive BOLD response, cross-line at maximum).

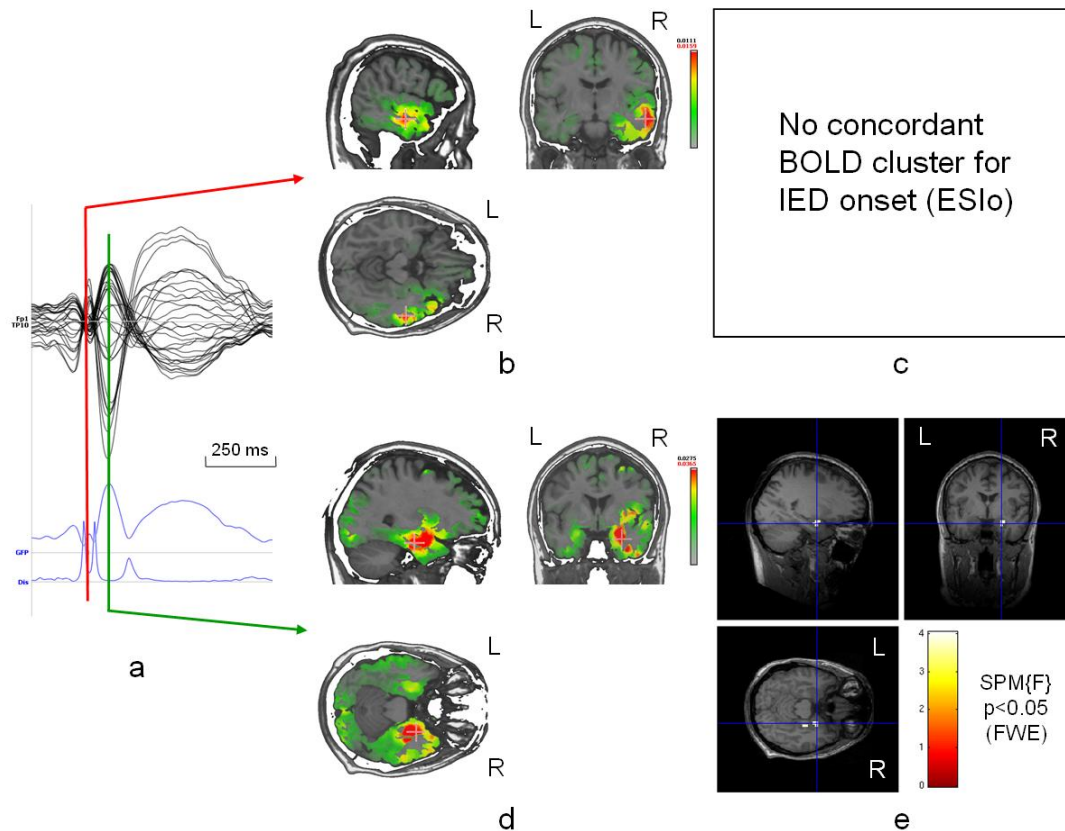


Figure 5.3: Discordant ESI and BOLD changes

Patient 1: ESI and EEG-fMRI SPM{F} map (canonical HRF and 2 derivatives, FWE corrected) overlaid on coregistered T1-weighted image; a) Averaged intra-MR IED of the most frequent IED (right temporal). The first rising phase of the averaged IED and Global Field Power is used for IED onset (ESlo, red line) and a later timeframe for IED propagation (ESlp, +80 ms, second maximum of the averaged IED, green line); b) EEG source imaging at IED onset (ESlo) in right lateral temporal cortex; c) there is no concordant medial temporal BOLD response, even for aggregated IED (right temporal, right posterior temporal, right temporo-occipital); d) EEG source imaging of the next maximum of the averaged IED showing a shift of maximal source activity to right medial temporal lobe (ESlp); e) Right medial temporal BOLD cluster concordant with ESlp (positive BOLD response for aggregated IED, cross-line at maximum); the positive statistical maximum is in the right anterior cingulate cortex (not seen). Intracranial EEG was concordant with ESlo (see section 5.4.3).

5.5 Discussion

The purpose of this study was to use ESI in order to extract more information from the temporally blurred BOLD patterns revealed by EEG-fMRI analysis. In this respect, the temporal resolution of ESI and its feasibility on the same dataset seems an ideal combination.

We were able to validate our starting hypotheses: the source of IED onset estimated with ESI was concordant with one fMRI BOLD cluster in 10/12 feasible cases and propagation to another concordant fMRI BOLD cluster was demonstrated in half of the cases. Moreover, the statistical maximum of BOLD changes was concordant with the electric source in a minority of cases and negative BOLD changes could also be concordant with the electric source.

Our study compared BOLD correlates of IED to electric source imaging performed on the same set of IED acquired inside the MR scanner. This represents an important step when comparing non-invasive modalities and opens the possibility of including features of single events to model BOLD signal changes (amplitude, morphology, spectral characteristics), as has previously been applied to event-related potentials (Debener, Ullsperger et al. 2005). Moreover the analysis of simultaneously acquired data eliminates bias associated with separate single modality sessions, such as the spatial extent and propagation of IED which may be altered by experimental conditions and clinical context (i.e. sleep-wake stage, medication, time since last seizure). This is particularly relevant in epilepsy as the pattern of spontaneous IED generation cannot be identically reproduced across sessions. Using the same set of IED for both analyses is methodologically stringent from the viewpoint of the comparison of the results of both modalities but this is not standard practice for ESI, as studies usually include only selected spikes with good signal to noise ratio.

Our aim was not to assess whether ESI or fMRI was better at localising the epileptic focus with respect to intracranial EEG recording as a gold standard. Good concordance between ESI, EEG-fMRI and subdural grid EEG recording in a single patient has been reported in an early EEG-fMRI paper (Seeck, Lazeyras et al. 1998) and, more recently, a study of 5 patients with focal epilepsy concluded that the results of ESI using multiple equivalent dipoles and clusters of significant BOLD responses were concordant both with each other and with intracranial recording (Benar, Grova et al. 2006). Another study using a distributed inverse solution also showed good concordance between both modalities and intracranial EEG recordings in 3 patients with focal epilepsy (Grova, Daunizeau et al. 2008). Concordance between ESI and BOLD increases confidence in both modalities and therefore in the localising information they provide. In our study, intracranial EEG recordings confirmed the spatio-temporal pattern of propagation in the 3 patients for which they were available.

Previous studies evaluated the concordance of ESI and BOLD responses to IED in focal epilepsy using different ESI methodology but always acquired the EEG recording for the ESI in a separate session outside the scanner, generally with additional electrode coverage (Lemieux, Krakow et al. 2001; Benar, Grova et al. 2006; Boor, Jacobs et al. 2007; Grova, Daunizeau et al. 2008). Our study shows that MR-related EEG artefacts and the application of correction algorithms do not preclude ESI on intra-MR EEG. This is consistent with previous studies which reported only minor distortion of IED after EEG correction, compared to outside the scanner environment (Benar, Gross et al. 2002; Benar, Aghakhani et al. 2003; Salek-Haddadi, Lemieux et al. 2003; Salek-Haddadi, Diehl et al. 2006).

5.5.1 Concordance and sources of uncertainties

An exact overlap between fMRI and ESI results is not expected due to the different nature of the two signals: EEG arises from the sum of synchronised post-synaptic activity while BOLD response originates from haemodynamic changes related to total synaptic activity, this signal being partly localised at the site of metabolic change and partly in distally draining veins, the latter effect being dependent on the scanner field strength (Logothetis, Pauls et al. 2001; Turner 2002). Additionally, changes in EEG and BOLD signal might be caused by different cellular populations which might or might not overlap spatially (Nunez and Silberstein 2000). Experimental measurements on the sensory cortex of monkeys showed an average distance of 10 mm between activated subdural micro-electrodes and fMRI centroids in 45% of observations (Disbrow, Slutsky et al. 2000). In this work, there was good agreement when measuring distances between peak local field potential, estimated with ESI, and the maximal activated voxel in the nearest BOLD cluster in order to quantify the spatial concordance between the two techniques and 6-33 mm are within the range of the above studies in animals, considering the added uncertainty of ESI. The possible sources of error in our ESI analysis include the ill-posed nature of the inverse problem, the use of standardised electrode positions (based on the 10-20 electrode position system), a sampling distance of 4-6 mm between solution points and the bias towards superficial sources. Regarding fMRI data, distortion and drop-out of fMRI signal especially at air-tissue interfaces, smoothing of fMRI data and coregistration of anatomical and EPI images can lead to degradation in sensitivity and localisation accuracy. Furthermore, the varying number of spikes captured during the EEG-fMRI recordings is an additional source of uncertainty, which affects both modalities equally but makes inter-subject comparisons more difficult.

All the above factors contribute to the inter-subject variability of the peak-to-peak distance observed in our study. It must be emphasized, however, that epileptic activity can never be pinpointed to a cortical region at a microscopic level because it involves the participation of large neuronal networks. IED detectable on the scalp EEG and hence modelled with either ESI or EEG-fMRI require the involvement of at least 6 cm² of cortex (Tao, Baldwin et al. 2007). This argues in favour of our choice of a sub-lobar scale for determining spatial concordance between the electro-clinical data and the two imaging techniques. Our spatial concordance is better than that reported in previous studies comparing dipole models of ESI with clusters of BOLD changes correlated to IED (Lemieux, Krakow et al. 2001; Bagshaw, Kobayashi et al. 2006). This adds evidence to the argument that distributed inverse solutions are better suited as a model of the widespread cortical activity such as involved in the onset and propagation of IED (Michel, Murray et al. 2004; Liu, Ding et al. 2006). Nevertheless, further studies are needed to determine the origin of the discrepancies between ESI and BOLD in epilepsy, and how they relate to factors such as cortical location.

In our study, the number of scalp electrodes (32 vs 64) did not influence the validity of the results. This is not surprising as our 64-channel cap had an increased electrode density but not an increased coverage of the scalp compared to the 32-channel cap. A more crucial factor than electrode number to increase the precision of ESI would be to improve spatial coverage, notably with lower temporal electrodes.

5.5.2 ESI and EEG-fMRI of IED in the medial cortex

In the cases with a medial frontal epileptogenic focus (patients 5 and 8), we found that the ESI maximum was lateralised to the contra-lateral hemisphere, whereas the BOLD responses were concordant with other electro-clinical data. False

lateralisation of midline activity with ESI can arise due to slight displacement of the electrode cap or topography of activated gyri and sulci (Michel, Lantz et al. 2004). Although these results have to be considered discordant in view of our criteria, they still provide valuable information to help interpret the multiple BOLD clusters, because they indicate a medial frontal IED focus despite limited spatial accuracy. In these cases, it is the strongly lateralised, spatially well-defined EEG-fMRI results, concordant with electro-clinical information that were helpful to correct the mislateralisation of interhemispheric ESI results, further highlighting complementarity between the two techniques. Such mislateralisation is not uncommon in cases where the EEG source is localised in the interhemispheric cortex, due to small imprecisions in electrode placement or source imprecision caused by polarity inversion of EEG events (interhemispheric gyri are “inverted” with respect to the surface).

5.5.3 ESI and EEG-fMRI in temporal lobe IED

The two other discordant cases (studies 1 and 4) illustrate the different methodological limitations affecting EEG-fMRI and ESI in patients with temporal lobe IED and thereby also illustrate the advantage of combining these imaging techniques for a better understanding of the underlying disease. Patient 1 showed a right occipito-temporal neocortical BOLD change corresponding to ESI for onset of IED, but there was no significant BOLD change linked to the other 2 sets of IED. In a secondary analysis, we combined all three types of temporal IED thereby potentially increasing sensitivity, if the three event types share a common haemodynamic substrate (Salek-Haddadi et al, 2006). The resulting map revealed a significant hippocampal response that was concordant with ESI. Taken together, this suggests that in the case of a widespread irritative zone, the medial temporal structures can represent a common denominator in the epileptic network of each

distinct IED type; a result confirmed by intracranial EEG in this case. This is in line with previous group analysis of patients with temporal lobe epilepsy using EEG-fMRI (Laufs, Hamandi et al. 2007). The statistical maximum of BOLD changes localised in the ipsilateral anterior cingulate gyrus was consistent with propagation from the hippocampus to other structures belonging to the limbic network. This case illustrates both the interesting neurophysiological speculation that can arise from EEG-fMRI findings as well as the ambiguity of labelling/categorisation of IED.

In patient 4 (left medial occipital cortical dysplasia with left and right temporal IED) only a very small cluster of significant voxels was obtained for the less frequent right temporal spikes whereas the more numerous left temporal IED had no associated significant BOLD change. There was also no significant corrected BOLD signal change in the lesional occipital lobe. Possible explanations for this result include signal drop-out in the basal temporal lobe, which limits sensitivity to BOLD signal changes in this location (Bagshaw, Aghakhani et al. 2004). Moreover, insufficient EEG electrode coverage, especially of the lower temporal regions can limit ESI localisation (Lantz, Grave de Peralta et al. 2003; Sperli, Spinelli et al. 2006). The absence of BOLD changes in the lesion could be due to an abnormal neuro-vascular coupling. Despite these limitations, our findings are consistent with intracranial studies of epileptic networks in patients with temporal lobe epilepsy, that describe a strong interaction of the epileptogenic activity in medial temporal and neocortical regions (Bartolomei, Wendling et al. 2001). While some authors consider that ESI is not able to recover isolated temporal medial activity (Ebersole 1997; Merlet and Gotman 2001; Gavaret, Badier et al. 2004) other studies suggested the opposite, at least when the entorhinal cortex was involved (Lantz, Ryding et al. 1997; Pacia and Ebersole 1997; Zumsteg, Friedman et al. 2006; James, Britz et al. 2008). Previous EEG-fMRI studies focusing on patients with temporal lobe epilepsy showed only rare temporal medial BOLD responses despite

the presence of hippocampal atrophy in several patients (Kobayashi, Bagshaw et al. 2006; Laufs, Hamandi et al. 2007). BOLD responses were also found in the contralateral temporal lobe and extra-temporal areas, such as the peri-insular/opercular cortex (as in patients 1 and 2). Further studies, involving better lower temporal electrode coverage and systematic intracranial validation, are necessary to assess the usefulness of EEG-fMRI to solve this ESI dilemma and help determine whether the combined methods can help discriminate between medial and lateral temporal epileptogenic foci.

5.5.4 ESI as a marker of propagation

When the two techniques give concordant localisation, the higher temporal resolution of ESI may be used to attempt to discriminate between BOLD clusters related to early vs. late IED components and provide dynamic information about the network. The rising phase of IED has been shown to be the best estimate for the localisation of IED onset, while source activity related to later timeframes indicates propagation (Lantz, Spinelli et al. 2003; Ray, Tao et al. 2007). In our study, when ESI showed propagation, this second region of maximal local field potential was related to a second concordant BOLD cluster in 6/12 cases. It remains unclear why the remaining cases showed no significant BOLD cluster concordant with ESI although, in 2/6 of these, a BOLD cluster concordant with ESI was observed in data uncorrected for multiple comparisons. This could reflect an inadequate model of the BOLD signal due to lack of IED, poor representation of the IED-related BOLD time course by the basis set of the HRF chosen in this study, although significant deviations are probably rare (Salek-Haddadi, Diehl et al. 2006; Lemieux, Laufs et al. 2008) or poor representation of the baseline (Salek-Haddadi, Friston et al. 2003). There was no clear cut difference in the number of IED for studies with BOLD cluster concordant with ESI compared to those without. The localisation

and propagation patterns revealed by EEG in 3 patients were in line with the ESI results. While this increases confidence in ESI-defined propagation in the other patients without intracranial recording, it is not possible to be sure if incorrect ESI or a lack of sensitivity of EEG-fMRI is the reason for any mismatch.

5.5.5 Revisiting the importance of the cluster containing the most significant BOLD increase

Previous EEG-fMRI studies have analysed EEG-fMRI results with particular attention paid to the maximal significant positive BOLD cluster in the hope of identifying a unique marker of epileptogenicity (Salek-Haddadi, Diehl et al. 2006). These authors assessed concordance at a lobar level between BOLD response at 1.5T and non-invasive clinical data (interictal/ictal EEG, abnormality on structural MRI if available). They showed that the cluster of maximal positive statistical value was generally concordant with the presumed focus at the lobar level. The other, less significant clusters, and in particular those corresponding to BOLD decreases, were suggested to reflect IED propagation or distant activation/deactivation of neuronal networks in response to IED. In this study, we found that the BOLD cluster containing the global statistical maximum was often not the closest to the region of IED onset as identified by ESI. In one case, intracranial EEG confirmed that a BOLD cluster other than that containing the global maximum was the main IED generator (patient 5). If ESI had not suggested this region for IED onset, the concordant very small cluster of positive BOLD change may have been overlooked. Therefore, even very small clusters of BOLD change should be a priori considered as potential candidates for localising the IED generator. In this case, the most significant positive and negative BOLD responses (supplementary motor cortex and precuneus, respectively) were distant from the intracranial spiking electrode contacts. However, when concordance is assessed only at a lobar level, the

maximal positive BOLD cluster and ESlo are found to be concordant found in 5 additional cases (cases 1abc, 2, 3, 6a, 7a) increasing concordance to 75% (9/12) cases, which is similar to the 74% (17/23) value in Salek-Haddadi et al. (2006). The finding that the most significant BOLD cluster does not reliably indicate the primary generator of IED is consistent with ictal SPECT studies, where the area of maximal perfusion usually correspond to area of seizure propagation rather than to the ictal onset zone.(Van Paesschen, Dupont et al. 2007).

5.5.6 ESI and negative BOLD responses

In some cases, we found that the closest BOLD cluster to ESlo results corresponded to a negative BOLD change. Negative IED-related BOLD changes have been increasingly reported both close to and distant from epileptogenic foci (Kobayashi, Bagshaw et al. 2006; Salek-Haddadi, Diehl et al. 2006; Jacobs, Kobayashi et al. 2007). They have been attributed to a decrease in metabolic demand (deactivation), relying on the assumption that neurovascular coupling is maintained in the irritative zone both during baseline and IED generation, for which there is some limited evidence mainly in relation to generalised discharges (Stefanovic, Warnking et al. 2005; Carmichael, Hamandi et al. 2008; Hamandi, Laufs et al. 2008). Whereas distant negative BOLD changes have generally been attributed to IED-induced changes in the brain resting state, BOLD decreases local to the presumed focus are more difficult to interpret. Some authors have suggested a local vascular steal or surround neuronal inhibition with low metabolic demand as possible mechanisms (Shmuel, Yacoub et al. 2002; Bagshaw, Aghakhani et al. 2004). Decrease in excitatory input (“deactivation”) has been related to BOLD decreases whereas neuronal inhibitory activity is intrinsically a metabolically demanding process associated with increase of the BOLD signal (Lauritzen and Gold 2003). Despite findings in animals and humans that a negative BOLD

response was associated with decreased neuronal activity during a visual task (Shmuel, Yacoub et al. 2002; Shmuel, Augath et al. 2006) this is not necessarily the case for epileptic activity. First, highly synchronised oscillations responsible for epileptic discharges seen on the EEG are not necessarily paired with regional increases of total synaptic activity. Concurrent decreases of the rest of the network activity (or decreased inhibitory activity) could result in negative BOLD response caused by a net decreased metabolism, as also seen with interictal FDG-PET (Van Paesschen, Dupont et al. 2007). MR perfusion studies of IED-related perfusion changes are difficult to conduct since a high rate of IED is needed due to the low signal-to-noise ratio of perfusion imaging. Second, fMRI and optical imaging studies have revealed a mismatch between brain oxygenation and perfusion in animal models of epilepsy (Bahar, Suh et al. 2006; Schridde, Khubchandani et al. 2008) which has also been reported in intra-operative recording of neocortical seizures in the human cortex (Zhao, Suh et al. 2007). Therefore, BOLD negative responses could occur even if synaptic activity and metabolic demand are increased. Intracranial recordings of epileptogenic activity showed that negative BOLD changes was associated with a relative decrease of low frequency power compared to positive BOLD changes (Benar, Grova et al. 2006). Since low frequency components of IED correspond to slow waves associated to increased inhibition, a reduction in low-frequency power could reflect a reduced inhibition (and therefore a reduced metabolic demand) associated with epileptic activity in regions showing negative BOLD changes.

ESIs closest to regions of BOLD decrease were found predominantly in the temporal lobe in our study. In 2 cases that exhibited only BOLD decreases, we did not find positive BOLD changes with concordant anatomic localisation and in the 2 other cases positive BOLD changes were located at much greater distance. This suggests that a potential ESI inaccuracy is not sufficient to explain our findings. In

patient 2, there was interplay between right medial and lateral temporal activity, with both regions being active at onset and maximum activation, switching from lateral to medial structures. Even if we reason that the true IED onset zone were in reality closer to the cluster of BOLD increase located in the medial temporal region, it would still be important to understand the pathological significance of BOLD decreases in the region of lateral temporal propagation which generated IED detected on the scalp EEG.

Therefore, both positive and negative BOLD changes should be considered when evaluating epileptic networks with EEG-fMRI, especially in the context of pre-surgical evaluation. A greater number of patients with intracranial EEG recording is needed to confirm the significance of “secondary” clusters of BOLD increase or decrease concordant with ESI localisation.

5.6 Conclusion

In conclusion, simultaneous ESI and EEG-fMRI appears to be a methodologically robust way of combining both modalities, which can provide new information on the dynamics of epileptic networks. It can be used to provide temporal differentiation of the often complex patterns of IED-related BOLD changes that are encountered with EEG-fMRI studies, and in particular to increase confidence in the location of the primary focus when spatially concordant. The high temporal resolution of ESI can improve the localising value of EEG-fMRI, while the spatial definition provided by the BOLD clusters may increase confidence in the ESI localisation. This synergy could improve the clinical decision making, for instance when defining regions of interest for intracranial EEG recording. More cases with invasive validation are needed to assess the clinical relevance of this multimodal imaging tool.

6 CONTINUOUS EEG SOURCE IMAGING ENHANCES ANALYSIS OF EEG-FMRI IN FOCAL EPILEPSY

6.1 Summary

Objectives: Methodological improvements in EEG-fMRI are needed to increase sensitivity and specificity for localising the epileptogenic zone. We investigated whether the estimated EEG source activity improved models of the BOLD changes in EEG-fMRI data, compared to conventional event-related designs based solely on the visual identification of IED.

Methods: Ten patients with pharmaco-resistant focal epilepsy underwent EEG-fMRI. EEG Source Imaging (ESI) was performed on intra-fMRI averaged IED to identify the irritative zone. The continuous activity of this estimated IED source (cESI) over the entire recording was used for fMRI analysis (cESI model). The maps of BOLD signal changes explained by cESI were compared to results of the conventional IED-related model.

Results: ESI was concordant with non-invasive electro-clinical data in 13/15 different types of IED. The cESI model explained significant additional BOLD variance in regions concordant with video-EEG, structural MRI or, when available, intracranial EEG in 10/15 IED. The cESI model allowed better detection of the BOLD cluster, concordant with intracranial EEG in 4/7 IED, compared to the IED model. In 4 IED types, cESI-related BOLD signal changes were diffuse with a pattern suggestive of contamination of the source signal by artefacts, notably incompletely corrected motion and pulse artefact. In one IED type, there was no significant BOLD change with either model.

Discussion: Continuous EEG source imaging can improve the modelling of BOLD changes related to interictal epileptic activity and this may enhance the localisation of the irritative zone.

6.2 Introduction

Most interictal EEG-fMRI studies are based on models that do not account for variations of the BOLD response to individual IED, although amplitude and morphology of IED on scalp EEG have been reported to be different in patients with and without BOLD response to IED (Krakow, Woermann et al. 1999) (see Chapter 2.5.1 for details). Moreover, modelling only IED detected on scalp EEG would often not reflect the abundant underlying epileptic activity that can be recorded by intracranial EEG (Tao, Ray et al. 2005).

In the present study, we used continuous Electrical Source Imaging (cESI) to obtain a continuous estimate of the activity of the IED source and used this estimated activity as a parametric model of the BOLD signal changes to test the following hypothesis:

- 1) The proposed parametric modelling of epileptic activity explains additional variance of the BOLD compared to a modelling of IED as discrete events.
- 2) There is spatial concordance between the ESI-correlated BOLD signal changes, the source of IED onset defined by ESI and other non-invasive or invasive imaging modalities. In other words, cESI reflects fluctuations in interictal epileptic activity.
- 3) This improved model of interictal BOLD fluctuations allows a better understanding of the epileptic networks in some patients, as validated with intracranial EEG recordings.

6.3 Methods

6.3.1 Patients and electro-clinical data

Patients with refractory focal epilepsy undergoing pre-surgical assessment were selected from the pool of EEG-fMRI data acquired on a 3T MR scanner between January 2004 and October 2008 according to the same criteria as in the previous study (see section 5.3.1.).

In 10 patients fulfilling the criteria (one EEG-fMRI recording each), we identified 15 separate IED types that were used for analysis, resulting in 15 IED-type specific analysis. Clinical, electrophysiological and imaging data of the patients are given in Table 6.1. All patients had cryptogenic focal epilepsy except for patient 4 who had focal cortical dysplasia in the left occipital cortex, patient 7 who had left hippocampal sclerosis and patient 10 who had a left frontal sub-cortical lesion (detectable as increased signal on FLAIR images).

6.3.2 EEG-fMRI acquisition

EEG-fMRI was recorded as described in section 4.1.

Patients P4, P6, P7, P8 and P9 had EEG with 62 recording electrodes and the others with 30 recording electrodes.

IED type	Gender, age	Seizure semiology	MRI	IED focus (scalp EEG)	Number of IED during fMRI (Number of 20-min fMRI sessions)	Intra-cranial EEG
1	M, 31y.	Bizzare vague sensation, CPS with dystonic posture L hand	N	R T	189 (2)	R T lat post
2	M, 30y.	Aphasic SPS No aura, CPS	N	L T	161 (2)	na
3	F, 48y.	No aura, CPS with oral and manual automatisms	N	L T	197 (2)	na
4a	M, 21y.	CPS, oral automatisms, R clonic jerks, SGS	FCD L medial occipital	L T	312 (2)	L Occ medial
4b				R T	56 (2)	
5	M, 27y.	Cloni R face/arm --> SGS	N	R F	2239 (2)	R Fmedial ant
6a	M, 19y.	Epilepsia partialis continua L leg --> rare SGS	N	Central midline	206 (3)	R medial F-Par
6b				R F-central	121 (3)	
6c				R F	10 (3)	
7	M, 33y.	Olfactory-gustatory aura, CPS	L HS	L T	33 (2)	na
8a	M, 22y.	No aura, CPS with L head version	N	Bil F	269 (3)	na
(8b)				Bil F polyspikes#	101 (3)	
9a	M, 25y.	Epigastric , auditory, gustatory or heautosopic aura, tonic posture R hand	N	L F-T	38 (3)	na
9b				L F polar	35 (3)	
9c				L Par	23 (3)	
10a	F, 37y.	No aura, CPS	L F white matter lesion	L F and Bil F L>R	72 (2)	na
(10b)				R F#	11 (2)	

Table 6.1: Clinical, electrophysiological and imaging data:

R/L/Bil: right/left/bilateral; T: temporal; F: frontal; Par: parietal; Occ: occipital; post: posterior; SPS/CPS : Simple/Complex Partial Seizure, SGS : Secondly Generalised tonic-clonic Seizure, FCD : Focal Cortical Dysplasia, HS : Hippocampal Sclerosis. # not considered for further analysis as good quality ESI was not possible, see text).

6.3.3 EEG analysis and Electrical Source Imaging (ESI)

EEG analysis and ESI was performed as described in sections 4.1.3 and 4.1.4.

6.3.4 Source activity based on continuous ESI (cESI)

For each IED type, we defined a region of interest (ROI) consisting of 5 neighbouring ESI solution points around the maximum estimated current density at ESI onset (ESI_o). Given the spatial resolution of the solution space (around 5x5x5 mm³), this ROI corresponds to a volume of approximately 625 mm³. Due to the local dependency constraint that is implemented in the LAURA source localisation algorithm, the selected ROI is representative of a larger area of activity of a few cubic centimetres. The averaged current density of this ROI was determined for each time point of the whole intra-MR EEG recording, giving the function cESI (Figure 6.1). In each case, a control ROI was identified as a region of minimal increase of activity during IED, as estimated visually by inspecting the solution space. The source activity for this region was labelled cESI_c. This cESI_c parameter was intended to account for artefacts in the source activity signal which may arise from motion, myogenic artefacts or pulse artefacts (similarly to the EEG trace) thereby potentially affecting source estimation diffusely throughout the brain. The choice of a single control region might not represent the global artefact or fluctuation of physiological activity but this represents a compromise to ensure a good degree of specificity of the cESI regressor to epileptic activity, while avoiding a strong reduction of sensitivity due to the spatial dependency constraint of ESI mentioned above.

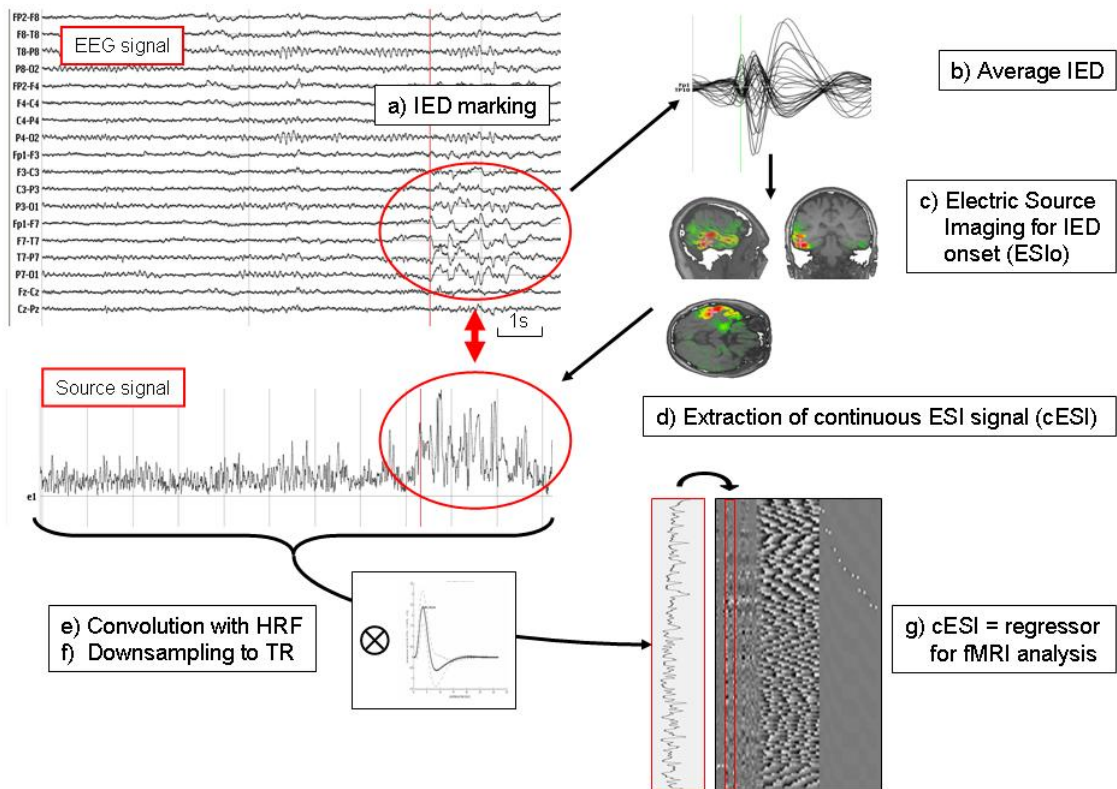


Figure 6.1 : Summary of the analysis strategy:

a) IED are marked on EEG recording; b) IED are averaged; c) Electric Source Imaging is performed at averaged IED onset (ESIo change in fig); d) continuous ESI: cESI is extracted for the entire EEG in the region of ESIo; e) the signal is convolved with the Haemodynamic Response Function; f) the result of convolution is down-sampled to the scanner repetition time (TR); g) the resulting vector is incorporated as a regressor into the General Linear Model for fMRI analysis.

6.3.5 fMRI analysis

fMRI datasets were preprocessed as described in section 4.1.5 .

6.3.5.1 Parametric model: cESI model

An embedded modelling strategy was employed to assess the contribution of the source activity regressors to the mapping of network involved in interictal epileptic activity. A GLM was built, including the effects of the individual IED, each represented as a stick function, cESI and cESI_c, convolved with the canonical HRF, its time derivative and dispersion derivative to account for variable slice delay and variations of the HRF across brain regions and individuals. Subsequently, the convolved cESI and cESI_c functions were down-sampled to the repetition time of the fMRI sequence (TR) to yield parametric regressors. Convolution and down-sampling were performed in Matlab 7.3 (Mathworks, Natick, MA, USA). The IED and cESI regressors represent effects of interest, and cESI_c represents a confounding effect. Realignment parameters and 'scan nulling' regressors, as described in section 4.1.5 were also introduced in the model. In addition, 'EEG nulling' regressors were used to cancel the effect of time periods in which the EEG was contaminated by artefacts. For this purpose, the EEG and cESI signal were reviewed in parallel and artefact-contaminated segments were visually identified. A Heaviside function (similarly to the 'scan nulling' regressors) which covered the duration of the scan corresponding to the artefact-affected event and the following two scans, was introduced in the GLM as a way of limiting the impact of these artefacts on the correlation between cESI and BOLD signals. In datasets containing more than one type of IED with different localisations (i.e. with different presumed underlying generators) one GLM was built for each cESI/cESI_c but each GLM contained all IED regressors. Given the high number of regressors and confounds, we preferred not to include all cESI/cESI_c in the same GLM to avoid an excessive reduction of the degrees of freedom in the

model. Baseline drift was removed by applying a high-pass filter with a cut-off of 1/128 Hz.

For each cESI model we obtained two SPM{F} contrast maps to estimate the following effects: 1) cESI-related BOLD signal changes to show variance of the BOLD signal related to the activity of the estimated IED source that was not accounted for by the IED (cESI SPM{F} maps); 2) combined IED and cESI (cESI+IED SPM{F} maps) to map BOLD signal changes related to all available information about epileptic activity. The resulting maps were corrected for multiple voxel comparisons (Family wise error, $p < 0.05$).

Figure 6.1 summarises the analysis strategy for cESI-informed fMRI analysis.

6.3.5.2 Conventional IED model

This “conventional” model was built similarly to the GLM analysis described in the previous study (see section 4.1.5 and 5.3.3).

6.3.6 Assessment of Concordance

For each model, the three resulting SPM{F} maps were evaluated for spatial concordance with prior hypothesis regarding localisation of the epileptic focus. Since only 4/10 patients had concordant intracranial EEG recording and only 3/10 had surgical resection we based our concordance assessment on non-invasive electro-clinical data and structural imaging with validation from intracranial EEG when available.

We labelled as “Concordant (C)” the maps in which all statistically significant clusters (excepting those belonging to the DMN, see next page) were located in the same lobe as prior knowledge of focus localisation. The “Concordance plus (C+)” label was applied to maps in which the most statistically significant cluster was located in the same lobe as prior knowledge of focus localisation but where additional clusters were

present in other lobes than the presumed focus but in regions known to be structurally and functionally connected to it (i.e. limbic network in temporal lobe epilepsy, contralateral frontal lobe in frontal lobe epilepsy, occipito-temporal distribution in occipital lobe epilepsy). Diffuse BOLD changes involving all lobes bilaterally, with no distinct clusters of BOLD changes, were labelled as “Discordant (D)”. In some cases, BOLD maps showed clusters clearly belonging to the Default Brain Network (DMN: medial parietal = precuneus, bilateral associative temporal-parietal cortex, bilateral medial fronto-polar, thalamus) (Raichle, MacLeod et al. 2001). These were not considered for the assessment of concordance, even when they included the global statistical maximum. These regions exhibit haemodynamic changes that are time-locked to IED in TLE (Laufs, Hamandi et al. 2007) or in bilateral spike-wave discharges (Hamandi, Salek-Haddadi et al. 2006) . Although their role in IED generation is unclear, these brain regions are involved in the modulation of brain activity that strongly interact with, but are not part of, the irritative zone.

The same criteria for concordance were used to label the ESI solutions with respect to the presumed or confirmed localisation of the epileptic focus.

To assess the potential clinical relevance of the cESI model, we also determined if the concordant BOLD clusters obtained with the cESI model gave additional information regarding the localisation of the IED generators, as compared with the conventional IED model. We restricted this comparison to cases in which intracranial EEG was available as a gold standard localising tool.

6.3.7 Exploration of factors influencing the degree of concordance

We considered a number of EEG data quality and event morphology indicators as possible explanatory factors for the degree of concordance of the cESI-related GLM results.

First, we considered characteristics of the EEG signal: number of IED, morphology and amplitude of IED, presence or absence of consecutive slow wave or focal slowing of EEG background. Second, we considered possible contamination of the scalp EEG signal and consequently in the source signal as a result of incomplete correction of the pulse-related artefact, by calculating the proportion of QRS complexes in which pulse artefact correction failed, due to an artefacted ECG signal preventing the precise marking of the cardiac QRS complex. Third, we calculated the correlation between $cESI$ and $cESI_c$ (after convolution with HRF) to estimate the spatial specificity of $cESI$ signal.

Differences between the group of concordant cases (C and C+) and the group of discordant cases D were tested with Mann-Whitney non-parametric tests for independent samples.

6.4 Results

6.4.1 Concordance and clinical relevance

The results of ESI and $SPM\{F\}$ BOLD maps are summarised in Table 6.2.

In total, 17 types of IED were identified. ESI was of poor quality in 2/17 IED types (cases 8b and 10b: polyspikes with low signal to noise of average IED and unstable ESI , see 5.4.1 for details) so that 15 IED types were considered for further analysis. ESI was spatially concordant with electro-clinical data in 13/15 IED types and with 7 intracranial EEG studies (4 patients). The 2 discordant cases (patient 4, IED types 4a, 4b) are discussed in detail below.

In 14/15 IED types we observed significant BOLD signal changes related to all epileptic activity (combined $cESI+IED$ $SPM\{F\}$ maps), as illustrated in Figure 6.2. In 10 of these IED types, the pattern of BOLD signal changes was concordant (3 C, 7 C+) with electro-clinical localisation of the irritative zone and structural lesion.

Clusters were also found in regions concordant with the DMN in 4 of these 10 cases. A significant amount of BOLD variance was attributed to the cESI regressor alone in 7 of the 10 concordant cases (Figures 6.3 and 6.4) and in these 7 cases the most statistically significant clusters (outside the DMN) were concordant with electro-clinical and structural imaging data. Significant cESI-related or cESI+IED-related BOLD changes (cESI model) were concordant with the IED-related results (IED model), in all cases except case 4a/b (see below). In the 7 IED types (1, 4a, 4b, 5, 6a, 6b, 6c: 4 patients) in whom intracranial EEG was available, the use of the cESI model clearly increased the size of the concordant clusters in 4/7 and showed similar results to those obtained with the IED model in the 3/7 remaining cases.

In 4 IED types (7, 9a,b,c: 2 patients), a pattern of bilateral, diffuse cESI-related BOLD signal changes was found, affecting all lobes particularly around large vessels (interhemispheric fissure, sylvian fissure, around brainstem (Figures 6.5 and 6.6). These spatial maps are similar to spatial maps obtained by mapping BOLD changes related to motion or cardiac (pulse-related) confounds. In 1/15 IED type (patient 6c, 10 IED), no significant cESI or cESI+IED-related BOLD change was revealed.

6.4.2 Illustrative case reports

In patient 1 (cryptogenic right TLE), the SPM{F} map for combined cESI+IED revealed BOLD clusters in the right hippocampus, and regions of the DMN (Figure 6.2). This was concordant with intracranial EEG, which showed a majority of IED originating from the right hippocampus with independent or synchronous lateral temporal IED, explaining the localisation of ESI in the right lateral temporal cortex. By comparison, the SPM{F} map for IED in the simpler model showed only very small clusters in the right cingulate cortex and the right hippocampus.

In patient 4 (left occipital focal cortical dysplasia, bilateral anterior temporal IED), the epileptogenic zone was presumed to be localised in the left occipital lobe because the seizures were characterised by a visual aura and a focal cortical dysplasia was evident on structural MRI. However, interictal EEG showed left and right anterior temporal IED (left-sided predominance; 88%) and, ESI showed left and right anterior temporal sources. BOLD changes related to left-sided anterior temporal cESI were revealed in the left occipital region, concordant with the MRI lesion (Figure 6.3). BOLD signal change related to right temporal cESI+IED were also found in the left occipital and temporal regions. Subsequent intracranial EEG recording confirmed a left occipital epileptogenic zone and the patient was seizure free 12 months after left occipital resection. In contrast, for the IED model, there was no significant IED-related BOLD change.

In patient 5 (right frontal lobe epilepsy): SPM_F maps for cESI showed bilateral medial and lateral frontal BOLD clusters with a right-sided predominance. Intracranial recording confirmed an extensive right frontal irritative zone predominating in the medial region. The patient continues to have seizures after a limited right anterior frontal resection that did not include the strongest cESI BOLD cluster. The cESI model showed a larger BOLD cluster in the medial frontal cortex, than did the IED model, with more discrete involvement of the DMN (Figure 6.4).

In the other concordant patients, no intracranial EEG recording was performed: In patient 2 (left temporal lobe epilepsy), maps obtained with the cESI model showed only a left temporal BOLD cluster compared to a more widespread map of BOLD clusters obtained with the IED model (left temporal, left insula, DMN). In patient 3 (left temporal lobe epilepsy), results of cESI model and IED model showed similar spatial maps. In patient 6 (right frontal/right fronto-central: 6a, 6b, 6c), results were similar with both cESI- and IED-models; 6c showed no significant BOLD changes with either model. In patients 8 (bilateral frontal IED) and 10 (left frontal, bilateral frontal IED),

multifocal BOLD clusters included right and left frontal clusters respectively, which were concordant with electro-clinical data and ESI.

Table 6.2 (next page): Results of ESI, conventional and parametric EEG-fMRI analysis.

BOLD clusters are presented with decreasing statistical scores. *Regions belonging to the Default Brain Network of the brain, not considered localising. R/L/Bil : Right/Left/Bilateral ; F/P/T/O : Frontal/Parietal/Temporal/Occipital lobes ; SMA: Supplementary Motor Area ; FC : Fronto-Central ; Cing : Cingulate gyrus ; operc : opercular ; Thal : Thalamus ; WM : white matter ; Ant/post/pol/mid : anterior/posterior/polar/middle, lat/med: lateral/medial. n.s.: non-significant; C/C+/D/--: Concordant/Concordant+/Discordant/no result available. Cluster smaller than 5 voxels were not reported in this Table except if they coincided with the statistical maximum or if no larger cluster was present. n.a.: not applicable (no intracranial EEG recording available).

IED type	Scalp EEG focus	ESI	Conventional IED model	Parametric cESI model			Additional information obtained from cESI+IED model compared to IED model (icEEG as gold standard)
			F(IED) (FWE)	EEG source activity: F(cESI) (FWE)	All epileptic activity (EEG source and IED F(cESI+IED) (FWE) Only additional clusters to cESI column on the left	Concordance cESI/cESI+IED	
1	RT	RTlat	RCing ant, RTmed	Bil Pmed*, Bil TP*, RFmed	+ RTmed	D/C+	Larger cluster R hippocampus
2	LT	LTlat	Bil Pmed*, LTsup, Linsul, RTsup, LTP	n.s.	+ LTinf	--/C	n.a.
3	LT	LTlat	Bil Pmed*, LTP*, Linsul, LTlat, LTmed, Rcereb	Bil Pmed*, LTmed, LTP*, LTlat, Linsul, LF	(idem cESI)	C+/C+	n.a.
4a	LT	LTant	n.s.	LOmed	(idem cESI)	C/C	New L occipital cluster
4b	RT	RTpol	RTP	n.s.	+ LOmed + LTinf	--/C	New L occipital cluster
5	RF	RForb	Bil TP*, Bil Pmed*, RFmed, Bil Thal, RFoperc	Bil Thal, RSMA, RFmed, Bil TP*, Bil Pmed*, R>>L Flat	(idem cESI)	C+/C+	Larger R medial frontal clusters
6a	Vertex	L>R central med	Rparacentral lobule	Rparacentral lobule, Lcereb	(idem cESI)	C+/C+	Similar, no additional information
6b	RFC	RFC lat	RFmid	RFmid, RTsup	(idem cESI)	C+/C+	Similar, no additional information
6c	RF	RFlat	n.s.	n.s.	n.s.	--/--	Similar, n.s.
7	LT	LTmed	n.s.	RFant (max) Diffuse bilateral all lobes	(idem cESI)	D/D	n.a.
8	RF	RFant	RFsup, Bil BG, LFsup, LFpol, Bil TP*, Lcereb, LFmed	LFant, Bil Foperc, LTP*, Bil Tsup, LPmed*	+ RFsup/med, RTP*, Bil Tlat, RPmed*, LFant, R Thal	C+/C+	n.a.
9a	LFpol	LFpol	n.s.	LFpost (max) Diffuse bilateral all lobes	(idem cESI)	D/D	n.a.
9b	LFinf /LTant	LTlat	LTsup	LFpost (max) Diffuse bilateral all lobes	(idem cESI)	D/D	n.a.
9c	LP	LPlat	n.s.	LFpost (max) Diffuse bilateral all lobes	(idem cESI)	D/D	n.a.
10	biF	LFmid	LFmid, Bil TP*, Bil Fmed, LFoperc, RFmid	n.s.	+ ROmed, Bil TP*, LFsup, LFmid, RCing ant, LPmed*, LTlat	--/C+	n.a.

Table 6.2 (Legend on previous page): Results of ESI, conventional and parametric EEG-fMRI analysis.

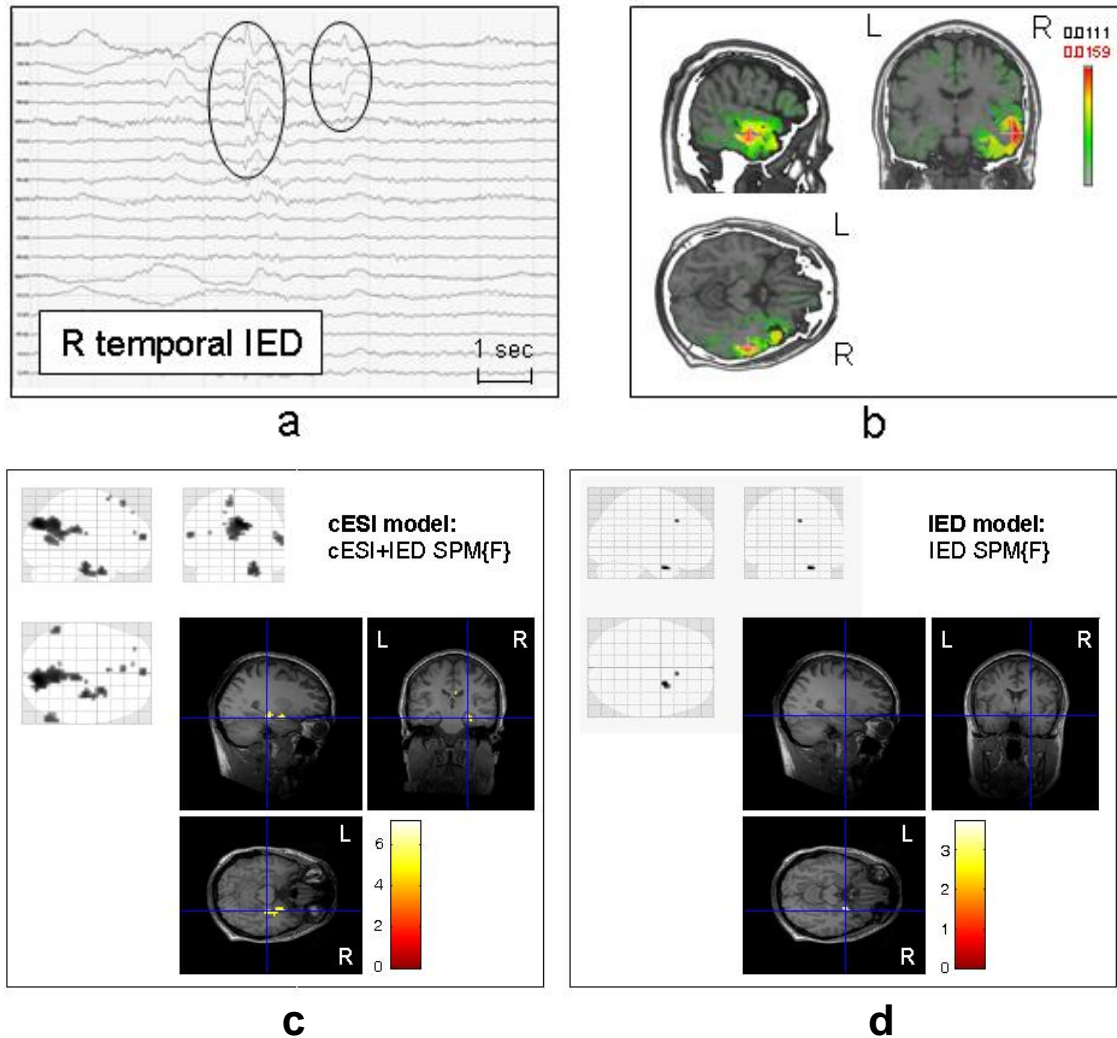


Figure 6.2 : IED model vs parametric model : temporal lobe focus

Case 1: Scalp EEG, ESI, cESI- and IED-related BOLD changes (SPM{F} maps, family-wise error corrected $p < 0.05$) : a) Right temporal and temporo-occipital IED (black circles); b) result of ESI showing right lateral temporal source; c) cESI model: combined cESI+IED SPM{F} maps: clear anatomical localisation in the right hippocampus with additional regions of the Default Mode Network (DMN); d) IED model: IED-related BOLD changes: very small BOLD cluster in the right anterior cingulate gyrus (maximum) and right hippocampus. Intracranial EEG confirmed right temporal medial and lateral IED with predominance in the medial structures. The 'glass brain' SPM{F} maps were normalised for display purposes only; the overlay on T1-weighted image is in individual space.

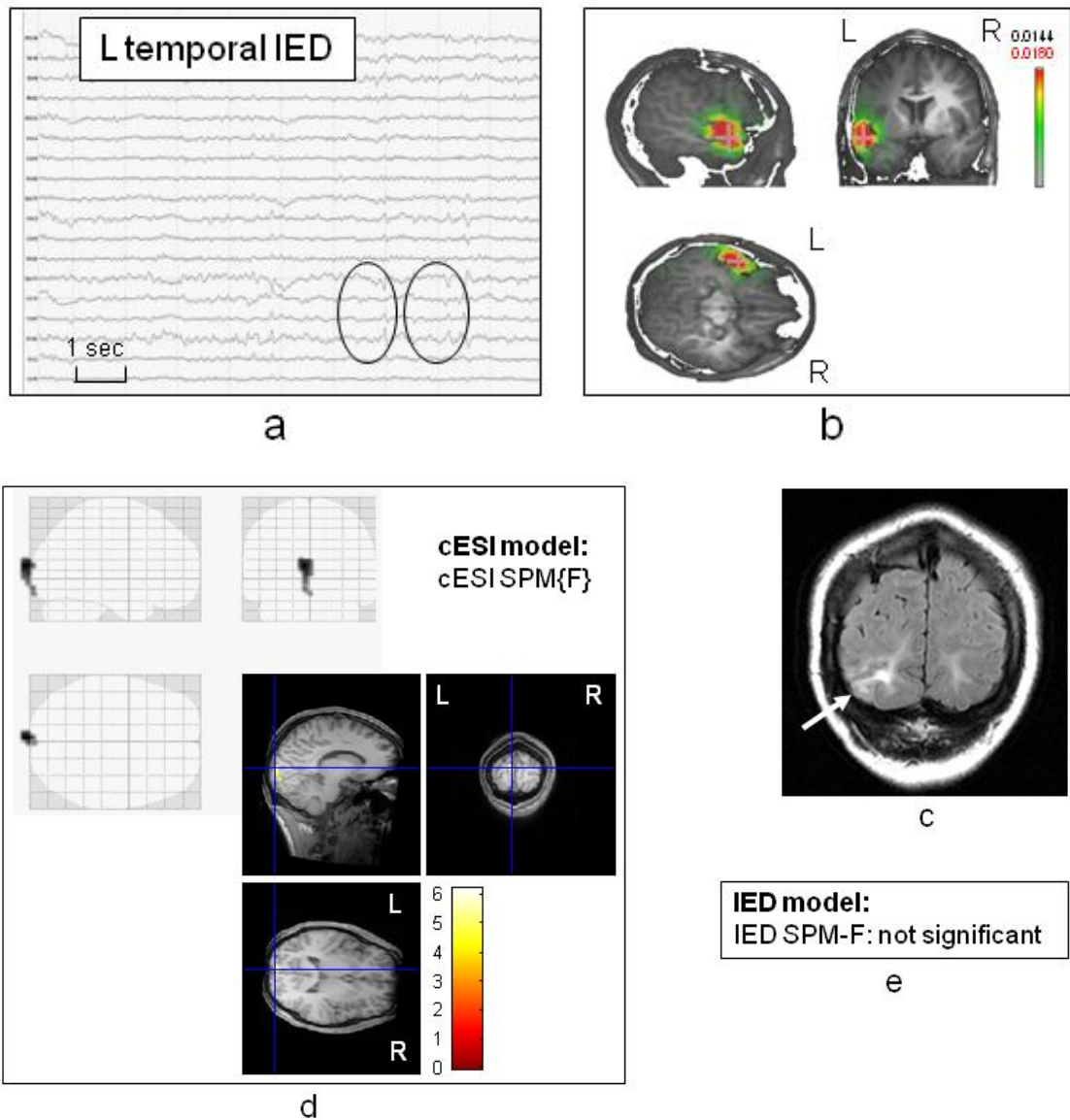


Figure 6.3 : IED model vs parametric model : occipital focus

Case 4a : Scalp EEG, ESI, cESI- and IED-related BOLD changes (all are SPM{F} maps, family-wise error corrected $p < 0.05$) : a) scalp EEG showing left anterior temporal IED (black circles); b) result of ESI showing left anterior temporal source; c) left occipital focal cortical dysplasia seen as signal increase in the white matter on coronal FLAIR image (white arrow); d) cESI model: cESI SPM{F} maps: left occipital BOLD cluster co-localised with MRI lesion; e) IED model: no significant IED-related BOLD change. Intracranial EEG with subdural electrodes confirmed a left occipital epileptogenic zone. The 'glass brain' SPM{F} maps were normalised for display purposes only; the overlay on T1-weighted images is in individual space.

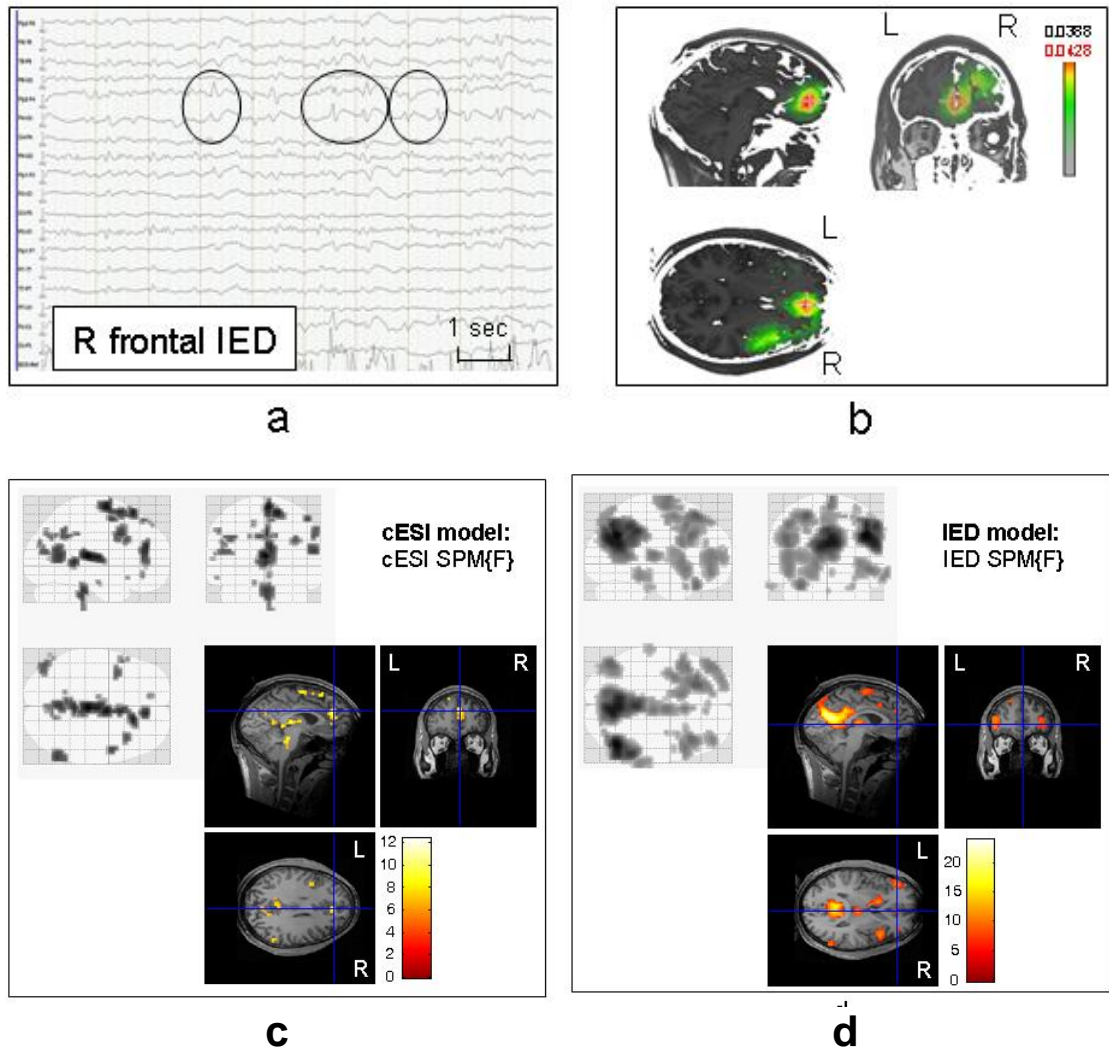


Figure 6.4 : IED model vs parametric model : frontal focus

Case 5: Scalp EEG, ESI, cESI- and IED-related BOLD changes (all are SPM{F} maps, family-wise error corrected $p < 0.05$) : a) Right frontal IED on scalp EEG (black circles); b) result of ESI showing right medial frontal source; c) cESI model: cESI-related BOLD changes: significant BOLD changes in the right medial frontal lobe, concordant with ESI. d) IED model: IED-related BOLD changes: Much smaller BOLD cluster in the anterior right medial frontal lobe (crossline) and predominance of frontal lateral clusters and DMN-related BOLD clusters. Intracranial EEG recording with depth electrodes confirmed the right medial frontal localisation. The 'glass brain' SPM{F} maps were normalised for display purposes only; the overlay on T1-weighted images is in individual space.

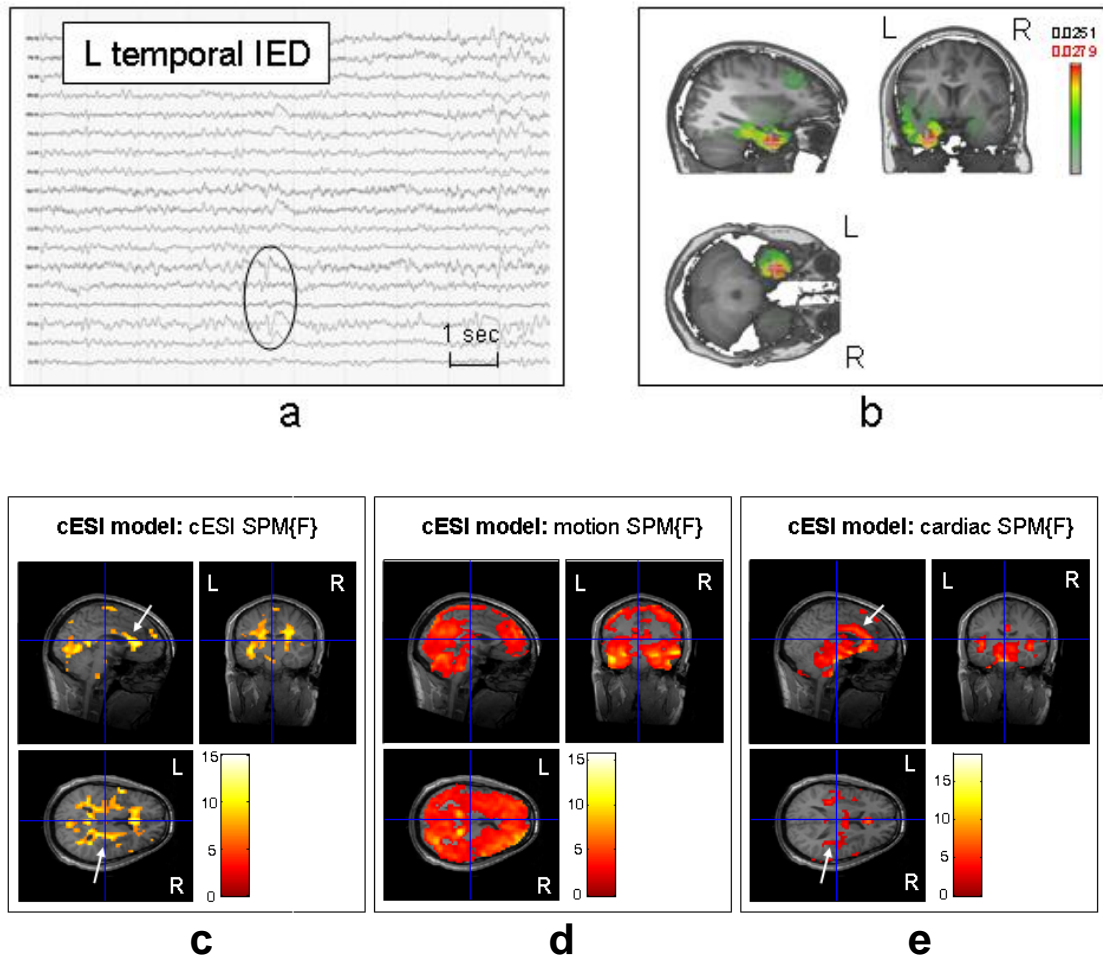


Figure 6.5: Discordant case

Case 7: Scalp EEG, ESI and cESI-related BOLD changes (all are SPM{F} maps, family-wise error corrected $p < 0.05$): a) Left temporal IED (black circles); b) result of ESI showing left inferior temporal source; c) cESI model: cESI-related BOLD changes: diffuse bilateral BOLD changes affecting all lobes with very high statistical value in regions of large vessels (superior midline, sylvian fissure, around brainstem) and white matter with spatial similarity to the SPM{F} map of cardiac confounds suggesting residual cardiac artefact (white arrows); d) motion-related BOLD changes e) cardiac-related BOLD changes (white arrows show spatial similarities with cESI-related BOLD clusters).

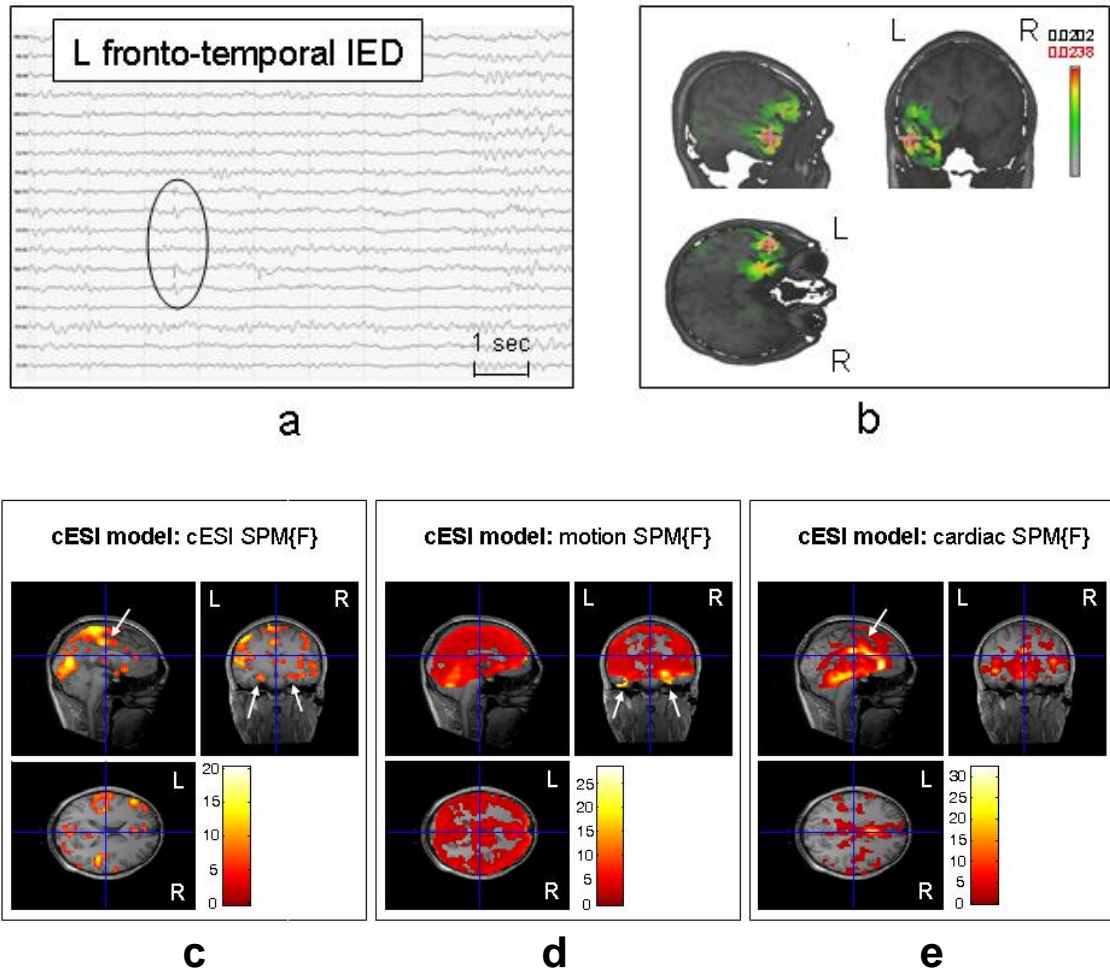


Figure 6.6: Discordant case

Case 9a: Scalp EEG, ESI and cESI- related BOLD changes (all are family-wise error corrected $p < 0.05$) : a) Left fronto-temporal IED (black circles), b) result of ESI showing left anterior lateral temporal source; c) cESI model: cESI-related BOLD changes: diffuse bilateral BOLD changes affecting all lobes, with very high statistical value in regions of large vessels (superior midline, sylvian fissure, around brainstem) with spatial similarity to the SPM{F} map of cardiac and motion confounds suggesting residual motion and cardiac artefact (white arrows); d) motion-related BOLD changes; e) cardiac-related BOLD changes (white arrows show spatial similarities with cESI-related BOLD clusters).

6.4.3 Factors that influence the degree of concordance

The discordant group generally showed diffuse bilateral cortical changes which showed spatial similarity with maps of motion- or pulse- artefacts, so that these maps presumably reflected contamination of cESI by artefacts (Table 6.2). The number of IED was significantly lower in the discordant (D) group than in the concordant (C/C+) group (median 34 vs. 193, $Z=2.83$, $p=0.002$). There was no group difference in morphology of IED, presence of subsequent slow wave or focal slowing of EEG background (qualitative estimation, no statistics performed on these ordinal variables). There was no difference between the groups regarding correlation of the signal derived from the IED source and the control region (median 0.85 vs. 0.76, $Z=1.00$, $p=0.32$). Looking at the variance explained by confounds modelling motion or pulse artefacts, we found that the BOLD changes associated with the cardiac confounds also affected the perisylvian areas whereas the BOLD changes associated with motion showed a diffuse cortical localisation. The analysis of the quality of the QRS labelling on the ECG for correction of pulse-related artefacts showed that there was a greater percentage of missed R-peak markers in the discordant group (median 2.00% vs. 0.08%, Mann-Whitney test $Z=2.00$, $p=0.046$) (Table 6.3).

IED type	Scalp EEG focus	ESI	IED during fMRI (fMRI sessions)	Correlation cESI vs cESI _c	% R markers missed	cESI Concordance cESI/ cESI+IED
1	RT	RTlat	189 (2)	0.51	0.08	D/C+
2	LT	LTlat	161 (2)	0.86	0,04	--/C
3	LT	LTlat	197 (2)	0.67	0.04	C+/C+
4a	LT	LTant	312 (2)	0.95	0.05	C/C
4b	RT	RTpol	56 (2)	0.90	0.05	--/C
5	RF	RForb	2239 (2)	0.28	0.12	C+/C+
6a	Vertex	L>R central med	206 (3)	0.78	1.8#	C+/C+
6b	R FC	RFClat	121 (3)	0.88	1.8#	C+/C+
6c	RF	RFlat	10 (3)	0.79	1.8#	--/--
7	LT	LTmed	33 (2)	0.85	0.66	D/D
8a	RF	RFant	370 (3)	0.52	3.80	C+/C+
9a	LFpol	LFpol	38 (3)	0.85	2.00	D/D
9b	LFinf/LTant	LTlat	35 (3)	0.93	2.00	D/D
9c	LP	LPlat	23 (3)	0.83	2.00	D/D
10a	biF	LFmid	72 (2)	0.74	0.08	--/C+

Table 6.3: Factors influencing the degree of concordance:

EEG characteristics and results of SPM for IED-based GLM and parametric model. #: persistent residual gradient artefact on ECG channel, but cardiac rhythm was very regular. R/L/Bil: Right/Left/Bilateral; F/P/T/O: Frontal/Parietal/Temporal/Occipital lobes; Ant/post/pol/mid: anterior/posterior/polar/middle, lat/med: lateral/medial. C/C+/D/--: Concordant/Concordant+/ Discordant/no result available (See Table 5.2).

6.5 Discussion

Using continuous ESI (cESI) of the IED source as a model for interictal BOLD signal changes, we have been able to validate our starting hypotheses by showing that:

- 1) In models that also included IED-based effects, cESI explained significant amounts of additional variance of the BOLD signal in 10/15 IED studies. In 4 of these 10 cases, the use of cESI revealed a concordant BOLD cluster that had not been found with the conventional analysis.
- 2) There was generally good spatial concordance between the cESI-related BOLD changes and the presumed localisation of the epileptic focus suggested by structural imaging and electro-clinical data. In 4/7 cases this improved localisation was validated by subsequent intracranial EEG recordings, confirming the clinical benefit of this methodological improvement. cESI-correlated changes were also found distant from the region of IED onset, mostly in regions known to be part of the DMN (Aghakhani, Kobayashi et al. 2006; Hamandi, Salek-Haddadi et al. 2006; Laufs, Hamandi et al. 2007).
- 4) Discordant cases had fewer IED and cESI was probably contaminated by uncorrected artefacts in these cases.

These observations suggest that, in most cases studied here, cESI can reflect the activity of the epileptic focus rather than mostly independent fluctuations in background activity. Its inclusion as a predictor of BOLD changes in GLM could lead to improved mapping of the BOLD changes associated with interictal epileptic activity in selected cases with frequent IED.

6.5.1 Methodological considerations

Our choice of continuous ESI as a parametric regressor to model the BOLD signal was motivated by the following considerations:

- 1) EEG-fMRI has low sensitivity, predominantly due to the requirement for a significant number of clearly visible scalp IEDs;
- 2) Simultaneous scalp and intracranial studies have shown that IED visible on scalp EEG usually involve at least 6-10 cm² of excited cortex (Tao, Ray et al. 2005) and that as little as 1:2000 IED recorded by intracranial electrodes can be visually detected with scalp electrodes (Alarcon, Guy et al. 1994).
- 3) Projection of the EEG signal in source space can allow the detection of additional events for GLM analysis, increasing the statistical power of the analysis (Liston, De Munck et al. 2006). Projection of the signal into source space offers an elegant spatial filter for the EEG signal (Brookes, Vrba et al. 2009) and the resultant source signal should be more robust to artefact contamination than the EEG signal (see below).
- 4) Two recent studies have validated the use of ESI performed on the averaged IED detected in the MR scanner during fMRI acquisition results for the localisation of the IED onset (Groening, Brodbeck et al. 2009; Vulliemoz, Thornton et al. 2009) (see Chapter 5).
- 5) Taking the amplitude of IED into consideration rather than using a one-size-fits-all approach such as in the “event-related” approach to fMRI data analysis (IED model) used in this study might improve the modelling of BOLD changes.

The proposed approach represents a more quantitative EEG-based modelling strategy for BOLD signal fluctuations related to epileptic activity than the approach based on visual identification of IED, categorisation and representation as stick functions. In contrast to the method described by Liston et al. (Liston, De Munck et al.

2006), we did not limit the additional projected source-derived regressor to epochs corresponding to a specific waveform, but instead wanted to assess the BOLD correlates of the entire recording, while accounting for various sources of noise in the GLM. Another approach would be to parameterise the visually-identified IED; indeed our results suggest such an approach would probably benefit the IED-based model. In terms of the range of strategies available for the analysis of simultaneously acquired EEG-fMRI data in patients with epilepsy, our study can be positioned between visual IED-based GLM and data-driven approaches such as ICA of the EEG (Jann, Wiest et al. 2008; Marques, Rebola et al. 2009) or fMRI (Rodionov, De Martino et al. 2007). While the ICA approaches are potentially superior for identifying artefacts in the EEG signal, the selection of an “epileptic independent component” remains subjective and hence components containing more subtle activity may not be recognised. In that respect, the value of cESI is that it contains all activity including the one which can be potentially left out by ICA. The cESI regressor is based on the estimated source of IED that were concordant with the electro-clinical data. Therefore, cESI contains prior spatial knowledge about the localisation of the epileptic activity, whereas temporal ICA decomposition of the EEG is purely data-driven and relies on the temporal correlation with visually identified IED to select the epileptic component. The ESI solution varies smoothly across solution points and, therefore, the cESI regressor is not strongly influenced by the inherent uncertainty of source localisation. Conversely, this lack of spatial specificity means that the regressor is likely to incorporate activity remote from the true generator. This is one of the reasons for the inclusion of a control cESI regressor in the model.

Along with these potentially beneficial factors, this more user-independent analysis in source space carries significant challenges. In the spontaneous EEG, IED account only for a small proportion of the data and the Signal to Noise Ratio (SNR) is much lower than for individual or averaged IED, causing the cESI to be contaminated by

noise. By first defining a region of interest based on ESI of averaged IED, we maximised the epileptic contribution in cESI. We postulated that the underlying ongoing epileptic activity, as recorded from intracranial recordings in similar patients, would be reflected in the source signal despite some contamination with noise. Electrode motion-artefacts and myogenic artefacts contaminating the scalp EEG are projected into source space, corrupting the ESI signal. Recent ESI simulation and experimental studies showed that the signal to noise ratio was increased through projection in source space as interference is correlated across EEG channels (Brookes, Mullinger et al. 2008). The authors used “beamformer”, an inverse solution based on a spatial filter and suggested that the same benefit should be obtained with other ESI strategies, particularly distributed linear inverse solution as used in our study. However, Visual inspection of the scalp EEG and cESI signal, however, revealed residual artefacts surviving the projection in source space and the cESI regressor remains more confounded by residual artefacts than the marking of IED by experts. Therefore, we used additional “scan nulling” regressors (Lemieux, Salek-Haddadi et al. 2007) to account for the variance of the BOLD signal in the volumes acquired during these time intervals. Additionally, despite a conservative analysis strategy to remove variance caused by motion and cardiac pulsations, we found consistent results in the discordant cases, that were strongly suggestive of residual artefacts as shown by spatial similarity with the map of signal changes related to cardiac confounds (as modelled by the linear “Time After Pulse” methods (Liston, Lund et al. 2006)) and motion confounds (Figures 6.5 and 6.6). We found that the pulse-artefact correction was significantly better in concordant cases. The effect of cardiac cycle variability (Shmueli, van Gelderen et al. 2007) and other non-linear cardiac effects (Wan, Iwata et al. 2006) or respiratory effects (Birn, Diamond et al. 2006) might help explain this residual contamination. We were not able to assess the residual pulse-related activity by formal comparison of the low frequency content of the EEG spectrum inside/outside the MR scanner due to the different levels of

arousal between the two recordings in most patients. Moreover, the discordant cases had significantly fewer IED, and therefore a lower SNR of the epileptic activity in cESI and an increased effect of residual confounds (cases with fewer than 40 IED were all discordant and all cases with concordant BOLD cluster related to cESI had more than 100 IED). This association between concordant cases and a high number of IED suggests that the major part of the cESI regressor explaining the variance was the parametrisation of the IED rather than fluctuation of the signal in the absence of detected IED.

Clusters that were localised in regions overlapping with the DMN were not considered in the assessment of concordance. Such classification was made on visual inspection of the BOLD maps. A more user-independent approach could be based on the identification of the DMN by ICA in individual subjects and the use of a mask for discarding overlapping BOLD changes related to epileptic activity. The DMN-related BOLD changes were variably associated with IED (e.g. patient 5) or with cESI (e.g. patient 1). This was probably due to insufficient statistical power of IED-related BOLD changes in the latter case.

Different EEG frequency bands have been associated with distinct haemodynamic spatial signatures in healthy subjects (Laufs, Krakow et al. 2003; Mantini, Perrucci et al. 2007). A future refinement of our analysis strategy will be to decompose the source signal in separate frequency bands to build parametric regressors. This would allow us to be more specific about the BOLD changes associated with source activity at different frequencies.

6.5.2 Neurophysiological and clinical relevance

Our results suggest that the use of continuous ESI as a parametric regressor for EEG-fMRI analysis can improve the modelling of interictal BOLD fluctuations in focal

epilepsy. In 7 IED types (4 patients) with concordant results, intracranial recording was available as a gold standard for localising the IED generators. Compared with the conventional IED model, we found that cESI model revealed a new or larger concordant BOLD cluster in 4/7 cases.

In most patients, we found good spatial concordance between cESI-related BOLD changes and non-invasive localisation of the epileptogenic focus (lesion on structural MRI, electro-clinical data). This suggests that the cESI signal reflects the activity of the epileptic focus. Although the epileptic activity may interact with the physiological activity of resting state networks (as illustrated by DMN BOLD clusters in 4/10 concordant cases), we would expect a different spatial distribution of BOLD signal changes if the cESI signal was dominated by non-epileptic activity (systematic involvement of resting state networks, absence of clusters localising the epileptogenic focus).

Case 4a is particularly instructive from a clinical perspective. Occipital BOLD changes were observed in relation to anterior temporal IED and anterior temporal ESI, probably reflecting IED propagation along occipito-temporal pathways (Aykut-Bingol and Spencer 1999). A left occipital epileptogenic zone was identified by subsequent subdural EEG recording. The BOLD changes appeared to take place at the epileptogenic zone, “upstream” from bilateral anterior temporal IED, which reflect propagation areas and an irritative zone with a much larger extent than the epileptogenic zone. This effect may be related to BOLD changes preceding IED as has been shown in some cases of focal epilepsy, mostly in relation to generalised IED (Hawco, Bagshaw et al. 2007; Lemieux, Laufs et al. 2008; Jacobs, Levan et al. 2009; Vaudano, Laufs et al. 2009). Other studies rather suggested a “downstream” effect, with IED modulating BOLD signal and presumably neuronal activity in distant regions involved in the epileptogenic network, such as the DMN (Kobayashi, Bagshaw et al. 2006; Salek-Haddadi, Diehl et al. 2006; Laufs, Hamandi et al. 2007)

and the limbic network (Kobayashi, Bagshaw et al. 2006) in medial temporal epilepsy. One hypothesis to explain this neurovascular uncoupling might be that high frequency activity (frequently associated with focal cortical dysplasia) or closed electric field generated by interneurons was timelocked to the IED but was not detected in our scalp recording. This activity could have more haemodynamical correlates than the propagated temporal activity that was however, easier to detect on the scalp. Another hypothesis could be that distortion and drop out known to affect the inferior temporal lobes prevented the observation of temporal BOLD changes related to the temporal IED.

The availability of invasive EEG recording and post-operative outcome data in larger patient groups will allow us to further validate the proposed method.

6.6 Conclusion

Continuous EEG source imaging could improve the modelling of the BOLD signal in interictal studies of patients with focal epilepsy. This could enhance our ability to localise the irritative zone in selected pre-surgical epilepsy cases using EEG-fMRI. We have identified specific features (number of IED, low residual pulse-related artefact) which might be helpful to select patients in whom our model would be more likely to have clinical relevance. The validation and gains in sensitivity and specificity of the method need to be addressed in larger groups of patients.

7 SIMULTANEOUS INTRACRANIAL EEG AND fMRI OF INTERICTAL EPILEPTIC DISCHARGES IN HUMANS

7.1 Summary

Objectives: Intracranial EEG (icEEG) has greater sensitivity and spatial specificity than scalp EEG but limited spatial sampling. We performed simultaneous icEEG and functional MRI recordings in epileptic patients to study the haemodynamic correlates of intracranial Interictal Epileptic Discharges (IED).

Methods: Two patients undergoing icEEG with subdural and depth electrodes as part of the presurgical assessment of their pharmaco-resistant epilepsy participated in the study. They were scanned on a 1.5T MR scanner following a strict safety protocol. Simultaneous recordings of fMRI and icEEG were obtained at rest. IED were subsequently visually identified on icEEG and their fMRI correlates were mapped using a GLM.

Results: On scalp EEG-fMRI recordings performed prior to the implantation, no IED were detected. The recording of icEEG-fMRI was well tolerated and no adverse health effect was observed. Intra-MR icEEG was comparable to that obtained outside the scanner. In both patients, significant IED-related haemodynamic changes were revealed, both close to the most active electrode contacts and at distant sites. In one case, results showed an epileptic network including regions that could not be sampled by icEEG, in agreement with findings from magneto-encephalography, offering some explanation for the persistence of post-operative seizures in this patient.

Discussion: icEEG-fMRI allows the study of whole-brain human epileptic networks with unprecedented sensitivity and specificity. This could help improve our understanding of epileptic networks with possible implications for epilepsy surgery.

7.2 Introduction

In patients who are candidates for epilepsy surgery, intracranial EEG (icEEG) remains the gold-standard to localise the epileptogenic zone and reveal propagation of epileptic activity. The technique has high sensitivity and spatial discrimination compared to scalp recording but limited spatial sampling. Simultaneous fMRI could mitigate these limitations and provide a new source of information about the organisation of distributed epileptic networks. Additionally, by allowing the recording of epileptic electrical activity and fMRI signals within the same small region, the underlying local neurovascular coupling can be investigated.

The parameters whereby simultaneous intracranial EEG and fMRI (icEEG-fMRI) can be recorded in humans without significant additional health risk have recently been published (Carmichael, Thornton et al. 2010). Here, we investigated haemodynamic changes correlated with intracranial epileptiform activity in the first two patients with focal epilepsy who underwent icEEG-fMRI and we tested the following hypotheses:

- 1) BOLD signal changes can be found at the immediate vicinity of focal epileptic activity precisely localised and sampled by intracranial EEG. This would confirm a correct data quality despite artefacts caused by the presence of the intracranial electrodes as well as a preserved neurovascular coupling during focal interictal epileptic activity.
- 2) Whole-brain BOLD changes correlated to focal IED provide potentially useful clinical information that is complementary to the limited spatial sampling of intracranial EEG.

7.3 Methods

7.3.1 Patients

All patients with refractory focal epilepsy undergoing intracranial EEG for presurgical assessment of their epilepsy between June and September 2009 were considered for participation in the study between the end of the clinical icEEG recording and planned removal of the intracranial electrodes. We present the first 2 patients whom we were able to recruit and scan during this period. Patients were only recruited if they were in good general health, tolerated a post-operative clinical MRI electrode localisation scan and did not have evidence of damage to any electrodes (based on CT and clinical recordings). Prior to implantation of intracranial electrodes (AdTech, Racine, WI, USA), both patients underwent scalp EEG-fMRI acquisitions using our standard protocol (see chapter 4), during which no epileptiform abnormality was detected.

7.3.2 Case reports

7.3.2.1 Patient 1

Patient 1 was a 42 year-old left-handed female with pharmaco-resistant cryptogenic left frontal lobe epilepsy. From the age of 18 she suffered from multiple daily complex motor seizures starting with stiffening or a feeling of tension in the right arm, sometimes evolving to impaired awareness. Structural MRI (3 Tesla) was unremarkable. Long-term video-EEG recording showed occasional (ca. 10/hour) low-amplitude left paracentral IED with no localisable ictal pattern. Magnetoencephalography (MEG, 275-channel CTF Omega whole cortex magneto-meter, VSM MedTech, Coquitlam, BC, Canada; 40 min recording) was also performed. Source analysis of the 30 IED recorded during MEG (Equivalent Current Dipole on the patient's own segmented cortex and a 3-shell boundary element method realistic

head model) suggested left frontal IED propagating from a posterior frontal medial focus to the pericentral cortex near the hand motor cortex.

Intracranial subdural electrodes were implanted for coverage of the left frontal lobe (Figure 7.4.a). Subdural recording from the left medial frontal cortex was not possible due to prominent bridging veins. During the clinical recording, icEEG showed small amplitude very focal IED over the pre- and post-central cortex. Seizures onset was localized to the pre- and post-central cortex. Cortical resection in this region was tailored by icEEG findings and electrocorticography and histological examination revealed gliosis without dysplasia. Follow-up 3 months after surgery revealed persistent simple partial seizures (70% frequency reduction) and moderate weakness of the left hand.

7.3.2.2 Patient 2

Patient 2 was a 31 year-old right-handed female with pharmaco-resistant cryptogenic left temporal epilepsy. From the age of 6 she has suffered from complex partial seizures with epigastric aura, dysgeusia followed by loss of awareness, eye and head version to the right, followed by secondary tonic-clonic generalisation. Structural MRI showed no abnormality. Long-term video-EEG recording demonstrated IED and seizures onset in the left temporal electrodes.

Intracranial electrodes were implanted for coverage of the left lateral and medial temporal lobe (Figure 7.5.a). The clinical icEEG revealed IED involving almost exclusively the left amygdala and hippocampus, with some propagation to the basal temporal lobe and only rare IED involving the lateral grid. Seizure onset was localised to the left hippocampus. She subsequently underwent left anterior temporal lobe resection and pathology was an atypical pattern of hippocampal sclerosis (end folium sclerosis). At follow-up 3 months after surgery, seizures were less severe but simple partial seizures remained.

7.3.3 Data acquisition

7.3.3.1 MRI

MRI was performed using a 1.5T Siemens Avanto scanner (Siemens, Erlangen, Germany) between the end of the diagnostic invasive EEG recording and removal of the icEEG electrodes. To limit heating, we used a head transmit and receive RF coil, low SAR (Specific Absorption Rate) sequences ($\leq 0.1\text{W/Kg}$, head average), as described elsewhere (Carmichael, Thornton et al. 2008; Carmichael, Thornton et al. 2010). The following scans were performed: 1) localiser, 2) FLASH T1-volume (TR 150ms/TE 4.49 ms/flip angle 25°), 3) two 10-minute gradient echo EPI fMRI scans (TR 3s/TE 40ms/ flip angle 90° , 38×2.5 mm slices with 0.5mm gap, 3×3 mm in plane resolution, 200 volumes), during which intracranial EEG was recorded.

7.3.3.2 icEEG

EEG electrode leads were routed directly to the vertex before replacing the bandage. The cables connecting the electrodes to the amplifiers for the clinical recordings were replaced by shorter cables (length 90 cm) to minimize radio-frequency induced risk of heating and laid out precisely in relation to the scanner (Carmichael, Thornton et al. 2008; Carmichael, Thornton et al. 2010). For icEEG recording we used the same hardware and software system as for scalp EEG-fMRI (see section 4.1.1).

7.3.4 icEEG analysis

MR gradient-related artefacts were removed with the strategy used for scalp EEG-fMRI recordings as described in section 4.1.3. On the icEEG corrected for scanning-related artefacts, pulse-related artefacts were small compared to the epileptiform activity and did not interfere with IED identification. Therefore, no correction was performed for the pulse-related artefact.

IED were identified and labelled. For the purpose of fMRI modelling, IED were grouped according to their most active contact and spatial extent (number of contacts involved).

7.3.5 fMRI

fMRI time-series were corrected for slice acquisition time. After this step fMRI preprocessing was performed similarly to scalp EEG-fMRI recordings as described in section 4.1.5.

7.3.5.1 Mapping epileptic networks: whole brain IED-related BOLD changes

For fMRI analysis, IED were modelled as single-events (as in chapters 5 and 6 or as blocks in case of sustained IED activity) and then convolved with the canonical Haemodynamic Response Function. Motion-related effects were included in the GLM in the form of the 6 realignment parameters. SPM_t contrasts (positive and negative) were used to generate SPM_t maps, with a significance threshold of $p < 0.001$ uncorrected for multiple comparisons overlaid onto the coregistered T1-weighted volumetric image.

7.3.5.2 Detecting focal BOLD changes in the irritative zone

Given the potential for local signal alteration around the icEEG electrodes and resulting BOLD sensitivity reduction (Deichmann, Josephs et al. 2002), we wanted to confirm that local correlation between epileptic icEEG events and BOLD signal could be measured with our technique. Clinical intracranial macro-electrode contacts typically record electric signals within a distance of about 1 cm (Lachaux, Rudrauf et al. 2003) and therefore record events directly from a known brain region (in contrast to scalp EEG-fMRI recordings, where the EEG represents the weighted sum of

distributed generators). Therefore we looked for IED-correlated BOLD changes in this region using a volume of interest reflecting the recording volume (VOI: 1-cm radius sphere around the electrode contact location with the strongest epileptic activity). Having an a priori defined VOI, the p-value of the local maxima at a given threshold (here $p < 0.05$) represents the statistical significance of the result with strong control of Family-wise type I error (Friston 1997). The VOI analysis is an application of the small volume correction tool in SPM. Instead of establishing the significance of a correlation between the predicted and measured BOLD signal for each voxel over the entire brain (using random field theory for multiple comparisons) it performs the statistical threshold correction over the pre-specified VOI, taking into account its shape and volume. Therefore the result is not a map, but the presence or absence of a significant finding within the VOI.

7.4 Results

Neither patient reported any discomfort, headache or neurological symptom during or immediately following the icEEG-fMRI sessions. During electrode removal, careful visual inspection of the neighbouring brain tissue did not reveal any sign of adverse effect and no unusual abnormality was noted in histological examination.

In both patients, the corrected icEEG and intracranial IED were similar, on visual inspection, to icEEG recorded outside the scanner with the same equipment (Figures 7.1 and 7.2) and with the previous clinical EEG recording. MRI image quality was sufficient to obtain significant correlations to IED (see below and Figure 7.3).

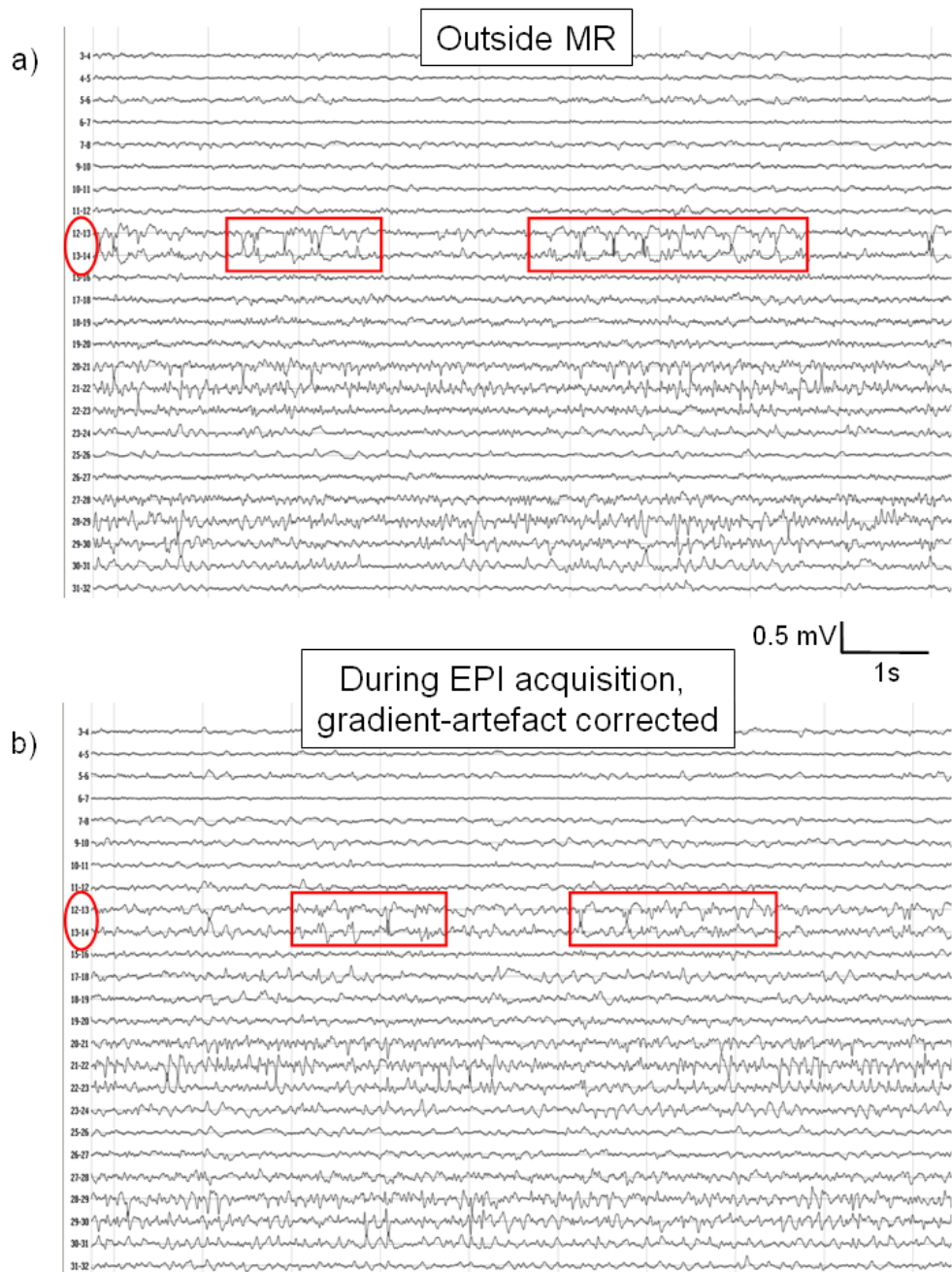


Figure 7.1: EEG outside and inside the MR scanner : patient 1.
 (Legend see next page)

Figure 7.1 (see previous page): EEG outside and inside the MR scanner : patient 1.

Representative sample of intracranial EEG from Patient 1, bipolar montage on parts of a 8x8 contacts grid (1-8: superior row front to back; etc). Top: outside the MR scanner; bottom: inside the MR-scanner after correction of MR-gradient artefacts. For the contacts with the most prominent epileptic activity (red circle, see Figure 7.4), the runs of IED were marked as blocks (red boxes). Note the good quality of the corrected EEG inside the scanner similarity to the recording outside the scanner.

Figure 7.2 (see next page): EEG outside and inside the MR scanner: patient 2.

Representative sample of intracranial EEG in Patient 2: colour ellipses correspond to the colours of the electrodes as displayed in Figure 7.5 (yellow: depth electrode to amygdala, medial to lateral; orange: idem to hippocampus; red: basal subdural strips, medial to lateral; green: sample of temporal lateral subdural grid); Top: icEEG recorded outside the MR scanner; bottom: ic EEG recorded inside the MR-scanner after correction of MR-gradient artefacts. Short arrows: IED restricted to medial temporal lobe (hippocampus>amygdala); long arrows: IED recorded in the medial temporal and basal temporal lobe. Empty arrows: prominent slow-wave activity in the hippocampus is also observed. Note the good quality of the corrected EEG inside the scanner and its similarity to the recording outside the scanner.

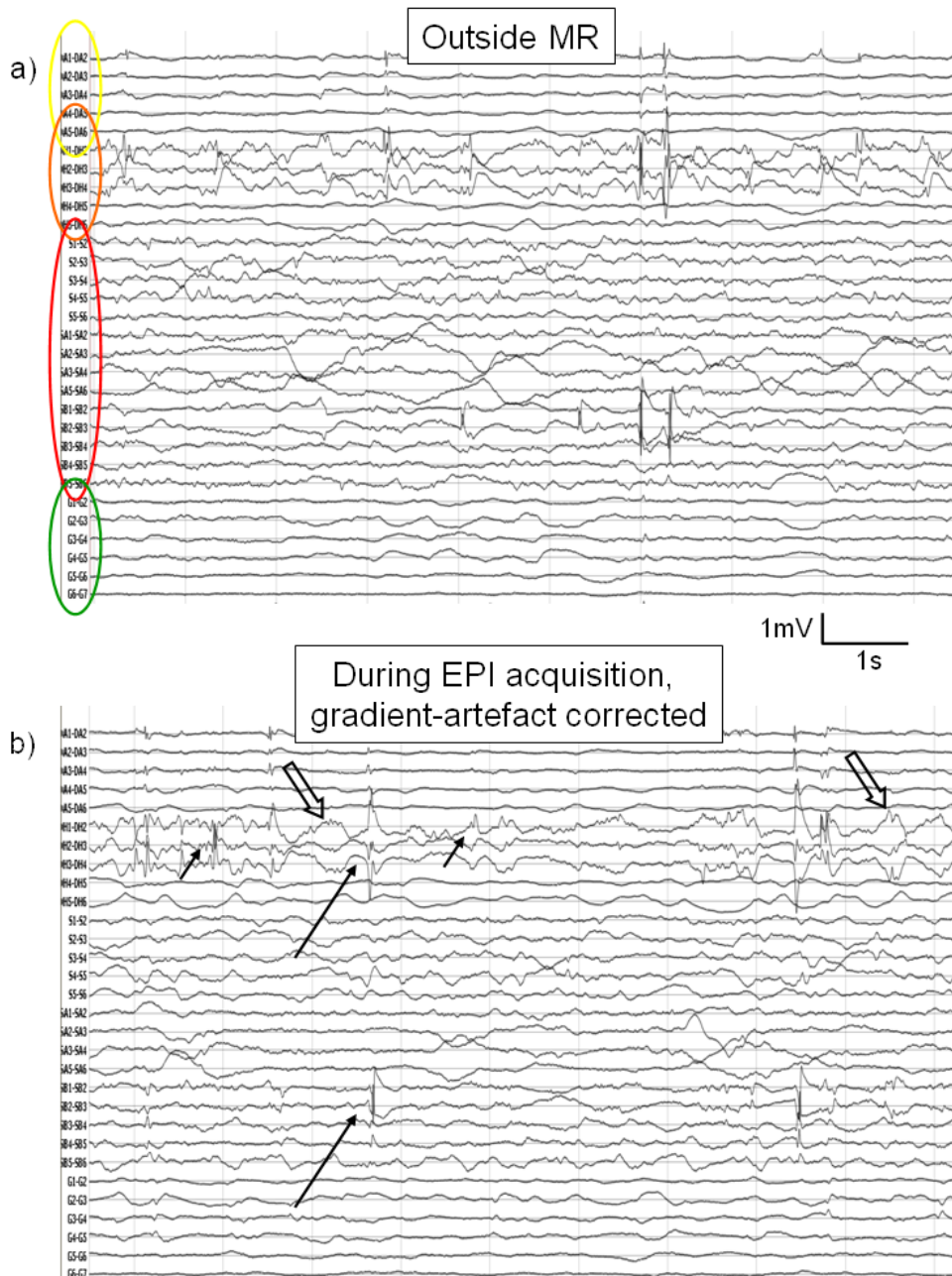


Figure 7.2: EEG outside and inside the MR scanner : patient 2.
 (legend see previous page)

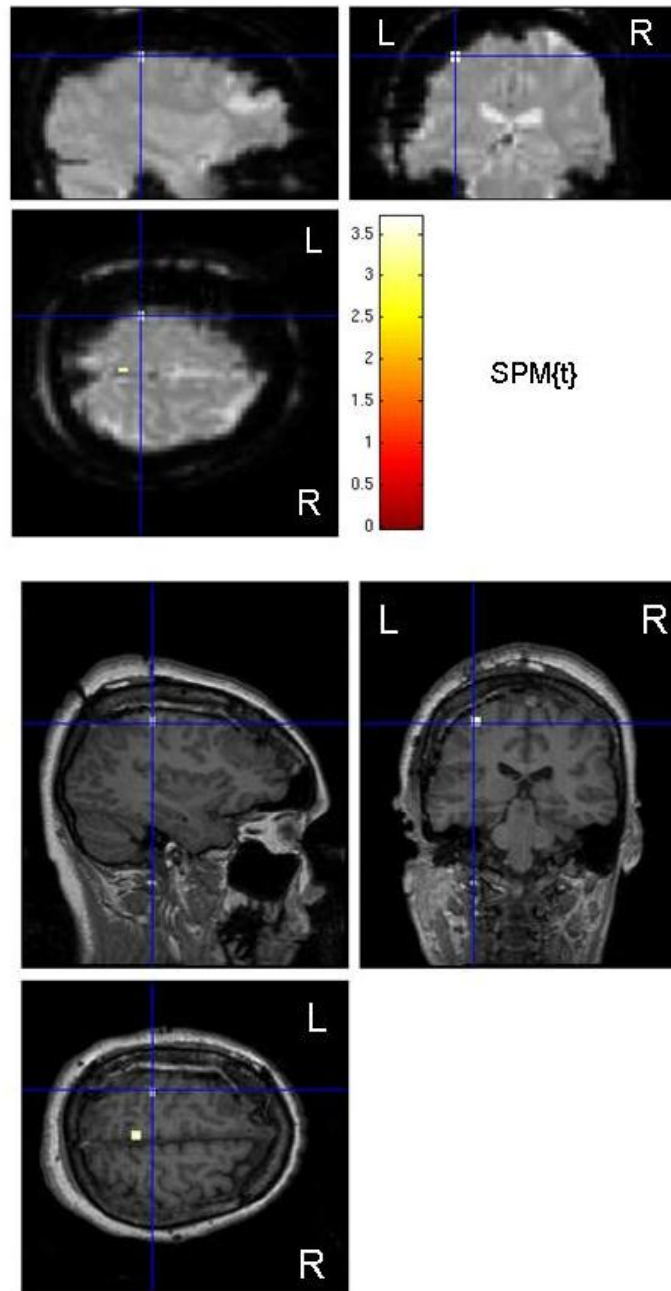


Figure 7.3: Quality of MRI data.

BOLD changes in patient 1, overlaid on mean EPI image (left) and T1 (right, same as Figure 7.4): a cluster of significant IED-related BOLD changes was found in the immediate vicinity of the electrodes (crosshair) despite the artefact caused by the subdural electrodes. Comparison with the T1 image shows that a significant amount of the visible brain asymmetry is due to brain displacement caused by the implantation of the subdural grid with additional signal loss and image distortion caused by the presence of the intracranial electrodes.

Cases	Type of IED	Events in 20 min EPI recording
Patient 1	Runs of small amplitude IED in the left peri-central cortex	Total time of IED blocks / baseline = 0.26
Patient 2	Left amygdala >> hippocampus	N= 23
	Left hippocampal>>amygdala IED	N= 59
	L amygdala + hippocampus	N= 202
	L amygdala + hippocampus + basal temporal	N= 146
	L hippocampus : small IED and large amplitude consecutive slow-wave	N= 222

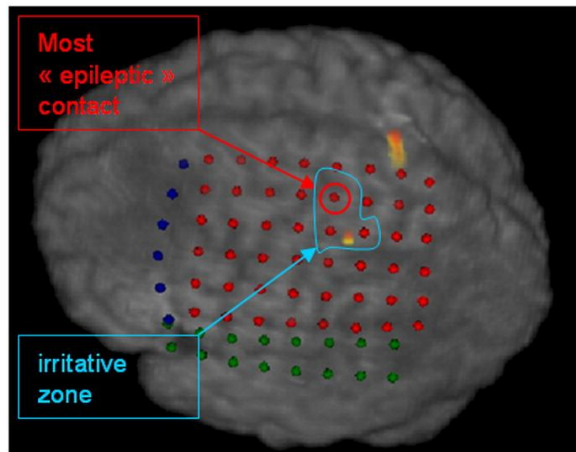
Table 7.1: Interictal Epileptiform Discharges (IED) during fMRI

(see Figures for illustration of EEG traces and localisation of electrode contacts).

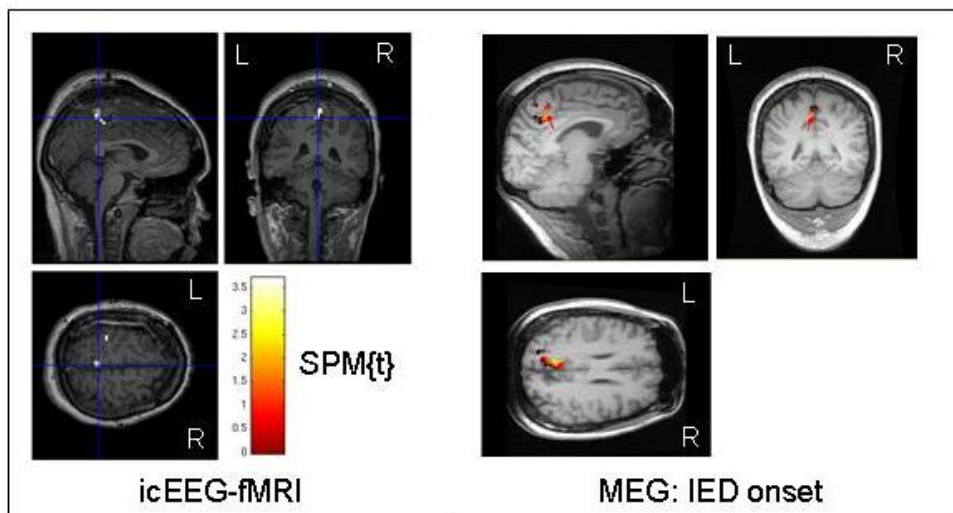
7.4.1 Patient 1

Similarly to the clinical icEEG findings, very abundant (persistent and at times almost continuous >100/min) low amplitude IED were recorded over the left pre-central and post-central cortex and the involved contacts also showed important physiological activity corresponding to the resting mu rhythm of the pericentral cortex (Figures 7.1 and 7.4, Table 7.1). This resting rhythms recorded from subdural electrodes had the typical morphology with relatively sharp components that were in part difficult to discriminate from pathological activity. IED were marked in the contact with most IED (and corresponding to seizure onset zone) in the pre-central cortex. They occurred in runs of spikes, spike-waves and polyspike-waves and these runs were modelled as constant-amplitude blocks in the fMRI modelling because the identification of individual pathological EEG events in a background physiological oscillations such as the Mu rhythms (resting oscillations which can take a “spiky” character) would have been extremely difficult visually and certainly subject to high observer subjectivity in this patient.

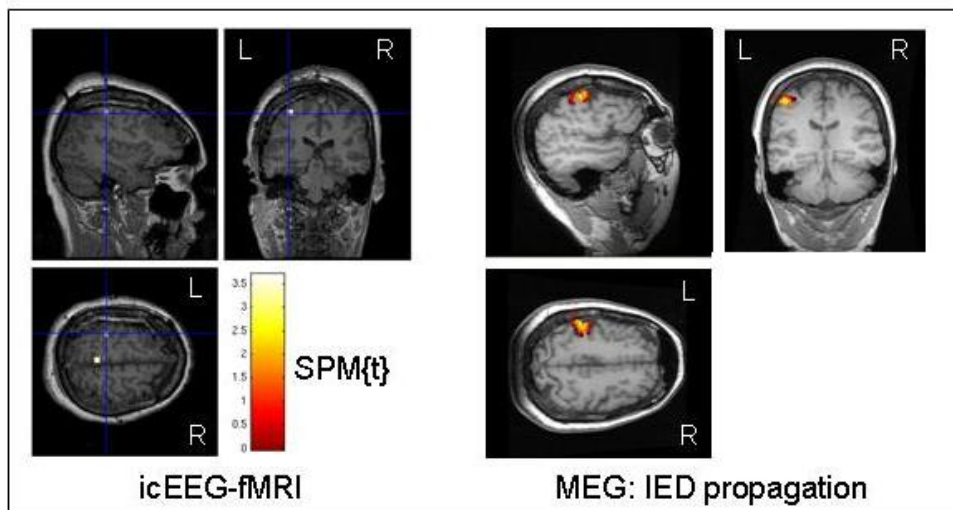
Whole brain SPM{t} maps revealed negative BOLD changes in the left post-central gyrus in close proximity to the spiking contacts that were located near the hand motor cortex (as identified by the “omega” curvature of the precentral gyrus on structural MRI); peak BOLD magnitude: -0.5%, peak t-value: 3.35; extent: 4 voxels, estimated distance between cluster maximum and most active contact = 13 mm), and in the left frontal medial cortex (-1%; peak t-value 3.38; 13 voxels, 18 mm to most active contact). There was good spatial concordance between these BOLD changes and the localisation of IED sources estimated from the MEG recording for the medial frontal cluster and the lateral frontal cluster (Euclidian centre-to-centre distance = 7 mm and 14 mm, respectively) (Figure 7.3). The VOI analysis confirmed significant local negative correlation around the most spiking contact ($p=0.005$).



a



b



c

Figure 7.4: Intracranial electrode position and BOLD changes : patient 1 (legend see next page).

Figure 7.4 (previous page): Intracranial electrode position and BOLD changes : patient 1. a) Subdural electrodes positions overlaid onto post-implantation T1-weighted MRI: one subdural grid (6x8 contacts) over the lateral left frontal lobe (red dots) and three additional strips (1x8 contacts each, blue and green dots) for comprehensive lateral fronto-temporal coverage. Blue line: irritative zone (where IED are recorded); red line: contact demonstrating maximal epileptic activity; b-c) Left panels: statistical maps of BOLD changes correlated to IED showed a left medial frontal (at crosshair in b) and a left lateral frontal cluster (at crosshair in c); right panels: Results of MEG analysis showing IED onset in medial frontal lobe propagating to lateral frontal lobe (courtesy of Dr F. Rugg-Gunn). There is good spatial concordance between MEG sources and BOLD changes.

7.4.2 Patient 2

Very frequent IED (>30/min) were observed, involving the left amygdala (depth electrode), the left hippocampus (depth electrode), and, less frequently, the left basal temporal cortex (strip electrode) (Figures 7.2 and 7.5, Table 7.1). Rare IED (N = 2) were recorded on the lateral temporal grid. SPM_t maps of IED with the largest field (involving the amygdala, hippocampus and basal temporal lobe) showed strong negative BOLD changes in the medial parietal (-1%; peak t-value: 4.27; 101 voxels) and lateral parieto-occipito-temporal cortex bilaterally. These BOLD changes show very good spatial concordance with the posterior part of the Default Mode Network (Raichle, MacLeod et al. 2001). The VOI-based analysis revealed positive correlation in the anterior hippocampus (p=0.002).

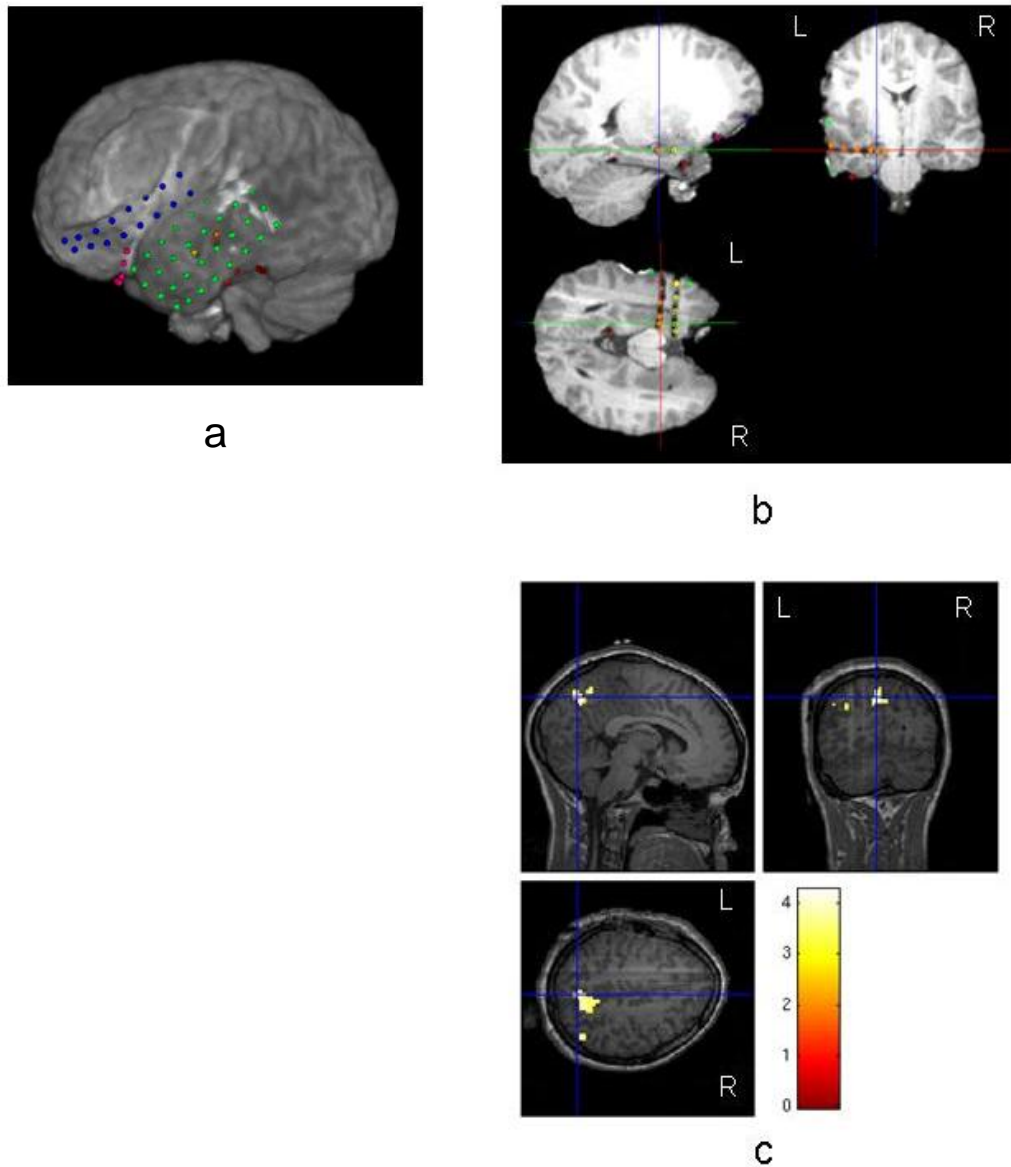


Figure 7.5: Intracranial electrode position and BOLD changes : patient 2. a) Subdural electrodes positions overlaid onto post-implantation T1-weighted MRI: two six-contact depth electrodes (lateral-medial orientation) in the left amygdala (yellow dots) and hippocampus (orange dots). Lateral temporal coverage was obtained by a subdural grid (4x8 contacts, green dots), basal temporal coverage was accomplished using 3 subdural strips (1x8 contacts, red dots); 1 subdural strip (2x8 contacts, blue dots) was placed over the inferior frontal cortex; b) Coronal view showing the position of the depth electrode in the hippocampus (orange dots, crosshair at most active contact); c) Statistical maps of BOLD changes showed bilateral medial and lateral parietal negative changes correlated to IED.

7.5 Discussion

In this first report of simultaneous icEEG and fMRI recordings in humans, no adverse effects were observed following a strict data acquisition protocol, and icEEG data quality allowed clear identification of IED. Our objectives were 2-fold: firstly, to demonstrate the technique's capability to reveal IED-related BOLD changes over the whole brain using a simple modelling approach similar to that used for scalp EEG-fMRI; secondly, to verify if it was possible to detect significant IED-BOLD coupling from signals recorded from within the same region. We have validated our working hypotheses:

- 1) We showed significant IED-related BOLD changes in the immediate vicinity of the focus localised by icEEG, suggesting good data quality and spatial concordance between neuronal and BOLD changes in focal epileptic activity (neurovascular coupling).
- 2) We also observed distant BOLD changes related to specific interictal discharge patterns, illustrating a potential advantage of simultaneous icEEG-fMRI for investigating whole-brain epileptic networks over icEEG alone and scalp EEG-fMRI.

7.5.1 Methodological considerations

To ensure patient safety, we used the following data acquisition protocol: a 1.5T scanner with a head transmit-receive coil; RF power limited to 0.1W/Kg head-average; exact cable lengths and placement in the scanner bore and exact EEG recording equipment configuration. This approach was devised based on previous specific testing on a test object with the same arrangement and a safety margin to account for any differences between in-vitro safety studies and patient/electrode configurations (Carmichael, Thornton et al. 2008; Carmichael, Thornton et al. 2010).

Despite MR image artefacts (distortion and drop out) near the intracranial electrode contacts, IED-related BOLD changes within 1.0 cm of the active electrode were detected. This demonstrates that the technique can detect BOLD signal changes local to the electrode contacts and can therefore be applied to investigate local icEEG-fMRI coupling in epilepsy. A more systematic investigation of data quality issues that will require a larger group of subjects with different implantation strategies is currently underway in our laboratory. In the future, optimisation of imaging sequences and intracranial electrodes (e.g. using material with lower magnetic susceptibility) should further improve fMRI data quality and detection sensitivity.

The richness of epileptic events and their variability (morphology, amplitude) observed in both patients make IED labelling a difficult and user-dependant task, as evident from Table 7.1. In patient 1, we opted for a block design since individual events were so numerous and difficult to individualize. In patient 2, we clustered the event principally according to their spatial extent. A finer classification of events based on user-independently measured features such as amplitude or spectral components might improve the model.

Differences in the event-to-slice timing can be accounted for by using a flexible basis set for the HRF. Due to the frequency of events in this study the time from events to slice acquisition was critical to define expected signal changes hence we used slice timing correction. Moreover, due to the exquisite definition of the events in our data and for the sake of model simplicity, we assumed that the IED-related BOLD changes were canonical as previously shown to be a correct estimation in the case of focal discharges recorded on the scalp (Lemieux, Laufs et al. 2008). Therefore SPM_t tests were used rather than SPM_F tests across all HRF regressors, as performed in Chapters 5 and 6. However, since IED-related BOLD changes can significantly depart from a canonical response even in focal epilepsy, it might be interesting to use a more flexible model of the HRF and probably also to investigate possible non linear

effect with a volterra expansion of the regressor. Moreover, the availability of co-localised icEEG-fMRI signals will allow more systematic assessment of inter-regional and inter-individual variability in epileptic event-related haemodynamic changes and the study of the EEG correlates of this variability.

The SPM{t} maps showed significant IED-related BOLD changes with magnitude (0.5 to 1%) and extent (4 to 101 voxels) within the range of commonly observed scalp IED-related BOLD effects at this field strength (Krakow, Woermann et al. 1999; Benar, Gross et al. 2002). The location of the clusters was concordant with non-invasive electroclinical data or with distant regions known to show haemodynamic changes related to focal temporal lobe IED (Laufs, Hamandi et al. 2007). Thus, it is highly unlikely that these results are due to insufficient control of false positives. Given icEEG's great sensitivity, the generators of detected IED on icEEG can be weaker and of smaller spatial extent than for IED detected on scalp EEG. We would therefore expect the associated haemodynamic changes to occur over a smaller brain region and to be of smaller magnitude, which could cause difficulties to detect icEEG IED-related BOLD changes in some cases, highlighting the need for a careful modelling of the baseline. Although simultaneous scalp recordings were not available, the small IED field and, in patient 2, the deep localisation of the IED focus make it unlikely that these events would have been detected with scalp EEG electrodes, consistent with the lack of IED in previous scalp EEG-fMRI recording for both patients. The high frequency of events narrows the dynamic range of the relatively slow haemodynamic response compared to expected BOLD changes in scalp EEG-fMRI studies, which model rarer events that originate from larger areas of active cortex (Tao, Ray et al. 2005). In addition, possible non-linear effects (de Zwart, van Gelderen et al. 2009) related to very close occurrence of successive IED might also play a role (Bagshaw, Hawco et al. 2005; Salek-Haddadi, Diehl et al. 2006).

In addition to the fMRI artefacts due to the depth electrode, the detection of IED-related hippocampal BOLD changes with scalp EEG-fMRI is limited by the difficulty of recording temporal medial IED even when using fMRI protocols optimised for the basal temporal lobe (Bagshaw, Torab et al. 2006; Kobayashi, Bagshaw et al. 2006). In patient 2, we found a highly significant correlation between hippocampal IED and BOLD signal changes from within the same region.

7.5.2 Neurophysiological relevance

In fMRI studies the starting hypothesis is that focal neuronal activity is coupled to haemodynamic changes, so that focal BOLD changes can be interpreted as reflecting changes of neuronal activity (Logothetis 2008). In non-human primates, BOLD changes are best correlated to synaptic activity (local field potential) (Logothetis, Pauls et al. 2001) but the coupling between cortical evoked potentials and haemodynamic responses might not show perfect spatial match (Disbrow, Slutsky et al. 2000). In humans, non-invasive cerebral perfusion measurements suggested preserved neurovascular coupling in relation to generalised IED (Stefanovic, Warnking et al. 2005; Carmichael, Hamandi et al. 2008; Hamandi, Laufs et al. 2008). The non-invasive study of the neurovascular coupling during epileptic activity in humans is limited by the poor sensitivity and low spatial resolution of scalp EEG (Alarcon, Guy et al. 1994) and the resulting suboptimal characterisation of the baseline state. By contrast, simultaneous recording of local neuronal activity and haemodynamic changes presented here revealed co-localised haemodynamic changes to the most active icEEG contact as well as distant changes, concordant with invasive animal studies (Englot, Mishra et al. 2008).

In patient 1, we observed negative BOLD changes at the site of IED. These could reflect alterations of the neurovascular coupling due to local pathology or reflect an imbalance between excitatory and inhibitory neuronal processes (Logothetis 2008)

with decreased metabolic demand in the case of the very focal IED. This could be reversed in the case of IED involving larger patches of cortex and detectable on scalp EEG. The observation that, in scalp-EEG studies, most IED-correlated BOLD changes concordant with the epileptic zone are positive supports this alternative hypothesis (Kobayashi, Bagshaw et al. 2006; Salek-Haddadi, Diehl et al. 2006) (see sections 2.2.2 and 5.5.6 for additional discussion of negative BOLD changes related to epileptic activity).

In patient 2, we found a highly significant local correlation between hippocampal IED and BOLD signal changes within the same region (1 cm around the most spiking contact) by using the spatial specificity of the icEEG recording. We also observed prominent slow wave activity in the hippocampus (Figure 7.2), whereas slow waves were not a prominent feature of spiking contacts in Patient 1 (Figure 7.1). This is consistent with previous reports of increased slow wave spectral power at electrodes close to positive vs. negative BOLD changes (Benar, Grova et al. 2006). In addition, we found distant IED-related BOLD changes in the medial parietal cortex (precuneus) and lateral occipito-temporo-parietal cortex that are localised in regions shown to participate in the Default Mode Network (DMN) of the brain (Raichle, MacLeod et al. 2001). This is consistent with previous observations of DMN involvement in temporal lobe epileptic activity (Kobayashi, Bagshaw et al. 2006; Salek-Haddadi, Diehl et al. 2006; Laufs, Hamandi et al. 2007) and with the coupling between the hippocampus and the DMN revealed by functional connectivity studies (Raichle, MacLeod et al. 2001).

7.5.3 Clinical relevance

The mapping of BOLD changes related to intracranial IED can provide useful information about the epileptic network, circumventing low spatial resolution (typically

1cm³ around the electrode contact (Lachaux, Rudrauf et al. 2003)) and restricted brain coverage of icEEG. In the two patients studied here, intracranially recorded IED were very focal and invisible to scalp EEG so that only icEEG allowed modelling of the BOLD changes to confirm focal icEEG findings or to reveal changes at sites not explored by icEEG electrodes.

In patient 1, scalp IED were recorded during long-term EEG (mostly during drowsiness or sleep) and during MEG but not during scalp EEG-fMRI. These differences in activity are common and can result from source orientation or fluctuations of brain state across recording sessions. The icEEG-fMRI showed left frontal medial IED-related BOLD change and a weaker left lateral BOLD change, concordant with MEG results showing left medial frontal IED onset with propagation to the left lateral frontal cortex (Figure 7.3). The concordance of the two results and persistence of the seizures after surgery limited to portions of the left lateral pre- and post-central cortex support an important role of the medial frontal cortex in the epileptic network of this patient. This could not be investigated by icEEG alone for technical reasons (see case reports), while icEEG-fMRI allowed for whole brain investigation providing complementary information. This example suggests that the icEEG-fMRI results, and the consequently improved knowledge of the epileptic network, could result in a better planning of epilepsy surgery and estimation of the odds of seizure freedom. Larger studies will allow better definition of the sensitivity, specificity and clinical relevance of icEEG-fMRI as a presurgical mapping tool for patients with pharmaco-resistant epilepsy.

In patient 2, icEEG-fMRI confirmed medial temporal BOLD changes related to hippocampal spikes, adding to the hypothesis of medial temporal lobe epilepsy.

The purpose of this study was mostly to validate the methodological developments surrounding the use of icEEG-fMRI in epilepsy. It is difficult at this stage to ascertain the clinical utility of icEEG-fMRI and more patients are certainly needed. The proven

safety of the procedure makes it however a clearly unique research tool to investigate neuro-vascular coupling at a fine scale.

7.6 Conclusion

This study showed that simultaneous intracranial EEG and fMRI recording can be performed safely if a strict safety protocol is followed. Despite interactions between the two systems, intracranial EEG and fMRI data were of good quality, allowing exploration of whole-brain BOLD changes related to epileptic activity. In 2 patients with focal epilepsy, we found BOLD changes at immediate proximity of the intracranial electrode contacts showing interictal epileptic activity. Remote changes were found, notably in areas not sampled by intracranial electrodes. This suggests a complementary role of intracranial EEG-fMRI for revealing additional parts of the epileptic network that could have a clinical relevance for epilepsy surgery.

8 CONNECTIVITY OF THE SUPPLEMENTARY MOTOR AREA IN JUVENILE MYOCLONIC EPILEPSY AND FRONTAL EPILEPSY

8.1 Summary

Objectives : Subtle structural abnormalities of frontal lobe grey and white matter have been described in cryptogenic frontal lobe and idiopathic generalised epilepsies. The Supplementary Motor Area (SMA) has a role in motor control. Epileptic seizures affecting the frontal lobe and involving the SMA are characterised by a typical asymmetric tonic posturing. Moreover, motor networks are dysfunctional in Juvenile Myoclonic Epilepsy (JME). We tested the hypothesis that SMA structural connectivity is different in focal frontal lobe epilepsy (FLE) and JME compared to healthy controls.

Methods : Diffusion Tensor Imaging and probabilistic tractography were used to map the structural connectivity of the SMA, defined by motor functional MRI, in 15 patients with JME, 36 patients with FLE and 18 healthy controls.

Results : Structural connectivity of the SMA was significantly altered in JME compared to controls (reduced fractional anisotropy and increased mean diffusivity). In FLE there was no significant difference compared to controls and in all groups there was stronger connectivity in the left hemisphere (higher fractional anisotropy) compared to the right. There was no difference in SMA connectivity between patients with medial or lateral frontal lobe epileptic foci.

Discussion : Altered white matter connectivity is the structural correlate of functional frontal lobe abnormalities in JME. In FLE, the structural connectivity of the SMA was preserved, suggesting a robust motor network that is not compromised by long standing epilepsy involving the medial frontal lobes.

8.2 Introduction

In lesional and non-lesional focal epilepsies, recent imaging studies have found structural abnormalities in brain structures that appear normal using conventional clinical MRI protocols (Eriksson, Rugg-Gunn et al. 2001; Rugg-Gunn, Eriksson et al. 2001) as well as altered structural connectivity (Eriksson, Symms et al. 2002; Widjaja, Blaser et al. 2007). In Frontal Lobe Epilepsy (FLE), seizures often affect motor networks with asymmetric tonic posturing being a classical ictal sign indicating involvement of the Supplementary Motor Area (SMA) in the medial frontal cortex (Loddenkemper and Kotagal 2005). There is also evidence suggesting impaired motor excitability in FLE (Badawy, Curatolo et al. 2007; Loscher, Dobesberger et al. 2007; Nardone, Venturi et al. 2008).

In Juvenile Myoclonic Epilepsy, an Idiopathic Generalised Epilepsy (IGE) syndrome characterised by myoclonic jerks, tonic-clonic seizures and, occasionally, absence seizures (Janz 1985), there is evidence of functional and structural abnormalities in the frontal lobes, despite normal conventional brain MRI, with impaired executive functions (Pascalichio, de Araujo Filho et al. 2007), hyperexcitability of the motor cortex (Manganotti, Bongiovanni et al. 2000; Badawy, Curatolo et al. 2007), and abnormalities revealed by PET, MRI and EEG source imaging studies (Koepp, Richardson et al. 1997; Woermann, Sisodiya et al. 1998; Duncan 2005; Deppe, Kellinghaus et al. 2008; Holmes, Quiring et al. 2009)}.

In this study we used tractography to determine the SMA connectivity in FLE and JME compared to control subjects. We hypothesised that FLE and JME would be associated with abnormal structural connectivity of the SMA compared to controls, reflecting dysfunction of motor control systems.

8.3 Methods

8.3.1 Patients and controls

15 patients with JME, 36 patients with FLE and 18 healthy controls participated in this study. All patients were on antiepileptic medication.

The diagnosis of FLE was made based on non-invasive data including history, seizure semiology (especially of initial motor system involvement), video-EEG monitoring, structural MRI and, in some patients, PET. FLE patients were only recruited if sufficient concordant data were available for lateralisation of the epileptic focus (unilateral or asymmetric ictal signs, unilateral or asymmetric interictal or ictal EEG, causative MRI lesion) and patients were categorised as right FLE (R-FLE) or left FLE (L-FLE). Further labelling as medial or lateral FLE was also performed if localising signs were present: for medial FLE, early bilateral tonic posturing (with or without asymmetric fencing position) or hyperkinetic seizures with concordant EEG abnormalities (bilateral frontal, limited to the midline or absent) and/or a medial MRI lesion; for lateral FLE, early ictal unilateral tonic or clonic manifestations together with supporting interictal/ictal EEG and structural imaging. The clinical data as well as the lateralisation and localisation of the presumed epileptogenic zone are detailed in Table 8.1. 29/36 patients had initial or early motor system involvement during their seizures. The vast majority of FLE patients were pharmaco-resistant with only 2/36 patients seizure free for >6 months at time of scanning.

The JME patients were recruited by the same experts according to the following inclusion criteria: unequivocal seizure history compatible with JME (morning myoclonic jerks and generalised tonic-clonic seizures, with or without absences); normal neurological examination; EEG recording showing generalised epileptic discharges with a normal background; normal conventional structural MRI; good seizure control with antiepileptic treatment but no seizure freedom without

medication. All but 2/15 JME patients had been free of generalised tonic-clonic seizures for >4 months before scanning and only 2 additional patients had persistence of frequent absences or myoclonic jerks >1/month.

8.3.2 Motor fMRI

8.3.2.1 Paradigm

Subjects were asked to perform externally paced joystick movements in four directions (up, down, right, left) with their right hand following a visual cue (white dot). This task was part of a working memory task (“dotback”) in which the subjects were asked to point with the joystick towards the current dot (“0-dotback” condition), the previous dot (“1-dotback” condition) or two dots earlier (“2-dotback” condition). Thirty-second blocks of each condition, alternating with 15-second resting blocks were repeated five times in pseudo-random order (Kumari, Peters et al. 2009). Previous animal and human studies showed that externally paced, unilateral hand movement was able to activate the contralateral primary motor cortex and the bilateral SMA, especially during visually guided movements (Picard and Strick 1996; Picard and Strick 2003).

8.3.2.2 fMRI acquisition and analysis

Motor fMRI consisted of 272 single shot gradient-echo echo-planar image volumes (EPI; TE/TR 25/2500 msec, flip angle 70°, FOV 24x24cm² with in-plane resolution of 3.75x3.75 mm², 50 interleaved slices with 2.4 mm thickness and 0.1 mm gap). Preprocessing in individual space was similar to fMRI preprocessing of EEG-fMRI datasets (see section 4.1.5). A GLM was built containing the blocks of the dotback task and the 6 realignment parameters as confounds. After estimation of the model, a contrast was made for the motor task (0-dotback) and a Student t-test (family-wise error correction, p=0.05) was used to generate maps of BOLD signal changes

(SPM{t}). If these maps failed to show bilateral activation of the medial frontal lobe (SMA), we used the uncorrected t-maps ($p=0.001$) with small volume correction in a sphere of 1cm radius considered to include the medial frontal cortex where the SMA location was expected. Given the strong prior information for the localisation of the SMA activation, this small volume correction was considered sufficient.

8.3.3 Diffusion Tensor imaging acquisition and preprocessing

8.3.3.1 Acquisition and preprocessing

This was done as described in section 4.2.

8.3.3.2 Tractography

The SPM{t} maps were coregistered to the b0 image using a 6-degrees of freedom rigid-body transformation and overlaid onto the FA image which has very good discrimination between grey and white matter. As a seed region for tractography, we placed a 6mm radius sphere (105 voxels) in the white matter of the gyrus corresponding to the peak of SPM{t} maps in the medial frontal lobe. A midline exclusion mask was drawn above the corpus callosum to prevent spurious tracking through the interhemispheric fissure.

Probabilistic tractography was carried out as described in chapter 4. Spurious tracts leaving the top of the brain due to FA noise in the extra-cerebral structures were truncated with an axial mask.

8.3.3.3 Quantitative tract description

The mean FA and MD of the tracts were calculated for a threshold of 0.1 probability of connection in individual subject.

The tracts were then normalised (see section 4.2.2) and the volume of the normalised tract was calculated. Commonality maps of left/right SMA tracts were created seeded

from the left/right SMA in all subject groups (controls, R-FLE, L-FLE, JME). Commonality maps of seed regions were also created to show the variation in tractography seeding related to functional-based seeding in individual subject space.

8.3.3.4 Group statistics

Group statistics were conducted in SPSS 14.0 (www.spss.com). Non-parametric tests (Kruskal-Wallis or Mann-Whitney U, χ^2) were used to test for differences in age, age of onset and handedness between groups. We used univariate ANOVAs to test for interhemispheric and intergroup differences of FA, MD and nTV of SMA tracts between controls and JME, and between controls, R-FLE and L-FLE, with statistical significance at $p < 0.05$. If ANOVA yielded significant results when comparing 3 groups, Duncan's post-hoc test was used (with control group as control category) for pair-wise group comparisons. In a secondary analysis, we used an ANOVA to test for intergroup difference in FA results between JME and pooled FLE patients.

8.4 Results

FLE patients were divided into 18 R-FLE and 18 L-FLE. Further localisation was possible in 25/36 FLE patients (15 medial: 7 left, 8 right ; 12 lateral : 6 left, 6 right). There was no difference in age between R-FLE, L-FLE and controls (Chi-square=0.64 ; df=2 ; p=0.795), between JME and controls (z=0.652; n.s.) or between JME and pooled FLE patients (z=-0.476; n.s.). There was no difference in age of onset between R-FLE and L-FLE (z=0.975 ; n.s.). There was no difference in handedness across all groups (Chi-square=4.72 ; df=3 ; p=0.193) (Table 8.1).

8.4.1 SMA tractography

Figure 8.1a shows the commonality maps in 15 JME patients for the normalised left SMA seed region, defined using motor fMRI in individual subjects, and overlaid on a normalised FA map. Figure 8.1b shows the commonality map for the resulting SMA tracts. The main variability of the SMA, as localised with motor fMRI, is along the anterior-posterior axis.

FA values of SMA-seeded tracts were within the range of other reported tracts in healthy controls and patients with epilepsy (Powell, Parker et al. 2006; Yogarajah, Powell et al. 2008).

8.4.2 Juvenile Myoclonic Epilepsy

There were no significant interhemispheric differences for FA, MD or nTV. The mean FA of the defined SMA tracts was 8% lower in JME than in controls (p=0.004) and mean MD was 7% higher in JME than controls (p=0.004). There was no intergroup difference in nTV (Table 8.2). There was a trend for a higher mean FA in the left than

the right hemisphere across both patient and control groups (6%) but this did not reach statistical significance ($p=0.056$) (Table 8.2, Figure 8.2).

8.4.3 Frontal Lobe Epilepsy

Mean FA of SMA tracts was 5% higher in the left than the right hemisphere (R-FLE, L-FLE and controls $p=0.04$). Post-hoc analysis limited to right-handed subjects showed similar results and was not carried out in the very small group of left-handed subjects. There was no significant difference in FA between groups of R-FLE, L-FLE and controls. There were no significant interhemispheric or intergroup differences for MD or nTV. There were no significant differences in FA, MD or nTV between medial FLE, lateral FLE and controls (Table 8.2, Figure 8.2). In a secondary analysis, age (controls and patients) and age of disease onset had no significant effect on FA or MD measures, when included as a covariate (together with tract side and focus side).

8.4.4 Comparison between FLE and JME

The (left and right) SMA tracts of JME patients had a mean FA 8% lower than the (left and right) tracts of the pooled FLE patients ($p=0.005$).

	JME	LFLE	RFLE	Controls
Number (M:F)	15 (6:9)	18 (11:7)	18 (8:10)	18 (8/10)
Medial/lateral/ not localised	na	7 :6 :5	8 :6 :4	na
Age (median, range in years)	39 ^{#†} (26-49)	34 ^{§†} (18-46)	31.5 ^{§†} (18-46)	31.5 ^{§#} (22-49)
Age of onset (median, range, y)	14 (7-20)	9 (1-19) *	10 (2-40) *	na
Handedness (Right:Left)	15:0 **	14:4 **	16:2 **	14:4 **
Clinical MRI :				
- No lesion	15	13	9	18
- Glioma		1	3	
- Cortical Dysplasia		1	2	
- DNT		0	3	
- Trauma		1	0	
- Abscess		1	0	
- Unspecified		1	1	

Table 8.1 : Clinical characteristics of patients and controls.

M :F= Male :Female ; JME=Juvenile Myoclonic Epilepsy, L-FLE/R-FLE :Left/Right Frontal Lobe Epilepsy ; DNT : Dysembrioplastic Neuroepithelial Tumour. na : not applicable. * No significant difference (Chi-square= 4.72; df=3; p=0.193) [§]No significant difference (Chi-square=0.64; df=2; p=0.795). [#] No significant difference (z=0.652). [§]: no difference in age between R-FLE, L-FLE and controls (Chi-square=0.64 ; df=2 ; p=0.795). [#]: no difference in age between JME and controls (z=0.652; n.s.). [†]:No difference in age between JME and FLE (R and L pooled) (z=-0.476; n.s.). *: no difference in age of onset between R-FLE and L-FLE (z=0.975 ; n.s.). **: no difference in handedness across all groups (Chi-square=4.72 ; df=3 ; p=0.193).

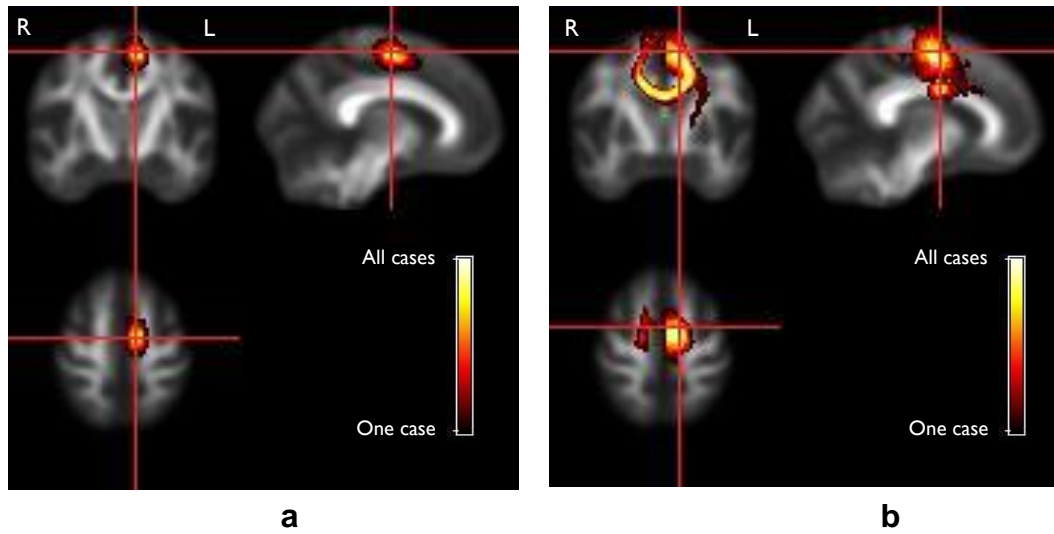


Figure 8.1 : Commonality maps of SMA connectivity for Juvenile Myoclonic Epilepsy

Group commonality maps in 15 JME patients: (a) left SMA seed region (white matter of the gyrus with maximum SMA activation in motor fMRI). The functional definition of SMA in individual subjects explains the spread of the seed regions after normalisation to the template; (b) results of left SMA tractography showing predominant connection with the contralateral SMA but also descending cortico-spinal fibres and a small connection to the primary motor cortex. The colour scale reflects the proportion of cases where the voxel was included in the tract (white=all cases, dark red=one case only).

Group (N)	Fractional Anisotropy (FA)		Mean Diffusivity (MD, 10 ⁻³ mm ² /s)		Normalised Tract Volume (nTV, mm ³)	
	Mean (s.d.)		Mean (s.d.)		Mean (s.d.)	
	L [§]	R [§]	L	R	L	R
Controls (18)	0.366 * (0.040)	0.342 * (0.039)	0.869 # (0.069)	0.888 # (0.068)	11342 (2198)	9881 (1851)
JME (15)	0.332 * (0.038)	0.319 * (0.037)	0.930 # (0.084)	0.946 # (0.104)	11000 (3008)	10291 (2777)
L-FLE (18)	0.355 (0.033)	0.333 (0.040)	0.904 (0.073)	0.931 (0.085)	10779 (2283)	10092 (2161)
R-FLE (18)	0.354 (0.052)	0.348 (0.052)	0.897 (0.084)	0.898 (0.100)	11232 (2613)	11393 (2718)
Medial FLE (15) (7 left, 8 right)	0.376 (0.035)	0.349 (0.050)	0.875 (0.065)	0.908 (0.117)	11066 (2378)	9911 (2046)
Lateral FLE (12) (6 left, 6 right)	0.337 (0.034)	0.343 (0.337)	0.918 (0.070)	0.920 (0.075)	10875 (2225)	11391 (2404)

Table 8.2 : Quantitative SMA tractography analysis

Fractional Anisotropy (FA), Mean Diffusivity (MD) and normalised Tract Volume (nTV) for the SMA tracts in both hemispheres and for control and patient groups (L/R : left/right). [§]Across all groups, there was a 5% higher FA in the left hemisphere compared to the right (p=0.04). *Mean FA was 8% lower in JME compared to controls (p=0.004) and #mean MD was 7% higher in JME than in controls (p=0.004).

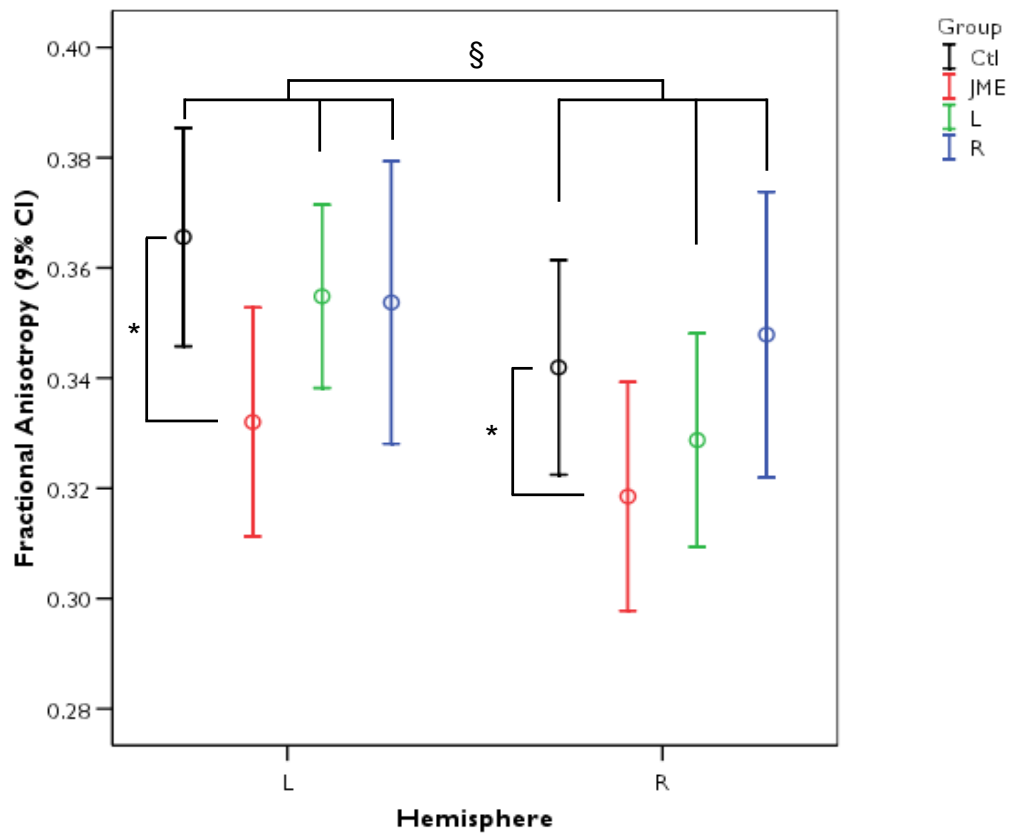


Figure 8.2 : Quantitative SMA tractography analysis

Fractional Anisotropy values of SMA tracts for controls, JME, R-FLE and L-FLE in the left and right hemispheres. In JME, mean FA was 8% lower than in controls (*, $p=0.004$). In the left hemisphere, mean FA was 5% higher (§, $p=0.04$) in L-FLE, R-FLE and controls. Left mean FA was also higher in the left hemisphere in JME but this did not reach statistical significance.

8.5 Discussion

Diffusion tensor tractography is a valuable non-invasive tool for visualizing and characterizing the neuro-anatomical substrate of motor networks (Johansen-Berg and Rushworth 2009). Using tractography with functionally determined seed-points, we compared the connectivity of the SMA in JME and FLE with controls. Our study showed very robust connectivity of the SMA. We validated our hypothesis that connectivity of the motor system is altered in JME compared to healthy controls.

Across all groups of FLE, JME and controls, we found a higher FA in the left hemispheric SMA tracts compared to the right. However, there was no difference between patients with FLE and controls. The biological processes underlying FA changes are still incompletely understood. Causes of anisotropy changes include changes in myelination, axonal membrane or axonal density. Differences in tracts crossing the tract of interest could also modify its anisotropy (Concha, Livy et al.; Beaulieu 2002; Johansen-Berg and Rushworth 2009). Prominent left-sided white matter motor tracts would be consistent with left-sided manual and language specialisation of the predominantly right-handed population studied here. These results are in keeping with hemispheric asymmetry of structural connectivity reported for language (Powell, Parker et al. 2006) and motor systems (Guye, Parker et al. 2003).

8.5.1 Juvenile Myoclonic Epilepsy

We found altered structural connectivity of the SMA in JME compared to controls. Reduced FA in the white matter indicates either decreased fibre density or decreased preferred orientation, and increased MD suggests reduced cell number or volume in the white matter and compensatory increase in extracellular space (Beaulieu 2002). Our findings of white matter abnormalities complement a growing body of studies

reporting anatomical and functional abnormalities of neuronal networks subserving motor functions in JME. These studies consistently point towards increased cortical cellular density and hyperexcitability. A number of MR volumetry studies of cortical grey matter found bilateral increases in cortical volume in the medial frontal cortex (Woermann, Sisodiya et al. 1998; Woermann, Free et al. 1999; Kim, Lee et al. 2007) although two other studies could not reproduce these findings (Betting, Mory et al. 2006; Roebeling, Scheerer et al. 2009). Limited data from autopsy studies of JME patients have also reported controversial microdysgenesis and increased neuronal density in the frontal lobe grey matter (Meencke and Janz 1984). An association between abnormal white matter connectivity assessed by DTI and increased cortical thickness has been found in malformations of cortical development (Eriksson, Rugg-Gunn et al. 2001; Gross, Bastos et al. 2005). While cortical abnormalities suggest abnormally packed cortical neurons, our study provides evidence for corresponding underlying abnormal white matter connectivity. Such abnormal connectivity could be linked to the abnormal electrophysiological properties of the motor cortex described in JME. For instance, the inhibitory input from the contralateral hemisphere (Grefkes, Nowak et al. 2011) could be reduced by altered SMA connectivity, leading to a reduction in intracortical inhibition, as documented by transcranial magnetic stimulation studies (Manganotti, Bongiovanni et al. 2000). This could be a consequence of altered via abnormal SMA projections. Further, magnetic resonance spectroscopy has shown reduced frontal N-acetyl-aspartate/choline ratio, notably in the medial frontal regions, suggesting neuronal loss in the motor network (Savic, Lekvall et al. 2000) that could parallel hyperexcitability of the motor cortex (Lin, Carrete et al. 2009). Additional evidence for neuroanatomical or functional abnormalities in JME come from a PET study in a group of patients with Idiopathic Generalised Epilepsy (IGE), including JME patients, that found increased binding of flumazenil to central benzodiazepine receptors in the cortex (Koepp, Richardson et al.

1997). This could either reflect increased grey matter cellular density or hyperexcitability with receptor upregulation.

Anatomical studies have shown that the SMA is connected to the primary motor cortex, the premotor cortex, the primary somato-sensory cortex, the striatum, the thalamus as well as the spinal motor neurons (Picard and Strick 1996). Our tractography findings show similar connectivity pattern to previous tractography studies of the medial frontal cortex in healthy subjects, with principal connections to the contralateral SMA and weaker tracts towards the striatum and along the cortico-spinal tract (Johansen-Berg, Behrens et al. 2004). Similar SMA connectivity has also been found in Gilles de la Tourette syndrome and correlated with the severity of the movement disorder (Thomalla, Siebner et al. 2009). However, our tractography study showed only a very weak connectivity between the SMA and the primary motor cortex, concordant with other tractography studies (Johansen-Berg, Behrens et al. 2004). The most likely explanation for it is the difficulty of tractography algorithms to succeed in crossing the very strong cortico-spinal tracts when tracking between the SMA and the primary motor cortex. Tracts seeded from the SMA are therefore very likely to be “attracted” by strong tracts such as the cortico-spinal tract or the transcallosal fibres. Reduced connectivity measured by tractography therefore mostly reflects reduction in transcallosal connectivity, which could be related to a reduced interhemispheric inhibition and hyperexcitability of the motor cortex. These convergent findings of structural abnormality in the medial frontal cortex of JME suggest a crucial role of the SMA in the pathophysiology of this condition, including the generation of myoclonic jerks. This enhances our understanding of this condition and could help tailor new treatment strategies such as transcranial magnetic stimulation or deep brain stimulation, in which therapeutical stimulation could compensate for the altered input delivered via abnormal white matter tracts. Reduced

SMA connectivity was not found in the pharmaco-resistant group of FLE patients suggesting that reduced anisotropy in JME is not a consequence of seizure activity.

Our findings are further supported by a separate study comparing FA and neuropsychological measures in a larger group of JME patients (O'Muircheartaigh, Vollmar et al. 2011) performed on an identical 3T-MRI scanner using the same protocol (O'Muircheartaigh, Vollmar et al. 2011). Using whole-brain VBM for grey matter and tract based spatial statistics (TBSS) for white matter diffusion MRI data, we revealed specific reductions in grey matter volume in the SMA as well as reductions in FA in underlying corpus callosum regions, which were associated with specific neuropsychological deficits in word naming tasks and expression scores.

8.5.2 Frontal Lobe Epilepsy

We did not find any change in structural connectivity of the SMA attributable to the lateralisation or the sublobar localisation (medial vs lateral) at a group level. This suggests that the motor system is a very robust neural network which is not affected by chronic FLE, not even in cases with frequent seizures involving the SMA. This has important implications for epilepsy surgery planning in the pericentral cortex and is also consistent with the lack of functional motor deficit in most patients with FLE without a motor cortex lesion. Electrophysiological studies have showed motor hyperexcitability in FLE (Loscher, Dobesberger et al. 2007; Nardone, Venturi et al. 2008) and a voxel-based study of MD in FLE reported significant MD increases within the motor network in some patients (Guye, Ranjeva et al. 2007) but our group results did not find abnormal structural connectivity paralleling these findings.

The groups of L- and R-FLE patients were heterogeneous with respect to cause and age of onset. Confirmation of our results from further studies with more homogeneous patient groups is needed but large groups of such patients are difficult to recruit.

There were no significant FA changes for the subgroups with lateral and medial FLE, as defined on the pattern of motor system involvement. However, the medial vs lateral localisation was based on the involvement of SMA as the symptomatogenic zone but not necessarily the ictal onset zone or the epileptogenic zone since formal validation with intracranial EEG recording or post-operative follow-up was only available in some patients. In contrast to JME, in which involvement of the motor system is intrinsic to the syndrome, further studies are needed with FLE patients showing a validated localisation of the epileptogenic zone within the motor system. This would allow a more specific study of SMA and motor system connectivity in FLE.

8.5.3 Methodological considerations

Motor plasticity has been reported in association with structural lesions of the motor cortex (Dancause 2006) and with epileptic activity (Lee, Shin et al. 2009) and this was one of the main reasons to base our tractography on seed regions defined by motor fMRI in individual subjects. Our localisation of medial frontal BOLD changes using the joystick task was concordant with other studies of the SMA using fMRI, PET or corticography (Picard and Strick 1996). In contrast to voxel-based measurements of diffusion parameters such as FA or MD in the white matter underlying abnormal cortical structures, diffusion parameters measured in whole tracts seeded from these regions explore white matter changes with a network-oriented approach. A similar strategy suggested abnormal white matter tracts in language and memory networks of patients with temporal lobe epilepsy (Powell, Parker et al. 2007; Yogarajah, Powell et al. 2008). In our study, FA was the most sensitive parameter, followed by MD, whereas nTV was less sensitive in detecting intergroup differences. Recognised limitations of diffusion based tractography include difficulty in dealing with crossing or 'kissing' fibres, even with probabilistic tractography and an algorithm to optimise the resolution of this ambiguity. The commonality maps found in our study were similar to

those obtained in a group of healthy subjects in another study (Johansen-Berg, Behrens et al. 2004). The bi-medial frontal connectivity is a good subcortical correlate of the bilateral grey matter changes found in other studies (Woermann, Free et al. 1999; Kim, Lee et al. 2007).

8.6 Conclusion

Using Diffusion Tensor Tractography, we found altered structural connectivity of the SMA in JME compared to controls, concordant with a growing body of evidence that there are subtle frontal lobe abnormalities in this condition. In contrast, SMA connectivity was not altered in FLE. This evidence of impaired motor networks in JME parallels electrophysiology studies which showed impaired recruitment of inhibition in JME but not in FLE (Klimpe, Behrang-Nia et al. 2009). The finding of preserved structural connectivity changes in FLE patients suggest that the white matter regions known to contain this part of the motor network should be spared by surgical procedures, even when the epileptic focus lies in the medial frontal region.

9 STRUCTURAL CONNECTIVITY OF EPILEPTIC NETWORKS

9.1 Summary

Objectives: This chapter focuses on the combination of functional imaging methods with structural connectivity tools, to study the underlying anatomical connections subserving epileptic networks. The neurophysiological hypothesis and methodological considerations applying to the use of different tools for localisation of the epileptic activity (ESI, MEG, EEG-fMRI, intracranial EEG) are discussed and an exploratory study on the combination of intracranial EEG and DTI tractography is presented.

Methods: One patient with medically refractory left parietal epilepsy symptomatic of a focal cortical dysplasia was studied. The structural connectivity of the seizure onset zone defined with intracranial EEG was mapped with DTI tractography. The qualitative (spatial extent) and quantitative analysis of the tracts were compared with similar mapping in 20 controls, especially with respect to branches of the whole tract extending towards the region of non-contiguous seizure propagation defined on intracranial EEG. Voxel-based analysis of maps of Fractional Anisotropy (FA) between the patient and the controls was also performed and highlights the methodological constraints while raising suggestions for further studies.

Results: There was no patient specific tract connecting the seizure onset zone and the area of non-contiguous propagation. Higher FA was found in a region of interest connecting the seizure onset and propagation zones. This result was not confirmed by voxel-based analysis.

Discussion: The study of intralobar structural connectivity underlying non-contiguous propagation of epileptic seizure in a single patient presents several methodological challenges. DTI might lack sensitivity for the relevant small white matter tracts. Moreover, statistical comparison between single subjects and a group of control is

difficult and the normalisation of seed regions might have introduced additional confounds. Further studies looking at long range propagation and using improved tractography techniques are warranted.

9.2 Introduction

9.2.1 Epileptic networks

In the XIXth century, the eminent British neurologist Hughling Jackson first realised that the spread of focal epileptic symptoms across the body (for instance clonic jerks starting in the face then affecting the hand and arm) corresponded to the propagation of the epileptic activity in the brain : the eponymous Jacksonian “march” of epileptic symptoms (Jackson 1870). Intracranial EEG recordings show that the epileptic activity can spread locally but can also propagate to distant brain structures via white matter fibre tracts, generally along tracts that belong to physiological brain networks, as illustrated in Figure 9.1.

In principle, structural connections between brain structures involved in the epileptic network can be direct (monosynaptic connections) or indirect with cortical or subcortical relays (polysynaptic connections). Functional connectivity studies based on EEG, MEG or fMRI (Astolfi, Cincotti et al. 2007; Guggisberg, Honma et al. 2008; Bettus, Guedj et al. 2009) can be used to draw inferences about correlation between the activity (neuro-electric or haemodynamic) of different brain structures. However, most of these techniques do not inform on the direction of the flow of information (no “causality” information) and do not distinguish between correlated activity mediated by direct anatomical connections or due to a common input without direct connections between the studied regions. Alternatively, models of effective connectivity, such as Dynamic Causal Modelling, are based on an underlying model of neuro-electric

activity and haemodynamic changes and give inferences about the directionality of the functional coupling between brain regions (see 2.6.2.4).

Structural connectivity studies can investigate the anatomical connections underlying epileptic networks. Therefore, structural connectivity may shed light on the architecture of these networks and could distinguish between direct and indirect connections. This chapter focuses on the structural connectivity of the epileptic network using DTI tractography.

The wider concept of “epileptic network” encompasses overlapping networks that can be specifically studied :

- Structural connectivity of the irritative zone : structural connections between brain regions involved in the irritative zone and best mapped with functional imaging of the interictal epileptic activity as described in chapter 2 with ESI and EEG-fMRI.
- Structural connectivity of the seizure onset zone : structural connections of the seizure onset zone, ideally defined by intracranial EEG recordings.
- Structural connectivity between the seizure onset zone and the structures involved in ictal symptoms and signs (the symptomatogenic zone): this is of particular interest to better understand early seizure propagation and ictal semiology in individual patients.

In patients who are candidates for epilepsy surgery, a better knowledge of these first two networks would help better delineate the epileptogenic zone to be surgically removed or disconnected.

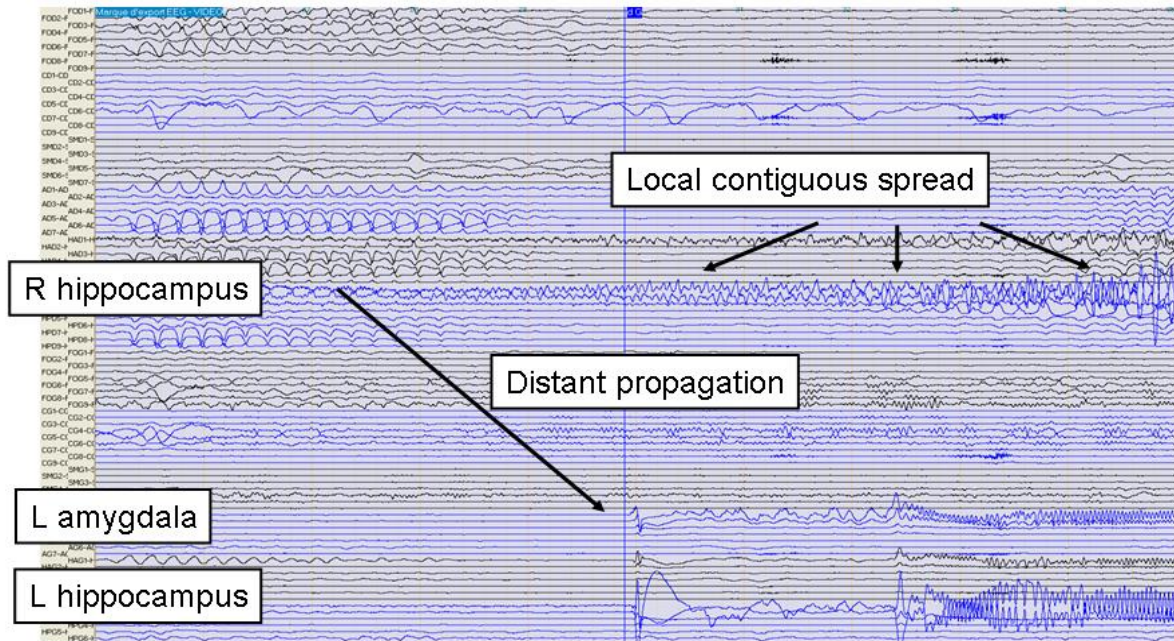


Figure 9.1 : Connectivity of epileptic networks on intracranial EEG

Illustrative intracranial EEG in a patient with right temporal lobe epilepsy. The seizure starts in the electrode contacts located in the right hippocampus. There is recruiting focal activity with increasing amplitude and number of contacts involved, suggesting contiguous spread along cortico-cortical junctions or short intralobar subcortical tracts. There is also distant propagation to the contralateral medial temporal structures that necessarily occurs via white matter fibre tracts.

9.2.2 Mapping the structural connectivity of epileptic networks

The literature contains only sparse studies investigating brain structural connectivity based on functionally defined epileptic activity (see 3.6.7). Methodological limitations developed below can partly account for this paucity.

9.2.2.1 Precise functional localisation of epileptogenic structures

Investigating the structural connectivity of the epileptic network requires a precise localisation of the involved brain structures in order to define seed regions for the tractography. A good anatomical resolution is paramount for the reliability of the tracking as shifting the seed region by the magnitude of one gyrus can of course lead to radically different connections. Non-invasive methods to localise epileptic activity generally focus on interictal activity for ease of recording and analysis.

- ESI : a sublobar localisation can be obtained with state-of-the-art recording conditions (number and position of electrodes for ESI, see section 2.3.1.2) and analysis strategies. The same level of accuracy is expected with MEG studies.
- EEG-fMRI : The spatial resolution of the technique has the order of magnitude of a voxel (typically $3 \times 3 \times 3 \text{ mm}^3$) but multiple clusters of BOLD changes are often found, lowering specificity. Moreover, the potential mismatch between neuroelectric activity and the BOLD changes captured by EEG-fMRI can be of several millimetres (see section 2.6.1) and this imprecision is then carried over in the tractography seed placement. The yield of these functional localising tools is limited by the need to record a sufficient number of IED. However, recent development of EEG-fMRI analysis might provide localising information even in patients in whom no IED is recorded during EEG-fMRI, provided IED have been detected during prolonged video-EEG telemetry (Grouiller, Spinelli et al. 2010).

- Intracranial EEG recording can localise the seizure onset zone and irritative zone with infra-centimetric precision allowing for a precise placement of seed regions (Diehl, Tkach et al. 2010) but the number of investigated patients is much smaller.

9.2.2.2 Mapping small tracts

Despite considerable methodological advances, the mapping of small white matter tracts (intralobar cortico-cortical connections, long-range small fibre tracts) with tractography is still difficult for the following reasons:

- As for fMRI, DTI voxels are the order of magnitude of $3 \times 3 \times 3 \text{ mm}^3$, therefore much larger than some white matter fibre bundles.
- In some parts of the brain, the reliability of the tracking algorithm is affected by colocalised large fibre tracts and can have difficulty to resolve “crossing” or “kissing” tracts (see section 3.3.1).

9.2.2.3 Altered vs aberrant connections

As already mentioned, structural brain connectivity is altered at the site of epileptic activity (with mainly reduced FA and increased MD) (Guye, Ranjeva et al. 2007; Focke, Yogarajah et al. 2008) but remote changes inside and outside the irritative zone make these changes not sufficiently specific for localising the epileptic activity based on diffusion imaging. Moreover, diffusion changes extending beyond cortical lesions have been well documented (Eriksson, Rugg-Gunn et al. 2001). The existence of aberrant white matter connections existing in patients with epilepsy but not in healthy subjects has been suggested (Bhardwaj, Mahmoodabadi et al. 2010) but is still a matter of debate. Therefore, studying the structural connectivity of epileptic networks should focus on quantitative changes in specific tracts involved in the propagation of the epileptic activity.

9.2.2.4 Abnormal connectivity at the individual level

Connectivity of the epileptogenic zone in localisation-related epilepsy is mainly limited to the study of series of individual cases, except in a few well-defined conditions such as medial temporal lobe epilepsy with hippocampal sclerosis or idiopathic focal epilepsy with centro-temporal spikes. As a consequence, the determination of altered connections has to be done by comparing one patient with a group of controls. This type of analysis has a much lower statistical power than comparing connectivity between two groups, as done in the vast majority of tractography studies.

9.2.3 Combined icEEG and DTI study of the structural connectivity of the seizure onset zone

Given the above considerations, we explored the changes in structural connectivity of the seizure onset zone, compared to healthy controls in a situation defined with very strict inclusion criteria :

- Seizure onset zone defined by intracranial EEG with non-ambiguous findings.
- Evidence of non-contiguous seizure propagation : evidence on intracranial EEG of propagation to distant cortical regions without contiguous spread (i.e. some electrode contacts between onset and propagation structures showing no epileptic activity).

We hypothesized that:

- 1) the structural connectivity between the seizure onset and the propagation zone in single patients would be altered compared to a group of controls;
- 2) the propagation tract would show different quantitative alterations compared to other tracts seeded from the seizure onset zone. This would help

disentangling connectivity changes related to a structural epileptogenic lesion vs epileptic activity *per se*.

At the time when data was gathered for this study in early 2009, only two patients from the telemetry unit of the NHNN who had had intracranial EEG fulfilled the EEG inclusion criteria and had pre-implantation DTI. One of them did not have a pre-implantation DTI acquisition with the latest acquisition. This prevented comparison with healthy controls and this case was excluded from analysis. The patients implanted in the following 4 months months did not show intracranial findings compatible with the inclusion criteria.

9.3 Case Report

This 20 year-old woman suffered from left parietal epilepsy symptomatic of a focal cortical dysplasia. Seizure semiology consisted in daily complex partial seizures with tonic posturing of the right arm and automatisms of the left arm. Frequent secondary generalisation had occurred in the past. Interictal and ictal scalp EEG showed left parietal epileptic activity. Intracranial EEG was performed to confirm the seizure onset zone and map the eloquent cortex (mainly language). Left parietal lateral seizure onset occurred simultaneously in a cluster of contacts of the subdural grid with early propagation to a non-contiguous contact in the left posterior paramedian parietal cortex, as illustrated in Figure 9.2.

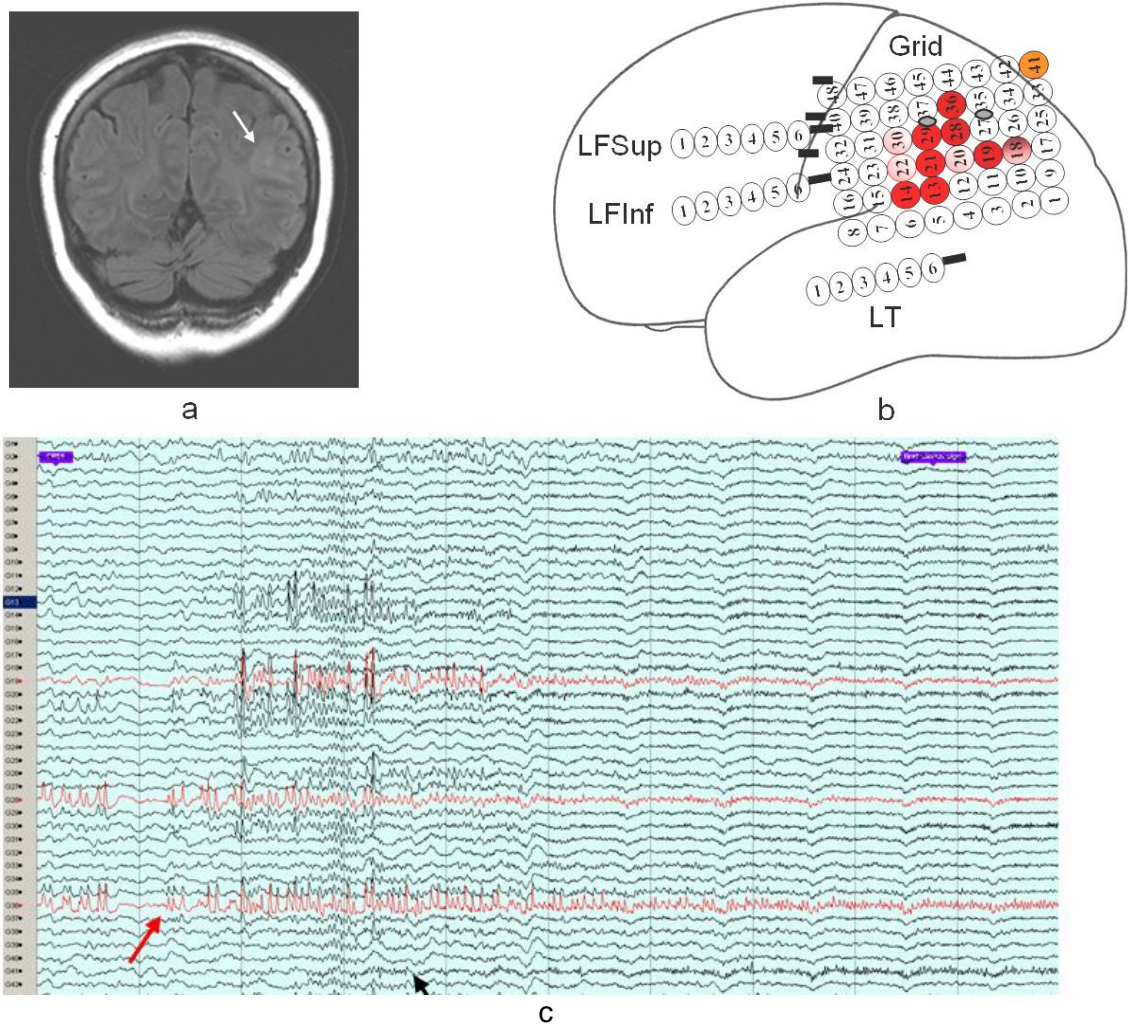


Figure 9.2: Intracranial seizure onset in focal cortical dysplasia

a) Coronal FLAIR MRI showing the signs of focal cortical dysplasia in the left parietal cortex (arrow) characterized by blurring of the grey-white matter and hyperintensity of the white matter. b) Schematic diagram of intracranial electrode positions with colour coding of subdural grid contacts (numbered circles) involved in seizure onset: dark red→orange = maximal→minimal involvement. LFSup, LFIInf, LT=left frontal superior, inferior and left temporal strips, not involved in the seizure onset. Note that propagation to contact 41 (orange) occurred in a non-contiguous fashion, suggesting subcortical propagation via cortico-cortical white matter tracts. Grey ovals represent intracerebral depth electrodes. c) Seizure onset on intracranial recording: Red channels correspond to dark red contacts in the schematic diagram. Red arrow: left lateral parietal ictal onset (contact 36); black arrow: early non-contiguous propagation to paramedian posterior parietal cortex (contact 41). b and c: courtesy of Dr Beate Diehl, EEG Telemetry Unit, National Hospital for Neurology and Neuropsychiatry.

9.4 Methods

9.4.1 Localisation of the seizure onset zone as tractography seed

The position of the icEEG electrodes was coregistered to the anatomical images (T1-weighted image) according to a routine strategy for patients with intracranial EEG recordings using BiImageSuite (<http://www.bioimagesuite.org/>) (analysis performed by Dr Roman Rodionov, ION). Computed Tomography (CT) images acquired after intracranial implantation were coregistered to structural (T1-weighted) MRI. The brain image was then extracted from the T1 image (skull stripping) and the artefacts created by the contacts of the intracranial electrodes were segmented from the CT images.

Precise co-registration of these T1-based images with diffusion-weighted images used for tractography is difficult because of image distortion and rigid coregistration can lead to imprecision of a few millimetres in some brain regions. Non-linear methods implemented in SPM5 for normalisation were tested but did not lead to a better coregistration. Therefore we visually compared the T1-weighted images (containing icEEG electrodes) with the FA images to localise the seizure onset and seizure propagation regions of interest on the FA image. A 6mm radius sphere was drawn in the underlying white matter of these two regions of interest to serve as seed regions for the tractography (SOZ seed S_{soz} ; propagation seed S_p). The size of the seed regions was motivated by the difficulty to map tracts in this region with smaller seed regions (5mm) and the unspecific tracking that resulted from larger regions (8mm).

9.4.2 Tractography: one-seed vs two-seed

We used the tractography methods described in section 4.2 in two ways :

- One-seed tractography from the S_{soz} .
- Two-seed tractography starting from the S_{soz} with the condition that the tracts should travel through or terminate in the S_p . In a preliminary analysis, no tract was found when using two seed regions Therefore; tracking was limited to one seed region.

Tracts were thresholded at 0.01 (1% probability of connection).

9.4.3 Tractography in healthy controls

A group of 20 healthy controls was chosen as a comparison. They had no history of neurological or psychiatric disease and age ranged from 22-49 years (mean 33.2 ± 8.6 years) The FA map of the patients was normalised to an FA template as described in section 4.2.2. The transformation parameters of this normalisation were applied to obtained normalised seed regions (wS_{soz} and wS_p). These normalised seeds were then back normalised on the brain of individual healthy controls using a back normalisation routine written in Matlab and provided by Dr Niels Focke (UCL Institute of Neurology) and the accurate localisation of this two-step normalised seeds ($w'wS_{\text{soz}}$ and $w'wS_p$) was visually verified by overlay on individual FA images.

The tractography procedure was run in each individual control data set with the same parameters as for the patient.

9.4.4 Qualitative tractography and commonality maps

The tracts of the patient and the 20 controls were normalised to the FA template. With the procedure described in section 4.2.2, commonality maps of the tract seeded from the $w'w S_{\text{soz}}$ were derived. The patient's individual tract was overlaid onto this commonality map to investigate the existence of patient specific tracts.

9.4.5 Quantitative tract analysis

To investigate quantitative differences between the patient and the control group, mean FA and MD values were calculated for two sets of tracts in the patient and the healthy controls :

- the whole tract seeded from the SOZ;
- the tract included in the white matter region lying between both seed regions.

This “tract of interest” was delineated manually on normalised FA maps and back normalised to the individual space of the patient and controls.

9.4.6 Voxel-based analysis of FA maps

In addition, a voxel-based comparison of FA maps was performed to look for significant differences in FA between the patient and the control group. Normalised FA maps were smoothed with a cubic gaussian kernel (5mm full-width at half maximum). The data were explored with a statistical threshold of $p < 0.001$ uncorrected and subsequent small volume correction was performed in a 20 mm radius sphere in the parietal lobe.

9.5 Results

9.5.1 Qualitative tractography and commonality maps

The map of the structural connectivity of the seizure onset zone of the patient is shown in Figure 9.3. This connectivity map is overlaid onto the commonality map of the connectivity of the homologous region in the 20 controls. The normalised seed regions wS_{soz} and wS_p are overlaid on the same figure. There was no part of the patient tracts that extended beyond the commonality map of the controls.

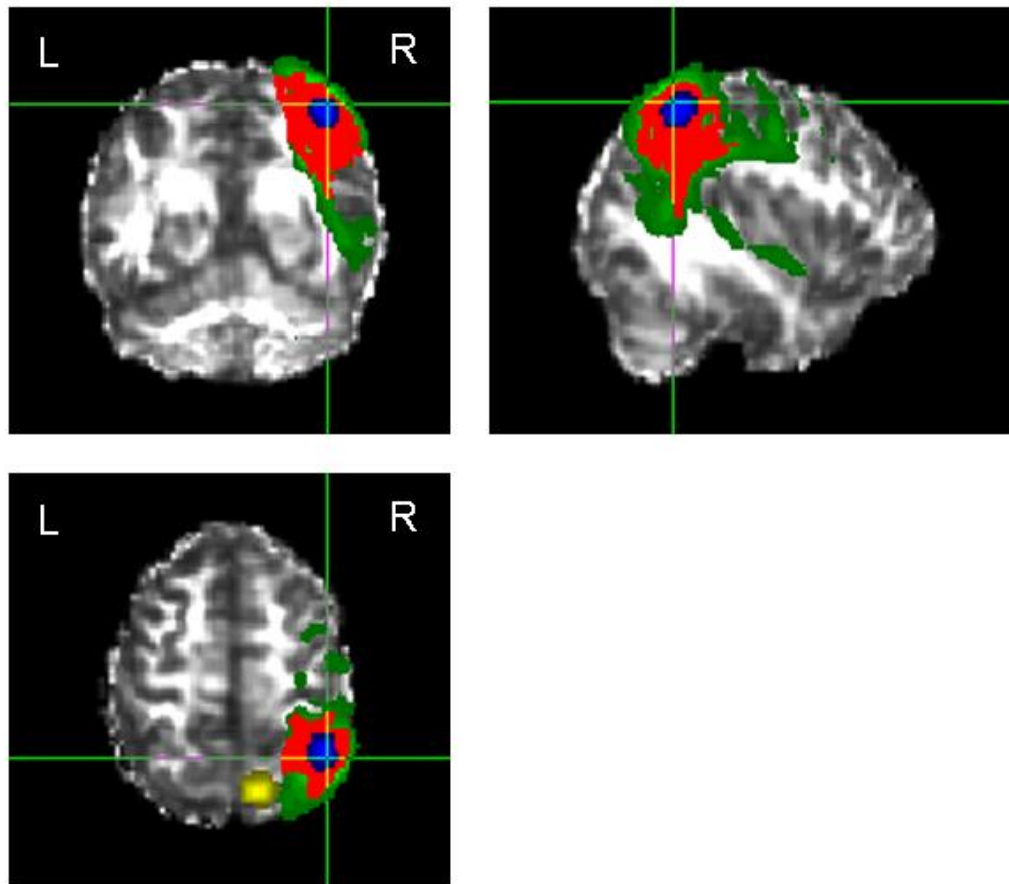


Figure 9.3 : Commonality map of seizure onset zone connectivity.

Connectivity of the seizure onset zone in the patient (red) overlaid onto the normalised FA map. The commonality map of 20 healthy controls (green) is also overlaid. There is no part of the tract that is patient specific (i.e. outside the commonality map of the controls). The seeds corresponding to seizure onset zone (blue) and propagation zone (yellow) are represented.

9.5.2 Quantitative tract analysis

Figure 9.4 shows the manually-defined “tract of interest” between SOZ and propagation area, overlaid onto the normalised FA image. FA and MD in this tract of interest and in the whole tract seeded from the S_{SOZ} are shown in Figure 9.5. In the patient, there was high FA and low MD in this tract of interest compared to controls (patient: FA=0.260, MD=2.56; control group mean and standard deviation: FA 0.192 ± 0.025 , MD 3.13 ± 0.59). After correction for multiple comparisons (Bonferroni, 4 correlations analysis), there was no significant correlation in the controls between age and mean FA resp MD in the tract of interest ($p=0.12$, resp $p=0.25$) or between age and mean FA in the whole tract ($p=0.64$). Only a correlation between age and MD in the whole tract was just significant after correction ($r=0.54$; $p=0.044$). However, in the whole tract, there was no visual trend for the FA and MD values in the patient tract compared to the controls and the patient’s values were concordant with the average of the control group (patient: FA=0.272, MD=2.69; control group mean and standard deviation: FA 0.271 ± 0.020 , MD 2.70 ± 0.28).

9.5.3 Voxel-based analysis of FA maps

The voxel-based statistical parametric mapping of the FA maps showed multifocal bilateral FA increase in the patient (Figure 9.6). There was a small cluster of FA increase in the parietal cortex and this cluster survived small-volume correction ($p<0.0005$, family-wise error correction). However, this cluster was not spatially overlapping the tract of interest.

Lower FA in the patient compared to the control group was found in the thalamus bilaterally as well as in scattered voxels but not in the left parietal lobe.

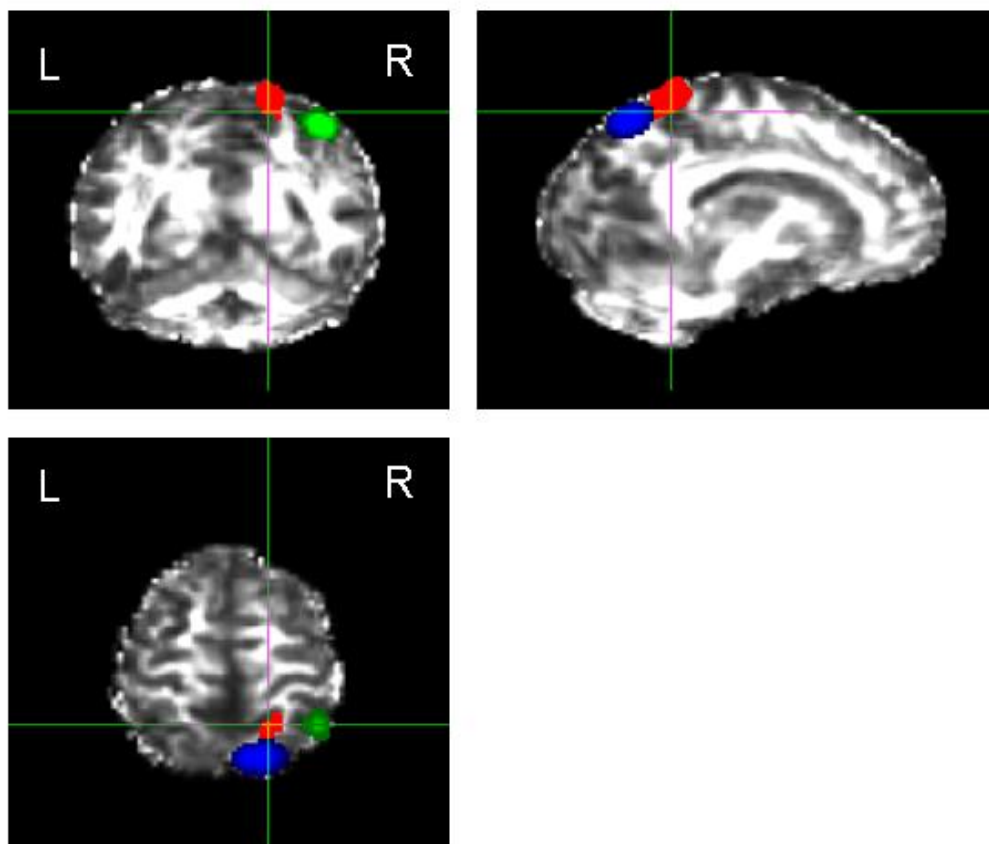


Figure 9.4 : Seizure propagation

Seed regions in the white matter underlying the seizure onset zone (green) and the seizure propagation zone (blue). Tract of interest (red) (see text).

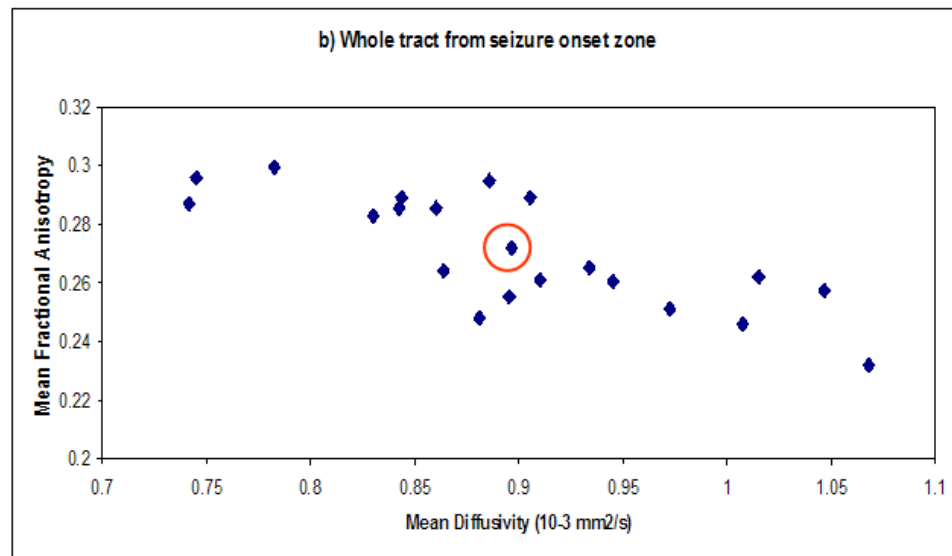
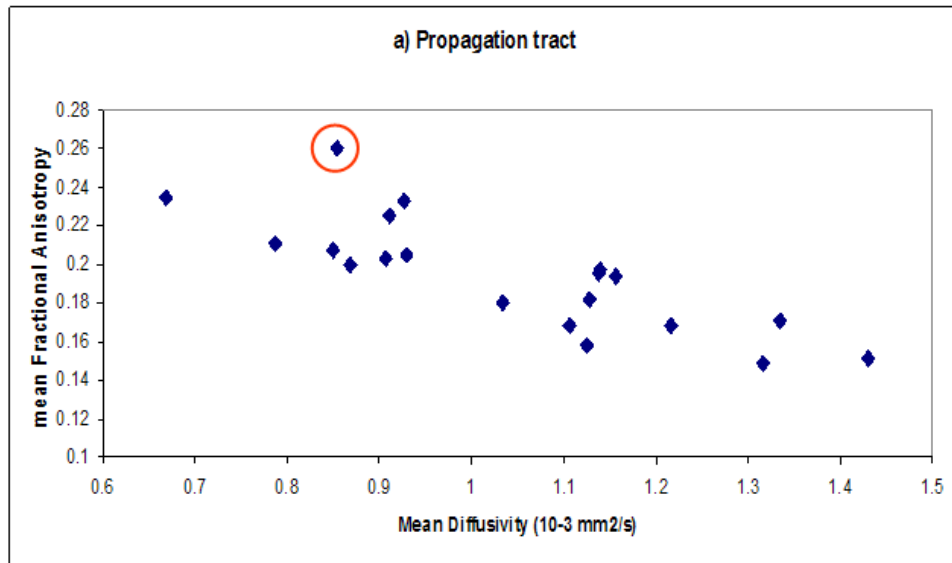


Figure 9.5: Quantitative tract analysis

Mean FA and MD of patient and controls for the tract of interest (top) and the whole SOZ connectivity tract (bottom). Red circles identify the patient data. There is a comparatively striking high FA and low MD in the tract of interest of the patient, while the patient data are within the range of the control group in the whole SOZ connectivity tract.

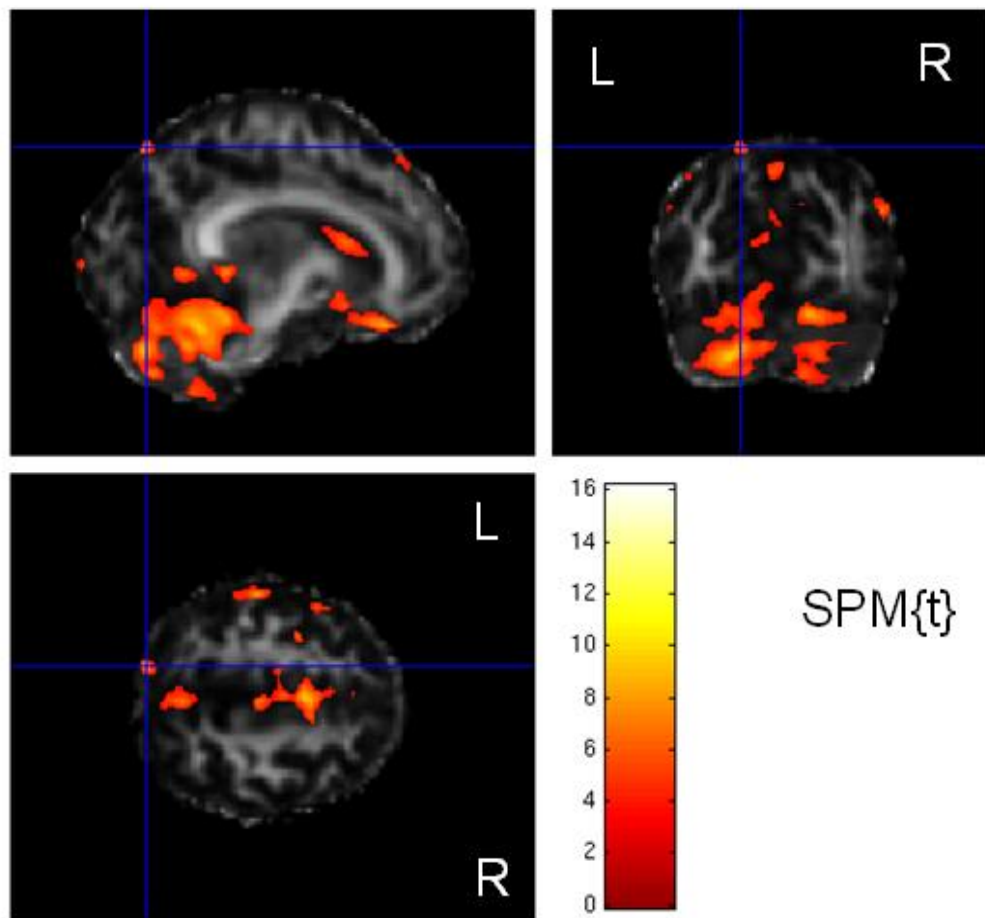


Figure 9.6: voxel-based analysis of FA maps: patient > controls

SPM{t} test looking for voxels where the FA is higher in the patient compared to 20 controls ($p < 0.001$ uncorrected). Bilateral multifocal significant clusters were found, one of them (cross-line) in the paramedian parietal lobe, the region identified as belonging to the epileptic network. This cluster survived small-volume correction but did not overlap with the tract of interest defined above (see text).

9.6 Discussion

9.6.1 Neuroanatomical significance

In this study of the structural connectivity of the S_{SOZ} estimated with icEEG-based DTI tractography, no patient tract could be found that could not be found amongst the controls. Tractography did not reveal direct anatomical connections between the seizure onset zone and the region of seizure propagation.

This patient had a structural abnormality (focal cortical dysplasia) in the vicinity of the SOZ. Previous studies have shown areas of significant FA decreases which frequently extend beyond the lesion visible on clinical MRI suggesting subtle structural abnormalities and reduced connectivity (Rugg-Gunn, Eriksson et al. 2001). We found rather opposite changes in a tract of interest investigating the seizure propagation revealed by icEEG. Within a user-defined region assumed to contain white matter fibres connecting the two regions, mean FA and MD were in favour of increased connectivity (higher FA, lower MD) in the patient compared to controls. In the whole connectivity map tracked from the SOZ, we found no difference in the patient compared to control.

Therefore, our current results do not allow the validation or rejection of our starting hypotheses but rather suggest that the methodology should be improved to answer them. First, the absence of a structural connection between the two regions of interests probably points out at the limited sensitivity of current tractography techniques (see section 8.6.2 methodological considerations) and suggests that our findings should be interpreted with caution. Second, our finding of increased FA along a tract directed towards (but not reaching) the zone of seizure propagation, while the global connectivity of the seizure onset zone was not different from controls, needs to be confirmed by future studies. If confirmed, this finding might be in favour of increased connectivity along the path of propagation meaning either that seizure

propagation along the “path of least resistance”, represented by the higher FA or that propagation acts as a stimulating neurobiological signal that reinforces the specific connection used, within regionally altered connectivity.

Bilateral cerebellar FA reduction predominating on the side of the epileptic focus were consistent with structural cerebellar alterations (atrophy) found in patients with focal epilepsy (Liu, Lemieux et al. 2005). The history did not reveal any chronic use of the antiepileptic drug phenytoin, which could also cause cerebellar atrophy.

9.6.2 Methodological considerations

Some limitations apply to this exploratory study.

First the normalisation and back normalisation procedures between individual FA and the normalised FA are performed in several steps. Despite visual verification, some degree of imprecision in coregistration and localisation is intrinsic to the procedure. All steps were carried out manually resulting in a significant time of processing so that automatisisation should be obtained for investigating larger groups of patients. Improved normalisation tools accounting for non-linear deformation could be used to minimize the imprecision of the normalisation to a template map and intersubject variability (Ashburner 2007; Klein, Andersson et al. 2009).

Second, FA differences between the patient and the control group were found in voxels belonging predominantly to the grey matter. Altered structural connectivity would rather be expected to be related to white matter FA changes. It is possible that a subtle focal cortical atrophy associated with the malformation of brain development presented by the patient resulted in fewer voxels with “cortical” FA signal and therefore a larger average FA in the tract of interest and relevant voxels in the voxel-based analysis. This would be concordant with the results of the voxel-based analysis which failed to show significant FA changes in the white matter of the tract of interest

but showed a small region of increased FA in the parietal cortex concordant with the tract of interest of uncertain significance. However, given the multifocal changes in the voxel-based analysis, such comparison is speculative at this stage. As a next step to demonstrate its validity, our approach should be tested on additional patients exhibiting seizure propagation to a different lobe (e.g. temporal to frontal), well documented by icEEG and therefore involving the mapping of larger white matter tracts. This would potentially yield more reliable results than the study of intralobar connections, for the application to small patient groups compared to healthy controls.

Third, the comparison of one patient with a group of requires a small variability in the control group to obtain statistical significance, when measuring a small deviation of this variable in a patient. Moreover, data shuffling with testing for significant differences of each healthy control compared to the N-1 other controls would be necessary to avoid false positive findings. The increasing number of patients undergoing intracranial EEG in most epilepsy centres and the wider availability of good quality diffusion imaging protocols and tractography software will help build small patient groups and increase the statistical power of such studies. Multicentric studies would help recruit patients more quickly but harmonisation of acquisition protocols for DTI is needed as well as comparative studies checking for scanner specific differences as systematic differences can be present even in nominally identical scanners (Vollmar, O'Muircheartaigh et al. 2010). The correction of this bias reduces intersubject variability, therefore potentially increasing the statistical power of group analysis.

Fourth, the tractography algorithm was not able to reveal direct tracts connecting the SOZ and the propagation area despite clear propagation between these regions shown by icEEG and absence of contiguous cortical spread. Several hypotheses can account for this : the resolution of DTI and tractography could be insufficient to map small tracts connecting both regions; the angular threshold might be too conservative

to map strongly curved fibres and studies with variable angular thresholds would be useful; finally, the unctiguous propagation shown by icEEG could have no direct underlying anatomical connections, occuring via subcortical relays in the basal ganglia and thalamus. A combination of the first two hypotheses is the most likely cause of this unsuccessful tracking and future improvement in DTI resolution are needed. A combination of structural connectivity studies with functional and effective connectivity models could help answer the third hypothesis by comparing the likelihood of models of direct vs indirect structural connectivity.

Finally, the patient belonged to the youngest quartile of the group but her age was within 1 standard deviation of the mean of the control group. Moreover, we found no clear correlation between age and FA/MD that could have explained our findings.

9.6.3 Perspectives

With the current resolution of DTI and non-invasive functional localisation of epileptic activity, future studies might concentrate on regional structural connectivity changes rather than precise voxel-to-voxel connectivity, with seed regions defined by non-invasive tools (ESI, EEG-fMRI). Precise prior hypothesis regarding individual pattern of propagation, as identified by electro-clinical semiology will be needed to guide the placement of the seed regions. In addition to using fMRI to reveal epileptic networks with simultaneous EEG-fMRI or with a functional connectivity approach (He, Shulman et al. 2007) EEG strategies estimating connectivity and causality relationships between brain regions (Astolfi, Babiloni et al. 2004) or combinations of these techniques could be applied to map epileptic networks. Such information about the functional coupling between brain structures could be compared to structural connectivity patterns in specific patient groups as well as in individual cases compared to controls.

Ongoing methodological development in diffusion imaging and tractography as well as new analysis strategies will help to map smaller tracts and better resolve the ambiguity related to fibre crossing. In Diffusion Spectrum Imaging (DSI), a much greater number of diffusion directions and intensities are acquired (typically 256-512, compared to 60 with the current DTI sequence used in this work) (Wedeen, Hagmann et al. 2005; Hagmann, Jonasson et al. 2006). Such methodological improvement could improve the mapping of crossing tracts but further improvements such as reducing scan duration and reproducibility studies are needed to assess the real potential of the technique. Connectivity-based cortical parcellation has been shown to help segregating neighbouring cortical regions involved in different networks (Johansen-Berg, Behrens et al. 2004). Such a strategy could be used to investigate the cortical and subcortical plasticity in longstanding epileptic activity.

9.7 Conclusion

The study of structural connectivity of the networks involved in epileptic activity requires a precise localisation of the epileptiform activity with non-invasive or invasive methods and a tracking strategy with sufficient resolution to display intralobar midrange fibre length (50-100 mm) typically involved in propagation of the interictal and ictal epileptic activity. Our exploratory study shows that quantitative tracks statistics can be applied to single patients and control groups to investigate such connectivity. However, several methodological caveats limit the significance to our preliminary findings.

SECTION 3

DISCUSSION

10 OVERALL DISCUSSION

10.1 Summary of the principal findings and methodological considerations

10.1.1 Combining ESI and EEG-fMRI

ESI can be reliably performed on the scalp EEG recorded during fMRI acquisition, after correction of MR gradient-related and pulse-related artefacts. Spatial concordance between ESI and BOLD changes was obtained in more than 80% of cases. The use of continuous ESI of the source of IED improved the modelling of BOLD changes related to interictal epileptic activity.

10.1.2 Interictal epileptic networks in focal epilepsy

Performing ESI on the EEG recorded during EEG-fMRI helped distinguishing between BOLD changes related to onset vs propagation of epileptic discharges. ESI allowed mapping the propagation of IED between regions involved in the epileptic networks revealed by ESI. The statistical maximum of BOLD changes corresponded to the source of the epileptic activity only in a third of the patients. Other positive BOLD changes, even with very small spatial extent, or negative BOLD changes could be spatially concordant with the neuroelectric source of IED. Moreover, the continuous activity of the IED source had BOLD correlates that were concordant with the localisation of focal epileptic activity, thereby extending the yield of EEG-fMRI.

However, the sensitivity and specificity of EEG-fMRI in focal epilepsy still needs to be improved. The methodological developments presented in this work do not tackle the problem of EEG-fMRI datasets in which no IED are found (Salek-Haddadi, Diehl et al. 2006). In other patients, the finding of multiple BOLD changes remote from the

presumed epileptic focus is puzzling and cannot be further explained by propagation estimated by simultaneous ESI. Findings in the resting state networks probably represent upstream or downstream modulation of activity rather than propagation of epileptic activity. However, some of the discordant findings, notably asymmetric BOLD changes contralateral to the presumed focus, are difficult to explain with our anatomical and physiological knowledge and there are often no strong arguments justifying to classify them as artefacts. This highlights the fact that EEG-fMRI reveals networks of functionally connected regions rather than single focal epileptic sources underlining our limited current understanding of such networks.

10.1.3 Intracranial EEG-fMRI

Intracranial EEG-fMRI was performed without adverse effects in 2 patients with epilepsy. Despite the interactions between icEEG and fMRI, data quality was sufficient to obtain IED related BOLD changes both locally and over the whole brain. BOLD changes occurred in the immediate vicinity of very focal IED recorded with icEEG. Distant BOLD changes were also found, sometimes in brain structures not sampled by icEEG.

Compared to scalp EEG, the abundance of interictal events on intracranial EEG and their variability complicated greatly the labelling of IED, requiring user-dependant choices regarding the grouping of the IED and the contrasts to be tested. We also used a very strict canonical HRF function without testing for non-canonical responses. Testing the validity of the assumption of linearity underlying the neuro-vascular coupling in such instance of very frequent IED is also needed.

10.1.4 Structural connectivity of physiological and epileptic networks

Tractography seeded from motor fMRI activations showed altered structural connectivity of the motor network in patients with JME compared to controls. There were no changes of SMA structural connectivity between patients with frontal lobe epilepsy and controls.

Within the motor system, we focused on the SMA connectivity as previous studies had reported structural abnormalities in the medial frontal cortex in patients with JME and the rest of the motor system projections were not explored. The connectivity changes illustrated by this study are limited to connections of the SMA, particularly those to the cortico-spinal tract and, via the corpus callosum, to the contralateral SMA. Other functionally important connections of the SMA are only poorly represented, notably the anatomically well identified connection between the SMA and the primary motor cortex could not be found. This illustrates the tendency of the tracking algorithm to be “attracted” by large tracts despite continuous methodological development to improve this problem.

The study of structural connectivity of epileptic networks requires the combination of functional and structural imaging tools to accurately localise the seed regions for subsequent tractography and was limited by important methodological challenges. The seizure onset zone defined by icEEG currently offers the best spatial precision for exploring structural connectivity with tractography. Qualitative and quantitative results can be obtained and compared to a group of controls.

However, as illustrated in Chapter 9, the current resolution of DTI-based tractography might not be able to map intralobar connections that are typically involved in propagation of epileptic activity. The user-dependent choice of the size of the seed region, as well as its manual placement, are also a source of bias and error. Our

choice was based on a compromise to combine stability and specificity: too small a seed region would reduce the stability of tracking and make it more dependent on the exact location of the seed region, while too large a seed would include nearby tracts that would confound the study. A systematic optimisation of the size and location of the seed regions would require testing a series of values and select the most stable solution. Moreover, comparison between individual patients and a control group and the usually high intersubject variability make it difficult to obtain statistically significant abnormalities in individual patients.

10.2 General discussion and future research directions

In this thesis, the general methodological aim was to combine neuro-imaging tools to better understand the functional and structural organisation of both pathological and physiological neuronal networks in the epileptic brain. The clinical and neurophysiological relevance of each study as well as its specific methodological limitations have been discussed above in the relevant sections. In the following section, I discuss the global relevance of this work, in the light of methodological limitations, and propose future research directions in each subsection.

10.2.1 Methodological discussion and perspectives

10.2.1.1 Beyond “conventional” EEG-fMRI studies of patients with epilepsy

More than 15 years after the first reports of simultaneous EEG and fMRI recordings in patients with epilepsy (Ives, Warach et al. 1993; Warach, Ives et al. 1996; Lemieux, Allen et al. 1997; Seeck, Lazeyras et al. 1998), the information extracted from the EEG for fMRI analysis remains, by large, the visual coding of IED (or in rare cases,

seizures) by clinical experts who cluster their findings into groups according to their spatial localisation, field and morphology. EEG-fMRI results show reproducibility (Gholipour, Moeller et al. 2010) but inaccurate IED marking can lead to significantly different results or lack of significant findings (Flanagan, Abbott et al. 2009). Using this IED-based strategy, up to 70% of scalp EEG-fMRI studies (depending on inclusion criteria) show no IED-related BOLD changes, even at 3T, either because no IED is recorded in the scanner or because of lack of statistical power. Other techniques to complement or validate EEG-fMRI studies have used recordings on separate sessions with the limitation that resting brain activity (vigilance, drugs) and hence spontaneous epileptic activity can be different across sessions (Benar, Grova et al. 2006; Grova, Daunizeau et al. 2008).

BOLD changes related to interictal epileptic activity reveal a complex network involving multiple cortical and subcortical structures. The addition of simultaneous ESI allows better localisation of the starting point of this interictal activity and following its “march” across the network. Similarly to the study described in chapter 5, simultaneous ESI and EEG-fMRI has recently been applied in children (Groening, Brodbeck et al. 2009) and has allowed to identify distinct networks but common mechanisms of IED propagation in children suffering from epileptic encephalopathy with Continuous Spike and Wave during Sleep (Siniatchkin, Groening et al. 2010), a form of focal electrical status epilepticus with severe cognitive consequences. Moreover, instead of following the spread of the epileptic activity, ESI can also be focused on the temporal course of its source, as shown in chapter 6 : the modelling of the BOLD signal changes by the continuous activity of the IED source enhanced the localisation of the epileptic focus.

The aim of EEG-fMRI (and more globally fMRI) analysis is to build a model containing variables explaining the largest possible amount of variance of the BOLD signal by inclusion of regressors describing the effect of interest and adding parameters to

describe effects of no interest (confounds) that help explain the BOLD signal changes (motion, pulse, other physiological confounds). Since scalp epileptic activity represents only the “tip of the iceberg” of pathological cortical activity (Tao, Ray et al. 2005), the modelling of epileptic activity by a continuously varying variable constitutes a logical improvement of the modelling of BOLD signal changes in resting state fMRI of patients with epilepsy. Such EEG-based parametrisation of fMRI analysis has also been proposed in the field of cognitive neurosciences by parametrising single evoked responses using behavioural variables or neurophysiological features (signal amplitude, latency time-frequency characteristics) (Debener, Ullsperger et al. 2006; Bagshaw and Warbrick 2007; Porcaro, Ostwald et al. 2010), again to obtain a more detailed modelling of the BOLD signal changes. Such a single-event approach could be used to parametrise EEG spikes following several labelling categories (topography, morphology, amplitude, etc). However, this possibility would raise the issue of selecting the most neurophysiologically relevant feature(s) for analysis and neurophysiologic rationale for the choice of such features of interest should be considered before analysis.

Parametric fMRI regressors such as continuous epileptic source activity estimated by ESI reflect the combination of epileptic activity, physiological brain activity and some contamination by EEG artefacts. In parallel to our study, other strategies have been reported for building EEG-informed parametric epilepsy-specific regressors for fMRI. These techniques are based on independent component analysis in an attempt to isolate the epileptic activity (factor) from the EEG signal and avoid confounding factors such as motion, eyeblinks or cardiac artefacts (Marques, Rebola et al. 2009; Formaggio, Storti et al. 2010) but comparative studies with conventional General Linear Model analysis suggested that they require the presence of more IED to reveal the epileptic networks (Moeller, Levan et al. 2010).

The use of ESI or cESI combined with fMRI as presented in chapters 5 and 6 and the inclusion criteria imposed by these studies make the technique available only to datasets with spikes in the scanner. All EEG-fMRI studies suffer from recruitment biases depending on the tested hypothesis. Early studies preferentially included patients with abundant interictal epileptic activity outside the scanner (Lazeyras, Blanke et al. 2000; Al-Asmi, Benar et al. 2003; Salek-Haddadi, Diehl et al. 2006) and intra-MR IED were obtained in about two thirds of datasets. More recently, studies with a strong interest in invasive validation recruited any patient considered for intracranial recording with, consequently, a much reduced proportion of patients with IED during fMRI (Thornton, Vulliemoz et al.). Inclusion criteria for ESI reduced the proportion of cases in which our methodological advances are applicable. Future studies should aim at broadening applicability to increase clinical relevance.

In fMRI analysis, the inclusion of additional knowledge about variables of the system improves the description of the system, reduces the residual error (unexplained variations of the measurements) and should improve the statistical analysis of variables of interest. Sleep stages are related to changes resting state network, epileptic activity and their haemodynamic correlates (Moehring, Moeller et al. 2008). The physiological rhythms of resting brain activity have clear BOLD correlates, as shown initially for the posterior alpha rhythm and subsequently for other frequency bands (Laufs, Krakow et al. 2003; Tyvaert, Levan et al. 2008). The inclusion of these effects in the fMRI analysis might enhance the mapping of the epileptic networks. Likewise, the BOLD correlates of specific spectral changes of the EEG related to epileptic activity are unknown (IED-related time-frequency changes). Alternatively, instead of segregating the signal into spectral frequency bands, EEG-fMRI studies could benefit from modelling spatial features of the EEG such as topographic maps, which are frequency independent. The occurrence and duration of physiological “resting state” EEG maps on the scalp EEG of resting subjects has recently been

shown to correlate with fMRI resting state networks (Britz, Van De Ville et al. 2010; Musso, Brinkmeyer et al. 2010) and such properties have been explained by the scale-invariance of topographic EEG features (Van De Ville, Britz et al.). Preliminary results exploring the BOLD correlates of epilepsy specific EEG maps suggest that such EEG features could be used to inform fMRI analysis in patients with epilepsy even when no IED are detected during fMRI recording (Grouiller, Spinelli et al. 2010). Of course, validation with invasive techniques is mandatory for such new analysis strategies.

10.2.1.2 Characterisation of neurovascular coupling

The coupling between neuro-electric activity and haemodynamic changes in the human brain, a fundamental factor in the interpretation of fMRI studies, is still incompletely understood. This is particularly true in brain structures with lesions or pathological neuro-electric activity such as epileptiform discharges. Several results in this thesis bring some insight into this issue. The concordance of ESI, IED-related BOLD changes and BOLD changes related to continuous ESI suggest a mostly preserved neuro-vascular coupling in the concordant cases. From a modelling point of view, the use of HRF derivatives provides some flexibility for inter-individual or intra-individual regional variations. Further increase in sensitivity could be obtained by fitting the HRF to individual datasets, however at the cost of specificity (Grouiller, Vercueil et al. 2010).

Haemodynamic changes preceding detectable IED (early BOLD) have been repeatedly reported but it is still unclear whether they have neuroelectric correlates (Hawco, Bagshaw et al. 2007; Jacobs, Levan et al. 2009) or represent instances of non-canonical haemodynamic response functions (Rathakrishnan, Moeller et al. 2010). Extracting new features from the EEG to improve the modelling of the BOLD signal might also help to identify neuro-electrical changes occurring before the IED. Similarly, early cortical haemodynamic changes, preceding IED and subcortical

haemodynamic changes, have also been found in idiopathic generalised epilepsy (Moeller, LeVan et al. 2010) and tend to support the hypothesis that generalised spike-wave discharges might originate from cortical rather than subcortical modulation (Vaudano, Laufs et al. 2009). However, these cortical drivers could be located far from the scalp (i.e. in the precuneus, deep in the interhemispheric fissure), therefore related to scalp EEG changes yet undetected.

Near Infra Red Spectroscopy (NIRS) is a non-invasive technique using sensors placed on the scalp that measures variations in oxyhaemoglobin and deoxyhaemoglobin at a rate similar to EEG and therefore higher than fMRI. In animals, the technique revealed a complex pattern of oscillatory pre-IED haemodynamic changes revealed by the high temporal resolution (Osharina, Ponchel et al. 2010). In clinical research, NIRS can be combined with EEG at bedside or with corticography during open skull surgery to measure haemodynamic changes related to interictal or ictal epileptic activity but can only measure neocortical structures (close to the scalp and sensors).

In our icEEG-fMRI study, preserved neurovascular coupling was suggested by the findings of significant BOLD changes within 1 cm of intracranial electrode contacts where IED were recorded. This illustrates the potential dual advantage of icEEG-fMRI: exploring BOLD changes related to very focal recording of neuro-electric activity, while providing whole-brain maps of this activity recorded with exquisite spatial selectivity. More studies are required to further investigate the relationship between positive/negative BOLD changes and neuro-electric activity recorded with icEEG. The results of these studies might help understand the origin of concordant negative BOLD changes correlated to scalp IED. The possibility to record simultaneous icEEG-fMRI is a unique window open on the human brain to further explore the neurovascular coupling at rest and during a task, notably with time-frequency approaches. There is ongoing development of several data analysis

strategies aiming at building global explanatory models of brain function including neuro-electric (EEG/MEG) and haemodynamic (fMRI) recordings. These models, such as Dynamic Causal Modelling (DCM), are based on an underlying microscale model of neuro-vascular interactions which could be refined by knowledge gained from icEEG-fMRI studies.

Standard intracranial electrodes can now record very high frequency oscillations such as fast ripples (350Hz-500Hz) that have been shown to play a critical role in cognitive processes. In patients with epilepsy, these high frequency oscillations could be a better marker of epileptogenicity, as preliminary evidence suggests that their resection is associated with a better outcome of epilepsy surgery (Jacobs, Zijlmans et al. 2010; Jacobs, Zijlmans et al. 2010).

Micro-electrodes can sample multi-unit or, rarely, single-unit activity and allow a much better recording of high frequency activity. They are increasingly used in combination with conventional clinical contacts. The feasibility of simultaneous fMRI and microelectrode recordings in human would be a further significant step to characterise neurovascular coupling in the human brain. These recordings would allow detailed time-frequency-haemodynamic correlation of physiologic cognitive functions in basic neuroscience (depending on the patient-specific brain structures sampled for clinical purposes) as well as a refinement of models of epileptic networks. Feasibility and safety studies will prove difficult to accomplish, because the precise estimation of local heating (and potential tissue damage) at the tip of a very thin microwire is far from trivial.

10.2.1.3 EEG source imaging

Whereas any detectable interictal activity on the scalp EEG could be marked and used for fMRI analysis, ESI of interictal epileptic activity requires spikes, sharp waves (or slow waves) for a robust application. Therefore, patients with low amplitude fast EEG activity, as commonly encountered in focal cortical dysplasia could not be

analysed, although there is increasing evidence suggesting that such EEG transients might have a higher localising value than IED (Andrade-Valenca, Dubeau et al. 2011). Time-frequency based analysis might help to estimate the source of these EEG patterns.

The use of topography-based or time-frequency-based (Michel, Grave de Peralta et al. 1999) approaches might also help broaden the applicability of ESI to low-amplitude fast EEG activity, seizure onset and spike-less datasets. These approach offer great promises to gather neurophysiologically meaningful information from the EEG to guide fMRI analysis should be applied also to datasets with no spike.

However, the use of techniques exploring event-related that do not have a fixed time-lag to the event might be needed rather than the usual averaging that cancels most of the signal that is not time-locked to the event.

10.2.1.4 Structural brain connectivity in patients with epilepsy

Whole-brain studies of connectivity can be performed by building connectivity matrices describing the strength of connection between pairs of grey matter regions (cortical and subcortical). Methodologically, in addition to technological issues such as computing power, such amounts of connectivity data generated will also require dedicated statistical tools to define the statistical relevance of the findings, especially to reduce the risk of false positive results. Moreover, data reduction strategies must be applied to deliver a small number of results qualifying the dataset and allow interpretation. Graph theoretical analysis offers the possibility of data reduction and describes a complex large network by identifying its major nodes and connections (Bullmore and Sporns 2009) and highlighting the core of the functional or structural network (“the connectome”). A very large multicentric study in healthy controls (>1400 subjects) has identified how factors such as age and gender influence the functional connectome measured with fMRI (Biswal, Mennes et al. 2010). Similarly, the

structural connectome has been well characterised in healthy controls (Hagmann, Cammoun et al. 2008), including its modifications during late brain development (Hagmann, Sporns et al.) and correlations between the structural and functional connectomes have been found (Hagmann, Sporns et al.; Honey, Sporns et al. 2009).

Another interesting approach is cortical parcellation informed by structural connectivity. Such studies used tractography to delineate cortical (Johansen-Berg, Behrens et al. 2004) or subcortical (thalamus) structures (Draganski, Kherif et al. 2008) based on their specific connectivity profile and showed good correspondence with functional segregation of cortical regions using various fMRI tasks. The application of these techniques in specific brain regions could reveal the structural changes associated with epilepsy without the need for a priori parcellation hypothesis.

10.2.2 Neurobiological discussion and perspectives

10.2.2.1 Functional epileptic networks

The results presented in this work support the view that epileptic activity is organised in complex multifocal cortical and subcortical neuronal networks that influence the activity in well known physiological networks (see next point) and that a refined modelling of epileptic activity is needed to improve their characterisation. Moreover, haemodynamic activity near the generators of focal epileptic activity can vary from increase to decreases suggesting that the balance between inhibition and excitation and total regional metabolic demand may be region- and patient-specific. Local negative BOLD changes related to epileptic activity revealed by simultaneous icEEG-fMRI are concordant with previous findings obtained in separate sessions which suggested reduced inhibition. Further work is needed to explore the icEEG frequency spectral changes in icEEG-fMRI studies. Moreover, the feasibility and safety of simultaneous scalp EEG recording and icEEG-fMRI needs to be investigated. Such

technique would bridge the gap between scalp EEG-fMRI and icEEG-fMRI and would help answer some important questions raised by scalp EEG-fMRI such as the intracranial electrophysiological correlates of early or negative BOLD responses to scalp IED.

10.2.2.2 Interaction between epileptic and physiologic activity in the brain

IED-related BOLD changes are frequently found distant to the epileptogenic zone and to propagation structures, notably in the default mode network and the causal relationship between changes in these resting states and epileptic activity is controversial. EEG-fMRI allows documentation of interictal epileptic activity during fMRI acquisition and is therefore critical for studying the alteration of the DMN and other resting states in the course of longstanding pathological neuroelectrical activity which is the hallmark of epilepsy. Studying icEEG-fMRI patients in whom electrodes cover regions involved in the DMN for clinical purposes would help to clarify the causality and flow of neuronal information between epileptic and resting state networks. However, these are very rare clinical situations. The addition of individual cognitive data would help to understand the clinical relevance of these interactions and better understand cognitive alterations in patients with epilepsy.

10.2.2.3 Structural and functional connectivity of brain networks

The structural anatomical connections that underlie functional networks are critical for the mapping of propagation pathways used by epileptic activity. White matter tracts belonging to physiological brain networks are the vast majority of these connections, with probably only a small minority of “aberrant connections”, found in patients with significant abnormalities of brain development. However, the involvement of these tracts in epileptic networks appears to be associated with altered structural connectivity which in turn might correlate with abnormal function of physiological networks in patients with epilepsy.

The large-scale more user-independent strategies described above should soon be mature enough to be applied to models of brain disease and in particular to epilepsy. They should first be tested in homogeneous groups of patients with, for instance unilateral temporal lobe epilepsy and hippocampal sclerosis who are post-operatively seizure-free to obtain robust results in a group of well-defined epileptic syndrome.

The highly pathognomonic neuro-electric activity of epileptic discharges with a high signal to noise ratio and the unique opportunity to record intracranial EEG for clinical purposes in a subset of patients make the study of epileptic networks and their interactions with physiological networks an interesting model of functional and structural (when a lesion is present) brain dysfunction. Alternatively to the widely used functional connectivity using fMRI, functional brain networks can be studied more directly and with additional temporal resolution using electrophysiological techniques, instead of haemodynamic (fMRI) recordings, an advantage particularly relevant in the case of epilepsy. Network characterisation based on graph theoretical analysis can be applied to intracranial EEG (David, Bastin et al. 2011) and their comparison with structural connectivity pattern would be a promising extension of the intracranial EEG-Tractography study described in chapter 8. For non-invasive data acquired with EEG or MEG, various strategies, notably using Granger causality (Astolfi, Babiloni et al. 2004) or approaches based on coherence (Guggisberg, Honma et al. 2008; Brookes, Hale et al. 2011) allow the study of functional connectivity between EEG/MEG sources. The limitations of these techniques are the difficulty to non-invasively record epileptic activity in some patients and the uncertainties inherent to source estimation techniques. Nevertheless, these techniques based on neurophysiological recordings represent a more direct measurement of neuro-electrical activity and some have the advantage of allowing a time-varying approach with a temporal resolution much higher than with fMRI. Comparison between functional connectivity approaches based on neuro-electrical vs haemodynamics signals in animals suggested that the

variability of haemodynamic responses could confound the causality analysis (David, Guillemain et al. 2008). Therefore, the study of the correlations between neuro-electrical functional connectivity and structural connectivity in epilepsy would certainly shed a new light on the organisation of epileptic networks and more generally on the large-scale transfer of neuronal signals in the brain.

10.2.2.4 Translation to cognitive neuroimaging

From a cognitive neuroscience perspective, the strategies of ESI and EEG-fMRI combination applied in this work could be applied to cognitive studies. One way would be to model the ongoing epileptic activity as a covariate in cognitive fMRI performed on patients with epilepsy. Another way could consist in estimating both the source of neuro-electric activity and its BOLD correlates from simultaneous recordings. On top of representing a significant gain in data acquisition time and patient/subject comfort, this would also avoid a contamination by different brain state across different recording session. The possibility of icEEG-fMRI offers even more attractive opportunities to study specific physiological brain responses using task protocols customized to the individual patient according to the brain structures sampled by icEEG (Jerbi, Vidal et al. 2010). However, given recruitment, logistical and ethical limitations, icEEG-fMRI will probably remain an imaging technique applied in selected patients (with electrode implantation customised according to the clinical context) focusing in delivering important clinical information about the epileptic network as well as a unique scientific tool to validate hypotheses on neuro-vascular coupling and models of brain function.

10.2.2.5 Revisiting idiopathic generalised epileptic syndromes

The finding of altered SMA structural connectivity in patients with JME shows the power of DTI tractography to investigate structural brain connectivity and reveal structural changes despite normal appearing routine MRI. Our changes were congruent with an increasing body of studies in this epileptic syndrome that reported

altered motor networks with functional and structural imaging techniques (O'Muircheartaigh, Vollmar et al. 2011; Vollmar, O'Muircheartaigh et al. 2011). These findings of subtle structural abnormalities are concordant with the new classification approach of epileptic syndromes that recommends to abandon the term "idiopathic" for the cause of epileptic syndromes (in favour of "genetic" in the case of JME) (Berg, Berkovic et al. 2010).

10.3 Clinical implications and perspectives

10.3.1 Mapping epileptic networks for epilepsy surgery

In patients with medically intractable focal epilepsy, non-invasive information that helps localising focal epileptic activity is crucially needed to select patients for intracranial studies, and to refine the placement of intracranial electrodes. The improvement in scalp EEG-fMRI analysis and interpretation of its results presented in this work could have important implications for epilepsy surgery by enhancing the localisation of onset of epileptic activity and its patterns of propagation. Recent studies suggested that EEG-fMRI could help predict the post-operative outcome (Thornton, Laufs et al. 2010) with focal BOLD responses colocalised with the resection area being associated with a seizure-free outcome whereas more widespread BOLD changes predicting a poorer outcome. Improving the issue of sensitivity and specificity by reducing the number of inconclusive EEG-fMRI studies with the methods applied in this thesis and further developments to understand multifocal network patterns in specific epileptic syndromes, positive vs negative BOLD changes are needed. They would represent a precious step towards transforming this research tool into a recognised clinical tool for routine use in presurgical non-invasive mapping. While its useful contribution for guiding intracranial electrode is accepted, future studies are needed to assess the reliability of EEG-fMRI for predicting post-operative seizure outcome in individual patients. Moreover, the mapping of whole-brain haemodynamic changes related to intracranial EEG IED allows compensating for the limited spatial sampling of intracranial electrodes. The identified relevant structures could be targeted by a complementary implantation or be integrated in the prognosis implication and decision making regarding tailored resection. In selected patients with concordant multimodal localising tools (MRI, ESI, EEG-fMRI, PET) these developments might eventually allow tailored surgical resections without the need for

intracranial EEG recordings, but the clinical relevance of icEEG-fMRI needs however to be addressed in larger clinical populations.

A limited but highly interesting application of EEG-fMRI is in patients who serendipitously present subclinical seizures or seizures with little motion during fMRI acquisition. Small series of such patients have allowed to map the regions involved in seizure onset and propagation (Thornton, Rodionov et al. 2010) and have shown that different structures are involved in interictal and ictal networks (Tyvaert, Hawco et al. 2008). The addition of video recordings to EEG-fMRI could help in the characterisation of these ictal events and in the identification of confounds (Chaudhary, Kokkinos et al. 2010), although the ability of video to model clinical ictal features in seizures that are not grossly contaminated by motion remains to be documented.

Focal brain lesions and long-standing pathological neuronal activity in patients with epilepsy might lead to abnormal organisation of physiological networks with or without functional impairment. A precise mapping of these networks including cortical regions and subcortical connections will represent precious information for neurosurgeons for tailoring resections that spare these physiological networks. Current developments in this direction will need to compensate for distortions affecting MR images when coregistering them into a neuronavigation for per-operative localisation. Also, the current complexity of most analysis needs to be translated into more automated analysis protocols if such improvement is to be used in more than very few clinical centres with close links to research facilities.

Currently, of all the techniques used in this work, ESI is probably the closest to routine clinical use, but require high density recordings for a sensitivity, specificity and localisation accuracy comparable to other widely used localising structural (MRI) or functional (PET, SPECT) techniques (Brodbeck, Spinelli et al. 2011). EEG-fMRI and tractography still require additional validation in larger surgical populations and

clarification of their limitations (as discussed above in Section 10.2.1). For all these techniques, the research-oriented centre-specific strategies for data recording and analysing should certainly continue but should be paralleled by regularly updated guidelines approved by opinion leaders in the field, to standardize the use of these techniques. Also, these techniques are currently mostly applied in clinical centres benefitting from strong collaboration with developers for the time-intensive and not user friendly analysis. Automatisation and simplifications of analysis procedures are also necessary to make such tool clinically viable.

To optimize surgical planning, the results of functional and structural mapping will need to be implemented into neurosurgical navigation tools used in the operating theatres. This goal requires strict application of coregistration pipelines to achieve robust and reliable image overlay. It is very important that interpretation of these images is made in the light of the distortion between the brain anatomy and the different imaging modalities and acquisition protocols.

10.3.2 Mapping epileptic networks for neuromodulation

Some patients with medically refractory epilepsy are not suitable candidates for surgery, either because the epileptic activity is not unifocal or because there is a high risk that a focal resection would lead to intolerable deficits. Alternative treatment strategies are currently being investigated. Based on the experience in movement disorders, neuromodulation with deep brain electrical stimulation (DBS) via chronically implanted electrodes is increasingly applied in selected patients with epilepsy with the objective of desynchronising targeted structures for inhibiting epileptic activity and the range of targets and parameters is currently explored (Kahane and Depaulis 2010). Some studies have shown significant seizure reduction by targeting the site of focal epileptic activity, such as the amygdalo-hippocampal structures in medial temporal lobe epilepsy (Vonck, Boon et al. 2002; Boex, Vulliemoz

et al. 2007). The stimulation of neocortical structures in extratemporal lobe epilepsy with on-demand stimulation is the subject of ongoing studies (Smith, Fountas et al. 2010). Other studies showed seizure reduction by stimulating subcortical structures such as the anterior nucleus (Fisher, Salanova et al. 2010) of the thalamus which was predominantly successful in patients with temporal lobe epilepsy (probably because this nucleus belongs to the limbic circuitry that was involved in these cases). Stimulation of the centro-median nucleus of the thalamus allowed a reduction of generalised seizures in patients with Lennox-Gastaut syndrome who suffer from medically refractory poorly localised epilepsy with multiple seizure types (Velasco, Velasco et al. 2006). A minority of patients with idiopathic generalised epilepsy also suffer from medically refractory generalised seizures and might be candidates for such treatment strategies. All these studies showed a clear room for improvement with respect to patient selection, precise site of stimulation and stimulation parameters. A better understanding of functional and structural epileptic networks will be crucial for the choice of a specific site of stimulation in individual patients and its successful application. A recent study showed that EEG-fMRI could identify the involvement of specific thalamus nuclei in idiopathic generalised epilepsy, lending support to the potential benefit of such technique (Tyvaert, Chassagnon et al. 2009). There are also reports suggesting a reduction of seizure frequency after focal transcranial magnetic stimulation targeting the estimated site of the epileptic focus (Fregni, Otachi et al. 2006). Similarly to DBS, the application of this technique might also benefit from a better characterisation of epileptic networks.

11 GENERAL CONCLUSION

In this thesis, I have combined neuro-imaging techniques to increase our understanding of brain networks involved in epileptic activity as well as its influence on physiological brain networks. By combining simultaneous ESI and EEG-fMRI, I obtained a better mapping of epileptic networks and described the dynamics of propagation in patients with focal epilepsy. In addition, the possibility to map whole-brain BOLD changes related to epileptic discharges recorded with intracranial electrodes offers a unique tool to map epileptic networks and to improve the understanding of neurovascular coupling in humans. Moreover, while tested here on resting-state brain activity, the combination of these techniques could be readily applied to the investigation of task-related brain activity, notably with cognitive paradigms. Finally, the demonstration of altered structural connectivity in an idiopathic form of epilepsy known to exhibit subtle structural abnormalities strengthens the role of tractography to study disease-modified brain networks.

Throughout this work I have discussed the methodological considerations of each technique and analysis strategy that was used and I evaluated the potential clinical relevance with the best available evidence.

Studies of epileptic networks using combinations of functional haemodynamic and neuro-electric tools as well as structural imaging methods are needed. These could use one modality to constrain the other or, in a more symmetrical approach, compare functional and structural connectivity maps built in parallel. Such approaches could build on recent methodological developments in healthy subjects to investigate the effect of pathological neuro-electrical activity of functional and structural brain networks. Beyond their neuroscientific interest, these future studies will improve the understanding of neural mechanisms underlying epilepsy and the medical and surgical management of patients with epilepsy.

LIST OF REFERENCES

- Aghakhani, Y., A. P. Bagshaw, et al. (2004). "fMRI activation during spike and wave discharges in idiopathic generalized epilepsy." *Brain* **127**(Pt 5): 1127-44.
- Aghakhani, Y., D. Kinay, et al. (2005). "The role of periventricular nodular heterotopia in epileptogenesis." *Brain* **128**(Pt 3): 641-51.
- Aghakhani, Y., E. Kobayashi, et al. (2006). "Cortical and thalamic fMRI responses in partial epilepsy with focal and bilateral synchronous spikes." *Clin Neurophysiol* **117**(1): 177-91.
- Agirre-Arrizubieta, Z., G. J. Huiskamp, et al. (2009). "Interictal magnetoencephalography and the irritative zone in the electrocorticogram." *Brain* **132**(Pt 11): 3060-71.
- Ahlfors, S. P., G. V. Simpson, et al. (1999). "Spatiotemporal activity of a cortical network for processing visual motion revealed by MEG and fMRI." *J Neurophysiol* **82**(5): 2545-55.
- Al-Asmi, A., C. G. Benar, et al. (2003). "fMRI activation in continuous and spike-triggered EEG-fMRI studies of epileptic spikes." *Epilepsia* **44**(10): 1328-39.
- Alarcon, G., C. N. Guy, et al. (1994). "Intracerebral propagation of interictal activity in partial epilepsy: implications for source localisation." *J Neurol Neurosurg Psychiatry* **57**(4): 435-49.
- Alexander, D. C., G. J. Barker, et al. (2002). "Detection and modeling of non-Gaussian apparent diffusion coefficient profiles in human brain data." *Magn Reson Med* **48**(2): 331-40.
- Allen, P. J., O. Josephs, et al. (2000). "A method for removing imaging artifact from continuous EEG recorded during functional MRI." *Neuroimage* **12**(2): 230-9.
- Allen, P. J., G. Polizzi, et al. (1998). "Identification of EEG events in the MR scanner: the problem of pulse artifact and a method for its subtraction." *Neuroimage* **8**(3): 229-39.
- Alpherts, W. C., J. Vermeulen, et al. (2006). "Verbal memory decline after temporal epilepsy surgery? A 6-year multiple assessments follow-up study." *Neurology* **67**(4): 626-31.
- Andrade-Valenca, L. P., F. Dubeau, et al. (2011). "Interictal scalp fast oscillations as a marker of the seizure onset zone." *Neurology* **77**(6): 524-31.
- Ashburner, J. (2007). "A fast diffeomorphic image registration algorithm." *Neuroimage* **38**(1): 95-113.
- Ashburner, J. and K. Friston (1997). "Multimodal image coregistration and partitioning--a unified framework." *Neuroimage* **6**(3): 209-17.
- Assaf, B. A. and J. S. Ebersole (1997). "Continuous source imaging of scalp ictal rhythms in temporal lobe epilepsy." *Epilepsia* **38**(10): 1114-23.
- Astolfi, L., F. Babiloni, et al. (2004). "Time-varying cortical connectivity by high resolution EEG and directed transfer function: simulations and application to finger tapping data." *Conf Proc IEEE Eng Med Biol Soc* **6**: 4405-8.
- Astolfi, L., F. Cincotti, et al. (2007). "Comparison of different cortical connectivity estimators for high-resolution EEG recordings." *Hum Brain Mapp* **28**(2): 143-57.
- Aubert, A., L. Pellerin, et al. (2007). "A coherent neurobiological framework for functional neuroimaging provided by a model integrating compartmentalized energy metabolism." *Proc Natl Acad Sci U S A* **104**(10): 4188-93.
- Aykut-Bingol, C. and S. S. Spencer (1999). "Nontumoral occipitotemporal epilepsy: localizing findings and surgical outcome." *Ann Neurol* **46**(6): 894-900.
- Babajani, A. and H. Soltanian-Zadeh (2006). "Integrated MEG/EEG and fMRI model based on neural masses." *IEEE Trans Biomed Eng* **53**(9): 1794-801.
- Babiloni, F., C. Babiloni, et al. (2002). "Cortical source estimate of combined high resolution EEG and fMRI data related to voluntary movements." *Methods Inf Med* **41**(5): 443-50.
- Badawy, R. A., J. M. Curatolo, et al. (2007). "Changes in cortical excitability differentiate generalized and focal epilepsy." *Ann Neurol* **61**(4): 324-31.
- Bagshaw, A. P., Y. Aghakhani, et al. (2004). "EEG-fMRI of focal epileptic spikes: analysis with multiple haemodynamic functions and comparison with gadolinium-enhanced MR angiograms." *Hum Brain Mapp* **22**(3): 179-92.
- Bagshaw, A. P., C. Hawco, et al. (2005). "Analysis of the EEG-fMRI response to prolonged bursts of interictal epileptiform activity." *Neuroimage* **24**(4): 1099-112.
- Bagshaw, A. P., E. Kobayashi, et al. (2006). "Correspondence between EEG-fMRI and EEG dipole localisation of interictal discharges in focal epilepsy." *Neuroimage* **30**(2): 417-25.
- Bagshaw, A. P., L. Torab, et al. (2006). "EEG-fMRI using z-shimming in patients with temporal lobe epilepsy." *J Magn Reson Imaging* **24**(5): 1025-32.
- Bagshaw, A. P. and T. Warbrick (2007). "Single trial variability of EEG and fMRI responses to visual stimuli." *Neuroimage* **38**(2): 280-92.

- Bahar, S., M. Suh, et al. (2006). "Intrinsic optical signal imaging of neocortical seizures: the 'epileptic dip'." Neuroreport **17**(5): 499-503.
- Barnes, G. R., P. L. Furlong, et al. (2006). "A verifiable solution to the MEG inverse problem." Neuroimage **31**(2): 623-6.
- Bartolomei, F., F. Wendling, et al. (2001). "Neural networks involving the medial temporal structures in temporal lobe epilepsy." Clin Neurophysiol **112**(9): 1746-60.
- Baxendale, S. (2009). "The Wada test." Curr Opin Neurol **22**(2): 185-9.
- Baxendale, S. and P. Thompson (2010). "Beyond localization: the role of traditional neuropsychological tests in an age of imaging." Epilepsia **51**(11): 2225-30.
- Baxendale, S., P. Thompson, et al. (2006). "Predicting memory decline following epilepsy surgery: a multivariate approach." Epilepsia **47**(11): 1887-94.
- Beaulieu, C. (2002). "The basis of anisotropic water diffusion in the nervous system - a technical review." NMR Biomed **15**(7-8): 435-55.
- Behrens, T. E., H. J. Berg, et al. (2007). "Probabilistic diffusion tractography with multiple fibre orientations: What can we gain?" Neuroimage **34**(1): 144-55.
- Bell, G. S. and J. W. Sander (2009). "Suicide and epilepsy." Curr Opin Neurol **22**(2): 174-8.
- Bell, M. L., S. Rao, et al. (2009). "Epilepsy surgery outcomes in temporal lobe epilepsy with a normal MRI." Epilepsia.
- Benar, C., Y. Aghakhani, et al. (2003). "Quality of EEG in simultaneous EEG-fMRI for epilepsy." Clin Neurophysiol **114**(3): 569-80.
- Benar, C. G. and J. Gotman (2002). "Modeling of post-surgical brain and skull defects in the EEG inverse problem with the boundary element method." Clin Neurophysiol **113**(1): 48-56.
- Benar, C. G., D. W. Gross, et al. (2002). "The BOLD response to interictal epileptiform discharges." Neuroimage **17**(3): 1182-92.
- Benar, C. G., C. Grova, et al. (2006). "EEG-fMRI of epileptic spikes: concordance with EEG source localization and intracranial EEG." Neuroimage **30**(4): 1161-70.
- Berg, A. T., S. F. Berkovic, et al. (2010). "Revised terminology and concepts for organization of seizures and epilepsies: report of the ILAE Commission on Classification and Terminology, 2005-2009." Epilepsia **51**(4): 676-85.
- Bernasconi, A., N. Bernasconi, et al. (2011). "Advances in MRI for 'cryptogenic' epilepsies." Nat Rev Neurol **7**(2): 99-108.
- Betting, L. E., S. B. Mory, et al. (2006). "Voxel-based morphometry in patients with idiopathic generalized epilepsies." Neuroimage **32**(2): 498-502.
- Bettus, G., E. Guedj, et al. (2009). "Decreased basal fMRI functional connectivity in epileptogenic networks and contralateral compensatory mechanisms." Hum Brain Mapp **30**(5): 1580-91.
- Bhardwaj, R. D., S. Z. Mahmoodabadi, et al. (2010). "Diffusion tensor tractography detection of functional pathway for the spread of epileptiform activity between temporal lobe and Rolandic region." Childs Nerv Syst **26**(2): 185-90.
- Binder, J. R. (2010). "Functional MRI is a valid noninvasive alternative to Wada testing." Epilepsy Behav.
- Birn, R. M., J. B. Diamond, et al. (2006). "Separating respiratory-variation-related fluctuations from neuronal-activity-related fluctuations in fMRI." Neuroimage **31**(4): 1536-48.
- Biswal, B. B., M. Mennes, et al. (2010). "Toward discovery science of human brain function." Proc Natl Acad Sci U S A **107**(10): 4734-9.
- Blanke, O., G. Lantz, et al. (2000). "Temporal and spatial determination of EEG-seizure onset in the frequency domain." Clin Neurophysiol **111**(5): 763-72.
- Blume, W. T., H. O. Luders, et al. (2001). "Glossary of descriptive terminology for ictal semiology: report of the ILAE task force on classification and terminology." Epilepsia **42**(9): 1212-8.
- Boex, C., S. Vulliemoz, et al. (2007). "High and low frequency electrical stimulation in non-lesional temporal lobe epilepsy." Seizure **16**(8): 664-9.
- Bonelli, S. B., R. H. Powell, et al. (2010). "Imaging memory in temporal lobe epilepsy: predicting the effects of temporal lobe resection." Brain **133**(Pt 4): 1186-99.
- Bonilha, L., J. Halford, et al. (2007). "Microstructural white matter abnormalities in nodular heterotopia with overlying polymicrogyria." Seizure **16**(1): 74-80.
- Bonmassar, G., D. P. Schwartz, et al. (2001). "Spatiotemporal brain imaging of visual-evoked activity using interleaved EEG and fMRI recordings." Neuroimage **13**(6 Pt 1): 1035-43.
- Boon, P., M. D'Have, et al. (2002). "Ictal source localization in presurgical patients with refractory epilepsy." J Clin Neurophysiol **19**(5): 461-8.

- Boor, R., J. Jacobs, et al. (2007). "Combined spike-related functional MRI and multiple source analysis in the non-invasive spike localization of benign rolandic epilepsy." Clin Neurophysiol **118**(4): 901-9.
- Briellmann, R. S., R. M. Wellard, et al. (2005). "Seizure-associated abnormalities in epilepsy: evidence from MR imaging." Epilepsia **46**(5): 760-6.
- Britz, J., D. Van De Ville, et al. (2010). "BOLD correlates of EEG topography reveal rapid resting-state network dynamics." Neuroimage **52**(4): 1162-70.
- Brodbeck, V., A. M. Lascano, et al. (2009). "Accuracy of EEG source imaging of epileptic spikes in patients with large brain lesions." Clin Neurophysiol **120**(4): 679-85.
- Brodbeck, V., L. Spinelli, et al. (2011). "Electroencephalographic source imaging: a prospective study of 152 operated epileptic patients." Brain **134**(Pt 10): 2887-97.
- Brookes, M. J., J. R. Hale, et al. (2011). "Measuring functional connectivity using MEG: Methodology and comparison with fcMRI." Neuroimage.
- Brookes, M. J., K. J. Mullinger, et al. (2008). "Simultaneous EEG source localisation and artifact rejection during concurrent fMRI by means of spatial filtering." Neuroimage **40**(3): 1090-104.
- Brookes, M. J., J. Vrba, et al. (2009). "Source localisation in concurrent EEG/fMRI: applications at 7T." Neuroimage **45**(2): 440-52.
- Brookes, M. J., J. M. Zumer, et al. (2011). "Investigating spatial specificity and data averaging in MEG." Neuroimage **49**(1): 525-38.
- Brookings, T., S. Ortigue, et al. (2009). "Using ICA and realistic BOLD models to obtain joint EEG/fMRI solutions to the problem of source localization." Neuroimage **44**(2): 411-20.
- Bullmore, E. and O. Sporns (2009). "Complex brain networks: graph theoretical analysis of structural and functional systems." Nat Rev Neurosci **10**(3): 186-98.
- Buxton, R. B., E. C. Wong, et al. (1998). "Dynamics of blood flow and oxygenation changes during brain activation: the balloon model." Magn Reson Med **39**(6): 855-64.
- Buzsaki, G., K. Kaila, et al. (2007). "Inhibition and brain work." Neuron **56**(5): 771-83.
- Carmichael, D. W., K. Hamandi, et al. (2008). "An investigation of the relationship between BOLD and perfusion signal changes during epileptic generalised spike wave activity." Magn Reson Imaging **26**(7): 870-3.
- Carmichael, D. W., S. Pinto, et al. (2007). "Functional MRI with active, fully implanted, deep brain stimulation systems: safety and experimental confounds." Neuroimage **37**(2): 508-17.
- Carmichael, D. W., J. S. Thornton, et al. (2008). "Safety of localizing epilepsy monitoring intracranial electroencephalograph electrodes using MRI: radiofrequency-induced heating." J Magn Reson Imaging **28**(5): 1233-44.
- Carmichael, D. W., J. S. Thornton, et al. (2010). "Feasibility of simultaneous intracranial EEG-fMRI in humans: a safety study." Neuroimage **49**(1): 379-90.
- Carne, R. P., T. J. O'Brien, et al. (2004). "MRI-negative PET-positive temporal lobe epilepsy: a distinct surgically remediable syndrome." Brain **127**(Pt 10): 2276-85.
- Catani, M., D. K. Jones, et al. (2003). "Occipito-temporal connections in the human brain." Brain **126**(Pt 9): 2093-107.
- Chandra, P. S., N. Salamon, et al. (2006). "FDG-PET/MRI coregistration and diffusion-tensor imaging distinguish epileptogenic tubers and cortex in patients with tuberous sclerosis complex: a preliminary report." Epilepsia **47**(9): 1543-9.
- Chaudhary, U. J., V. Kokkinos, et al. (2010). "Implementation and evaluation of simultaneous video-electroencephalography and functional magnetic resonance imaging." Magn Reson Imaging **28**(8): 1192-9.
- Chelune, G. J. (1995). "Hippocampal adequacy versus functional reserve: predicting memory functions following temporal lobectomy." Arch Clin Neuropsychol **10**(5): 413-32.
- Choy, M., K. K. Cheung, et al. (2010). "Quantitative MRI predicts status epilepticus-induced hippocampal injury in the lithium-pilocarpine rat model." Epilepsy Res **88**(2-3): 221-30.
- Chupin, M., A. Hammers, et al. (2007). "Fully automatic segmentation of the hippocampus and the amygdala from MRI using hybrid prior knowledge." Med Image Comput Comput Assist Interv Int Conf Med Image Comput Comput Assist Interv **10**(Pt 1): 875-82.
- Ciccarelli, O., M. Catani, et al. (2008). "Diffusion-based tractography in neurological disorders: concepts, applications, and future developments." Lancet Neurol **7**(8): 715-27.
- Ciccarelli, O., G. J. Parker, et al. (2003). "From diffusion tractography to quantitative white matter tract measures: a reproducibility study." Neuroimage **18**(2): 348-59.

- Concha, L., C. Beaulieu, et al. (2009). "White-matter diffusion abnormalities in temporal-lobe epilepsy with and without mesial temporal sclerosis." *J Neurol Neurosurg Psychiatry* **80**(3): 312-9.
- Concha, L., C. Beaulieu, et al. (2007). "Bilateral white matter diffusion changes persist after epilepsy surgery." *Epilepsia* **48**(5): 931-40.
- Concha, L., D. W. Gross, et al. (2006). "Diffusion tensor imaging of time-dependent axonal and myelin degradation after corpus callosotomy in epilepsy patients." *Neuroimage* **32**(3): 1090-9.
- Concha, L., D. J. Livy, et al. "In vivo diffusion tensor imaging and histopathology of the fimbria-fornix in temporal lobe epilepsy." *J Neurosci* **30**(3): 996-1002.
- Connors, B. W. and M. J. Gutnick (1990). "Intrinsic firing patterns of diverse neocortical neurons." *Trends Neurosci* **13**(3): 99-104.
- Cook, P. A., M. Symms, et al. (2007). "Optimal acquisition orders of diffusion-weighted MRI measurements." *J Magn Reson Imaging* **25**(5): 1051-8.
- Cuffin, B. N. (1996). "EEG localization accuracy improvements using realistically shaped head models." *IEEE Trans Biomed Eng* **43**(3): 299-303.
- Dale, A. M., A. K. Liu, et al. (2000). "Dynamic statistical parametric mapping: combining fMRI and MEG for high-resolution imaging of cortical activity." *Neuron* **26**(1): 55-67.
- Dancause, N. (2006). "Neurophysiological and anatomical plasticity in the adult sensorimotor cortex." *Rev Neurosci* **17**(6): 561-80.
- Dauguet, J., S. Peled, et al. (2006). "3D histological reconstruction of fiber tracts and direct comparison with diffusion tensor MRI tractography." *Med Image Comput Comput Assist Interv Int Conf Med Image Comput Comput Assist Interv* **9**(Pt 1): 109-16.
- Daunizeau, J., O. David, et al. (2009). "Dynamic causal modelling: A critical review of the biophysical and statistical foundations." *Neuroimage*.
- Daunizeau, J., C. Grova, et al. (2007). "Symmetrical event-related EEG/fMRI information fusion in a variational Bayesian framework." *Neuroimage* **36**(1): 69-87.
- Daunizeau, J., A. E. Vaudano, et al. (2010). "Bayesian multi-modal model comparison: a case study on the generators of the spike and the wave in generalized spike-wave complexes." *Neuroimage* **49**(1): 656-67.
- David, O., J. Bastin, et al. (2011). "Studying network mechanisms using intracranial stimulation in epileptic patients." *Front Syst Neurosci* **4**: 148.
- David, O., I. Guillemain, et al. (2008). "Identifying neural drivers with functional MRI: an electrophysiological validation." *PLoS Biol* **6**(12): 2683-97.
- De Tiege, X., H. Laufs, et al. (2007). "EEG-fMRI in children with pharmaco-resistant focal epilepsy." *Epilepsia* **48**(2): 385-9.
- de Zwart, J. A., P. van Gelderen, et al. (2009). "Hemodynamic nonlinearities affect BOLD fMRI response timing and amplitude." *Neuroimage* **47**(4): 1649-58.
- Debener, S., K. J. Mullinger, et al. (2008). "Properties of the ballistocardiogram artefact as revealed by EEG recordings at 1.5, 3 and 7 T static magnetic field strength." *Int J Psychophysiol* **67**(3): 189-99.
- Debener, S., M. Ullsperger, et al. (2006). "Single-trial EEG-fMRI reveals the dynamics of cognitive function." *Trends Cogn Sci* **10**(12): 558-63.
- Debener, S., M. Ullsperger, et al. (2005). "Trial-by-trial coupling of concurrent electroencephalogram and functional magnetic resonance imaging identifies the dynamics of performance monitoring." *J Neurosci* **25**(50): 11730-7.
- Deichmann, R., O. Josephs, et al. (2002). "Compensation of susceptibility-induced BOLD sensitivity losses in echo-planar fMRI imaging." *Neuroimage* **15**(1): 120-35.
- Deneux, T. and O. Faugeras (2006). *Model-driven EEG/fMRI fusion of brain oscillations*. 3rd IEEE International Symposium on Biomedical Imaging: Nano to Macro; 6-9 April 2006.
- Deppe, M., C. Kellinghaus, et al. (2008). "Nerve fiber impairment of anterior thalamocortical circuitry in juvenile myoclonic epilepsy." *Neurology* **71**(24): 1981-5.
- Diehl, B., R. M. Busch, et al. (2008). "Abnormalities in diffusion tensor imaging of the uncinate fasciculus relate to reduced memory in temporal lobe epilepsy." *Epilepsia* **49**(8): 1409-18.
- Diehl, B., I. Najm, et al. (2001). "Postictal diffusion-weighted imaging for the localization of focal epileptic areas in temporal lobe epilepsy." *Epilepsia* **42**(1): 21-8.
- Diehl, B., Z. Piao, et al. (2010). "Cortical stimulation for language mapping in focal epilepsy: correlations with tractography of the arcuate fasciculus." *Epilepsia* **51**(4): 639-46.
- Diehl, B., M. R. Symms, et al. (2005). "Postictal diffusion tensor imaging." *Epilepsy Res* **65**(3): 137-46.

- Diehl, B., J. Tkach, et al. (2010). "Diffusion tensor imaging in patients with focal epilepsy due to cortical dysplasia in the temporo-occipital region: electro-clinico-pathological correlations." *Epilepsy Res* **90**(3): 178-87.
- Dinesh Nayak, S., A. Valentin, et al. (2004). "Characteristics of scalp electrical fields associated with deep medial temporal epileptiform discharges." *Clin Neurophysiol* **115**(6): 1423-35.
- Disbrow, E. A., D. A. Slutsky, et al. (2000). "Functional MRI at 1.5 tesla: a comparison of the blood oxygenation level-dependent signal and electrophysiology." *Proc Natl Acad Sci U S A* **97**(17): 9718-23.
- Draganski, B., F. Kherif, et al. (2008). "Evidence for segregated and integrative connectivity patterns in the human Basal Ganglia." *J Neurosci* **28**(28): 7143-52.
- Duncan, J. (2009). "The current status of neuroimaging for epilepsy." *Curr Opin Neurol* **22**(2): 179-84.
- Duncan, J. S. (2005). "Brain imaging in idiopathic generalized epilepsies." *Epilepsia* **46 Suppl 9**: 108-11.
- Duncan, J. S. (2010). "Imaging in the surgical treatment of epilepsy." *Nat Rev Neurol* **6**(10): 537-50.
- Dyrby, T. B., L. V. Sogaard, et al. (2007). "Validation of in vitro probabilistic tractography." *Neuroimage* **37**(4): 1267-77.
- Ebersole, J. S. (1997). "Defining epileptogenic foci: past, present, future." *J Clin Neurophysiol* **14**(6): 470-83.
- Ebersole, J. S. (1999). "EEG source modeling. The last word." *J Clin Neurophysiol* **16**(3): 297-302.
- Ebersole, J. S. and S. M. Ebersole (2010). "Combining MEG and EEG source modeling in epilepsy evaluations." *J Clin Neurophysiol* **27**(6): 360-71.
- El-Koussy, M., J. Mathis, et al. (2002). "Focal status epilepticus: follow-up by perfusion- and diffusion MRI." *Eur Radiol* **12**(3): 568-74.
- Ellmore, T. M., M. S. Beauchamp, et al. (2009). "Relationships between essential cortical language sites and subcortical pathways." *J Neurosurg* **111**(4): 755-66.
- Engel, J., Jr. (2006). "Report of the ILAE classification core group." *Epilepsia* **47**(9): 1558-68.
- Engelhorn, T., J. Weise, et al. (2007). "Early diffusion-weighted MRI predicts regional neuronal damage in generalized status epilepticus in rats treated with diazepam." *Neurosci Lett* **417**(3): 275-80.
- Englot, D. J., A. M. Mishra, et al. (2008). "Remote effects of focal hippocampal seizures on the rat neocortex." *J Neurosci* **28**(36): 9066-81.
- Eriksson, S. H., F. J. Rugg-Gunn, et al. (2001). "Diffusion tensor imaging in patients with epilepsy and malformations of cortical development." *Brain* **124**(Pt 3): 617-26.
- Eriksson, S. H., M. R. Symms, et al. (2002). "Exploring white matter tracts in band heterotopia using diffusion tractography." *Ann Neurol* **52**(3): 327-34.
- Fauser, S., A. Schulze-Bonhage, et al. (2004). "Focal cortical dysplasias: surgical outcome in 67 patients in relation to histological subtypes and dual pathology." *Brain* **127**(Pt 11): 2406-18.
- Federico, P., J. S. Archer, et al. (2005). "Cortical/subcortical BOLD changes associated with epileptic discharges: an EEG-fMRI study at 3 T." *Neurology* **64**(7): 1125-30.
- Fisher, R., V. Salanova, et al. (2010). "Electrical stimulation of the anterior nucleus of thalamus for treatment of refractory epilepsy." *Epilepsia*.
- Fisher, R. S., W. van Emde Boas, et al. (2005). "Epileptic seizures and epilepsy: definitions proposed by the International League Against Epilepsy (ILAE) and the International Bureau for Epilepsy (IBE)." *Epilepsia* **46**(4): 470-2.
- Flanagan, D., D. F. Abbott, et al. (2009). "How wrong can we be? The effect of inaccurate mark-up of EEG/fMRI studies in epilepsy." *Clin Neurophysiol* **120**(9): 1637-47.
- Flugel, D., M. Cercignani, et al. (2006). "Diffusion tensor imaging findings and their correlation with neuropsychological deficits in patients with temporal lobe epilepsy and interictal psychosis." *Epilepsia* **47**(5): 941-4.
- Focke, N. K., M. Yogarajah, et al. (2008). "Voxel-based diffusion tensor imaging in patients with mesial temporal lobe epilepsy and hippocampal sclerosis." *Neuroimage* **40**(2): 728-37.
- Foong, J. and D. Flugel (2007). "Psychiatric outcome of surgery for temporal lobe epilepsy and presurgical considerations." *Epilepsy Res* **75**(2-3): 84-96.
- Formaggio, E., S. F. Storti, et al. (2010). "Integrating EEG and fMRI in epilepsy." *Neuroimage* **54**(4): 2719-31.

- Fregni, F., P. T. Otachi, et al. (2006). "A randomized clinical trial of repetitive transcranial magnetic stimulation in patients with refractory epilepsy." *Ann Neurol* **60**(4): 447-55.
- Friston, K., L. Harrison, et al. (2008). "Multiple sparse priors for the M/EEG inverse problem." *Neuroimage* **39**(3): 1104-20.
- Friston, K. J. (1997). "Testing for anatomically specified regional effects." *Hum Brain Mapp* **5**(2): 133-6.
- Friston, K. J., P. Fletcher, et al. (1998). "Event-related fMRI: characterizing differential responses." *Neuroimage* **7**(1): 30-40.
- Friston, K. J., C. D. Frith, et al. (1991). "Comparing functional (PET) images: the assessment of significant change." *J Cereb Blood Flow Metab* **11**(4): 690-9.
- Friston, K. J., L. Harrison, et al. (2003). "Dynamic causal modelling." *Neuroimage* **19**(4): 1273-302.
- Friston, K. J., S. Williams, et al. (1996). "Movement-related effects in fMRI time-series." *Magn Reson Med* **35**(3): 346-55.
- Gavaret, M., J. M. Badier, et al. (2004). "Electric source imaging in temporal lobe epilepsy." *J Clin Neurophysiol* **21**(4): 267-82.
- Gavaret, M., J. M. Badier, et al. (2006). "Electric source imaging in frontal lobe epilepsy." *J Clin Neurophysiol* **23**(4): 358-70.
- Genovese, C. R., N. A. Lazar, et al. (2002). "Thresholding of statistical maps in functional neuroimaging using the false discovery rate." *Neuroimage* **15**(4): 870-8.
- Gholipour, T., F. Moeller, et al. (2010). "Reproducibility of interictal EEG-fMRI results in patients with epilepsy." *Epilepsia*.
- Gloor, P. (1985). "Neuronal generators and the problem of localization in electroencephalography: application of volume conductor theory to electroencephalography." *J Clin Neurophysiol* **2**(4): 327-54.
- Glover, G. H. (1999). "Deconvolution of impulse response in event-related BOLD fMRI." *Neuroimage* **9**(4): 416-29.
- Goldenholz, D. M., S. P. Ahlfors, et al. (2009). "Mapping the signal-to-noise-ratios of cortical sources in magnetoencephalography and electroencephalography." *Hum Brain Mapp* **30**(4): 1077-86.
- Goldman, R. I., J. M. Stern, et al. (2000). "Acquiring simultaneous EEG and functional MRI." *Clin Neurophysiol* **111**(11): 1974-80.
- Gong, G., L. Concha, et al. (2008). "Thalamic diffusion and volumetry in temporal lobe epilepsy with and without mesial temporal sclerosis." *Epilepsy Res* **80**(2-3): 184-93.
- Gong, G., Y. He, et al. (2009). "Mapping anatomical connectivity patterns of human cerebral cortex using in vivo diffusion tensor imaging tractography." *Cereb Cortex* **19**(3): 524-36.
- Gonzalez-Andino, S. L., O. Blanke, et al. (2001). "The use of functional constraints for the neuroelectromagnetic inverse problem: alternatives and caveats." *International Journal of Bioelectromagnetism* **3**(1): available online at: ijbem.k.hosei.ac.jp/2006-/volume3/number1 (last accessed 15-8-2009).
- Gotman, J., E. Kobayashi, et al. (2006). "Combining EEG and fMRI: a multimodal tool for epilepsy research." *J Magn Reson Imaging* **23**(6): 906-20.
- Grant, P. E. (2005). "Imaging the developing epileptic brain." *Epilepsia* **46 Suppl 7**: 7-14.
- Grave de Peralta Menendez, R., S. Gonzalez Andino, et al. (2001). "Noninvasive localization of electromagnetic epileptic activity. I. Method descriptions and simulations." *Brain Topogr* **14**(2): 131-7.
- Grefkes, C., D. A. Nowak, et al. (2011). "Modulating cortical connectivity in stroke patients by rTMS assessed with fMRI and dynamic causal modeling." *Neuroimage* **50**(1): 233-42.
- Groening, K., V. Brodbeck, et al. (2009). "Combination of EEG-fMRI and EEG source analysis improves interpretation of spike-associated activation networks in paediatric pharmacoresistant focal epilepsies." *Neuroimage* **46**(3): 827-33.
- Gross, D. W., A. Bastos, et al. (2005). "Diffusion tensor imaging abnormalities in focal cortical dysplasia." *Can J Neurol Sci* **32**(4): 477-82.
- Gross, D. W., L. Concha, et al. (2006). "Extratemporal white matter abnormalities in mesial temporal lobe epilepsy demonstrated with diffusion tensor imaging." *Epilepsia* **47**(8): 1360-3.
- Grouiller, F., L. Spinelli, et al. (2010). How to take all these inconclusive EEG-fMRI studies in epilepsy from the bin. 16th Annual Meeting of the Organization for Human Brain Mapping, Barcelona, Spain.
- Grouiller, F., L. Vercueil, et al. (2007). "A comparative study of different artefact removal algorithms for EEG signals acquired during functional MRI." *Neuroimage* **38**(1): 124-37.

- Grouiller, F., L. Vercueil, et al. (2010). "Characterization of the hemodynamic modes associated with interictal epileptic activity using a deformable model-based analysis of combined EEG and functional MRI recordings." *Hum Brain Mapp* [Epub ahead of print].
- Grova, C., J. Daunizeau, et al. (2008). "Concordance between distributed EEG source localization and simultaneous EEG-fMRI studies of epileptic spikes." *Neuroimage* **39**(2): 755-74.
- Grova, C., J. Daunizeau, et al. (2006). "Evaluation of EEG localization methods using realistic simulations of interictal spikes." *Neuroimage* **29**(3): 734-53.
- Guggisberg, A. G., S. M. Honma, et al. (2008). "Mapping functional connectivity in patients with brain lesions." *Ann Neurol* **63**(2): 193-203.
- Guggisberg, A. G., H. E. Kirsch, et al. (2008). "Fast oscillations associated with interictal spikes localize the epileptogenic zone in patients with partial epilepsy." *Neuroimage* **39**(2): 661-8.
- Gullmar, D., J. Hauelsen, et al. (2011). "Influence of anisotropic electrical conductivity in white matter tissue on the EEG/MEG forward and inverse solution. A high-resolution whole head simulation study." *Neuroimage* **51**(1): 145-63.
- Gupta, R. K., S. Saksena, et al. (2005). "Diffusion tensor imaging in late posttraumatic epilepsy." *Epilepsia* **46**(9): 1465-71.
- Guye, M., G. J. Parker, et al. (2003). "Combined functional MRI and tractography to demonstrate the connectivity of the human primary motor cortex in vivo." *Neuroimage* **19**(4): 1349-60.
- Guye, M., J. P. Ranjeva, et al. (2007). "What is the significance of interictal water diffusion changes in frontal lobe epilepsies?" *Neuroimage* **35**(1): 28-37.
- Hagler, D. J., Jr., M. E. Ahmadi, et al. (2009). "Automated white-matter tractography using a probabilistic diffusion tensor atlas: Application to temporal lobe epilepsy." *Hum Brain Mapp* **30**(5): 1535-47.
- Hagmann, P., L. Cammoun, et al. (2008). "Mapping the structural core of human cerebral cortex." *PLoS Biol* **6**(7): e159.
- Hagmann, P., L. Jonasson, et al. (2006). "Understanding Diffusion MR Imaging Techniques: From Scalar Diffusion-weighted Imaging to Diffusion Tensor Imaging and Beyond." *Radiographics* **26** Suppl 1: S205-23.
- Hagmann, P., O. Sporns, et al. "White matter maturation reshapes structural connectivity in the late developing human brain." *Proc Natl Acad Sci U S A*.
- Hakyemez, B., C. Erdogan, et al. (2005). "Apparent diffusion coefficient measurements in the hippocampus and amygdala of patients with temporal lobe seizures and in healthy volunteers." *Epilepsy Behav* **6**(2): 250-6.
- Hamandi, K., H. Laufs, et al. (2008). "BOLD and perfusion changes during epileptic generalised spike wave activity." *Neuroimage* **39**(2): 608-18.
- Hamandi, K., H. W. Powell, et al. (2008). "Combined EEG-fMRI and tractography to visualise propagation of epileptic activity." *J Neurol Neurosurg Psychiatry* **79**(5): 594-7.
- Hamandi, K., A. Salek-Haddadi, et al. (2004). "EEG/functional MRI in epilepsy: The Queen Square Experience." *J Clin Neurophysiol* **21**(4): 241-8.
- Hamandi, K., A. Salek-Haddadi, et al. (2006). "EEG-fMRI of idiopathic and secondarily generalized epilepsies." *Neuroimage* **31**(4): 1700-10.
- Hauser, W. A., J. F. Annegers, et al. (1993). "Incidence of epilepsy and unprovoked seizures in Rochester, Minnesota: 1935-1984." *Epilepsia* **34**(3): 453-68.
- Hawco, C. S., A. P. Bagshaw, et al. (2007). "BOLD changes occur prior to epileptic spikes seen on scalp EEG." *Neuroimage* **35**(4): 1450-8.
- He, B., X. Zhang, et al. (2002). "Boundary element method-based cortical potential imaging of somatosensory evoked potentials using subjects' magnetic resonance images." *Neuroimage* **16**(3 Pt 1): 564-76.
- He, B. J., G. L. Shulman, et al. (2007). "The role of impaired neuronal communication in neurological disorders." *Curr Opin Neurol* **20**(6): 655-60.
- Heiervang, E., T. E. Behrens, et al. (2006). "Between session reproducibility and between subject variability of diffusion MR and tractography measures." *Neuroimage* **33**(3): 867-77.
- Helmholtz, H. (1853). "Über die Methodes, kleinste Zeiteile zu messen, und ihre Anwendung für physiologische Zwecke. Original work translated in." *Philosophical Magazine* **6**: 313-25.
- Hermann, B. P., M. Seidenberg, et al. (1995). "Relationship of age at onset, chronologic age, and adequacy of preoperative performance to verbal memory change after anterior temporal lobectomy." *Epilepsia* **36**(2): 137-45.

- Holmes, M. D., J. Quiring, et al. (2009). "Evidence that juvenile myoclonic epilepsy is a disorder of frontotemporal corticothalamic networks." Neuroimage.
- Holmes, M. D., D. M. Tucker, et al. (2010). "Comparing noninvasive dense array and intracranial electroencephalography for localization of seizures." Neurosurgery **66**(2): 354-62.
- Honey, C. J., O. Sporns, et al. (2009). "Predicting human resting-state functional connectivity from structural connectivity." Proc Natl Acad Sci U S A **106**(6): 2035-40.
- Hufnagel, A., J. Weber, et al. (2003). "Brain diffusion after single seizures." Epilepsia **44**(1): 54-63.
- ILAE (1981). "Proposal for revised clinical and electroencephalographic classification of epileptic seizures. From the Commission on Classification and Terminology of the International League Against Epilepsy." Epilepsia **22**(4): 489-501.
- ILAE (1989). "Proposal for revised classification of epilepsies and epileptic syndromes. Commission on Classification and Terminology of the International League Against Epilepsy." Epilepsia **30**(4): 389-99.
- ILAE (2005). "ILAE Neuroimaging Commission Recommendations for Neuroimaging of Patients with Epilepsy ILAE Neuroimaging Commission." Epilepsia **38**(s10): 1-2.
- Ives, J. R., S. Warach, et al. (1993). "Monitoring the patient's EEG during echo planar MRI." Electroencephalogr Clin Neurophysiol **87**(6): 417-20.
- Jackson, J. H. (1870). A study of convulsions. Transactions of the St Andrews University Medical Graduates Association.
- Jacobs, J., F. Dubeau, et al. (2008). "Pathways of seizure propagation from the temporal to the occipital lobe." Epileptic Disord **10**(4): 266-70.
- Jacobs, J., E. Kobayashi, et al. (2007). "Hemodynamic responses to interictal epileptiform discharges in children with symptomatic epilepsy." Epilepsia **48**(11): 2068-78.
- Jacobs, J., P. Levan, et al. (2009). "Hemodynamic changes preceding the interictal EEG spike in patients with focal epilepsy investigated using simultaneous EEG-fMRI." Neuroimage **45**(4): 1220-31.
- Jacobs, J., M. Zijlmans, et al. (2010). "High-frequency electroencephalographic oscillations correlate with outcome of epilepsy surgery." Ann Neurol **67**(2): 209-20.
- Jacobs, J., M. Zijlmans, et al. (2010). "Value of electrical stimulation and high frequency oscillations (80-500 Hz) in identifying epileptogenic areas during intracranial EEG recordings." Epilepsia **51**(4): 573-82.
- James, C. E., J. Britz, et al. (2008). "Early neuronal responses in right limbic structures mediate harmony incongruity processing in musical experts." Neuroimage **42**(4): 1597-608.
- Jann, K., R. Wiest, et al. (2008). "BOLD correlates of continuously fluctuating epileptic activity isolated by independent component analysis." Neuroimage **42**(2): 635-48.
- Jansen, F. E., K. P. Braun, et al. (2003). "Diffusion-weighted magnetic resonance imaging and identification of the epileptogenic tuber in patients with tuberous sclerosis." Arch Neurol **60**(11): 1580-4.
- Janz, D. (1985). "Epilepsy with impulsive petit mal (juvenile myoclonic epilepsy)." Acta Neurol Scand **72**(5): 449-59.
- Jerbi, K., J. R. Vidal, et al. (2010). "Exploring the electrophysiological correlates of the default-mode network with intracerebral EEG." Front Syst Neurosci **4**: 27.
- Johansen-Berg, H., T. E. Behrens, et al. (2004). "Changes in connectivity profiles define functionally distinct regions in human medial frontal cortex." Proc Natl Acad Sci U S A **101**(36): 13335-40.
- Johansen-Berg, H. and M. F. Rushworth (2009). "Using diffusion imaging to study human connective anatomy." Annu Rev Neurosci **32**: 75-94.
- Kahane, P. and A. Depaulis (2010). "Deep brain stimulation in epilepsy: what is next?" Curr Opin Neurol **23**(2): 177-82.
- Kaltenhauser, M., G. Scheler, et al. (2007). "Spatial intralobar correlation of spike and slow wave activity localisations in focal epilepsies: a MEG analysis." Neuroimage **34**(4): 1466-72.
- Kanner, A. M. (2009). "Psychiatric issues in epilepsy: the complex relation of mood, anxiety disorders, and epilepsy." Epilepsy Behav **15**(1): 83-7.
- Kiebel, S. J., J. Daunizeau, et al. (2008). "Variational Bayesian inversion of the equivalent current dipole model in EEG/MEG." Neuroimage **39**(2): 728-41.
- Kikuta, K., Y. Takagi, et al. (2008). "Introduction to tractography-guided navigation: using 3-tesla magnetic resonance tractography in surgery for cerebral arteriovenous malformations." Acta Neurochir Suppl **103**: 11-4.

- Kilner, J. M., J. Mattout, et al. (2005). "Hemodynamic correlates of EEG: a heuristic." *Neuroimage* **28**(1): 280-6.
- Kim, C. H., B. B. Koo, et al. (2010). "Thalamic changes in temporal lobe epilepsy with and without hippocampal sclerosis: a diffusion tensor imaging study." *Epilepsy Res* **90**(1-2): 21-7.
- Kim, D. W., S. K. Lee, et al. (2009). "Predictors of surgical outcome and pathologic considerations in focal cortical dysplasia." *Neurology* **72**(3): 211-6.
- Kim, H., Z. Piao, et al. (2008). "Secondary white matter degeneration of the corpus callosum in patients with intractable temporal lobe epilepsy: a diffusion tensor imaging study." *Epilepsy Res* **81**(2-3): 136-42.
- Kim, J. H., J. K. Lee, et al. (2007). "Regional grey matter abnormalities in juvenile myoclonic epilepsy: a voxel-based morphometry study." *Neuroimage* **37**(4): 1132-7.
- Kinoshita, M., K. Yamada, et al. (2005). "Fiber-tracking does not accurately estimate size of fiber bundle in pathological condition: initial neurosurgical experience using neuronavigation and subcortical white matter stimulation." *Neuroimage* **25**(2): 424-9.
- Klein, A., J. Andersson, et al. (2009). "Evaluation of 14 nonlinear deformation algorithms applied to human brain MRI registration." *Neuroimage* **46**(3): 786-802.
- Klimpe, S., M. Behrang-Nia, et al. (2009). "Recruitment of motor cortex inhibition differentiates between generalized and focal epilepsy." *Epilepsy Res* **84**(2-3): 210-6.
- Knowlton, R. C., R. A. Elgavish, et al. (2008). "Functional imaging: II. Prediction of epilepsy surgery outcome." *Ann Neurol* **64**(1): 35-41.
- Knowlton, R. C., R. A. Elgavish, et al. (2008). "Functional imaging: I. Relative predictive value of intracranial electroencephalography." *Ann Neurol* **64**(1): 25-34.
- Kobayashi, E., A. P. Bagshaw, et al. (2006). "Temporal and extratemporal BOLD responses to temporal lobe interictal spikes." *Epilepsia* **47**(2): 343-54.
- Kobayashi, E., A. P. Bagshaw, et al. (2006). "Negative BOLD responses to epileptic spikes." *Hum Brain Mapp* **27**(6): 488-97.
- Kobayashi, E., A. P. Bagshaw, et al. (2006). "Grey matter heterotopia: what EEG-fMRI can tell us about epileptogenicity of neuronal migration disorders." *Brain* **129**(Pt 2): 366-74.
- Kobayashi, E., A. P. Bagshaw, et al. (2005). "Intrinsic epileptogenicity in polymicrogyric cortex suggested by EEG-fMRI BOLD responses." *Neurology* **64**(7): 1263-6.
- Kobayashi, K., H. Yoshinaga, et al. (2003). "A simulation study of the error in dipole source localization for EEG spikes with a realistic head model." *Clin Neurophysiol* **114**(6): 1069-78.
- Koepp, M. J., M. P. Richardson, et al. (1997). "Central benzodiazepine/gamma-aminobutyric acid A receptors in idiopathic generalized epilepsy: an [¹¹C]flumazenil positron emission tomography study." *Epilepsia* **38**(10): 1089-97.
- Koepp, M. J. and F. G. Woermann (2005). "Imaging structure and function in refractory focal epilepsy." *Lancet Neurol* **4**(1): 42-53.
- Koessler, L., C. Benar, et al. (2010). "Source localization of ictal epileptic activity investigated by high resolution EEG and validated by SEEG." *Neuroimage* **51**(2): 642-53.
- Konermann, S., S. Marks, et al. (2003). "Presurgical evaluation of epilepsy by brain diffusion: MR-detected effects of flumazenil on the epileptogenic focus." *Epilepsia* **44**(3): 399-407.
- Krakov, K., P. J. Allen, et al. (2000). "EEG recording during fMRI experiments: image quality." *Hum Brain Mapp* **10**(1): 10-5.
- Krakov, K., F. G. Woermann, et al. (1999). "EEG-triggered functional MRI of interictal epileptiform activity in patients with partial seizures." *Brain* **122** (Pt 9): 1679-88.
- Kumari, V., E. R. Peters, et al. (2009). "Dorsolateral prefrontal cortex activity predicts responsiveness to cognitive-behavioral therapy in schizophrenia." *Biol Psychiatry* **66**(6): 594-602.
- Kwan, P. and M. J. Brodie (2000). "Early identification of refractory epilepsy." *N Engl J Med* **342**(5): 314-9.
- Lachaux, J. P., D. Rudrauf, et al. (2003). "Intracranial EEG and human brain mapping." *J Physiol Paris* **97**(4-6): 613-28.
- Lansberg, M. G., M. W. O'Brien, et al. (1999). "MRI abnormalities associated with partial status epilepticus." *Neurology* **52**(5): 1021-7.
- Lantz, G., R. Grave de Peralta, et al. (2003). "Epileptic source localization with high density EEG: how many electrodes are needed?" *Clin Neurophysiol* **114**(1): 63-9.
- Lantz, G., C. M. Michel, et al. (1999). "Frequency domain EEG source localization of ictal epileptiform activity in patients with partial complex epilepsy of temporal lobe origin." *Clin Neurophysiol* **110**(1): 176-84.

- Lantz, G., C. M. Michel, et al. (2001). "Space-oriented segmentation and 3-dimensional source reconstruction of ictal EEG patterns." Clin Neurophysiol **112**(4): 688-97.
- Lantz, G., E. Ryding, et al. (1997). "Dipole reconstruction as a method for identifying patients with mesolimbic epilepsy." Seizure **6**(4): 303-10.
- Lantz, G., L. Spinelli, et al. (2003). "Propagation of interictal epileptiform activity can lead to erroneous source localizations: a 128-channel EEG mapping study." J Clin Neurophysiol **20**(5): 311-9.
- Laufs, H., J. Daunizeau, et al. (2008). "Recent advances in recording electrophysiological data simultaneously with magnetic resonance imaging." Neuroimage **40**(2): 515-28.
- Laufs, H. and J. S. Duncan (2007). "Electroencephalography/functional MRI in human epilepsy: what it currently can and cannot do." Curr Opin Neurol **20**(4): 417-23.
- Laufs, H., K. Hamandi, et al. (2007). "Temporal lobe interictal epileptic discharges affect cerebral activity in "default mode" brain regions." Hum Brain Mapp **28**(10): 1023-32.
- Laufs, H., K. Hamandi, et al. (2006). "EEG-fMRI mapping of asymmetrical delta activity in a patient with refractory epilepsy is concordant with the epileptogenic region determined by intracranial EEG." Magn Reson Imaging **24**(4): 367-71.
- Laufs, H., J. L. Holt, et al. (2006). "Where the BOLD signal goes when alpha EEG leaves." Neuroimage **31**(4): 1408-18.
- Laufs, H., K. Krakow, et al. (2003). "Electroencephalographic signatures of attentional and cognitive default modes in spontaneous brain activity fluctuations at rest." Proc Natl Acad Sci U S A **100**(19): 11053-8.
- Lauritzen, M. and L. Gold (2003). "Brain function and neurophysiological correlates of signals used in functional neuroimaging." J Neurosci **23**(10): 3972-80.
- Lawes, I. N., T. R. Barrick, et al. (2008). "Atlas-based segmentation of white matter tracts of the human brain using diffusion tensor tractography and comparison with classical dissection." Neuroimage **39**(1): 62-79.
- Lazeyras, F., O. Blanke, et al. (2000). "EEG-triggered functional MRI in patients with pharmacoresistant epilepsy." J Magn Reson Imaging **12**(1): 177-85.
- Lee, H. W., J. S. Shin, et al. (2009). "Reorganisation of cortical motor and language distribution in human brain." J Neurol Neurosurg Psychiatry **80**(3): 285-90.
- Lee, S. K., S. Mori, et al. (2003). "Diffusion tensor MRI and fiber tractography of cerebellar atrophy in phenytoin users." Epilepsia **44**(12): 1536-40.
- Lehmann, D. and W. Skrandies (1980). "Reference-free identification of components of checkerboard-evoked multichannel potential fields." Electroencephalogr Clin Neurophysiol **48**(6): 609-21.
- Leijten, F. S. and G. Huiskamp (2008). "Interictal electromagnetic source imaging in focal epilepsy: practices, results and recommendations." Curr Opin Neurol **21**(4): 437-45.
- Lemieux, L., P. J. Allen, et al. (1997). "Recording of EEG during fMRI experiments: patient safety." Magn Reson Med **38**(6): 943-52.
- Lemieux, L., K. Krakow, et al. (2001). "Comparison of spike-triggered functional MRI BOLD activation and EEG dipole model localization." Neuroimage **14**(5): 1097-104.
- Lemieux, L., H. Laufs, et al. (2008). "Noncanonical spike-related BOLD responses in focal epilepsy." Hum Brain Mapp **29**(3): 329-45.
- Lemieux, L., A. Salek-Haddadi, et al. (2007). "Modelling large motion events in fMRI studies of patients with epilepsy." Magn Reson Imaging **25**(6): 894-901.
- Lhatoo, S. D., J. K. Solomon, et al. (2003). "A prospective study of the requirement for and the provision of epilepsy surgery in the United Kingdom." Epilepsia **44**(5): 673-6.
- Lin, J. J., J. D. Riley, et al. (2008). "Vulnerability of the frontal-temporal connections in temporal lobe epilepsy." Epilepsy Res **82**(2-3): 162-70.
- Lin, K., H. Carrete, Jr., et al. (2009). "Magnetic resonance spectroscopy reveals an epileptic network in juvenile myoclonic epilepsy." Epilepsia **50**(5): 1191-200.
- Liston, A. D., J. C. De Munck, et al. (2006). "Analysis of EEG-fMRI data in focal epilepsy based on automated spike classification and Signal Space Projection." Neuroimage **31**(3): 1015-24.
- Liston, A. D., T. E. Lund, et al. (2006). "Modelling cardiac signal as a confound in EEG-fMRI and its application in focal epilepsy studies." Neuroimage **30**(3): 827-34.
- Liu, R. S., L. Lemieux, et al. (2005). "Cerebral damage in epilepsy: a population-based longitudinal quantitative MRI study." Epilepsia **46**(9): 1482-94.
- Liu, Z., L. Ding, et al. (2006). "Integration of EEG/MEG with MRI and fMRI." IEEE Eng Med Biol Mag **25**(4): 46-53.

- Liu, Z. and B. He (2006). "A new multimodal imaging strategy for integrating fMRI with EEG." Conf Proc IEEE Eng Med Biol Soc **1**: 859-62.
- Liu, Z., F. Kecman, et al. (2006). "Effects of fMRI-EEG mismatches in cortical current density estimation integrating fMRI and EEG: a simulation study." Clin Neurophysiol **117**(7): 1610-22.
- Loddenkemper, T. and P. Kotagal (2005). "Lateralizing signs during seizures in focal epilepsy." Epilepsy Behav **7**(1): 1-17.
- Logothetis, N. K. (2008). "What we can do and what we cannot do with fMRI." Nature **453**(7197): 869-78.
- Logothetis, N. K., J. Pauls, et al. (2001). "Neurophysiological investigation of the basis of the fMRI signal." Nature **412**(6843): 150-7.
- Loscher, W. N., J. Dobesberger, et al. (2007). "rTMS reveals premotor cortex dysfunction in frontal lobe epilepsy." Epilepsia **48**(2): 359-65.
- Luat, A. F., M. Makki, et al. (2007). "Neuroimaging in tuberous sclerosis complex." Curr Opin Neurol **20**(2): 142-50.
- Lüders, H. (2008). Textbook of epilepsy surgery. London, Informa Healthcare.
- Lux, H. D., U. Heinemann, et al. (1986). "Ionic changes and alterations in the size of the extracellular space during epileptic activity." Adv Neurol **44**: 619-39.
- MacDonald, B. K., O. C. Cockerell, et al. (2000). "The incidence and lifetime prevalence of neurological disorders in a prospective community-based study in the UK." Brain **123** (Pt 4): 665-76.
- Maier, A., M. Wilke, et al. (2008). "Divergence of fMRI and neural signals in V1 during perceptual suppression in the awake monkey." Nat Neurosci **11**(10): 1193-200.
- Mandelkow, H., P. Halder, et al. (2006). "Synchronization facilitates removal of MRI artefacts from concurrent EEG recordings and increases usable bandwidth." Neuroimage **32**(3): 1120-6.
- Manganotti, P., L. G. Bongiovanni, et al. (2000). "Early and late intracortical inhibition in juvenile myoclonic epilepsy." Epilepsia **41**(9): 1129-38.
- Mantini, D., M. G. Perrucci, et al. (2007). "Electrophysiological signatures of resting state networks in the human brain." Proc Natl Acad Sci U S A **104**(32): 13170-5.
- Marques, J. P., J. Rebola, et al. (2009). "ICA decomposition of EEG signal for fMRI processing in epilepsy." Hum Brain Mapp **30**(9): 2986-96.
- McDonald, C. R., M. E. Ahmadi, et al. (2008). "Diffusion tensor imaging correlates of memory and language impairments in temporal lobe epilepsy." Neurology **71**(23): 1869-76.
- McDonald, C. R., D. J. Hagler, Jr., et al. (2008). "Subcortical and cerebellar atrophy in mesial temporal lobe epilepsy revealed by automatic segmentation." Epilepsy Res **79**(2-3): 130-8.
- McGonigal, A., F. Bartolomei, et al. (2007). "Stereo-electroencephalography in presurgical assessment of MRI-negative epilepsy." Brain **130**(Pt 12): 3169-83.
- McIntosh, A. M., R. M. Kalnins, et al. (2004). "Temporal lobectomy: long-term seizure outcome, late recurrence and risks for seizure recurrence." Brain **127**(Pt 9): 2018-30.
- Meckes-Ferber, S., A. Roten, et al. (2004). "EEG dipole source localisation of interictal spikes acquired during routine clinical video-EEG monitoring." Clin Neurophysiol **115**(12): 2738-43.
- Meencke, H. J. and D. Janz (1984). "Neuropathological findings in primary generalized epilepsy: a study of eight cases." Epilepsia **25**(1): 8-21.
- Megevand, P., C. Quairiaux, et al. (2008). "A mouse model for studying large-scale neuronal networks using EEG mapping techniques." Neuroimage **42**(2): 591-602.
- Merlet, I. and J. Gotman (2001). "Dipole modeling of scalp electroencephalogram epileptic discharges: correlation with intracerebral fields." Clin Neurophysiol **112**(3): 414-30.
- Michel, C. M., R. Grave de Peralta, et al. (1999). "Spatiotemporal EEG analysis and distributed source estimation in presurgical epilepsy evaluation." J Clin Neurophysiol **16**(3): 239-66.
- Michel, C. M., G. Lantz, et al. (2004). "128-channel EEG source imaging in epilepsy: clinical yield and localization precision." J Clin Neurophysiol **21**(2): 71-83.
- Michel, C. M., M. M. Murray, et al. (2004). "EEG source imaging." Clin Neurophysiol **115**(10): 2195-222.
- Michel, C. M., G. Thut, et al. (2001). "Electric source imaging of human brain functions." Brain Res Brain Res Rev **36**(2-3): 108-18.
- Moehring, J., F. Moeller, et al. (2008). "Non-REM sleep influences results of fMRI studies in epilepsy." Neurosci Lett.

- Moeller, F., P. Levan, et al. (2010). "Independent component analysis (ICA) of generalized spike wave discharges in fMRI: Comparison with general linear model-based EEG-fMRI." Hum Brain Mapp **32**(2): 209-17.
- Moeller, F., P. LeVan, et al. (2010). "Absence seizures: individual patterns revealed by EEG-fMRI." Epilepsia **51**(10): 2000-10.
- Moeller, F., H. R. Siebner, et al. (2008). "Changes in activity of striato-thalamo-cortical network precede generalized spike wave discharges." Neuroimage **39**(4): 1839-49.
- Mohamed, I. S., H. Otsubo, et al. (2007). "Magnetoencephalography and diffusion tensor imaging in gelastic seizures secondary to a cingulate gyrus lesion." Clin Neurol Neurosurg **109**(2): 182-7.
- Mullinger, K., M. Brookes, et al. (2008). "Exploring the feasibility of simultaneous electroencephalography/functional magnetic resonance imaging at 7 T." Magn Reson Imaging **26**(7): 968-77.
- Munari, C., D. Hoffmann, et al. (1994). "Stereo-electroencephalography methodology: advantages and limits." Acta Neurol Scand Suppl **152**: 56-67, discussion 68-9.
- Musso, F., J. Brinkmeyer, et al. (2010). "Spontaneous brain activity and EEG microstates. A novel EEG/fMRI analysis approach to explore resting-state networks." Neuroimage **52**(4): 1149-61.
- Nahum, L., D. Gabriel, et al. (2011). "Rapid consolidation and the human hippocampus: intracranial recordings confirm surface EEG." Hippocampus **21**(7): 689-93.
- Nardone, R., A. Venturi, et al. (2008). "Cortical silent period following TMS in a patient with supplementary sensorimotor area seizures." Exp Brain Res **184**(3): 439-43.
- Nedelcu, J., M. A. Klein, et al. (1999). "Biphasic edema after hypoxic-ischemic brain injury in neonatal rats reflects early neuronal and late glial damage." Pediatr Res **46**(3): 297-304.
- Nelles, M., C. G. Bien, et al. (2006). "Transient splenium lesions in presurgical epilepsy patients: incidence and pathogenesis." Neuroradiology **48**(7): 443-8.
- Niedermeyer, E. and F. Lopes da Silva (2005). Electroencephalography. Philadelphia, Lippincott Williams & Wilkins.
- Nilsson, D., G. Starck, et al. (2007). "Intersubject variability in the anterior extent of the optic radiation assessed by tractography." Epilepsy Res **77**(1): 11-6.
- Nunez, P. L. and R. B. Silberstein (2000). "On the relationship of synaptic activity to macroscopic measurements: does co-registration of EEG with fMRI make sense?" Brain Topogr **13**(2): 79-96.
- O'Muirheartaigh, J., C. Vollmar, et al. (2011). "Focal structural changes and cognitive dysfunction in juvenile myoclonic epilepsy." Neurology **76**(1): 34-40.
- Oh, J. B., S. K. Lee, et al. (2004). "Role of immediate postictal diffusion-weighted MRI in localizing epileptogenic foci of mesial temporal lobe epilepsy and non-lesional neocortical epilepsy." Seizure **13**(7): 509-16.
- Osharina, V., E. Ponchel, et al. (2010). "Local haemodynamic changes preceding interictal spikes: a simultaneous electrocorticography (ECoG) and near-infrared spectroscopy (NIRS) analysis in rats." Neuroimage **50**(2): 600-7.
- Pacia, S. V. and J. S. Ebersole (1997). "Intracranial EEG substrates of scalp ictal patterns from temporal lobe foci." Epilepsia **38**(6): 642-54.
- Parker, G. J. and D. C. Alexander (2003). "Probabilistic Monte Carlo based mapping of cerebral connections utilising whole-brain crossing fibre information." Lect Notes Comput Sci **2732**: 684-95.
- Pascalichio, T. F., G. M. de Araujo Filho, et al. (2007). "Neuropsychological profile of patients with juvenile myoclonic epilepsy: a controlled study of 50 patients." Epilepsy Behav **10**(2): 263-7.
- Pasqual Marqui, R. D., K. Sekihara, et al. (2009). Imaging the electrical neuronal generators of EEG/MEG. Electrical Neuroimaging. K. T. Michel CM, Brandeis D, Gianotti LRR, Wackermann J. Cambridge, Cambridge University Press: 49-77.
- Patel, M. R., A. Blum, et al. (1999). "Echo-planar functional MR imaging of epilepsy with concurrent EEG monitoring." AJNR Am J Neuroradiol **20**(10): 1916-9.
- Picard, N. and P. L. Strick (1996). "Motor areas of the medial wall: a review of their location and functional activation." Cereb Cortex **6**(3): 342-53.
- Picard, N. and P. L. Strick (2003). "Activation of the supplementary motor area (SMA) during performance of visually guided movements." Cereb Cortex **13**(9): 977-86.
- Pierpaoli, C., P. Jezzard, et al. (1996). "Diffusion tensor MR imaging of the human brain." Radiology **201**(3): 637-48.

- Plummer, C., A. S. Harvey, et al. (2008). "EEG source localization in focal epilepsy: where are we now?" Epilepsia **49**(2): 201-18.
- Porcaro, C., D. Ostwald, et al. (2010). "Functional source separation improves the quality of single trial visual evoked potentials recorded during concurrent EEG-fMRI." Neuroimage **50**(1): 112-23.
- Powell, H. W., G. J. Parker, et al. (2008). "Imaging language pathways predicts postoperative naming deficits." J Neurol Neurosurg Psychiatry **79**(3): 327-30.
- Powell, H. W., G. J. Parker, et al. (2005). "MR tractography predicts visual field defects following temporal lobe resection." Neurology **65**(4): 596-9.
- Powell, H. W., G. J. Parker, et al. (2007). "Abnormalities of language networks in temporal lobe epilepsy." Neuroimage **36**(1): 209-21.
- Powell, H. W., G. J. Parker, et al. (2006). "Hemispheric asymmetries in language-related pathways: a combined functional MRI and tractography study." Neuroimage **32**(1): 388-99.
- Prichard, J. W., J. Zhong, et al. (1995). "Diffusion-weighted NMR imaging changes caused by electrical activation of the brain." NMR Biomed **8**(7-8): 359-64.
- Prilipko, O., J. Delavelle, et al. (2005). "Reversible cytotoxic edema in the splenium of the corpus callosum related to antiepileptic treatment: report of two cases and literature review." Epilepsia **46**(10): 1633-6.
- Raichle, M. E., A. M. MacLeod, et al. (2001). "A default mode of brain function." Proc Natl Acad Sci U S A **98**(2): 676-82.
- Rathakrishnan, R., F. Moeller, et al. (2010). "BOLD signal changes preceding negative responses in EEG-fMRI in patients with focal epilepsy." Epilepsia **51**(9): 1837-45.
- Ray, A., J. X. Tao, et al. (2007). "Localizing value of scalp EEG spikes: a simultaneous scalp and intracranial study." Clin Neurophysiol **118**(1): 69-79.
- Richardson, M. P., P. Grosse, et al. (2006). "BOLD correlates of EMG spectral density in cortical myoclonus: description of method and case report." Neuroimage **32**(2): 558-65.
- Ritter, P. and A. Villringer (2006). "Simultaneous EEG-fMRI." Neurosci Biobehav Rev **30**(6): 823-38.
- Rodionov, R., F. De Martino, et al. (2007). "Independent component analysis of interictal fMRI in focal epilepsy: comparison with general linear model-based EEG-correlated fMRI." Neuroimage **38**(3): 488-500.
- Roebeling, R., N. Scheerer, et al. (2009). "Evaluation of cognition, structural, and functional MRI in juvenile myoclonic epilepsy." Epilepsia.
- Rosenow, F. and H. Luders (2001). "Presurgical evaluation of epilepsy." Brain **124**(Pt 9): 1683-700.
- Rossini, P. M., C. Altamura, et al. (2004). "Does cerebrovascular disease affect the coupling between neuronal activity and local haemodynamics?" Brain **127**(Pt 1): 99-110.
- Roth, B. J., D. Ko, et al. (1997). "Dipole localization in patients with epilepsy using the realistically shaped head model." Electroencephalogr Clin Neurophysiol **102**(3): 159-66.
- Rugg-Gunn, F. J., S. H. Eriksson, et al. (2001). "Diffusion tensor imaging of cryptogenic and acquired partial epilepsies." Brain **124**(Pt 3): 627-36.
- Rugg-Gunn, F. J., S. H. Eriksson, et al. (2002). "Diffusion tensor imaging in refractory epilepsy." Lancet **359**(9319): 1748-51.
- Rush, S. and D. A. Driscoll (1969). "EEG electrode sensitivity--an application of reciprocity." IEEE Trans Biomed Eng **16**(1): 15-22.
- Ryvlin, P., S. Bouvard, et al. (1998). "Clinical utility of flumazenil-PET versus [18F]fluorodeoxyglucose-PET and MRI in refractory partial epilepsy. A prospective study in 100 patients." Brain **121** (Pt 11): 2067-81.
- Salek-Haddadi, A., B. Diehl, et al. (2006). "Hemodynamic correlates of epileptiform discharges: an EEG-fMRI study of 63 patients with focal epilepsy." Brain Res **1088**(1): 148-66.
- Salek-Haddadi, A., K. J. Friston, et al. (2003). "Studying spontaneous EEG activity with fMRI." Brain Res Brain Res Rev **43**(1): 110-33.
- Salek-Haddadi, A., L. Lemieux, et al. (2002). "Role of functional magnetic resonance imaging in the evaluation of patients with malformations caused by cortical development." Neurosurg Clin N Am **13**(1): 63-9, viii.
- Salek-Haddadi, A., L. Lemieux, et al. (2003). "EEG quality during simultaneous functional MRI of interictal epileptiform discharges." Magn Reson Imaging **21**(10): 1159-66.
- Salek-Haddadi, A., L. Lemieux, et al. (2003). "Functional magnetic resonance imaging of human absence seizures." Ann Neurol **53**(5): 663-7.

- Salek-Haddadi, A., M. Merschhemke, et al. (2002). "Simultaneous EEG-Correlated Ictal fMRI." Neuroimage **16**(1): 32-40.
- Salmenpera, T. M., M. R. Symms, et al. (2006). "Postictal diffusion weighted imaging." Epilepsy Res **70**(2-3): 133-43.
- Sander, J. W. and S. D. Shorvon (1996). "Epidemiology of the epilepsies." J Neurol Neurosurg Psychiatry **61**(5): 433-43.
- Savic, I., A. Lekkval, et al. (2000). "MR spectroscopy shows reduced frontal lobe concentrations of N-acetyl aspartate in patients with juvenile myoclonic epilepsy." Epilepsia **41**(3): 290-6.
- Scherg, M., T. Bast, et al. (1999). "Multiple source analysis of interictal spikes: goals, requirements, and clinical value." J Clin Neurophysiol **16**(3): 214-24.
- Schoene-Bake, J. C., J. Faber, et al. (2009). "Widespread affections of large fiber tracts in postoperative temporal lobe epilepsy." Neuroimage.
- Schridde, U., M. Khubchandani, et al. (2008). "Negative BOLD with large increases in neuronal activity." Cereb Cortex **18**(8): 1814-27.
- Scott, R. C., D. G. Gadian, et al. (2002). "Magnetic resonance imaging findings within 5 days of status epilepticus in childhood." Brain **125**(Pt 9): 1951-9.
- Scott, R. C., M. D. King, et al. (2003). "Hippocampal abnormalities after prolonged febrile convulsion: a longitudinal MRI study." Brain **126**(Pt 11): 2551-7.
- Seeck, M., F. Lazeyras, et al. (1998). "Non-invasive epileptic focus localization using EEG-triggered functional MRI and electromagnetic tomography." Electroencephalogr Clin Neurophysiol **106**(6): 508-12.
- Seeck, M. and L. Spinelli (2004). "Intracranial monitoring." Suppl Clin Neurophysiol **57**: 485-93.
- Sekihara, K. and S. S. Nagarajan (2004). Neuromagnetic source reconstruction and inverse modeling. In: He B, editor. Modeling and Imaging of Bioelectric Activity - Principles and Applications. New York, Kluwer Academic/Plenum Publishers.
- Shmuel, A., M. Augath, et al. (2006). "Negative functional MRI response correlates with decreases in neuronal activity in monkey visual area V1." Nat Neurosci **9**(4): 569-77.
- Shmuel, A., E. Yacoub, et al. (2002). "Sustained negative BOLD, blood flow and oxygen consumption response and its coupling to the positive response in the human brain." Neuron **36**(6): 1195-210.
- Shmueli, K., P. van Gelderen, et al. (2007). "Low-frequency fluctuations in the cardiac rate as a source of variance in the resting-state fMRI BOLD signal." Neuroimage **38**(2): 306-20.
- Sierra, A., T. Laitinen, et al. (2010). "Diffusion tensor MRI with tract-based spatial statistics and histology reveals undiscovered lesioned areas in kainate model of epilepsy in rat." Brain Struct Funct.
- Simister, R. J., M. A. McLean, et al. (2009). "Proton MR spectroscopy of metabolite concentrations in temporal lobe epilepsy and effect of temporal lobe resection." Epilepsy Res **83**(2-3): 168-76.
- Siniatchkin, M., K. Groening, et al. (2010). "Neuronal networks in children with continuous spikes and waves during slow sleep." Brain **133**(9): 2798-813.
- Siniatchkin, M., A. van Baalen, et al. (2007). "Different neuronal networks are associated with spikes and slow activity in hypsarrhythmia." Epilepsia **48**(12): 2312-21.
- Sirotnin, Y. B. and A. Das (2009). "Anticipatory haemodynamic signals in sensory cortex not predicted by local neuronal activity." Nature **457**(7228): 475-9.
- Smith, J. R., K. N. Fountas, et al. (2010). "Closed-loop stimulation in the control of focal epilepsy of insular origin." Stereotact Funct Neurosurg **88**(5): 281-7.
- Song, S. K., S. W. Sun, et al. (2002). "Dysmyelination revealed through MRI as increased radial (but unchanged axial) diffusion of water." Neuroimage **17**(3): 1429-36.
- Sotero, R. C. and N. J. Trujillo-Barreto (2007). "Modelling the role of excitatory and inhibitory neuronal activity in the generation of the BOLD signal." Neuroimage **35**(1): 149-65.
- Spencer, S. and L. Huh (2008). "Outcomes of epilepsy surgery in adults and children." Lancet Neurol **7**(6): 525-37.
- Sperli, F., L. Spinelli, et al. (2006). "Contralateral smile and laughter, but no mirth, induced by electrical stimulation of the cingulate cortex." Epilepsia **47**(2): 440-3.
- Sperli, F., L. Spinelli, et al. (2006). "EEG source imaging in pediatric epilepsy surgery: a new perspective in presurgical workup." Epilepsia **47**(6): 981-90.
- Spinelli, L., S. G. Andino, et al. (2000). "Electromagnetic inverse solutions in anatomically constrained spherical head models." Brain Topogr **13**(2): 115-25.

- Stefan, H., C. Hummel, et al. (2003). "Magnetic brain source imaging of focal epileptic activity: a synopsis of 455 cases." *Brain* **126**(Pt 11): 2396-405.
- Stefan, H., C. Nimsky, et al. (2006). "Periventricular nodular heterotopia: A challenge for epilepsy surgery." *Seizure*.
- Stefan, H., S. Rampf, et al. (2010). "Magnetoencephalography adds to the surgical evaluation process." *Epilepsy Behav.*
- Stefanovic, B., J. M. Warnking, et al. (2005). "Hemodynamic and metabolic responses to activation, deactivation and epileptic discharges." *Neuroimage* **28**(1): 205-15.
- Strobel, A., S. Debener, et al. (2008). "Novelty and target processing during an auditory novelty oddball: a simultaneous event-related potential and functional magnetic resonance imaging study." *Neuroimage* **40**(2): 869-83.
- Sutherland, W. W., A. N. Mamelak, et al. (2008). "Influence of magnetic source imaging for planning intracranial EEG in epilepsy." *Neurology* **71**(13): 990-6.
- Szabo, K., A. Poepel, et al. (2005). "Diffusion-weighted and perfusion MRI demonstrates parenchymal changes in complex partial status epilepticus." *Brain* **128**(Pt 6): 1369-76.
- Takanashi, J., H. Oba, et al. (2006). "Diffusion MRI abnormalities after prolonged febrile seizures with encephalopathy." *Neurology* **66**(9): 1304-9; discussion 1291.
- Tao, J. X., M. Baldwin, et al. (2007). "Cortical substrates of scalp EEG epileptiform discharges." *J Clin Neurophysiol* **24**(2): 96-100.
- Tao, J. X., A. Ray, et al. (2005). "Intracranial EEG substrates of scalp EEG interictal spikes." *Epilepsia* **46**(5): 669-76.
- Taoka, T., M. Sakamoto, et al. (2005). "Diffusion tensor imaging in cases with visual field defect after anterior temporal lobectomy." *AJNR Am J Neuroradiol* **26**(4): 797-803.
- Tassi, L., N. Colombo, et al. (2005). "Electroclinical, MRI and neuropathological study of 10 patients with nodular heterotopia, with surgical outcomes." *Brain* **128**(Pt 2): 321-37.
- Thivard, L., C. Adam, et al. (2006). "Interictal diffusion MRI in partial epilepsies explored with intracerebral electrodes." *Brain* **129**(Pt 2): 375-85.
- Thivard, L., S. Lehericy, et al. (2005). "Diffusion tensor imaging in medial temporal lobe epilepsy with hippocampal sclerosis." *Neuroimage* **28**(3): 682-90.
- Thivard, L., M. L. Tanguy, et al. (2007). "Postoperative Recovery of Hippocampal Contralateral Diffusivity in Medial Temporal Lobe Epilepsy." *Epilepsia*.
- Thomalla, G., H. R. Siebner, et al. (2009). "Structural changes in the somatosensory system correlate with tic severity in Gilles de la Tourette syndrome." *Brain* **132**(Pt 3): 765-77.
- Thornton, R., H. Laufs, et al. (2010). "EEG correlated functional MRI and postoperative outcome in focal epilepsy." *J Neurol Neurosurg Psychiatry* **81**(8): 922-7.
- Thornton, R., S. Vulliemoz, et al. "Epileptic networks in Focal Cortical Dysplasia revealed using EEG-fMRI." *Annals of Neurology in press*.
- Thornton, R. C., R. Rodionov, et al. (2010). "Imaging haemodynamic changes related to seizures: comparison of EEG-based general linear model, independent component analysis of fMRI and intracranial EEG." *Neuroimage* **53**(1): 196-205.
- Thudium, M. O., A. R. Campos, et al. (2010). "The basal temporal approach for mesial temporal surgery: sparing the meyer loop with navigated diffusion tensor tractography." *Neurosurgery* **67**(2 Suppl Operative): 385-90.
- Toga, A. W., P. M. Thompson, et al. (2006). "Mapping brain maturation." *Trends Neurosci* **29**(3): 148-59.
- Tolias, A. S., F. Sultan, et al. (2005). "Mapping cortical activity elicited with electrical microstimulation using fMRI in the macaque." *Neuron* **48**(6): 901-11.
- Trivedi, R., R. K. Gupta, et al. (2006). "Diffusion tensor imaging in polymicrogyria: a report of three cases." *Neuroradiology* **48**(6): 422-7.
- Trujillo-Barreto, N., E. Martinez-Montes, et al. (2001). "A symmetrical Bayesian Model for fMRI and EEG/MEG Neuroimage Fusion." *International Journal of Electrobioimagnetism* **3**(1): Available online at <http://ijbem.k.hosei.ac.jp/2006-/volume3/number1> (last accessed 15-8-2009).
- Tuch, D. S., T. G. Reese, et al. (2003). "Diffusion MRI of complex neural architecture." *Neuron* **40**(5): 885-95.
- Tuch, D. S., V. J. Wedeen, et al. (2001). "Conductivity tensor mapping of the human brain using diffusion tensor MRI." *Proc Natl Acad Sci U S A* **98**(20): 11697-701.
- Turner, R. (2002). "How much cortex can a vein drain? Downstream dilution of activation-related cerebral blood oxygenation changes." *Neuroimage* **16**(4): 1062-7.

- Tyvaert, L., S. Chassagnon, et al. (2009). "Thalamic nuclei activity in idiopathic generalized epilepsy: an EEG-fMRI study." *Neurology* **73**(23): 2018-22.
- Tyvaert, L., C. Hawco, et al. (2008). "Different structures involved during ictal and interictal epileptic activity in malformations of cortical development: an EEG-fMRI study." *Brain* **131**(Pt 8): 2042-60.
- Tyvaert, L., P. Levan, et al. (2008). "Effects of fluctuating physiological rhythms during prolonged EEG-fMRI studies." *Clin Neurophysiol* **119**(12): 2762-74.
- Valdes-Sosa, P. A., J. M. Sanchez-Bornot, et al. (2009). "Model driven EEG/fMRI fusion of brain oscillations." *Hum Brain Mapp* **30**(9): 2701-21.
- Van De Ville, D., J. Britz, et al. (2010). "EEG microstate sequences in healthy humans at rest reveal scale-free dynamics." *Proc Natl Acad Sci U S A*.
- Van Paesschen, W. (2004). "Ictal SPECT." *Epilepsia* **45 Suppl 4**: 35-40.
- Van Paesschen, W., P. Dupont, et al. (2007). "The use of SPECT and PET in routine clinical practice in epilepsy." *Curr Opin Neurol* **20**(2): 194-202.
- VanLandingham, K. E., E. R. Heinz, et al. (1998). "Magnetic resonance imaging evidence of hippocampal injury after prolonged focal febrile convulsions." *Ann Neurol* **43**(4): 413-26.
- Vaudano, A. E., H. Laufs, et al. (2009). "Causal hierarchy within the thalamo-cortical network in spike and wave discharges." *PLoS One* **4**(8): e6475.
- Velasco, A. L., F. Velasco, et al. (2006). "Neuromodulation of the centromedian thalamic nuclei in the treatment of generalized seizures and the improvement of the quality of life in patients with Lennox-Gastaut syndrome." *Epilepsia* **47**(7): 1203-12.
- Vollmar, C., J. O'Muircheartaigh, et al. (2011). "Motor system hyperconnectivity in juvenile myoclonic epilepsy: a cognitive functional magnetic resonance imaging study." *Brain* **134**(Pt 6): 1710-9.
- Vollmar, C., J. O'Muircheartaigh, et al. (2010). "Identical, but not the same: intra-site and inter-site reproducibility of fractional anisotropy measures on two 3.0T scanners." *Neuroimage* **51**(4): 1384-94.
- Vonck, K., P. Boon, et al. (2002). "Long-term amygdalohippocampal stimulation for refractory temporal lobe epilepsy." *Ann Neurol* **52**(5): 556-65.
- Vulliemoz, S., R. Thornton, et al. (2009). "The spatio-temporal mapping of epileptic networks: combination of EEG-fMRI and EEG source imaging." *Neuroimage* **46**(3): 834-43.
- Wakamoto, H., D. C. Chugani, et al. (2008). "Alpha-methyl-L-tryptophan positron emission tomography in epilepsy with cortical developmental malformations." *Pediatr Neurol* **39**(3): 181-8.
- Wakana, S., A. Caprihan, et al. (2007). "Reproducibility of quantitative tractography methods applied to cerebral white matter." *Neuroimage* **36**(3): 630-44.
- Wan, X., K. Iwata, et al. (2006). "Artifact reduction for simultaneous EEG/fMRI recording: adaptive FIR reduction of imaging artifacts." *Clin Neurophysiol* **117**(3): 681-92.
- Wang, Y., A. Majors, et al. (1996). "Postictal alteration of sodium content and apparent diffusion coefficient in epileptic rat brain induced by kainic acid." *Epilepsia* **37**(10): 1000-6.
- Warach, S., J. R. Ives, et al. (1996). "EEG-triggered echo-planar functional MRI in epilepsy." *Neurology* **47**(1): 89-93.
- Wedeen, V. J., P. Hagmann, et al. (2005). "Mapping complex tissue architecture with diffusion spectrum magnetic resonance imaging." *Magn Reson Med* **54**(6): 1377-86.
- Wehner, T., E. Lapresto, et al. (2007). "The value of interictal diffusion-weighted imaging in lateralizing temporal lobe epilepsy." *Neurology* **68**(2): 122-7.
- Wendel, K., O. Vaisanen, et al. (2009). "EEG/MEG source imaging: methods, challenges, and open issues." *Comput Intell Neurosci*: 656092.
- Wetjen, N. M., W. R. Marsh, et al. (2008). "Intracranial electroencephalography seizure onset patterns and surgical outcomes in nonlesional extratemporal epilepsy." *J Neurosurg*.
- Wheeler-Kingshott, C. A. and M. Cercignani (2009). "About "axial" and "radial" diffusivities." *Magn Reson Med* **61**(5): 1255-1260.
- Widjaja, E., S. Blaser, et al. (2007). "Evaluation of subcortical white matter and deep white matter tracts in malformations of cortical development." *Epilepsia* **48**(8): 1460-9.
- Widjaja, E., S. Zarei Mahmoodabadi, et al. (2009). "Subcortical alterations in tissue microstructure adjacent to focal cortical dysplasia: detection at diffusion-tensor MR imaging by using magnetoencephalographic dipole cluster localization." *Radiology* **251**(1): 206-15.
- Wiebe, S., W. T. Blume, et al. (2001). "A randomized, controlled trial of surgery for temporal-lobe epilepsy." *N Engl J Med* **345**(5): 311-8.

- Wieshmann, U. C., M. R. Symms, et al. (1999). "Blunt-head trauma associated with widespread water-diffusion changes." Lancet **353**(9160): 1242-3.
- Wieshmann, U. C., F. G. Woermann, et al. (1997). "Development of hippocampal atrophy: a serial magnetic resonance imaging study in a patient who developed epilepsy after generalized status epilepticus." Epilepsia **38**(11): 1238-41.
- Woermann, F. G., S. L. Free, et al. (1999). "Abnormal cerebral structure in juvenile myoclonic epilepsy demonstrated with voxel-based analysis of MRI." Brain **122** (Pt 11): 2101-8.
- Woermann, F. G., S. M. Sisodiya, et al. (1998). "Quantitative MRI in patients with idiopathic generalized epilepsy. Evidence of widespread cerebral structural changes." Brain **121** (Pt 9): 1661-7.
- Yacoub, E. and X. Hu (1999). "Detection of the early negative response in fMRI at 1.5 Tesla." Magn Reson Med **41**(6): 1088-92.
- Yan, W. X., K. J. Mullinger, et al. (2010). "Physical modeling of pulse artefact sources in simultaneous EEG/fMRI." Hum Brain Mapp **31**(4): 604-20.
- Yogarajah, M. and J. S. Duncan (2008). "Diffusion-based magnetic resonance imaging and tractography in epilepsy." Epilepsia **49**(2): 189-200.
- Yogarajah, M., N. K. Focke, et al. (2009). "Defining Meyer's loop-temporal lobe resections, visual field deficits and diffusion tensor tractography." Brain **132**(Pt 6): 1656-68.
- Yogarajah, M., N. K. Focke, et al. (2010). "The structural plasticity of white matter networks following anterior temporal lobe resection." Brain **133**(Pt 8): 2348-64.
- Yogarajah, M., H. W. Powell, et al. (2008). "Tractography of the parahippocampal gyrus and material specific memory impairment in unilateral temporal lobe epilepsy." Neuroimage **40**(4): 1755-64.
- Yoon, H. H., H. L. Kwon, et al. (2003). "Long-term seizure outcome in patients initially seizure-free after resective epilepsy surgery." Neurology **61**(4): 445-50.
- Zhao, M., M. Suh, et al. (2007). "Focal increases in perfusion and decreases in hemoglobin oxygenation precede seizure onset in spontaneous human epilepsy." Epilepsia **48**(11): 2059-67.
- Zhong, J., O. A. Petroff, et al. (1993). "Changes in water diffusion and relaxation properties of rat cerebrum during status epilepticus." Magn Reson Med **30**(2): 241-6.
- Zijlmans, M., G. Huiskamp, et al. (2007). "EEG-fMRI in the preoperative work-up for epilepsy surgery." Brain **130**(Pt 9): 2343-53.
- Zumsteg, D., A. Friedman, et al. (2006). "Propagation of interictal discharges in temporal lobe epilepsy: correlation of spatiotemporal mapping with intracranial foramen ovale electrode recordings." Clin Neurophysiol **117**(12): 2615-26.